THE PROCEEDINGS OF THE PHYSICAL SOCIETY

VOL. 50, PART 5 | 1 *September* 1938 | NO. 281

SECONDARY-ELECTRON EMISSION FROM NICKEL, COBALT AND IRON AS A FUNCTION OF TEMPERATURE

BY L. R. G. TRELOAR, B.Sc., F.INST.P.

AND

D. H. LANDON, B.Sc.

A communication from the Research Staff of the M.O. Valve Company
Limited, at the G.E.C. Research Laboratories, Wembley, England

Received 16 *February* 1938. *Read* 10 *June* 1938

ABSTRACT. The evidence of other workers to the effect that the magnetic and structural changes which occur in ferromagnetic metals are accompanied by changes in the secondary-electron emission is critically discussed, and it is shown that this evidence is in many respects unsatisfactory. The authors have measured the secondary-emission coefficients for nickel, cobalt and iron at various primary voltages over a temperature range of about 400° c., and find in all cases either no change or a slight and gradual fall in the coefficient with rising temperature, the latter effect probably being due to surface gas. No evidence was obtained of any discontinuous changes in secondary emission at the transformation points, though a change of less than 5 per cent could readily have been detected.

§ 1. INTRODUCTION

It has been shown in a number of experimental investigations* that the coefficient of secondary-electron emission from a metal surface is, in general, independent of the temperature of the emitter. Exceptions to this general rule have been reported in the case of ferromagnetic metals and metals which undergo a change of crystal structure at a certain temperature; for such metals it appears from certain published results that there may be abrupt changes in secondary emission at the temperatures corresponding to the magnetic or structural changes. Owing to the theoretical significance which may be attached to these findings, and also to the fact that the previous works on the subject are open to serious criticisms, it was felt that a further experimental investigation of this matter was desirable.

---

* For summary of these investigations see Kollath(7).

§ 2. CRITICAL EXAMINATION OF PREVIOUS WORK

There have been two previous investigations dealing with the subject-matter of the present paper, the first due to Tartakowsky and Kudrjawzewa(1) and the second to Hayakawa(2). Tartakowsky and Kudrjawzewa studied the secondary emission of nickel as a function of temperature, using primary voltages in the neighbourhood of 30. According to their data, an example of which is reproduced in the broken curve in figure 1, when the temperature of the metal is raised from 150 to 350° C. there is a continuous increase in the secondary emission. This is followed by an abrupt fall at the Curie point (358°), i.e. the temperature at which the metal loses its ferromagnetic properties, and a further and more rapid rise up to 445°. Substitution of copper for nickel, in a control experiment, resulted in a uniform linear increase of secondary emission with temperature being obtained, the rate of increase being about 12 per cent per 100° rise of temperature. The sudden fall in the amount of the secondary emission which occurred in passing through the Curie point of nickel was held to show that the conduction electrons of the metal, which Tartakowsky and Kudrjawzewa suppose to give rise to the major portion of the secondary emission, are also responsible for its ferromagnetic properties.

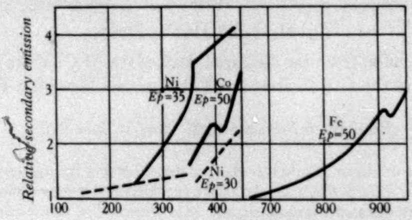

Figure 1. Variation of secondary emission with temperature. —— Hayakawa; - - - Tartakowsky and Kudrjawzewa.

In considering the experimental method by which these results were obtained, it is clear that the authors were not able to collect and measure all the secondary electrons emitted by their target. They could not, therefore, measure the secondary-emission coefficient, i.e. the ratio of the number of secondary electrons emitted by the target to the number of primary electrons incident upon it. What they actually measured was the current due to a comparatively small fraction of the emitted secondaries which entered a Faraday cage placed at a distance from the target. Now the ratio of this measured current to the total secondary emission must have been determined by the orbits of the secondary electrons leaving the target, and the orbit of a particular electron will depend on its direction and velocity of emission, on the potential-distribution in the space outside the target, and also on the magnetic field, if any, in the space. It follows that the data of Tartakowsky and Kudrjawzewa cannot be directly related to the secondary-emission coefficient, or to any other quantity having a precise physical significance, unless the following conditions were satisfied, over the temperature range employed: (1) constancy of angular distribution of the emitted secondaries; (2) constancy of energy distribution of the emitted secondaries; (3) constancy of potential of the glass walls; (4) absence of stray magnetic field due to the current in the filament used to heat the target.

It is not possible to say whether these conditions were satisfied, but the absence of any mention of their importance in the paper gives rise to some doubt as to the validity of the results obtained.

A further difficulty is presented by the large variation in the secondary emission from nickel over the temperature range on either side of the Curie point, and by the variation with temperature observed with copper, both of which effects were passed over without comment by the authors, though they would certainly not have been anticipated on the basis of earlier results.

Hayakawa(2) studied the variation of secondary emission with temperature for nickel, iron, cobalt and certain nickel-iron alloys, using primary voltages from 20 to 125. He found in all cases a large variation of secondary emission with temperature. Typical examples of his results are reproduced in figure 1. For nickel and iron the slope of the curve relating secondary emission with temperature changed abruptly at the Curie point, whilst for iron and cobalt there was a kink in the curve at the temperature corresponding to a change in the crystal structure. Analogous results were obtained with the nickel-iron alloys. The data were interpreted by Hayakawa in the light of a theory developed by Richardson(3), and quantitative evidence was adduced in support of the view that the secondary electrons were identical with Richardson's "structure electrons".

Whilst Hayakawa's experimental arrangement is not open to the objections which have been brought against the work previously discussed, his data nevertheless present such curious anomalies that they cannot readily be accepted. His results are not expressed in terms of the secondary-emission coefficient, even though it is stated that both the primary and secondary currents could be measured. Moreover, it is difficult to form a clear idea as to what quantity the term "secondary electron emission" as used by the author is intended to represent. Presumably it bears some relation to the secondary-emission coefficient, but it is not a relation of proportionality, as an examination of his figures will show. For example, the rates of variation of this quantity with temperature shown in his figures 8 and 9 differ by a factor of 2 from those given in his figure 10 for the same material under the same conditions. Even greater discrepancies are apparent when his figures 12 and 13 are compared with figure 14. Finally, it must be observed that the secondary emission from nickel at primary voltages of 19·5 and 22 apparently falls to zero at a certain temperature. It is also remarkable that Hayakawa found even larger variations of secondary emission with temperature, unassociated with any transformations, than Tartakowsky and Kudrjawzewa did, though like them he does not consider that point worthy of discussion.

For these reasons it was felt that Hayakawa's data could not be accepted as establishing beyond doubt the existence of a relationship between secondary emission and metallic structure.

§ 3. STUDY OF NICKEL AND COBALT

In the present investigation of the variation with temperature, if such variation occurs, of the secondary-emission coefficient for nickel and cobalt, a very simple experimental system shown diagrammatically in figure 2 was employed. A short tungsten filament F mounted axially in a cylindrical anode A served as the source of electrons, some of which, after passing through the tube G of length 10 mm. and internal bore 0·5 mm., fell on a target T of the material under investigation. This target, which was in the form of a tube of rectangular section, could be heated by passing a current through an insulated tungsten filament H, and its temperature could be measured by means of the thermocouple Th. The couple, which consisted of a pair of 0·1 mm. platinum and platinum-iridium alloy wires obtained from Messrs Johnson Matthey, was welded on to the target and sealed through the glass envelope of the apparatus. The tube G terminated in a circular nickel disc D, 10 mm. in diameter. The target, shown in plan in figure 2 (b), was electrically but not thermally connected with segments SS' mounted on either side of its centre portion, the disc D and the target with its associated segments thus forming in effect a pair of parallel plates separated by a distance of 1·5 mm. The field in the neighbourhood of the centre of the target, when a potential-difference was applied between target and anode, was therefore approximately uniform and normal to the surface of the target. By this arrangement the necessity for the provision of a separate collecting-chamber was obviated, with the result that the target could be brought quite close to the electron gun G, and its dimensions, and therefore the energy required to heat it, could be kept small.

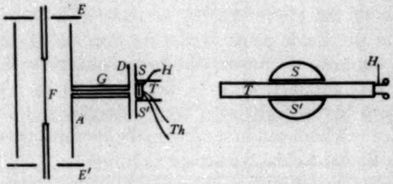

(a) (b)

Figure 2. Electrode system used in the measurements.

When the positive potential applied to the target was above that of the anode, only those secondary electrons emitted from the target with normal components of velocity sufficient to overcome the retarding potential difference were able to reach the anode, the remainder being returned to the target. In practice, therefore, a potential-difference of 150 v. between target and anode was sufficient to prevent the escape of all but a negligible fraction (probably less than 2 per cent) of the secondary electrons. This is illustrated by curve (b) in figure 3, which shows the variation of target current with target voltage, the anode voltage being fixed at 150 and the anode current maintained at 0·5 ma. by adjustment of the temperature of the filament *F*. It will be seen that the target current was constant for retarding potentials in excess of 100 v., indicating complete suppression of the secondary current. This limiting value of the target current was taken to be equal to the primary current over the range of voltages in which the field between anode and target was in such a direction that all the secondaries emitted from the target were drawn over to the anode, the secondary current in this region being therefore the difference between this and the observed current. The ratio of secondary to primary current, i.e. the secondary emission coefficient, was thus readily obtained.

To check that the primary target current was independent of the target voltage over the whole of the voltage range employed in the measurements, a separate experiment was carried out in which the target was replaced by an elongated cylindrical collecting-chamber 3·0 mm. in diameter and 40 mm. long. With an anode voltage of 150, the current to this collector, for various collector voltages, was as shown in figure 3, curve (*a*). This shows that the target current was independent of the target voltage to within 1½ per cent.

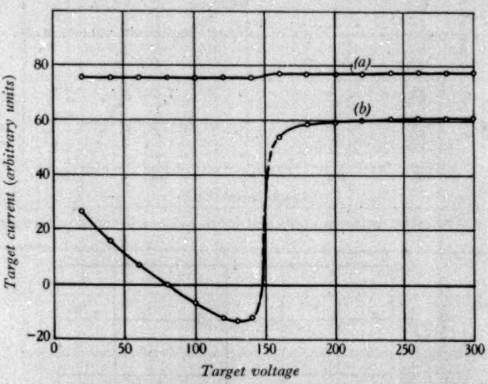

Figure 3. Variation of target current with target voltage.

On account of the imperfect insulation resistance of the heater coating at the higher temperatures employed, it was found necessary to supply the heating current from an insulated battery, the target being then connected to one end of the heater. All the measurements were made with sealed-off tubes containing barium getter.

In the first investigation the target was of nickel. This metal undergoes a magnetic transformation at 358° c. but has the same crystal structure at all temperatures. After a preliminary degassing for 1 hr. at a temperature of 1100° c., measurements of the secondary-emission coefficient were made as the temperature of the target was reduced from 525 to 110°. The results of these measurements, obtained with five different values of primary voltage, are shown in figure 4. There appears to be a slight and gradual change of secondary-emission coefficient with temperature, due probably to changes in the amount of gas adsorbed on the surface of the metal. No evidence was obtained, however, of any sudden change in the secondary-emission coefficient at the Curie point.

That no disturbing effect was produced by the magnetic field due to the heating current was proved by the fact that switching off the current during the cooling of the target produced no change in the secondary emission.

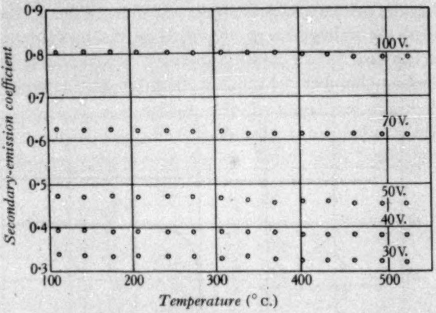

Figure 4. Secondary-emission coefficient for nickel as a function of temperature.

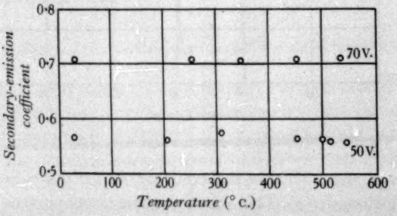

Figure 5. Secondary-emission coefficient for cobalt as a function of temperature.

The next metal studied was cobalt. The Curie point for cobalt is in the neighbourhood of 1150° C., and a change from a hexagonal lattice, which is stable at room-temperature, to a face-centred cubic lattice has been reported by a number of observers to occur at a temperature between 400 and 500° C. The exact temperature at which the transformation takes place is not definitely established; it probably depends among other things upon the purity of the sample of cobalt studied and upon the rate of cooling. In a recent work Marick(4) examined the structure of hot cobalt by X-ray diffraction and found the change to occur at about 490° C. during heating and at about 470° during cooling. The present experiments were concerned only with the structural change.

The cobalt was electrolytically deposited on to a nickel base to a thickness of about 0·05 mm. The target had been degassed before the assembly of the tube for 15 min. at 1000° C., and was subsequently heated to 1100° C. for a few minutes during the pumping. After the tube had been sealed off from the pump the latter treatment was repeated. Measurements of the secondary-emission coefficient were then made as the target-temperature was reduced in stages, 15 min. being allowed at each temperature for any possible time-lag in the occurrence of the transformation. As is shown in figure 5, there was no evidence of any appreciable change in the coefficient at any temperature from 20 to 340° C.

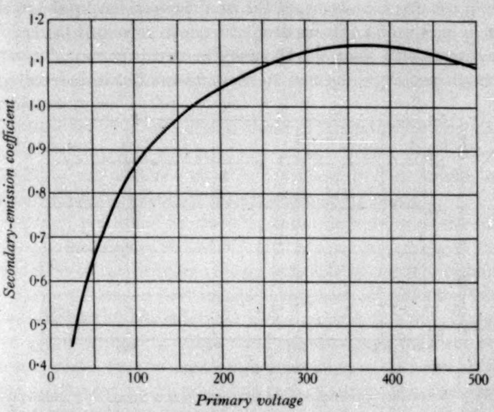

Figure 6. Secondary-emission coefficient for cobalt as a function of primary voltage.

Since there are few published data on the secondary-emission coefficient for cobalt, the curve of figure 6 is included in this paper. This gives the results of measurements of the coefficient, at room-temperature, for primary energies from 25 to 500 e.-v. Before taking these measurements the target was subjected to a further degassing at 1100° for 1 hr.

§ 4. STUDY OF IRON

In the study of iron the method of measuring secondary emission from filaments described in a previous paper by one of us$^{(5)}$ was employed. This method was not used in the case of nickel and cobalt on account of the difficulty of accurately measuring very low filament-temperatures, but it was particularly suitable in the case of iron where a higher range of temperatures was required.

The target filament was of soft iron and had a length of 50 mm. and a diameter of 0·12 mm. The cathode was 12 mm. in length, and as it was run at the temperature required to give a total emission of 0·5 ma., its effective emitting portion, on account of the end cooling, was probably not more than a 5 mm. length at its centre. The portion of the target filament subjected to electron bombardment was therefore also limited to a short length at its centre over which, under the conditions of operation, its temperature could be considered constant.

To avoid the possibility of contamination of the target by the evaporation of tungsten from the cathode, care was taken to avoid heating the cathode to a temperature higher than that necessary to give a space current of 0·5 ma. at any stage of the experiments. (The cathode filament had, however, been cleaned by flashing before the assembly of the tube.) Under these conditions a calculation showed that there was no possibility of contamination of the target occurring in this way.

In carrying out the measurements, the iron filament was heated to the required temperature by means of a current derived from an insulated battery. There was, of course, a potential-fall along the filament due to this current, but on account of the short length actually subjected to electron bombardment the potential-fall along the effective length of the filament was never more than 0·2 v. The target was shunted by a high resistance, to the centre point of which the high-potential lead was connected; with this arrangement the primary voltage remained unaffected by changes in heating current through the target. A separate experiment was carried out to determine the temperature of the iron filament in terms of the heating-current through it. In this experiment an iron filament of the same length and diameter as that used in the secondary-emission measurements was mounted in a bulb together with an indirectly-heated iron cylinder in such a way that the centre of the filament could be matched for brightness against the cylinder in the background. The temperature of the cylinder was measured by an attached thermocouple, and the temperatures of the filament and of the cylinder were taken to be equal when the filament disappeared against its background.

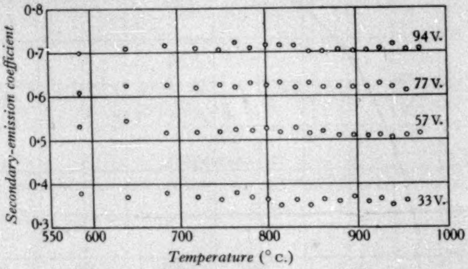

Figure 7. Secondary-emission coefficient for iron as a function of temperature.

The Curie point of iron is 770° c. and the transformation from a body-centred to a face-centred cubic lattice takes place at about 906° c. Both transformation points were included in the range of temperatures covered. In the carrying out of the experiment the target-temperature was first raised to 1000° c. for a few minutes for degassing purposes, and then maintained at 800° for 20 min. to ensure the transformation to the body-centred structure. The temperature was then reduced to 585° and measurements were made as it was raised in steps to about 950°. The results of these measurements are depicted in figure 7. It is clear that there is no appreciable change in the secondary-emission coefficient either at the Curie point or at the temperature at which the structural change occurs.

§ 5. CONCLUSION

The accuracy of the foregoing measurements was such that a change of 5 per cent in the secondary-emission coefficient either at the Curie point (for nickel and iron) or at the temperature of the crystalline transformation (for cobalt and iron) would have been apparent. From the fact that no such changes were detected it must be concluded that such transformations have no significant influence on the secondary-emission phenomenon.

These findings are in contrast with those of Tartakowsky and Kudrjawzewa and of Hayakawa referred to earlier in the paper. Reasons have, however, been given for doubting the evidence upon which those authors sought to prove the existence of discontinuous effects at the transformation points.

A further paper, published by Davis(6), has some bearing on the subject of the present investigation. Davis, in a study of the secondary-emission coefficient of cobalt as a function of the primary voltage, was able to obtain a stable and reproducible curve after prolonged heating at a yellow heat. If, after this condition had been achieved, the target was raised for a few minutes to a temperature near the melting point of cobalt (during which rapid evaporation of the metal occurred), an entirely different curve was obtained. Further heating at the previous temperature failed to cause a reversion to the preceding type of curve. The measurements were made with the target cold in all cases.

In attempting to explain this peculiar behaviour, Davis suggested that the appearance of the second form of curve might have been associated with a change from the face-centred to the hexagonal structure when the temperature was raised above 1150° C., a change for which there was a certain amount of evidence from other sources. Now, firstly, if there were such a reversion to the hexagonal structure above 1150°, it would be surprising if it were not reversible; that is to say, on the lowering of the temperature again into the 490–1150° region the metal would be expected to return to the face-centred cubic structure. Secondly, the evidence of Marick(4), who worked up to a temperature of 1187° C., suggests strongly that the reported change of structure at 1150° does not in fact exist.

A different explanation must therefore be sought for the phenomenon observed by Davis. It seems not unlikely that the diminution of secondary emission which he found after the high-temperature treatment may have been the result of etching of the surface produced by evaporation of the metal, for it is known that the effect of roughening the surface of a metal is to reduce its secondary emission.

§6. ACKNOWLEDGEMENT

The authors desire to tender their acknowledgement to the Marconiphone Company and the General Electric Company on whose behalf the work was done which has led to this publication.

REFERENCES

(1) Tartakowsky, P. and Kudrjawzewa, W. *Z. Phys.* **75**, 137 (1932).
(2) Hayakawa, K. *Sci. Rep. Tôhoku Univ.* **22**, 924 (1933).
(3) Richardson, O. W. *Proc. Roy. Soc.* A, **128**, 64 (1930).
(4) Marick, L. *Phys. Rev.* **49**, 831 (1936).
(5) Treloar, L. R. G. *Proc. Phys. Soc.* **48**, 488 (1936).
(6) Davis, M. N. *Proc. Nat. Acad. Sci.* **14**, 460 (1928).
(7) Kollath, R. *Phys. Z.* **38**, 202 (1937).

Figure 1.

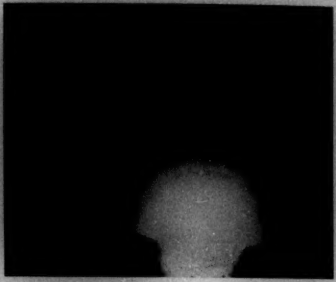

Figure 2.

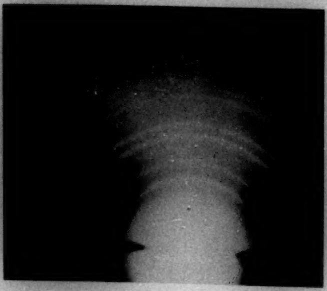

Figure 3.

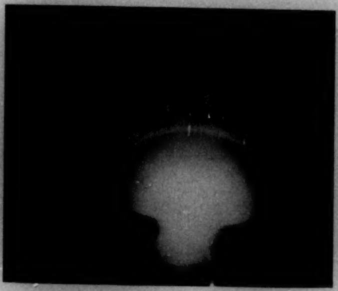

Figure 4.

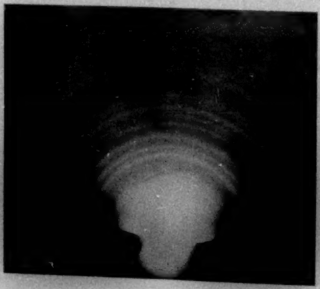

Figure 5.

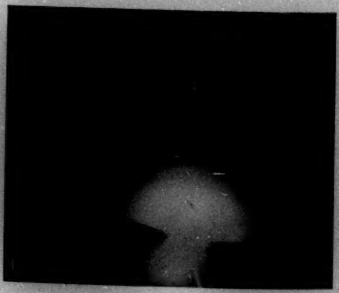

Figure 6.

To face page 635

DIFFRACTION OF ELECTRONS BY OXIDE-COATED CATHODES

BY JAMES A. DARBYSHIRE, M.SC., PH.D., A.INST.P.
Research Department, Ferranti Ltd., Moston, Manchester, 10

Received 3 *May* 1938. *Read in title* 24 *June* 1938

ABSTRACT. Electron-diffraction methods have been used to examine the surfaces of thermionic oxide-coated cathodes. The nickel cathodes were coated with a paste containing a solid solution of barium and strontium carbonates, and the diffraction camera was fitted up with ovens so that getter pellets could be fired off at suitable stages during the activation. These cathodes, after activation by heat treatment to give good emission, gave patterns of strontium oxide alone when no getter had been fired off, but gave patterns of magnesium oxide along with strontium oxide when the getter pellet (barium-magnesium alloy) had been fired off during the activation. Cathodes consisting of barium carbonate alone before activation gave patterns of barium oxide after activation, whereas cathodes consisting of strontium carbonate gave patterns of strontium oxide after activation.

§1. INTRODUCTION

In an earlier paper by Gaertner(1) it was pointed out that if oxide cathode surfaces are examined by means of X rays the depth of penetration of the rays is so great that the photographs do not give information about the active surface layers, but give the general composition of the cathode coating.

An X-ray examination has been carried out by Benjamin and Rooksby(2). The cathodes were activated in a high vacuum and the X rays were passed on to the cathode through thin-walled glass tubes. Thus the X-ray diffraction patterns were obtained without exposing the cathodes to air. Benjamin and Rooksby found that the activated layers consisted of mixed crystals of strontium oxide and barium oxide and that the proportion of barium oxide diminished if the cathodes were overheated, the emission having a maximum value corresponding to a cathode composition of approximately 60 per cent of strontium oxide and 40 per cent of barium oxide. They did not hope to find evidence on the presumably monatomic layer of alkali-earth metal on the cathode surface, which has often been considered to be responsible for the high emission that can be obtained from suitably activated cathodes.

Gaertner then repeated the experiments using electrons instead of X rays, and the detection of such a thin surface layer of barium became much more probable. Gaertner did not find any evidence for the existence of the barium layer; moreover his results differed from those obtained by Benjamin and Rooksby in that he obtained good patterns of strontium oxide by reflection from the cathode surface and little or no definite evidence of barium oxide.

It is known that barium oxide leaves the cathode by evaporation more readily than strontium oxide, and Gaertner came to the conclusion that the outer surface of a normally activated cathode losses its barium oxide component almost immediately, and strontium oxide remains predominant. Gaertner also obtained some hexagonal and tetragonal patterns. The hexagonal patterns, which appeared when the vacuum had not been good, remained unexplained. The tetragonal patterns were attributed to hydroxides of barium and strontium, and were found when the emission had been lost as a result of presence of water vapour.

The present work is a repetition of Gaertner's, under rather better vacuum conditions. It has been carried out in the hope of detecting the layer of barium on the surface and also to see if Gaertner's evidence for the apparent absence of barium oxide could be corroborated. The effect of getter-firing also has been investigated, and the contamination of the cathode-emitting surface due to it has been examined. The active surface of homogeneous single emitters, such as strontium oxide and barium oxide alone, has also been examined by electron-diffraction methods.

§2. APPARATUS

The electron-diffraction camera was of the Finch(3) type, and for most of the work a gas discharge tube, fed from a hydrogen supply through an adjustable leak, was used as the source of electrons. A thermionic hot-wire cathode was used also. This is more difficult to control and gave the same results as the gas discharge in hydrogen.

At first a good many attempts were made to obtain patterns from standard valve cathodes such as those used for the output pentode. This cathode is 3 mm. wide and 40 mm. long and was mounted so that the beam passed across the surface of the cathode in a direction parallel to the 3·0 mm. edge. However, no patterns of any value at all could be obtained in either the fresh or the activated state. These cathodes had been coated with the mixed barium and strontium carbonates by means of the aerograph spray gun, as used for valve-production. The next step was to increase the width of the cathode so that more of the cathode surface would present itself to the electron beam. The cathodes were made progressively wider until, when they were approximately 1 cm. wide, some type of pattern began to appear. The patterns were still very poor, however, until the spray method of coating was abandoned. It was found that much better photographs could be obtained if the carbonate suspension was allowed to drop on to the cathode from the tip of a glass rod. The cathode was then tilted up and down, so that the mixture could run all over the surface, and then the cathode was put away with the surface arranged in a perfectly horizontal plane, so that the mixture could dry to a uniform depth over its surface. If too much suspension was placed on the cathode, it took longer to dry, the surface was fairly rough, and poor photographs were obtained. Microscopic examination indicated that spraying, under various conditions, always gave a much rougher surface than the flow method. Rather thicker carbonate mixtures had to be used when the flow method was adopted.

The cathode, in its final form, consisted of a built-up nickel block, the active face being sheet nickel 0·5 mm. thick. The back face was made up of nickel sheet 0·150 mm. thick. These sheets both measured 10 mm. by 30 mm., and they were welded to the support wires of an ordinary valve stem, one sheet on each side. The space between the nickel sheets was filled up with ceramic insulators of the kind used in certain types of indirectly heated valve cathodes. Tungsten wires were threaded through the ceramics and connected up in series. The normal rating for such a cathode inside the diffraction camera at a temperature of approximately 800° C. would be 35 V., 1·5 amp.

The anode was a sheet of nickel, a little larger in area than the cathode, and was mounted on the same stem as the cathode and situated approximately 7 mm. from the active surface. The cathode lead and one of the heater leads were joined together and earthed to the diffraction camera. The other heater lead and the anode leads were brought out of the apparatus through insulated tubes of glass sealed with white wax of high melting point.

Another side flange on the apparatus carried a glass tube through which two pairs of thick-gauge wires were taken. These were attached, inside the camera, to two tungsten spirals which carried small quartz ovens. The tungsten wire was strong enough to hold the small quartz tube without any additional support. Two Kemet (barium-magnesium) getter pellets of standard type were placed in these ovens just before the apparatus was evacuated at the beginning of an experiment, and the getters could be fired off as desired during the processing and activation of the cathode.

§3. RESULTS

The carbonate mixture. The photographs of the unactivated cathodes were never very good, and different degrees of ball-milling made very little difference. The measurements of the principal lines were, however, quite consistent, and these are given in table 1 A photograph of the unactivated cathode is reproduced in figure 1.

Table 1. Unactivated carbonates; values of d/n (A.)

m	2·09
m	1·85
w	1·61
w	1·44
m	1·29
w	1·18
w	1·04
w	0·95

The material used was actually a solid solution of barium and strontium carbonates—containing approximately 57 per cent of barium carbonate and 43 per cent of strontium carbonate, and a calculation of the spacing of these carbonates gives so many values of d/n near to those in table 1 that it is useless to attempt to accord indices to the reflections observed. A further examination of cathodes coated initially with a mechanical mixture of approximately equal parts of barium carbonate and strontium carbonate is in progress.

The activated cathode. The cathode was then heated at a temperature of 1000° c. for four minutes. In some cases the activation was carried out by heat treatment only; in other cases additional activation was given after the heat treatment by drawing a current from the cathode at 800° c. for ten minutes. After activation the cathode was allowed to cool down to approximately 50° c. and a photograph was taken. The ring pattern was usually visible on the fluorescent screen, and so the cathode could be set at the best angle for reflection.

In many cases, when no getter had been fired off in the tube, the patterns were due to strontium oxide, but slight traces of other components could sometimes be seen. The measurements from such a pattern are given in table 2, along with the calculated values for strontium oxide in column 2. Column 3 gives the spacings found by Gaertner in the paper already referred to. A photograph of an activated layer is reproduced in figure 2.

Table 2. Activated cathode with no getter-firing; values of d/n (A.)

Activated cathode	Strontium oxide (calculated)	Gaertner
2·935	2·973	2·95
2·535	2·575	2·545
1·810	1·821	1·82
1·545	1·522	1·545
1·483	1·487	1·48
1·272	1·287	1·28
1·169	1·15	1·15
1·054	1·052	1·04
0·990	0·991	—
0·910	0·910	0·904
0·865	0·871	0·855

The patterns of strontium oxide, for which measurements are given in table 2, were obtained without firing any getter, and emission was quite good. The spacings agree so closely with those of strontium oxide that there is no evidence for a solid solution of the mixed oxides of strontium and barium. In some cases a number of extra lines appear and the patterns are so complex that a direct interpretation is not possible. In the later experiments, where getters were fired before and after activation, some excellent and well-defined patterns were obtained. A typical pattern of this type is reproduced in figure 3. Measurements from this pattern are given in table 3, and the values of d/n for barium, strontium, barium oxide are also given in columns 3, 4 and 5 respectively. It is evident that the pattern cannot be attributed to any of these substances. This type of pattern was obtained only when the Kemet getter (barium-magnesium alloy) had been fired within the tube. This pattern can be easily identified as that of magnesium oxide, and is found when the barium-magnesium getter cleans up the vacuum. A reflection photograph of magnesium oxide is reproduced in figure 4.

The cathode emission does not appear to drop in the least in consequence of this layer of magnesium oxide. A cathode was then sealed up on a standard valve pinch and activated on a bench pump. After activation the getter was fired and then the assembly was sealed off; it was later broken open and fixed in the diffraction camera for examination. A good pattern of magnesium oxide was again obtained, resembling in all respects that given by the cathodes which had been activated in the diffraction apparatus. It seems that the normal cathodes will also have a surface layer of magnesium oxide, as received from valve production, and so it was considered desirable to examine the emission from cathodes (Ferranti type D 4) specially coated with magnesium oxide in various ways. From a layer of magnesium oxide sprayed over the standard emitting surface (1 mg. per cm.^{2}), the total emission under specified conditions was 60 ma.; with magnesium oxide alone on cathode, it was 0·25 ma.; with magnesium oxide mixed in equal parts with the standard cathode spray it was 40 ma.; with the standard spray without any contamination by magnesium oxide it was 240 ma. These results indicate that any appreciably thick layer of magnesium oxide can seriously lower the cathode emission.

Table 3. Activated cathode with getter firing; value of *d*/*n* (A.)

Activated cathode after getter firing	Magnesium oxide	Barium	Strontium	Barium oxide
2·465	2·430	3·540	3·508	3·193
2·090	2·100	2·506	3·038	2·765
1·485	1·485	2·048	2·148	1·955
—	—	1·774	1·832	1·667
1·200	1·215	1·586	1·754	1·596
1·046	1·050	1·449	1·519	1·382
—	—	1·341	1·394	1·269
0·935	0·938	1·254	1·358	1·237
0·845	0·856	1·183	1·240	1·129
—	—	1·120	1·169	1·064
—	—	1·069	1·074	0·977
—	—	1·023	1·027	0·935

There is no doubt that on the normal valve assembly the cathode is not exposed to the direct path of the getter particles, and so the deposition of magnesium oxide would not be very great. There is every chance, however, that the cathode may receive some slight contamination from magnesium oxide, especially if the valve is very gassy before the getter is fired off. It must be remembered that in our experiment with the bench-pumped cathodes the bulb had to be broken open just before use, and if there was a deposit of metallic magnesium it would certainly oxidize to give magnesium oxide. The experiments do indicate, however, that the getter gives contamination, and our experiments in the diffraction chamber, where the contamination is certainly magnesium oxide, make it appear that it would also be magnesium oxide originally in the bench-pump evacuation. The bench-pump vacuum before getter-firing would not be as good as that in the diffraction chamber.

When this magnesium-oxide layer has appeared it cannot be removed by the most elaborate flashing schedules. The magnesium-oxide patterns are merely improved by reheating, and if the specimen is exposed to air after cooling down again the pattern is still magnesium oxide, even before any reheating. The pattern is definitely weaker and rather more diffuse after an exposure to atmospheric conditions, but it returns to its original type when reactivation is carried out.

On one occasion a different pattern was observed after getter-firing. This was carried out with the cathode coated with carbonates, but not heated at all. The surface remained unaltered after several exposures to air and gave a very sharply defined pattern of rings, figure 5. The cathode was of a rather dull metallic grey appearance, as opposed to the white surface previously observed. The material could not be barium or magnesium because of its stability in air, and was proved not to be magnesium oxide or barium oxide by measurement of d/n. So far, these rings are not understood. After the cathode had been heated up in vacuo and activated the pattern disappeared and became that of magnesium oxide. This took place without any additional getter-firing, and the material itself must have contained magnesium in some form.

Strontium carbonate alone. When the cathodes were coated with strontium carbonate alone, the patterns originally were poor, just as in the case of the mixture of barium and strontium carbonates. After activation the pattern of strontium oxide was plainly visible, provided no getter was fired, figure 6. If the getter was fired the pattern was that of the usual magnesium oxide + strontium oxide. If the cathodes were shielded from the getter beam the patterns were sometimes of strontium oxide and sometimes of strontium oxide + magnesium oxide. The emission from pure strontium-carbonate cathodes was, of course, very low. The following figures were taken from actual valve assemblies, to show the relative difference in the emission values of strontium oxide and barium oxide.

Table 4. Relative emission (ma.) under standard conditions

Barium carbonate	50
Strontium carbonate	9
Suitable mixture	170

Barium carbonate alone. Cathodes were coated with a barium-carbonate mixture and the patterns just after coating were very poor. After activation the patterns were not nearly as good as those from strontium carbonate, but in some cases they were good enough to allow the material to be identified as barium oxide. The emission from these cathodes was much better than that from the strontium-carbonate cathodes, in accordance with the figures given in table 4.

During experiments with very thin cathode coatings, it was suspected that nickel-oxide lines made their appearance during activation. This was later found not to occur, but while the matter was being investigated a rather interesting experiment was carried out on standard valve-production schedules. The cathodes of some output pentode valves of the Ferranti type PT 4D were oxidized to a pale blue colour by heating in air prior to their being sprayed with the mixed carbonates. These valves were assembled and were then given the normal production schedule for their type. After standard ageing, they showed about three times the normal softness current. They were re-aged and a little more getter was fired off; then they were within the recognized limits of hardness and the emission was quite up to the normal standard. These experiments with nickel oxide are hardly parallel to those carried out with magnesium oxide earlier, but they indicate that appreciable oxidation of the nickel base is not a serious matter.

The nickel-oxide rings were normal and did not give the extra reflections sometimes reported. This was true even if the oxidation was carried out in the highest vacuum obtainable consistently with oxidation of the surface.

§4. SUMMARY AND CONCLUSIONS

Gaertner reported some special patterns of hexagonal type when the cathode was partially poisoned by activation in a poor vacuum. He also reported a tetragonal structure when the cathode had been activated in a trace of moisture and completely poisoned. In some cases patterns were obtained in the present research which could not be explained in terms of known structures, but patterns corresponding to Gaertner's hexagonal and tetragonal types were not seen.

In general, however, Gaertner's conclusion that the activated oxide cathode presents a surface layer of strontium oxide has been verified. Gaertner's unactivated carbonate coating consisted of a mechanical mixture of the barium and strontium carbonates, whereas in the present research the carbonate was a solid solution of barium and strontium carbonates. In both cases, therefore, it appears that the final activated cathode has a surface layer of strontium oxide which presumably rests upon a solid solution of barium and strontium oxides, as was found by X-ray examination by Benjamin and Rooksby(2).

As regards the monatomic layer of barium postulated by Becker and Sears(4), we must remember that even if this layer were present it would not give an ordinary barium pattern. It would give either a typical two-dimensional grating pattern or a diffuse liquid pattern, according as the arrangement of barium atoms was regular or random. Now the lattice constant of strontium oxide is 5·150 A. and that of barium is 5·015 A., and so it is possible that the barium could be attached to the strontium-oxide lattice by linkage to the oxygen atoms of the strontium-oxide structure. If this were the case the adsorbed barium atoms would be virtually part of the strontium-oxide lattice and merely modify very slightly the intensity of the reflections from the strontium-oxide spacings, and its presence would be very difficult to detect even by electron-diffraction methods. If it were adsorbed in this way it would presumably be ionized and have a larger interatomic distance than would be natural for its ionic state, and the resultant surface field could perhaps give rise to the low work function and consequent high thermal emissivity of oxide-coated cathodes.

§5. ACKNOWLEDGEMENTS

In conclusion, I should like to thank Ferranti Ltd. for providing facilities for this research and for permission to publish the results. In particular my thanks are due to Mr A. L. Chilcot for many helpful suggestions and discussions.

REFERENCES

(1) Gaertner, H. *Phil. Mag.* **19**, 82 (1935).
(2) Benjamin, M. and Rooksby, H. P. *Phil. Mag.* **15**, 810 (1933) and **16**, 519 (1933).
(3) Finch, G. I. General discussion of the Faraday Society, September 1935. (Gurney and Jackson.)
(4) Becker and Sears. *Phys. Rev.* **38**, 2193 (1931).

THE FLASHING CHARACTER OF AERODROME FLOODLIGHT BEACONS

By W. M. HAMPTON, Ph.D., B.Sc., F.Inst.P.
AND
J. G. HOLMES, A.R.C.S., B.Sc., D.I.C., F.Inst.P.
Research Laboratory, Chance Brothers and Co. Limited

Received 22 *October* 1937. *Read* 2 *June* 1938

ABSTRACT. A simple mathematical method is developed for calculating the frequency of the flash, and the distribution of intensity during the flash, when a floodlight is tilted and rotated so as to form a flashing beacon. The results of a number of typical calculations are given as diagrams and these may be used to estimate the results given by other distributions and conditions which would not be so readily calculated. Comparison is drawn between the various methods of tilting and the ideal requirements of an airway beacon.

§1. INTRODUCTION

An aerodrome floodlight consists of an optical system so arranged as to emit light in a beam of narrow vertical divergence and wide horizontal divergence. Its purpose is, as its name implies, to illuminate the surface of an aerodrome to facilitate night landings.

An aerodrome beacon is intended to draw the attention of a distant pilot and to inform him of the name and position of the aerodrome which he is approaching. It has a flashing character which may be a distinctive Morse letter or may be only a regular flash similar to that of many marine lighthouses. It differs from a lighthouse in that it must give its indications in three dimensions, and it may consist either of a network of discharge tubes or of an optical system rotating about a vertical axis and projecting a beam whose intensity is high in the horizontal direction, with diminishing intensity up to about 20° above the horizontal. In the latter case, the intensity is usually so distributed that a pilot approaching the beacon at some given height and in some given state of the weather will receive substantially constant illumination after he has come within range of the beacon.

For reasons of economy, it is sometimes desired to make one apparatus serve for both purposes. The optical requirements for a floodlight are much more stringent than those for a beacon, and so the problem becomes that of finding the most efficient way of employing a typical floodlight apparatus as an aerodrome beacon. This paper is not concerned with either the type of floodlight or the mechanical details of mounting, but deals solely with the optical and geometrical aspects of the problem.

The obvious way of converting the floodlight to a beacon is to tilt it so that the beam becomes an elevated sheet, and then to rotate it about a vertical axis so that the whole azimuth is swept by the beam during one revolution and a flashing character is imparted. Three systems of tilting have been used in this country, but hitherto no details of the type of flash resulting from each have been computed. The three methods are: (I) tilting about an axis normal to the direction of maximum intensity—the general practice until 1932; (II) tilting about the direction of maximum intensity (British patent 426,222); (III) tilting about an axis inclined to the direction of maximum intensity (British patent 452,933).

This paper discusses the effects of these three methods and their compliance with the relevant requirements for a beacon, which are (*a*) that the beam-intensity should be a maximum along the horizontal, falling progressively as the elevation of the observer increases, with little or no light above 20° from the horizontal and (*b*) that the character of the flash—i.e. its duration and periodicity—should be independent of altitude. There are, of course, other requirements for a beacon, but these are not fundamental to an investigation of flash characteristics.

§ 2. THE GENERAL CASE OF A TILTING BEAM OF WIDE HORIZONTAL AND NARROW VERTICAL DIVERGENCE

Consider a very thin sheet of light emitted by an aerodrome floodlight at an angle β above the horizontal. This light lies on the surface of a cone whose semi-angle is $\pi/2-\beta$, whose axis is vertical and whose equation is:

$$z=\tan\beta\,.\,\sqrt{(x^2+y^2)} \qquad \text{......(1).}$$

Similarly, for light emitted at a divergence of $-\beta$, there will be a conical surface below the horizontal, which is given by the negative values of z in equation (1).

If the double cone be now tilted so that its axis is at an angle δ to the vertical OZ and lies in the XZ plane, the equation to the surfaces becomes

$$(z-x\tan\delta)^2-y^2\tan^2\beta\sec^2\delta=(z\tan\delta-x)^2\tan^2\beta \qquad \text{......(2).}$$

Reference should be made to figure 1, which illustrates the angles involved. This equation may be used either to define the limits of a beam, where β corresponds to the maximum divergence, or may be used to calculate the position of an elementary sheet of light at an angle β within the beam.

A pilot poised at an angle γ above the horizontal receives the same intersection of a rotating beam as he would see by flying in a circle round a vertical axis through the beacon while it is stationary. His course would be given by

$$\left.\begin{aligned} x&=\sin\theta\\ y&=\cos\theta\\ z&=\tan\gamma \end{aligned}\right\} \qquad \text{......(3),}$$

where the radius of his course is unity and θ is his horizontal angular position with reference to the Y axis.

Substituting (3) in (2) and solving for θ, we have

$$\sin\theta=\tan\gamma\cot\delta-\sec\gamma\sin\beta\,\mathrm{cosec}\,\delta \qquad \text{......(4).}$$

Alternatively, solving for β, we have

$$\sin \beta = \cos \gamma \cos \delta \, (\tan \gamma - \sin \theta \tan \delta) \qquad \text{......(4a)}.$$

Equation (4) gives two solutions for θ and $(\pi - \theta)$ corresponding to the four values of the angle in the horizontal plane which are the projections of the pilot's position when he enters and leaves the tilted beam. These solutions apply to the three types of floodlight beacon, since no restrictions have as yet been applied to the distribution of intensity.

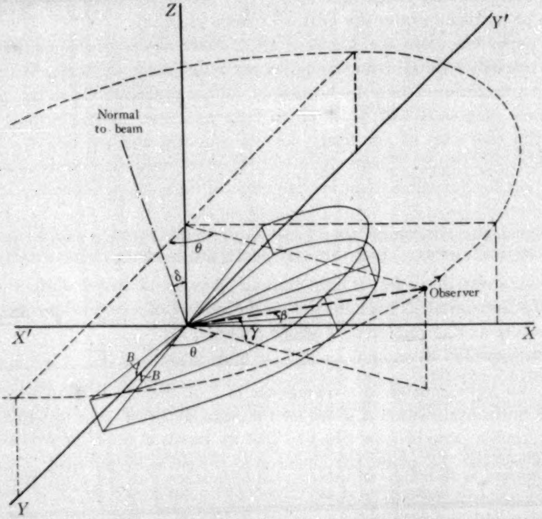

Figure 1. Isometric drawing of tilted beam.

§ 3. THE DISTRIBUTION OF LIGHT IN THE BEAM

The horizontal polar distribution of intensity (candle power) of certain types of floodlight may be represented sufficiently closely by the relation

$$I' = I_0 \cos \phi \qquad -\pi/2 < \phi < \pi/2 \qquad \text{......(5)},$$

where I' is the horizontal intensity at an angle ϕ away from the maximum intensity I_0. Various floodlights will have other distribution curves, but it has been found that all types which are suitable for tilting as beacons have distribution curves which lie between those represented by equation (5) and the following equation

$$I' = I_0 \cos^2 \phi \qquad -\pi/2 < \phi < \pi/2 \qquad \text{......(5a)}.$$

The two equations are shown graphically in figures 2*a* and 3. It will be seen later that the difference between these two limiting curves has only a small effect on the distribution in the tilted beam, and no effect on the flashing character of the beam.

The polar distribution in the vertical section of the beam at any value of ϕ is represented closely by the relations

$$I = I' \cos^2 (\pi\beta/2B) \qquad -B < \beta < B \qquad \text{......(6)},$$

where I is the intensity at (ϕ, β) and B is the vertical semidivergence of the beam at ϕ. This is shown in figure 2*b*. For purposes of calculation it is permissible to assume that B is independent of ϕ. The whole polar distribution of intensity from this floodlight is then given by the relation

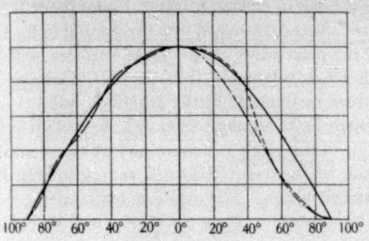

Figure 2 *a*.

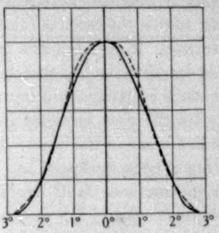

Figure 2 *b*.

Figure 2 *a*. Horizontal distribution of intensity. —— $\cos\phi$, equation (5); ·—·—· $\cos^2\phi$, equation (5 *a*); ——— 10 kw. lens floodlight; - - - - 9 kw. G.E.C. mirror floodlight.

Figure 2 *b*. Vertical distribution of intensity. ——— $\cos^2 (\pi\beta/2B)$, equation (6); - - - - 10 kw. lens floodlight.

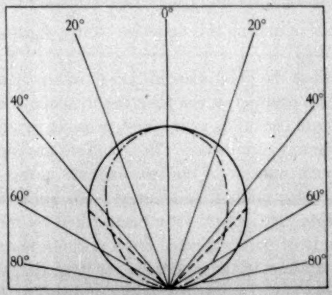

Figure 3. Horizontal polar distribution of intensity.
——— cosine, equation (5); - - - restricted cosine; —·— $\cos^2$, equation (5 *a*).

$$I = I_0 \cos\phi \cos^2 (\pi\beta/2B) \qquad -\pi/2 < \phi < \pi/2, \quad -B < \beta < B \quad \text{......(7)}.$$

Using equation (5 *a*) instead of equation (5), we may write the polar distribution of the $\cos^2$ type as follows

$$I = I_0 \cos^2\phi \cos^2 (\pi\beta/2B) \qquad -\pi/2 < \phi < \pi/2, \quad -B < \beta < B \quad \text{......(7}a\text{)}.$$

The restricted-cosine distribution is given by equation (7) with limits

$$-\pi/4 < \phi < \pi/4.$$

§4. APPLICATION OF THE THREE METHODS OF TILTING

In § 2 the general case of the tilting of a beam occupying 360° in azimuth has been considered. Equation (5) shows how the light from an actual floodlight only extends over 180° in azimuth and how the intensity in this region varies. The tilting represented by equation (2) applies to elevation of the beam about OY as axis, so that the beam is raised above OX and depressed into the ground in the OX' direction. It only remains to draw the polar curve on the tilted surfaces, with the peak intensity in the appropriate direction relative to OY, the axis of tilting, and the same equations will represent three methods of tilting described in § 1.

Let the peak intensity of the beam be at an angle α to OY, measured in the median plane of the beam. The value of this angle is determined by the method of tilting to be investigated and its values will be respectively $\pi/2$, zero or intermediate for the methods I, II or III described above. The relation between the polar coordinates ϕ and β of the ray seen by an observer at an elevation γ may be reduced to

$$\sin\gamma = \sin\beta\cos\delta + \sin\delta\cos\beta\sin(\phi+\alpha) \qquad \text{......(8).}$$

Assuming β to be small, we may write $\cos\beta$ as unity and the combination of equations (4*a*) and (8) will lead to

$$\sin(\phi+\alpha) = \sin\gamma\sin\delta + \cos\gamma\cos\delta\sin\theta \qquad \text{......(9).}$$

Less error is introduced in solving this equation from 4-figure tables than in solving equation (8).

Equation (7) describes the polar distribution of intensity and equation (9) gives the relation between the position of the observer in space and his position relative to the polar coordinates of the beam, so it is now possible to write down the intensity which he receives under any conditions. The equations are capable of exact solution but this is laborious and, in view of the approximate nature of equation (7), it is preferable to use a tabular method of solution. An abbreviated example of the calculation for the cosine distribution for a beam tilted by method III is shown in the appendix, the family of curves plotted from it being shown as figure 4*c*. The order adopted for the solution of the equations has been first to choose a value for δ and to solve equation (4*a*) for β at integral values of θ and γ. All values of β greater than a chosen value of B are neglected, and the limiting values of θ where $\beta = B$ give the flash-duration at each value of the elevation γ. The second stage has been to solve equation (9) for ϕ over the range of θ appropriate to each value of γ, and with the chosen value of α to represent the method of tilting. Finally, the above values of β and ϕ are inserted in equation (7) to give the intensity seen by a pilot under the conditions corresponding to the chosen values of θ, γ, δ and α. By plotting this intensity against θ at each value of γ, a family of curves is obtained for each case of δ and α, representing both the distribution of intensity throughout the duration of each flash and also the flashing character of the beacon at the various angles of elevation. The case worked out in the appendix and figure 4*c* is for method III where $\alpha = \pi/6$, the beam is elevated to $\delta = 20°$, and the value of the semi-

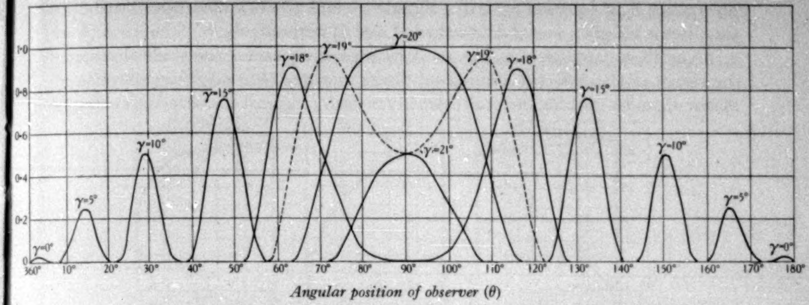

Figure 4 *a*. Distribution of intensity during flash received by observer. Method I. Elevation of observer γ; angle of tilt $\delta=20°$; direction of peak $\alpha=\pi/2$.

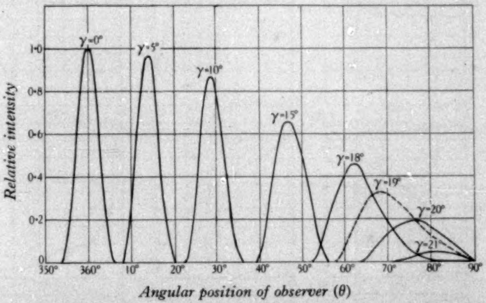

Figure 4 *b*. Distribution of intensity during flash received by observer. Method II. Elevation of observer γ; angle of tilt $\delta=20°$; direction of peak $\alpha=0$.

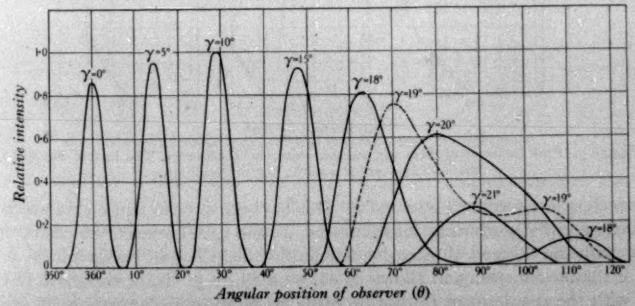

Figure 4 *c*. Distribution of intensity during flash received by observer. Method III. Elevation of observer γ; angle of tilt $\delta=20°$; direction of peak $\alpha=\pi/6$.

divergence B in equation (7) is 2°. Figures 4a and 4b show the cosine distribution for a beam tilted to $\delta = 20°$ by methods I and II respectively.

Even these families of curves are somewhat complex for ready visualization of the merits of the different methods of tilting, and a further stage has been to summarize them by plotting the peak intensity in flash I' against the observer's elevation

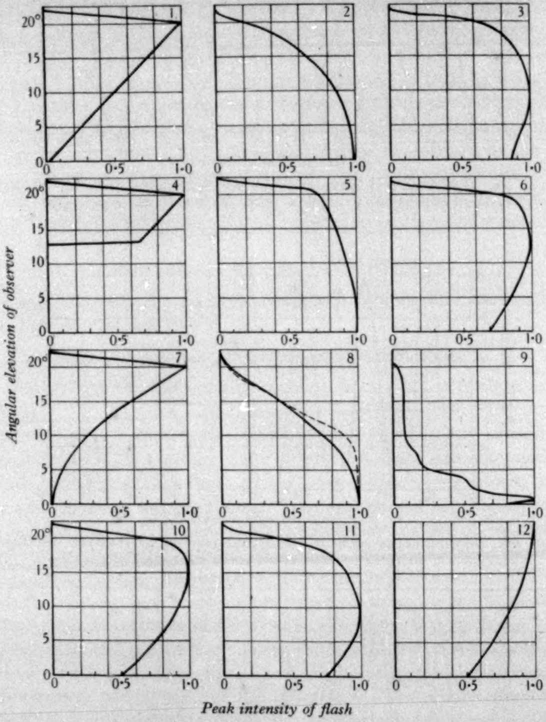

Figure 5. Peak intensity of flash and angular elevation of observer. The broken line gives the distribution for a 9-kw. mirror floodlight.

γ for each case determined by δ and α. This has been done in figure 5, in which the top line gives the summaries for figures 4a, 4b and 4c. These curves can be compared with the theoretical intensity-distribution described in paragraph (a) at the end of the introduction and shown as no. 9 on figure 5. The comparison of each case with the requirement (b) can be made by plotting flash-duration $\Delta\theta$ against elevation γ for each method of tilting as in figure 6.

It will be obvious that the effectiveness of a flash received by the observer will be determined by more factors than just the peak intensity and the gross duration. For a short flash the intensity is integrated by the eye over the duration of the flash, but knowledge of the mechanism of this integration is insufficient to enable us to carry the analysis to that stage. The effect of flashes which commence and end abruptly is known⁽¹⁾ for a range of illuminations from the threshold up to comparatively high levels, and van Vloten⁽²⁾ has derived a method of integrating flashes which have a trapezoidal distribution of intensity. It is, however, customary to describe a flash in terms of its peak intensity and of its gross duration, and this description is therefore retained in the present paper.

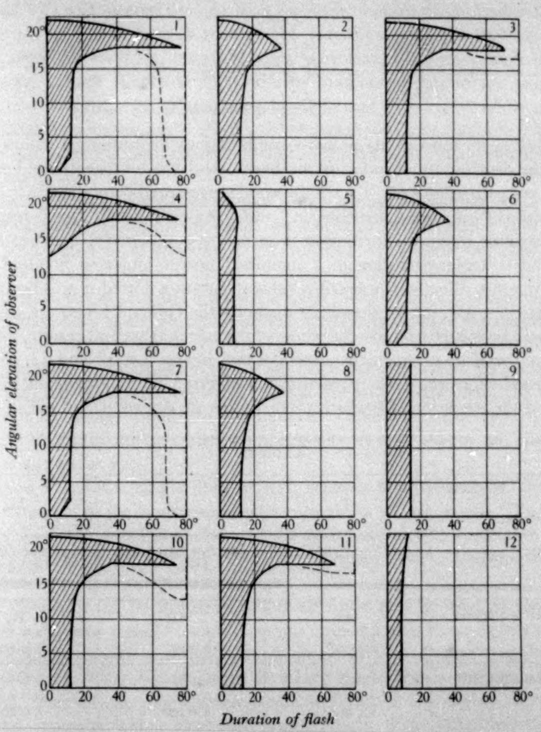

Figure 6. Duration of flash and angular elevation of observer.

§5. RESULTS OF ANALYSIS

Calculations have been made of the distribution of intensity in a number of typical cases with the numerical values shown in table 1.

Table 1

δ (deg.)	20, 30
α (rad.)	0, $\pi/6$, $\pi/4$, $\pi/2$
γ (deg.)	0, 5, 10, 15, 18, 19, 20, 21, 22
B (deg.)	± 2
θ	Integral values from $-5°$ to $185°$

In addition to the various possible combinations of numerical values given in table 1, the distribution of intensity has been calculated for floodlights having four different polar distributions. Two of these are represented by equations (7) and (7*a*) and are called "the cosine distribution" and "the cos^2 distribution" respectively. The "restricted cosine" distribution is given by equation (7) between narrower limits, and is a representation of a combined mirror and lens floodlight widely used in America. The fourth distribution is shown as a dotted line in figure 2*a* and represents the 9 kw. mirror floodlight made by the General Electric Company.

It would be wasteful to give the whole of the calculations and results, and typical results are therefore given in the appendix and figures 4*a*, 4*b* and 4*c*. The summarized results for twelve sets of calculations are given diagrammatically in figures 5 and 6, and the conditions for which these figures are drawn are set out in table 2.

Table 2

Method Distribution	I	II	III
Cosine	(1) See figure 4*a* $\alpha=\pi/2$ $\delta=20°$	(2) See figure 4*b* $\alpha=0$ $\delta=20°$	(3) See figure 4*c* $\alpha=\pi/6$ $\delta=20°$
Restricted cosine	(4) $\alpha=\pi/2$ $\delta=20°$	(5) $\alpha=0$ $\delta=30°$	(6) $\alpha=\pi/4$ $\delta=20°$
Cosine squared	(7) $\alpha=\pi/2$ $\delta=20°$	(8) $\alpha=0$ $\delta=20°$	(10) $\alpha=\pi/4$ $\delta=20°$
			(11) $\alpha=\pi/6$ $\delta=20°$
			(12) $\alpha=\pi/4$ $\delta=30°$
(9) Air Ministry beacon specification			

The presence of a second flash in each rotation is indicated in figure 6 by the dotted line.

§ 6. DISCUSSION OF RESULTS

The case of method III calculated in the appendix and shown in figure 4*c* may be considered first. An observer at ground level or at any elevation up to rather more than 15° will receive a single flash for each rotation of the beacon, the flash-intensity being within 85 per cent of the maximum and the flash-duration increasing from 12° to 16° of arc. Above 17° elevation, this comparative uniformity of character ceases. From 17° to 18° two consecutive flashes are seen in each rotation, the intensities at 18° elevation being 81 and 13 per cent of the maximum, and the durations 39° and 33°. Above 18° elevation, one long flash (72°) is seen, the intensity and duration both decreasing up to the limit of 22° elevation, above which there is no light.

Figures 4*a* and 4*b* have been plotted from a similar calculation of the intensity-distribution given by tilting the same beam of light by methods I and II respectively. By method I, an observer at ground level will receive two flashes equally spaced during each rotation, but an observer elevated between 0° and 18° will receive two flashes at unequal intervals in each rotation, the difference between the intervals increasing as the elevation increases. The duration of the flashes varies in the same way as for method III described above. At 18° the short interval has become zero and one long flash (72°) is seen, the duration of this flash decreasing to zero at 22° elevation. As regards the peak intensity of the flash, the horizontal intensity is extremely small but the intensity increases proportionately with the observer's elevation up to a maximum intensity at 20°. Above 20° the intensity decreases to zero at 22°.

Method II gives a single flash in each rotation at all elevations, the duration varying from 12° in the horizontal direction to 36° at 18° elevation. The maximum intensity is directed horizontally, and the peak intensity in each flash decreases smoothly to zero as the observer's elevation increases to 22°. The longer durations are associated with lower peak intensities.

The details of the performance described above may be read off the top three diagrams in figures 5 and 6. The diagrams 1, 4 and 7 in these figures all refer to method I and it may be seen that this will always give two flashes irregularly spaced in each rotation of the beacon, with very long single flashes between 18° and 22° elevation. Further, the highest intensities are given at the higher elevations, the horizontal intensity being negligibly small. Both these characteristics are the reverse of the requirements stated in § 1.

Method II is illustrated in diagrams 2, 5 and 8 and will always give a single flash of not greatly varying duration. The highest intensity is directed along the horizontal and the intensity falls progressively to zero at the higher angles. These characteristics are both in accordance with the original requirements, but the method has the disadvantage that as the beam from a floodlight is usually symmetrical, one-half of the light is directed on to the ground when the beam is tilted.

Method III endeavours to overcome this disadvantage by tilting the floodlight about some intermediate axis, so that the peak intensity is directed above the horizontal and less light is therefore lost. It is illustrated in diagrams 3, 6, 10, 11 and 12, and in general there are two flashes in each rotation at the higher elevations, one flash being of low intensity as in figure 4*c*. The intensity of the main flash increases as the elevation of the observer increases to some small angle, above which the intensity diminishes to zero at the limit of 22° elevation, with the exception of the case in diagram 12 of figures 5 and 6, which shows the state of affairs for a 30° tilt. Thus the result of saving light is to introduce some degree of irregularity into both the character and the intensity of the flash.

Figures 5 and 6 show that the difference between the cosine distribution and the $\cos^2$ distribution is a matter of intensity only. The flashing character is exactly the same and both show similar double flashes when the beam is tilted by methods I and III. The difference in intensity-distribution is most apparent when the beam is tilted by method I, but is not sufficient to be of practical importance. Other distributions which lie between these two, such as the G.E.C. 9 kw. mirror floodlight represented by the broken line in figure 5, will give similar results.

It appears then that method II is the one which gives closest adherence to the original requirements. The distribution which is essential for the operation of a projector as a floodlight necessitates the use of a wider beam than that required if the projector is operated as a beacon, and no method of tilting can redistribute the whole of the light in the beam to its best advantage. The essential difference between methods II and III is that the former puts the excess light into the ground while the latter puts it into the higher angles, where it is not necessarily of practical value. It should be noted that method III would be suitable to a system having a narrow beam-spread, and the analysis outlined above enables one to calculate the characteristics of any given beam when tilted.

§7. ACKNOWLEDGEMENTS

We are indebted to the General Electric Company for the data shown as the dotted curves in figures 2*a* and 5.

REFERENCES

(1) Blondel, A. and Rey, J. *J. de Phys.* (July 1911). *Illum. Engr, Lond.* (1912).
Toulmin-Smith, A. K. and Green, H. N. *Illum. Engr, Lond.* (Dec. 1933).
Hampton, W. M. *Illum. Engr, Lond.* (Feb. 1934).
(2) van Vloten, P. v. B. *Congrés International de Navigation*, Cairo (1926).

DISCUSSION

Dr W. S. Stiles enquired whether the methods to which figure 6 relates have been tested in practice, with results in accordance with the theory.

Author's reply. The three methods described have all been used in full-scale apparatus and observation has verified the calculations of flash-duration. The only way of obtaining the effective flash-intensity is to integrate the distribution of light in the flash by an empirical point-by-point method, which leads to a factor of the type $t/(a+t)$, where t is a measure of the duration and a is a constant depending on the intensity of illumination. The values of a are known for abrupt and for trapezoidal distributions, and the peak intensity is multiplied by this factor to give the effective intensity from which the range of the beacon can be calculated. For gradual distributions, such as are found in practice, the values of a are in general larger than for trapezoidal distributions of the same total duration, and the effective intensity is accordingly less. If the flash-duration is deliberately increased by defocusing the lamp, or by some similar method, the peak intensity is decreased proportionately and the effective intensity will be decreased slightly. It is therefore desirable in practice to have a flash as short and as intense as possible, with the intensity rising and falling sharply at each end.

APPENDIX

Cosine distribution. Beam tilted by method III. $\alpha=\pi/6$; $\delta=20^\circ$

θ (deg.)	Values of γ														
	0°			10°			18°			20°			21°		
	β (min.)	ϕ (deg.)	I	β (min.)	ϕ (deg.)	I	β (min.)	ϕ (deg.)	I	β (min.)	ϕ (deg.)	I	β (min.)	ϕ (deg.)	I
−2	41	−31·9	0·629												
0	0	−30·0	0·866												
2	−41	−28·2	0·653												
4	−82	−26·2	0·205												
23				108	−5·1	0·024									
25				71	−3·2	0·356									
30				−18	1·5	0·945									
35				−102	6·2	0·053									
55							82	26·8	0·203						
60							30	31·6	0·719						
65							−16	36·3	0·770	103	36·6	0·040			
70							−53	41·0	0·446	67	41·2	0·308			
75							−80	45·6	0·174	38	45·9	0·538	98	45·8	0·056
80							−103	50·3	0·032	17	50·5	0·607	78	50·6	0·173
85							−116	55·2	0·001	4	55·2	0·569	64	55·2	0·255
90							−120	60·0	0·000	0	60·0	0·500	60	60·0	0·250
95							−116	64·8	0·001	4	64·8	0·424	64	64·8	0·191
100							−103	69·7	0·017	17	69·5	0·334	78	69·4	0·096
105							−80	74·4	0·099	38	74·1	0·212	98	74·2	0·022
110							−53	79·0	0·112	67	78·8	0·079			
115							−16	83·7	0·070	103	83·4	0·006			
120							30	88·4	0·018						
125							82	—							
130															
Duration of flash	12°			14°			71°			52°			36°		
Peak intensity of flash	0·866			1·000			0·810			0·610			0·262		

THE MUTUAL SHUNT METHOD OF MEASURING SELF INDUCTANCE AT RADIO FREQUENCIES

By ALBERT CAMPBELL, M.A.

Received 25 *March* 1938. *Read* 10 *June* 1938

ABSTRACT. A simple method of measuring self inductance is described, in which the value is read directly on a mutual inductometer. Its secondary circuit, with an a.-c. ammeter in series, is put in parallel with the coil to be tested, the combination being connected, thro' the primary coil, to an a.-c. source of radio frequency giving constant current. The mutual inductance is now varied until the ammeter reads a minimum current, and then the self inductance is equal to the mutual inductance. This result does not involve resistance or frequency. Methods for eliminating the errors due to self and mutual capacitances in the inductometer are indicated.

§ 1. INTRODUCTION

For the measurement of self inductance at radio frequencies the most accurate methods are those in which resonance with a standard capacitor is used. These resonance methods are not always convenient, however, particularly when small inductances are to be measured over wide ranges of frequency. The null bridge methods, so useful at the lower frequencies, are not easy at radio frequencies, for the simpler current-measuring instruments (such as galvanometers with thermal converters or rectifiers) are mostly of square-law type and are very insensitive near zero reading. Thus for null methods more elaborate detectors have to be used.

§ 2. DESCRIPTION OF METHOD

I have recently devised a direct-reading system which quite avoids this difficulty. It is shown in the figure, where *B*, the coil to be tested, has resistance *R* and self inductance *L*.

In parallel with *B* there is an a.-c. ammeter *A* in series with the secondary coil of a mutual inductometer in which the mutual inductance *M* can be varied over a long range. The radio-frequency source is connected thro' the primary circuit of *M* as shown, with the point *E* earthed.

Let r and l be the total resistance and self inductance of the secondary branch, and i and i_2 the instantaneous values of the alternating currents as in figure 1, with effective values I and I_2. Then the current in *B* will be $(i-i_2)$, and if the a.c. is purely sinoidal and of pulsatance ω, we have

$$(R+Lj\omega)(i-i_2)=(r+lj\omega)\,i_2\pm Mj\omega i$$

or

$$[R+r+(L+l)\,j\omega]\,i_2=[R+(L\pm M)\,j\omega]\,i.$$

Taking the minus sign for M, we have

$$\frac{I_2^2}{I^2}=\frac{R^2+(L-M)^2\,\omega^2}{(R+r)^2+(L+l)^2\,\omega^2} \qquad \ldots\ldots(1).$$

Now if I is kept constant and M alone is varied, when the current I_2 shown by the ammeter is a minimum,

$$L=M \qquad \ldots\ldots(2).$$

Thus L is measured directly, and the result does not involve the frequency or the resistance R of the coil.

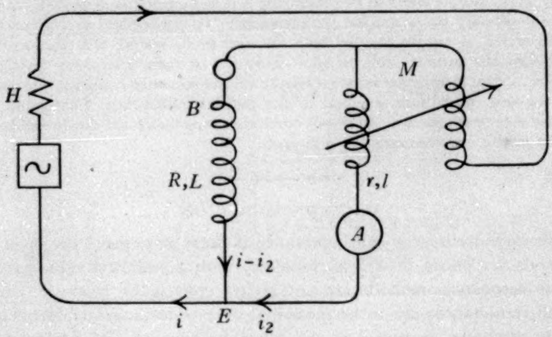

Figure 1.

It is best to obtain M by taking the mean of two values, above and below M, which give equal values of I_2. There is no need to know the calibration of the ammeter, and its scale may follow any law. As the result is independent of frequency, the wave form may contain harmonics. To ensure that I shall remain constant while M is varied, the outer circuit must contain impedance (as at H) much greater than that of the working part. The system may conveniently be named the "mutual shunt method".

It will be noticed that by reversing the connexions of one of the inductometer coils (i.e. changing the sign of M) negative self inductances can be measured over the same range.

§ 3. CORRECTION OF ERRORS DUE TO CAPACITANCES OF COILS

The simple theory just given becomes more complicated when the mutual inductance is not perfect, and the result obtained is affected by errors due to the self capacitances C_1 and C_2 and the mutual capacitance K of the primary and secondary coils of the varinductor used. As Butterworth(1) has shown, part of the total error increases with frequency, being proportional to ω^2. Moreover, when $L=0$ there is a zero error which increases with frequency. The errors become worse as the maximum range of M is increased. In the present application K usually causes more error than C_1 and C_2.

To get over these troubles I have constructed inductometers with relatively small self and mutual capacitances (by using single-layer coils and the like), and containing compensating systems to reduce the errors. The zero error can be largely reduced by putting in series with the L coil a resistance shunted by a capacitance and resistance in series. The remaining error, which varies as the reading of M is altered, is reduced by adding a closed tertiary circuit coupled to the primary and secondary circuits(2). Compensation can be obtained by proper choice of ρ, the resistance, and λ, the self inductance, of this auxiliary circuit. For small errors the compensation will hold over a good range of radio frequency, but in the more extreme cases it may be necessary to reset ρ for each frequency used. In the latter case it is necessary to know the frequency approximately.

§ 4. ACTUAL APPARATUS

I have constructed a number of inductometers of various ranges from 0 up to 300 μH., all meant to work up to frequencies of 800 kc./sec. and even higher. These instruments had their scales marked at 50 c./sec., and were adjusted to give minimum errors when testing L coils checked by the National Physical Laboratory or coils of calculable self inductance. For the complete set-up the a.-c. source is an oscillator with a single small valve (with filament current 0·075 amp., and anode voltage 120 v.), giving a variety of frequencies from 10 kc./sec. up to 800 kc./sec. The output coil can be turned so as to vary the coupling from 0 to the maximum; this is useful to prevent overloading the ammeter. For the ammeter a thermal converter (heater and thermojunction) was used at first, but for better sensitivity this was replaced by a small transformer connected to a full-wave copper-oxide rectifier and a moving-coil galvanometer. By the use of a Spot galvanometer (made by the Cambridge Instrument Company) the whole apparatus is made completely portable; it occupies very little space and can be run by dry cells.

§ 5. RESULTS

The following three examples illustrate the kind of results obtained:

Model	Range (μH.)
No. 1	−0·1 to +1·25
No. 2	−0·4 to +13
No. 3	−12 to 300

In each case the small residual zero errors were allowed for.

No. 1 could be read to 0·002 μH. even at the higher values. Without compensation it appeared to have very little error and no variation with frequency up to 800 kc./sec.

In No. 2, which was the one chiefly studied, the added compensations were quite automatic and reduced the error to less than 0·05 μH. at all points of the scale (e.g. less than 0·4 per cent at the top reading).

No. 3 without compensation showed a maximum error of about 30 per cent at 800 kc./sec. In its tertiary circuit a rheostat was arranged to be set at the proper resistance for each particular frequency. In this way the error was reduced to less than 2 μH. at all points of the scale.

When R is very large in comparison with $L\omega$ or $l\omega$, large errors may arise. Such extreme cases, which are not common in practice, cannot be dealt with by this method.

REFERENCES

(1) BUTTERWORTH, S. *Proc. Phys. Soc.* **33**, 312 (1921).
(2) CAMPBELL, A. and CHILDS, E. C. *Measurement of Inductance, Capacitance and Frequency*, p. 206 (1935).

DISCUSSION

Mr R. APPLEYARD. It is pleasant to realize that the problem of determining mutual inductance continues to engage the attention of electricians in this country, where it may be said to have had its origin. It is cheering, too, for us to remember that it has been intimately associated with the Physical Society. The account given to the Physical Society on November 27, 1886, by Professor G. Carey Foster, of a method of determining what was then a very elusive quantity gave the impetus to the investigation. At that time, it was thought likely that it would be of service in the design of dynamo-electric machinery. Between the years 1900 and 1907, when the work of Oliver Heaviside began to be appreciated and to yield tangible results, mutual inductance had to be measured in the factories—a laborious yet fascinating task. It remained fascinating, but it became far less laborious when, after the achievements of Heaviside and of Lord Rayleigh, the author placed in our hands his masterpiece, the inductometer. It was with this instrument that electricians were able to solve many of the practical difficulties in the design of loaded telegraph and telephone cables. He now presents them with means to measure small inductances at radio frequencies, and he deserves their gratitude. It is likely also that the instrument may prove of benefit when measurements have to be made in some of the subtle cases that arise in interference problems in telephony, where the quantities to be detected and gauged are next to nothing.

Telephone engineers are to-day concerned with mutual inductances of the order 1 mμH. (10^{-9} henry). They may require to know whether the inductance between two circuits is say 1, 2, 3, ..., 10, ..., 100 such units, to an accuracy within say $\frac{1}{2}$ or 1 unit. The range of frequency in these cases may be from 5000 c./sec. to 60,000 c./sec. The currents, where these mutual actions have to be determined, may be too small to be detected by a telephone. An amplifying system has therefore to be adopted.

Dr L. HARTSHORN. Mutual inductometers were first devised by the author nearly thirty years ago, and they have been standard laboratory instruments ever since. It is remarkable that Mr Campbell should at this stage be able to describe an application of the instruments which is novel and yet so beautifully simple. The single adjustment, and the lack of dependence of the readings on resistance or, to a first order of approximation, on frequency, are valuable features of the method for general testing purposes.

In connexion with the greater sensitivity obtained by the author with this method than with null bridge methods, it is interesting to note that for a coil of negligible resistance it becomes a null method. The curve connecting instrument reading and galvanometer deflection is rather like a resonance curve, which becomes flatter the higher the value of R. Thus although an increase of R tends to increase the sensitivity inasmuch as it causes the detector to operate at a more sensitive point on its characteristic curve, it also tends to diminish the sensitivity by flattening the response curve of the instrument. There is presumably an optimum condition for sensitivity, and it seems likely that it might be near the conditions obtained in the ordinary use of this instrument on typical coils.

At first sight it appears as if the self capacitance of the coil under test being added to that of the secondary coil of the inductometer must modify its calibration at the higher frequencies. In practice the compensating system would presumably be adjusted with a coil of known self capacitance in circuit. If the compensating circuit were set so that the values obtained by measurements on the standard coil included the effect of its self capacitance, then the instrument would subsequently give correctly the effective series inductance L_1 of any coil. If, however, the compensating circuit were set so that the values obtained for the standard coil excluded the effect of its self capacitance C, then the instrument would subsequently give the equivalent shunt inductance L_2 of a coil provided its self capacitance were equal to that of the standard. It is well known that $L_1 \doteqdot L_2/(1 - L_2 C\omega^2)$. The instrument would probably be used for measurements in which such differences are not important, but it is interesting to note that for routine tests on similar coils the compensating circuit could be adjusted so that the reading of the instrument would give either L_1 or L_2.

The use of a transformer and copper-oxide rectifier as a sensitive ammeter at such high frequencies is interesting. A thermal instrument would probably be much less satisfactory owing to its inability to stand the overloading which would be likely to occur in routine testing. Is the transformer of special design?

Dr D. Owen. The author's name is closely associated with the mutual inductometer, both in its development as an instrument of precision and in the devising of various new methods of measurement involving its aid. He now extends its application to very high frequencies, and the present communication embodies a simple method for the measurement of self inductance.

One or two questions suggest themselves. It would be of interest to know to what sources the zero error is to be assigned. The absence of any reference to the self capacity of the coil under test is noticeable; it is difficult to see how this useful datum is to be obtained by measurements at a single frequency. Again, the models no. 1 and no. 2 are designed to deal with self inductances of the small values which would be required normally for use at frequencies far above 800 kc./sec. On the face of it, this would appear to discount the value of the method as applied to short-wave coils.

AUTHOR'S REPLY. Mr Appleyard rightly points out the importance of Prof. Carey Foster's work. The Carey Foster bridge is still the simplest and best method of determining capacitance in terms of mutual inductance.

Dr Hartshorn notices that, for a given value of L, there should be an optimum value of R to give the best sensitivity. For this reason there is permanently mounted in the inductometer a resistance, for connection in series with the unknown coil, of such a value as to give satisfactory sensitivity for the whole range of M from 0 to the maximum, and over the whole working range of frequency.

The mutual shunt system can be worked as a null method, if desired, by making the closed tertiary circuit ρ, λ completely adjustable. If it is coupled to the primary and secondary circuits by mutual inductances m and μ respectively, then by adjustment of ρ, λ, m and for μ the current in the detector can be brought to zero, in which case

$$R=\frac{m\mu\lambda\omega^2}{\rho^2+\lambda^2\omega^2} \quad \text{and} \quad L=M+\frac{m\mu\rho}{\rho^2+\lambda^2\omega^2}.$$

If ρ can be made very small compared with $\lambda\omega$, these equations become much simpler, and it is possible that this null method might be useful in certain cases.

The inductometer is usually compensated so as to give the series L_1 of the coil under test. If L_2 is appreciably constant for the frequency range, it can be deduced by observing L_1 at two frequencies.

With regard to the sensitive detector used, I have to thank Mr W. L. Beck for kindly suggesting the use of a transformer in front of the rectifier. The transformer is of his design, with a closed magnetic circuit of mumetal.

In reply to Dr Owen: Butterworth's formula* does not perhaps quite meet the case, but it indicates that the zero error is due to the mutual capacitance between the primary and secondary coils. The method cannot determine the self capacitance of an unknown coil by a single reading at one frequency. By testing short-wave coils standardized by other methods, the models no. 1 and no. 2 might be compensated to read L_1 correctly at frequencies much higher than 800 kc./sec. Model no. 1 (to 1·2 μH.) would probably be satisfactory up to 8000 kc./sec., but it is hard to predict without sufficient experimental foundation.

---

* *Proc. Phys. Soc.* **33**, 312 (1921).

ANOMALOUS TRICHROMATISM AND ITS RELATION TO NORMAL TRICHROMATISM

By J. H. NELSON, A.R.C.S., B.Sc.
Imperial College of Science and Technology

Communicated by Dr W. D. Wright, 5 October 1937. Read 2 June 1938

ABSTRACT. The characteristics of six deuteranomalous observers and one protanomalous observer have been examined. In the case of the former it has been shown that, in contrast with what occurs in normal trichromatism and dichromatism, it is not possible to take mean values as representative of the deuteranomalous observer. This fact, combined with the results of the statistical survey with the Nagel anomaloscope, suggests that anomalous trichromatism is an intermediate state between dichromatism and normal trichromatism. In the case of the protanomalous this transition would seem to be of a continuous nature, but for the deuteranomalous there is a subsidiary maximum in the distribution curve.

§ 1. INTRODUCTION

It has been found by experiment that the majority of colours can be matched for the normal person by a mixture of red, green, and blue; and further, it has been shown that any colour quality can be uniquely expressed by an equation of the type

$$C = aR + bG + cB \qquad \text{......(1)},$$

where C is the colour quality, R, G and B the primary colours to be mixed, and a, b and c the proportions of the three primary colours, such that

$$a + b + c = 1 \qquad \text{......(2)}.$$

While the equation (1) will hold in all cases, it is found that some observers need have only two primary colours in order to match all other colours, and for others that only one primary is needed.

It can therefore be said that the colour-vision of all types of observers can be divided into three main groups, according as it is a function of one, two, or three variables. These three main groups are known as monochromats, dichromats and trichromats respectively. But although this classification is fundamental, there may be border-line cases.

In the investigation of the properties of the various types of colour-vision it has been found necessary to subdivide the main groups further. The first type, namely the monochromats, have not been further subdivided; while in their case there may be no more than one type of luminosity curve, no subdivision is possible from considerations of colour. The dichromats can be divided into three distinct classes; various names have been applied to them, but the most common are those introduced by von Kries, and since he introduced them so as to be independent of any theory, they will be used throughout this paper and assumed to have no theoretical significance. The classes of dichromats are protanopes, deuteranopes and tritanopes. Both the protanopes and deuteranopes are unable to distinguish colour-differences in the red-green region of the spectrum, and the tritanopes in the blue-green region of the spectrum; these last are rare. The former two types are defined by comparison of their luminosity curves with the normal. The protanopes are defined as having the maxima of their luminosity curves displaced towards the blue, while those of the deuteranopes are displaced towards the red, relative to the normal(1).

In the case of the trichromats there are two main classes, known as normal trichromats, to which class the majority of observers belong, and anomalous trichromats, who were first distinguished from the normal by Lord Rayleigh(2), who showed that in matching a yellow with a mixture of red and green the anomalous observer required more of either red or green than the normal to make a match. This latter class may again be subdivided and, as with the dichromats, the names to be given to the subdivisions are a subject for controversy. For the sake of uniformity of language, and since the names are already in use, the names protanomalous, deuteranomalous and tritanomalous will be used to distinguish the classes of anomalous trichromat. The definitions of these types are made from the region of the spectrum in which they are anomalous and from their luminosity curves in the same way as for the dichromats. But beyond this similarity of name and definition no further connexion with the dichromats is necessarily implied by the use of the names.

It is with anomalous trichromatism that this paper as a sequel to F. H. G. Pitt's work on dichromatism(1) is concerned. As yet the colour characteristics of anomalous trichromatic vision have not been fully investigated, and in consequence any physiological analysis must necessarily have been of a very speculative nature. The detailed characteristics of several anomalous observers are here given and an attempt has been made to relate the different types of colour-vision to one another. A statistical survey of a number of observers chosen at random has also been carried out, to discover where the observers whose characteristics have been determined came in relation to other observers, and to ensure that all the observers chosen were not of the same type.

§ 2. APPARATUS AND METHOD

The apparatus used was the Wright colorimeter(3), which is described elsewhere.

The procedure adopted in using the apparatus is as follows. One half of the field is filled with light from the test colour, and the other half with a mixture of light from the three primaries. A match is obtained for both colour and intensity by the observer's suitably adjusting the amount of red, green, and blue by means of the photometer wedges. In order that the observer may give an accurate match, he should keep looking away and looking back to rest his eyes. All measurements were taken in a darkened room, and after the observer had been dark-adapted for at least ten minutes. This period of dark-adaptation is to allow the observer to settle down and to give his eyes a preliminary rest; it is not an attempt to obtain a match in the dark-adapted state. Actually the final match is the same whether the observer has been dark-adapted for the full period of half an hour, or has been light-adapted, provided that the intensity of light-adaptation is not too high.

With the above arrangement the following characteristics for any observer may be determined: (1) the spectral coefficients, (2) luminosity and mixture curves, and (3) hue-discrimination data.

To determine the saturation-discrimination by adding small quantities of spectral colour to white, it is necessary to make some additions to the above apparatus. A diagram of the essential parts is shown in figure 1; a brass sector S, coated with magnesium oxide, is illuminated by light from a lamp as specified for the C.I.E. 1931 Standard Illuminant B(4). The sector is so arranged that both halves of the photometric field in the prism P are filled during one half of the revolution; and during the other half of the revolution monochromatic radiation of known wave-length is admitted to the top half of the field. This monochromatic radiation is obtained from the spectrum W_2, and the intensity is controlled by means of a calibrated photometer wedge. The intensity of the white S_B in the top half of the field may be controlled by neutral filters F, but it is advisable to use only the lightest filters, as the darker ones deviate considerably from neutrality. In the lower half of the field the intensity of the white is controlled by a very shallow photometer wedge. It is necessary to have the white of one half of the field so arranged that it can be varied continuously in intensity, and the use of a shallow wedge is probably the most satisfactory, as the deviation from neutrality would be negligible. The sector can be run at two speeds, fast to remove flicker between the white of the top half of the field and the monochromatic radiation, so that a discrimination step can be made between the mixture and the pure white in the lower half of the field; and slow, so that the intensities of the white and the monochromatic radiation may be compared by flicker.

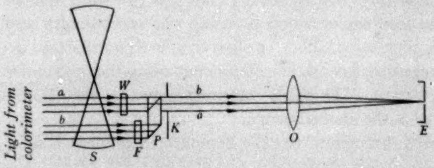

Figure 1. Diagram of optical system for saturation-discrimination.

For the statistical survey the Ishihara cards were used as a purely qualitative test, to determine whether the observer was deficient in colour sensitivity.

To divide the observers into their distinctive classes the Nagel anomaloscope was used. In this instrument one half of a photometric field is filled with monochromatic yellow, and the other with a mixture of monochromatic red and green. The intensity of the yellow is variable and also the ratio of red to green in the mixture, and thus it is possible to match the two halves of the field in colour and intensity. The instrument is calibrated so that for any observer the ratio of red to green required for the match can be found. Since it is possible to vary the red-to-green ratio from zero to infinity, it is possible, in the case of dichromats, to find the relative luminosity of the red and the green by matching each in turn with the yellow, and since it can be seen from their luminosity curves(1) that L_R/L_G for protanopes will be much less than L_R/L_G for deuteranopes, it is possible to distinguish between them.

The wave-lengths used for the red, yellow, and green were 0·650, 0·578 and 0·535 μ. respectively. In the case of the yellow it is usual to use 0·589 μ., and it is convenient to examine the relative advantages of setting the yellow of the anomaloscope at 0·578 μ. and 0·589 μ. respectively. In connexion with hue-discrimination the latter would have an advantage, but this would not be very large. On the other hand, in any one instrument the values of the wave-lengths for the red, yellow and green are all interdependent, and changing the yellow from 0·578 to 0·589 would cause a corresponding change in the red and green wave-lengths, but from the hue-discrimination curves it can be seen that this change would decrease the number of steps, and thus the difference in colour, between the red and the green. This would tend to make the settings less accurate. Thus it is probable that there is very little difference in the accuracy obtained by using one wave-length and the other. In order to test this conclusion, about 15 observers, both normal and deuteranomalous, were asked to make matches on the colorimeter, using the instrument primaries and a test-colour at 0·589 μ. The results obtained showed a very close agreement with those obtained from the anomaloscope.

The white used throughout was the Standard Illuminant B set up by the C.I.E. in 1931(4).

§ 3. UNITS AND METHODS OF EXPRESSING RESULTS

The trichromatic units have been based on two monochromatic matches, as in the W.D.W. system of units(5), but the same unit colours have not been used. In the W.D.W. system the units were based on matches at 0·5825 and 0·4940 μ., at which the red and green and the blue and green coefficients respectively are made equal. The advantage of this system for the purpose of research is that the resulting spectral coefficients will be independent of the macular pigmentation of the observer's eye, which makes it possible to eliminate one of the variables in an analysis of the curves. Moreover in the case of a normal observer the position of the white point will indicate the extent of the pigmentation. It was found that if the W.D.W. system were used to express the coefficients of a deuteranomalous observer, the negative red coefficients in the blue-green region of the spectrum would be very large and uncertain, and, while there is no objection to their being large, the uncertainty would directly influence the blue and green coefficients. It was therefore decided to reduce the values of the negative red in such a way as to reduce this uncertainty, but at the same time to keep the values large enough for comparison to be made between the results obtained by different observers. For this purpose a new unit colour was chosen at which to make the red and green coefficients equal, the other unit colour being the same as in the W.D.W. system. This new colour was at 0·6100 μ. for the deuteranomalous observers, and for convenience the system will be known as the J. H. N. (1) system of units.

In the case of protanomalous observers the negative red coefficients become inconveniently small when the W. D.W. system is used. In this case it is not convenient to move the unit colour to the region of 0·57 μ., since in this region the hue-discrimination is very poor, but precisely the same effect can be obtained by using 0·6100 μ. and making the ratio of the red-to-the green coefficient be as 10 is to 1. The other unit colour is again the same as in the W. D.W. system. This system will be known as the J. H. N. (2) system of units.

It is convenient to summarize these systems of units in tabular form, since the two types of anomalous trichromats have their final results expressed in two different ways, rendering direct comparison of their spectral coefficients impossible. They may, however, be compared with the normal observer's results expressed in their respective systems.

Table 1. Unit colours

	W. D. W. (μ.)	J. H. N. (1) (μ.)	J. H. N. (2) (μ.)
$R=G$	0·5825	0·6100	—
$10\,G=R$	—	—	0·6100
$B=G$	0·4940	0·4940	0·4940
Primaries R	0·6500	0·6500	0·6500
G	0·5300	0·5300	0·5300
B	0·4600	0·4600	0·4600

The luminosity curves are expressed in relation to the point of maximum luminosity, which in each case is made equal to unity. The results for all observers are thus comparable. The luminosity curves, which are for an equal-energy spectrum, are also split up into their three components, showing the relative luminosities of the red, green, and blue primaries needed to match each point of the spectrum. These and the subsequent curves are directly comparable with the corresponding normal curves.

The hue-discrimination is expressed as the least noticeable difference in wavelength at each point in the spectrum, when the intensities of the test and comparison fields are kept equal throughout the observation.

The saturation-discrimination is determined by finding the just noticeable difference in saturation from the white point S_B. If L_S is the intensity of any wavelength that has to be mixed with L_W, the intensity of S_B to produce a just noticeable difference, then the saturation-discrimination is expressed as the logarithm of the ratio $(L_W+L_S)/L_S$. A large value of this expression indicates a highly saturated spectral colour.

§ 4. STATISTICAL SURVEY AND RESULTS

In the statistical survey the observer was first asked to read the Ishihara cards, and any mistakes or hesitation were noted. In this way it was almost always possible to detect any deficiency, but only in a general way, dividing the observers into normal and abnormal. After they had read the cards all observers were asked to make a match on the Nagel anomaloscope. As only one match was taken, the observer was asked to look away at a dark card, and look back at the match once or twice, in order to make sure that the match was as accurate as possible. In the case of normal observers, some of whom repeated their readings after long intervals, it was found that this method gave results accurate to within about one scale division, while if a number of matches were taken by one observer the variation was between a half and one scale division. These figures may be compared with the variation of eight scale divisions between different normal observers. In the case of the anomalous trichromats the settings were not so exact, but as will be seen later from the hue-discrimination curves it would not be reasonable to expect the same accuracy.

The readings for the dichromats, which were used only for purposes of classification, were obtained by asking the observer to make two intensity matches, one between yellow and red and the other between yellow and green(1).

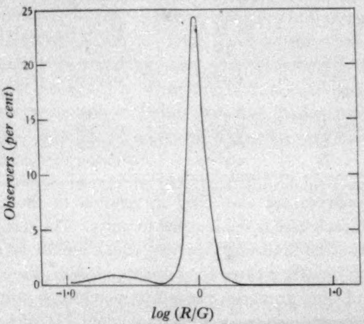

Figure 2. Distribution of R/G ratio for Nagel match.

The results of the survey are shown in table 2 as percentages of colour-defectives, and also in the form of a curve, figure 2, the ordinates of which represent the logarithm of the ratio of red to green in the match obtained, while the abscissae represent the percentage of observers giving that ratio. The ratio of red to green, by which the results are expressed, is comparable but not identical with the *Anomalquotient* introduced by Trendelenburg(6). In a general way the results obtained by the author agree with those obtained by Schmidt(7), as to the nature of the distribution of the anomalous trichromats. However, the latter finds a gap between the red-to-green ratio for the normal and for the deuteranomalous observers, while the author's results show only a dip in the distribution curve.

The results obtained for the percentages of various forms of colour-deficients are, as can be seen in table 2, somewhat higher than those obtained by other workers. Schmidt criticizes her own results as being too low since, as the readings were taken at a public exhibition, those who knew of their defect did not wish to show it. Some of the author's results were taken at the Physical Society's exhibition, where it was found that those who knew of their defect made a special point of presenting themselves.

Table 2. Results of statistical survey (males)

	Author	Schmidt(7)	Waaler(11)	v. Planta(12)
Total number	1338	6863	9049	2000
Protanopes (per cent)	1·27	1·09	0·88	1·60
Deuteranopes (per cent)	1·20	1·97	1·03	1·50
Protanomalous (per cent)	1·27	0·68	1·04	0·60
Deuteranomalous (per cent)	5·08	4·01	5·06	4·25
Total deficients (per cent)	8·82	7·75	8·01	7·95

§ 5. MEASUREMENT OF INDIVIDUAL CHARACTERISTICS

As a preliminary to recording the characteristics of each observer, several colour-matches were taken to accustom the observer to the apparatus; these results were recorded, and when the observer could give consistent results the measurement of the characteristics was started. The agreement to be considered as consistent was by no means the same for each observer, owing both to the variation in their defects and also to their inability to make scientific observations. For this latter reason it was found necessary to discontinue observations in some cases.

The following characteristics were measured for various observers; the exact experimental procedure in each case will be explained: (1) spectral coefficients; (2) equal-energy luminosity and spectral-mixture curves; (3) hue-discrimination; (4) saturation-discrimination; (5) coefficients of C.I.E. 1931 Standard Illuminant B.

(1) The method of basing the trichromatic units has been explained in § 3, the coefficients being based on two monochromatic matches. In practice the observer is asked to match the two unit colours before each set of readings. From these two matches, correction factors are obtained which must be applied to the readings from the photometer wedges controlling the intensities of the primaries in the mixture.

Throughout the readings for the coefficients three observations were taken on each match. In general the observer was asked to upset and reset each primary separately, but in some cases, especially in the yellow region, it was found necessary to ask the observer to upset both red and green primaries together, and to take a mean of more than three settings. In the case of each observer the final curves are a mean of several sets of results.

(2) The same observations were used to calculate both the trichromatic coefficients and the luminosity curves, and for this it was necessary to know the relative luminosities of the instrument primaries. These would, however, depend for their constancy on the condition of the instrument always remaining the same, and so the relative luminosities of the primaries needed to match the unit colours were found in each case, and were a constant for each observer.

This comparison was made by flicker, the apparatus being specially arranged(3). When the three primaries had been compared in this way, matches were made on the two unit colours and so the relative luminosities of the primaries needed for the matches could be calculated. These readings supplied a second correction factor to be applied to the wedge readings, after the application of the trichromatic unit-correction factor; but this factor, being a constant for the observer, could be used throughout the whole series of readings for any observer, any change in the apparatus being allowed for by the trichromatic unit-correction factor.

The luminosity curve given by the above method would refer to a spectrum having a particular energy-distribution depending on the source of light and the apparatus. In practice it is necessary to refer the curve to an equal-energy spectrum, and to do this it is necessary to correct for (1) the variation in the dispersion of the spectrum; (2) the energy-distribution of the source of light; and (3) selective absorption in the apparatus.

These measurements give constants of the apparatus and were originally taken by Pitt(1). As a check these constants were obtained by a slightly different method. To find the dispersion at various points in the spectrum, Pitt's method was to fit a narrow slit in front of the test colour prism, and then, by examining the exit pupil with an eye-piece, to determine the dispersion at various parts of the spectrum. From these readings a curve could be drawn showing the variation of the dispersion with the wave-length. As a check on these measurements the pointolite lamp was replaced by a mercury vapour lamp. The lines emitted could be viewed directly in the exit pupil with an eye-piece without the use of an additional slit in the spectrum, and so the dispersion was measured at the various wave-lengths emitted by the lamp. In the same way a curve was drawn showing the variation of the dispersion with wave-length.

In the case of the second and third corrections, the method adopted by Pitt was to take measurements for several normal observers, and then assuming that the mean point of maximum luminosity for these would be the same as for the C.I.E. 1931 Standard observer, to find the colour temperature of the lamp, assuming the energy-distribution to be Planckian; this made the maximum come to $0{\cdot}555\,\mu$., the maximum for the standard normal observer.

Owing to the smallness of the quantity of energy actually emitted, any direct measurement of the energy-distribution would be very tedious, if possible with any degree of accuracy. However, if it is assumed that the energy distribution is approximately Planckian when it emerges from the exit pupil, then the effective colour temperature of the source can be measured by measuring the colour obtained by reflecting back the whole of the spectrum W_1 with a white diffusing surface, and matching it with the instrument primaries. For this measurement the units were obtained by a match on the C.I.E. 1931 Standard Illuminant A(4). From the results of measurements of various colour temperatures, Judd(8) has drawn a locus in a colour triangle so that, given the colour of a source, its effective temperature can be found. It was found that the colour given by the source lay a little way off the curve for sources of Planckian distribution. The difference from the Planckian distribution, which was small, was assumed to be due to excess absorption of the blue, and so the colour temperature was found by joining the point given by the source to the blue origin, and the point where this line cuts the locus was taken as the effective colour temperature of the source as seen through the exit pupil. The results obtained by the two methods agreed very closely, the apparent colour temperature being 2600° K. in each case.

By measuring the energy-distribution in this way, both the energy-distribution of the source and the selective absorption in the apparatus can be corrected for at the same time, and with the curve for the variation in dispersion throughout the spectrum the equal-energy luminosity curves can be calculated. Further, the mixture curves can be calculated from the equal-energy luminosity curve, the spectral coefficients, and the relative luminosities of the primaries.

(3) In the measurements of the hue-discrimination it was necessary to fill both halves of the photometric field with light of approximately the same wave-length. To do this, two of the instrument primaries were removed and the third was set to the required wave-length to provide the colour comparison field. The test colour was arranged so that the wave-length could be controlled by the observer. The observer was asked to set the test colour so that there was the smallest distinguishable difference in colour between the two halves of the field, when the intensities were exactly the same. The intensity of the primary was controlled by means of the photometer wedge. In this way it was possible to find the difference limen due to colour alone at various points throughout the spectrum, and thus a curve could be drawn showing the difference limen at any point in the spectrum.

(4) The arrangement of the apparatus for the determination of the saturation-discrimination has been described in § 2. The test colour was removed and one of the primaries was set to the required wave-length, the other two being removed. In the first part of the experiment the observer was asked to match the intensity of the white field with that of the primary test field by flicker. During this measurement only the half of the field filled by both the primary and the white was visible. The speed of the sector was controlled by the observer so as to give the most accurate setting; five settings were usually taken. In the second part of the experiment both halves of the field were exposed, and the sector was run fast to remove flicker. The intensity of the primary was then set so that there was the smallest detectable difference in colour between the two fields, the intensities being kept equal throughout by means of the auxiliary wedge. In this way the intensities of the white and of the monochromatic radiation in the colour one step from the white could be found. This procedure was repeated at various points in the spectrum, and a curve showing the variation of the saturation-discrimination limen throughout the spectrum was drawn.

(5) For the measurement of the C.I.E. 1931 Standard Illuminant B a plane brass sheet covered with magnesium oxide was placed between the prisms *D* and *P*, with its plane normal to the direction of the light and so as to cut off the test colour beam. This surface was illuminated by the light from an N.P.L. standard lamp, the standard liquid filter being placed between the lamp and the surface.

§ 6. DISCUSSION OF RESULTS.

The results for all the observers are shown in figures 3 to 42. The characteristics of these curves will now be discussed, and the results for each observer compared.

The position of the observers on the Nagel distribution curve is shown in table 3, and compared with the normal mean and variation. It is immediately obvious that the position on the Nagel distribution curve cannot be taken as a measure of the defect of an observer as can his hue-discrimination curve, figures 4, 6, etc.

Table 3

Observer	log (R/G)
Normal, mean	0·000
extreme on the deuteranomalous side	−0·170
extreme on the protanomalous side	0·170
Deuteranomalous, A	−0·695
B	−0·705
C	−0·560
D	−0·580
E	−0·425
F	−0·430
G	−0·860
Protanomalous, L	0·615
M	0·295

To some extent, however, it must be borne in mind that the readings given by the anomalous observers on the Nagel anomaloscope, except possibly those for observers A and D, cannot be compared in accuracy with those given on the colorimeter, where several readings could be taken and the observer was more at ease.

From the first glance it can be seen that the curves are different in type for each observer, and no attempt to take a mean as representative of the deuteranomalous observer could possibly be made. While this may also be true for the protanomalous observers, it is impossible to make the assertion from the complete results of only one observer (observer L).

While, in relating the characteristics of any observer, the hue-discrimination and spectral-mixture curves would have a definite connexion, this connexion is not of a simple character, as has been shown by the work of von Helmholtz(9) and Schrödinger(10) and in the search for an empirical relation by Judd(8). It is therefore more convenient to discuss the curves for the hue-discrimination and the spectral coefficients together. The curves for observers A to F are shown together, as these are all deuteranomalous. These fall naturally into two groups, of which A, D, and F form one, and B, C, and E the other. In the case of the observer F only the spectral coefficients are shown. Both the spectral coefficients and the hue-discrimination curves of observers A and D are very similar in general shape to the normal. The points of minimum discrimination are in both cases moved towards the red, and the power of discrimination in the yellow is smaller than in the case of the normal.

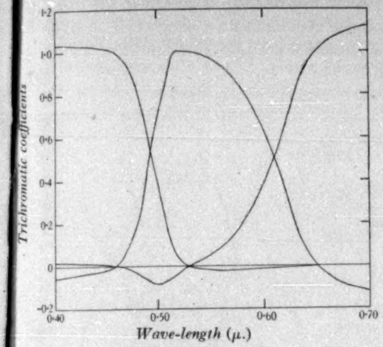

Figure 3. Spectral coefficients. J. H. N. (1) units. Observer A.

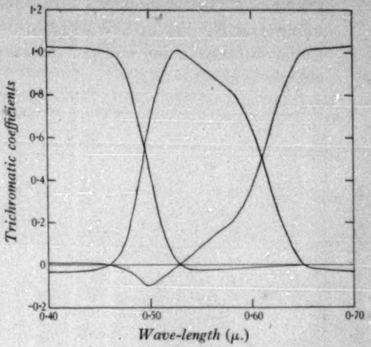

Figure 5. Spectral coefficients. J. H. N. (1) units. Observer D.

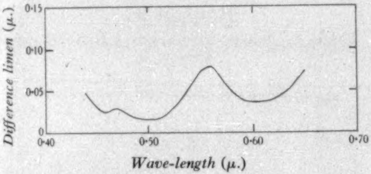

Figure 4. Hue-discrimination curve. Observer A.

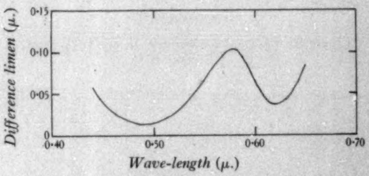

Figure 6. Hue-discrimination curve. Observer D.

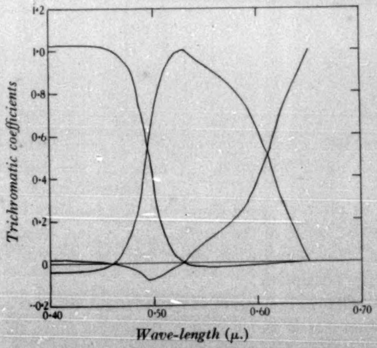

Figure 7. Spectral coefficients. J. H. N. (1) units. Observer F.

Observer A has a definite dip in the violet region, but this dip is absent in the case of observer D. The general shape of the spectral coefficients for observer F is also similar to that of the normal, although the coefficients change somewhat more sharply at about 0·54 μ.

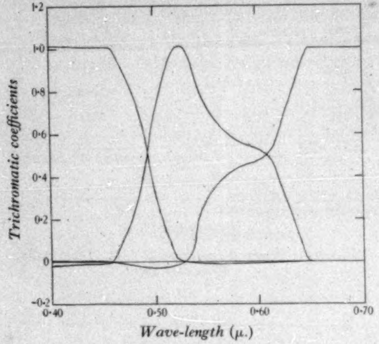

Figure 8. Spectral coefficients. J. H. N. (1) units. Observer B.

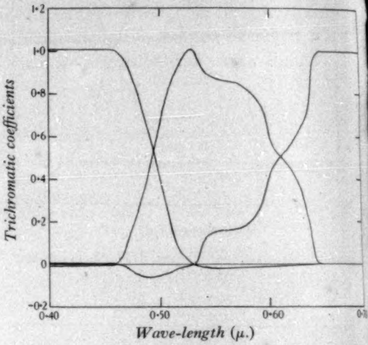

Figure 10. Spectral coefficients. J. H. N. (1) units. Observer C.

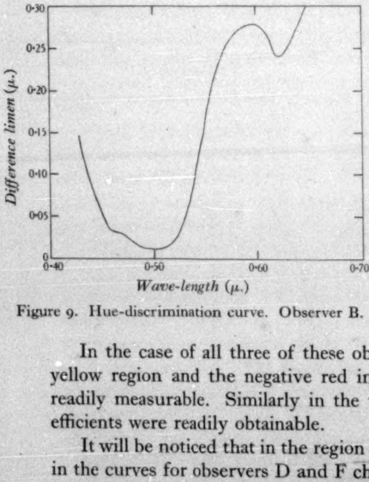

Figure 9. Hue-discrimination curve. Observer B.

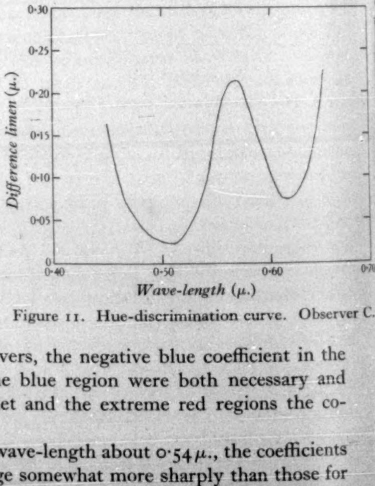

Figure 11. Hue-discrimination curve. Observer C.

In the case of all three of these observers, the negative blue coefficient in the yellow region and the negative red in the blue region were both necessary and readily measurable. Similarly in the violet and the extreme red regions the coefficients were readily obtainable.

It will be noticed that in the region of wave-length about 0·54 μ., the coefficients in the curves for observers D and F change somewhat more sharply than those for the normal and for observer A, the effect being to move the rather flat portion of the coefficient curves towards the red. It is the accentuation of this effect which differentiates the curves of observers B, C and E from those of observers A, D and F. It will be seen that with the presence of this flattening effect there is also a sharp rise in the value of the hue-discrimination limen. As far as the yellow region is concerned, observers C and E are somewhat similar, the difference limen has become large, and the point of minimum discrimination rather sharp. Observer B has even poorer discrimination, and the flattening of the coefficient curves and the point of minimum discrimination are moved farther towards the red. At the same time in the blue-green region observer B has a very small difference limen, comparable with those of observers A and D. It shows a semblance of a dip in the violet, while the limen for observers C and E is considerably larger.

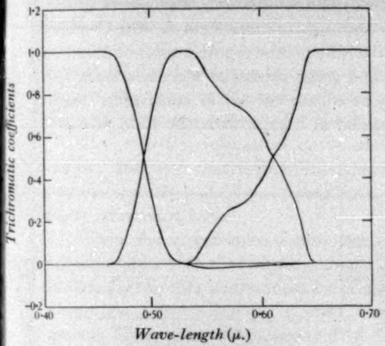

Figure 12. Spectral coefficients. J. H. N. (1) units. Observer E.

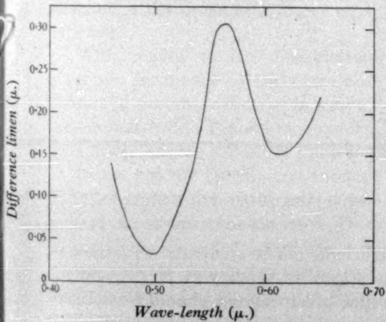

Figure 13. Hue-discrimination curve. Observer E.

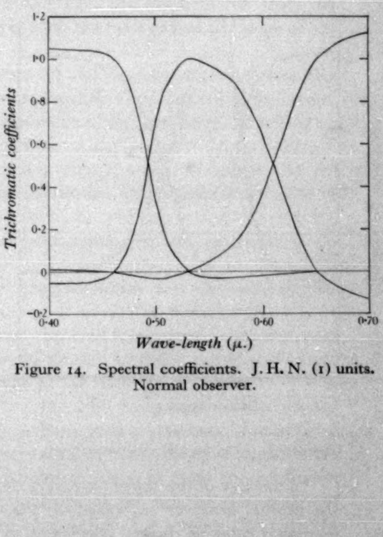

Figure 14. Spectral coefficients. J. H. N. (1) units. Normal observer.

The existence of the negative blue coefficient in the yellow region is somewhat doubtful in all three cases, but the measurements tended to confirm its presence.

Although somewhat uncertain in value, it was, with the negative red in the blue-green region, definitely necessary in order to obtain a match in the case of observers B and C, but a match was obtained in the blue-green region by observer E with only the blue and green primaries. In all three cases it was found possible to obtain a perfect match between 0·70 μ. and the red primary, and so no coefficients were measured in the extreme red. This would be expected also from the values of the hue-discrimination limen. In the violet in the case of observers B and C some difficulty was found in matching 0·43 μ. with the blue primary, and it was not possible to match 0·41 μ. In both these cases the red and green primaries were necessary for a satisfactory match, but the results were by no means certain or consistent. With observer E a perfect colour-match was obtained at 0·41 μ. with the blue primary alone.

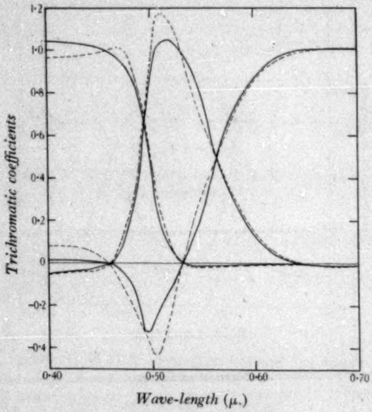

Figure 15. Spectral coefficients. J. H. N. (2) units. Observer L ——; normal observer – – – –.

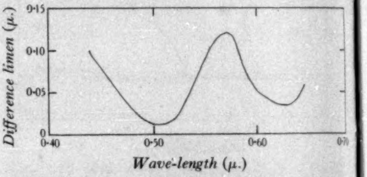

Figure 16. Hue-discrimination curve. Observer L.

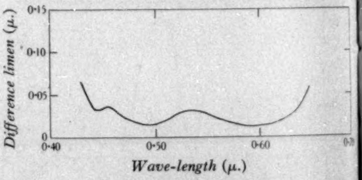

Figure 17. Hue-discrimination curve. Normal observe

In the case of the above observers the coefficients can be compared with those of the normal observer expressed on the same system of units, J. H. N. (1), and the increased value of the red coefficient in the blue-green regions should be noticed. This increase was not present in the case of observer B but, while the negative red was necessary, an accurate setting could not be obtained in the region.

As the results for only one protanomalous observer are given, it is impossible to talk of any stages of protanomaly except by comparison with the results for the deuteranomalous observers. The spectral coefficients for observer L are expressed in a different set of units, J. H. N. (2), from those for the deuteranomalous observers, and they may be compared with the coefficients of the normal observer expressed in the same units. In the yellow region both curves are of the same type, while at the same time the hue-discrimination is nowhere very poor, being comparable with that of observer D of the deuteranomalous observers. The angle of the red and green curves in the region of 0·54 μ. is not as sharp as in the case of the normal, but this is to be expected in view of the difference in the values of the negative red coefficient in the blue-green region, and there cannot be said to be any flattening of the curves like that which was present in the case of the deuteranomalous observers. However, it must be noticed that the rate of change of slope in the case of the normal curve is continuous from about 0·52 μ. to the extreme red, while this does not obtain in the case of observer L, his curve being convex between the extreme red and 0·56 μ. and concave between 0·56 and 0·52 μ. In the blue-green and violet regions the value of the red coefficient is less than the normal. In the former the negative red was necessary for the match and was readily measurable.

The hue-discrimination curve shows no secondary minimum in the violet region, and the discrimination extends farther into the extreme red than the normal, the value at 0·65 μ. being little poorer than the normal and the slope of the curve somewhat less.

When the equal-energy luminosity curves of the deuteranomalous observers are compared with that of the normal observer, the differences are not so striking as in the case of other characteristics. Even the position of the maximum, by which the observer is conventionally defined, does not show a displacement towards the red greater than those which occur in the variation among normal observers. In the case of the one protanomalous observer the maximum of the luminosity curve is definitely moved to the blue, and lies between the normal maximum and the position of the maximum found by Pitt for protanopes, the red luminosity being depressed.

With regard to the definition of the protanomalous and deuteranomalous observers by means of their luminosity curves, it would be more satisfactory to define the protanomalous as having a relatively low red luminosity, compared with the normal, while the deuteranomalous should be said to differ but slightly from the normal, giving relatively more importance to the red than the green.

In the case of the spectral-mixture curves, the differences between the normal and the anomalous become even more marked than in the coefficient curves. Again we find the curves of observers A, D and F very similar. A similarity of shape would of course be expected, since the mixture curves are derived from the coefficient curves and the luminosity curve with a knowledge of the relative luminosity of the primaries. The similarity of the mixture curves therefore implies that both the coefficients and the relative luminosities of the primaries are similar. The red curve is depressed nearly uniformly in comparison with the normal, while the green curve fills out in proportion. In the blue and violet regions the blue curve is depressed, and the red and green curves are nearer the axis, while the total luminosity is of the same order as the normal. The luminosity curve for observer D is broader than the normal, and there is a small irregularity in the red curve.

The curves for observers C and E are again very similar, but the differences between them and those for observer B have become more marked. The irregularity in the red curve is quite marked, but the total luminosity curve for observer E has a rather broader maximum than the normal and in consequence the green curves differ. In the case of observer B the red and green curves tend to run almost parallel over a long range, hence the red luminosity is increased relative to the green, and the curve falls very sharply just before 0·53 μ. The blue curves are still further depressed in all three cases, reaching a little more than one-fifth of the normal value for observer B. At the same time the red and green luminosities have become negligible in this region.

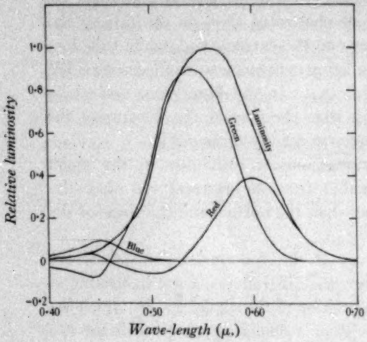

Figure 18. Luminosity and mixture curves for equal-energy spectrum. Normal trichromat.

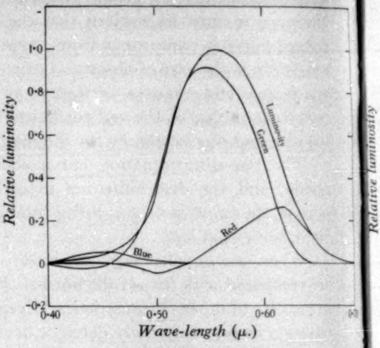

Figure 20. Luminosity and mixture curves for equal-energy spectrum. Observer D.

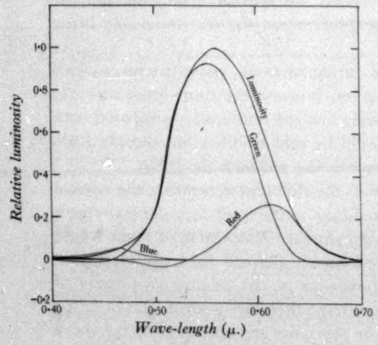

Figure 19. Luminosity and mixture curves for equal-energy spectrum. Observer A.

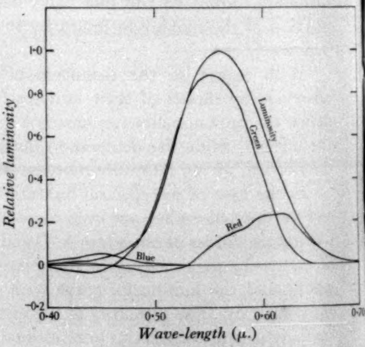

Figure 21. Luminosity and mixture curves for equal-energy spectrum. Observer F.

In consequence of the reduction of the total luminosity of the red region of the curve for observer L, the red mixture curve becomes very small, being comparable with the blue curve. Throughout the central region the green curve dominates the mixture, but in the violet region the negative green is small and the red is negligible, the mixture being dominated by the blue. In this region the blue luminosity is of the same order as the normal; thus since the red and green are less important, the blue is relatively more important for the protanomalous than for the normal observer. It is interesting to note that in spite of this blue dominance and consequent smallness of the change in relative composition with wave-length, the hue-discrimination is not made very much poorer than the normal.

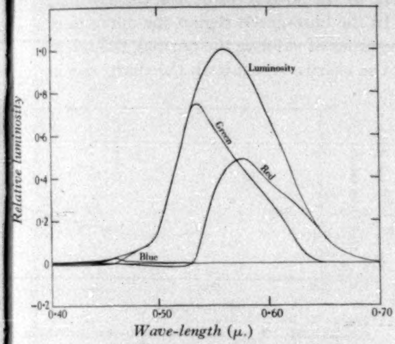

Figure 22. Luminosity and mixture curves for equal-energy spectrum. Observer B.

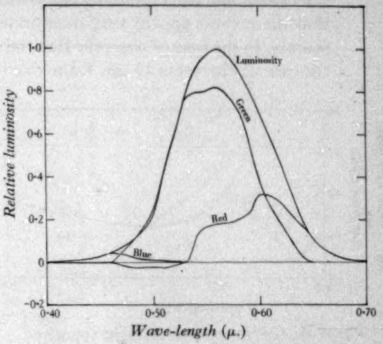

Figure 23. Luminosity and mixture curves for equal-energy spectrum. Observer C.

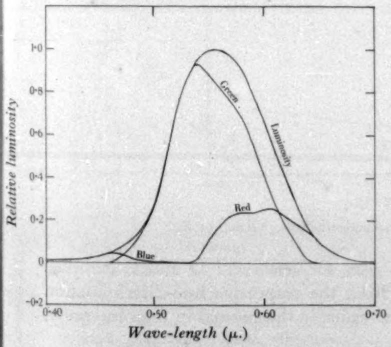

Figure 24. Luminosity and mixture curves for equal-energy spectrum. Observer E.

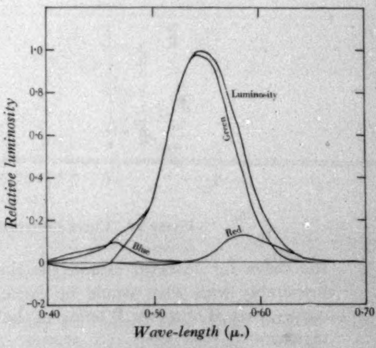

Figure 25. Luminosity and mixture curves for equal-energy spectrum. Observer L.

Saturation-discrimination curves have only been taken for observers B, D and E. We have seen that in the red-yellow-green region the hue-discrimination is low and in consequence the colours are all much more similar than in the case of the normal observer. Since the colours are very similar it is natural that the differences between them and white should be more nearly the same; thus it is to be expected that the saturation-discrimination will not change much with wave-length in this region. This is found in practice with all three observers, the value of the saturation-discrimination corresponding approximately to the lowest value for the normal; thus the colours appear very desaturated. In the blue-green region the curve rises sharply, in the case of observer B to the same order of value as the normal, though in the case of observers D and E the rise is not so sharp. Again both the sharp rise in the curve for observer B and the slower rises for observers D and E compare favourably with what would be expected from the respective hue-discrimination curves, that of observer B being of the same order as the normal in the blue-green region.

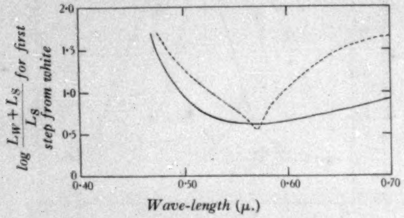

Figure 26. Curves for saturation-discrimination. Observer B. Dotted curve gives normal values for comparison.

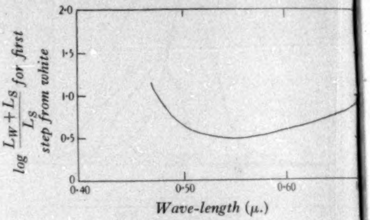

Figure 27. Curve for saturation-discrimination. Observer D.

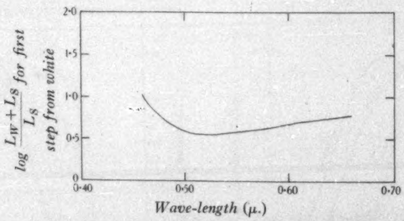

Figure 28. Curve for saturation-discrimination. Observer E.

The trichromatic coefficients have also been shown in the form of a colour-triangle. While the shape of the triangle will depend mainly on the choice of unit colours, the differences between the observers are readily shown by the differences in the grouping of the points for different wave-lengths and by the position of the white (S_B) point. The position of this white point may be compared with that of the normal observer shown in the same system. The difference between the normal and the anomalous position of the white point falls, for the observers shown, into roughly two classes. In the case of observers A, B, C and E it is displaced towards the yellow and the yellow-green, but in the case of observers D and F it is displaced predominantly towards the red.

The colour-triangles have been used to find the complementary wave-lengths for each observer. With the exception of the curve for observer C these are of the

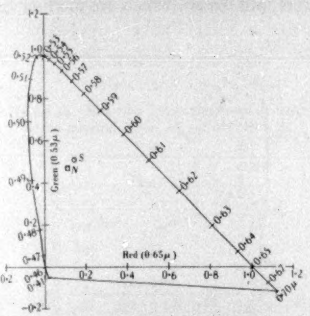

Figure 29. Spectral locus plotted in colour-triangle. J. H. N. (1) units. Observer A. *N*, white point for normal observer; *S*, white point for observer A.

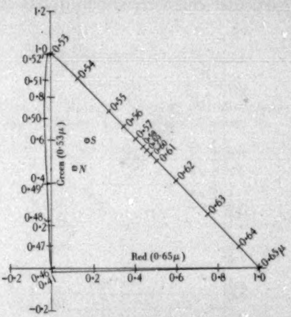

Figure 30. Spectral locus plotted in colour-triangle. J. H. N. (1) units. Observer B. *N*, white point for normal observer; *S*, white point for observer B.

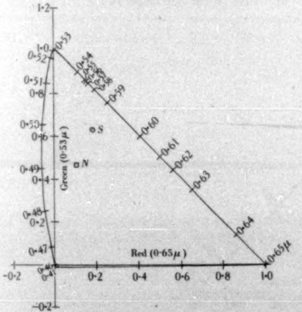

Figure 31. Spectral locus plotted in colour-triangle. J. H. N. (1) units. Observer C. *N*, white point for normal observer; *S*, white point for observer C.

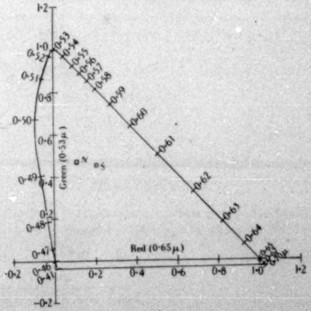

Figure 32. Spectral locus plotted in colour-triangle. J. H. N. (1) units. Observer D. *N*, white point for normal observer; *S*, white point for observer D.

same smooth type as for the normal, the curve for observer C being re-entrant at about 0·61μ. At the red end of the spectrum all the curves are of the same order as the normal, but there are considerable differences in the violet end, observers A, C, D and F requiring a wave-length between 0·58 and 0·60μ. to mix with 0·40μ., while observers B and E require between 0·54 and 0·56μ., the normal value being about 0·57μ. In the case of observer L there is a change in the red, the wave-length to be mixed with the extreme red being changed from about 0·50 μ. for the normal to about 0·49 μ. The change in the violet is of the same order, being from about 0·57 to 0·58 μ.

In the above discussion of results, it has been possible in the discussion of each particular characteristic to divide the observers into classes which are more or less similar. It is of interest to express these classes in a table; this has been arranged so that the members of group I are in general more similar to the normal than those of group II (table 4).

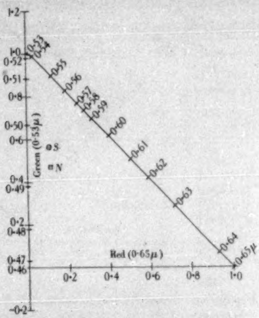

Figure 33. Spectral locus plotted in colour-triangle. J. H. N. (1) units. Observer E. *N*, white point for normal observer; *S*, white point for observer E.

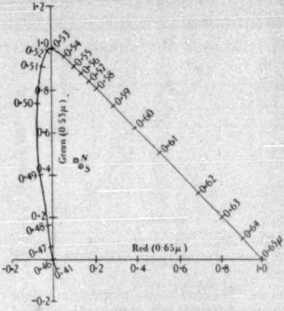

Figure 34. Spectral locus plotted in colour-triangle. J. H. N. (1) units. Observer F. *N*, white point for normal observer; *S*, white point for observer F.

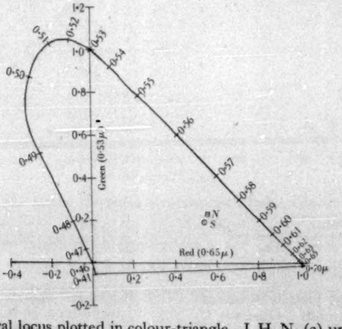

Figure 35. Spectral locus plotted in colour-triangle. J. H. N. (2) units. Observer L. *N*, white point for normal observer; *S*, white point for observer L.

In addition to the results obtained for observers A to F and L, observations were made by several other observers. Observer G (figure 43) is a deuteranomalous observer with approximately the same amount of defect as observer C, according to

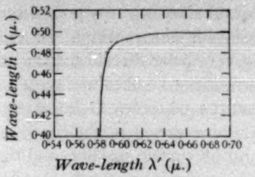

Figure 36. Relation between complementary wave-lengths λ and λ′, for observer A.

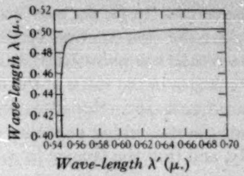

Figure 37. Relation between complementary wave-lengths λ and λ′, for observer B.

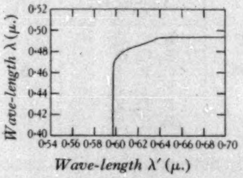

Figure 38. Relation between complementary wave-lengths λ and λ′, for observer C.

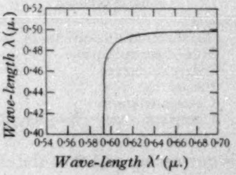

Figure 39. Relation between complementary wave-lengths λ and λ′, for observer D.

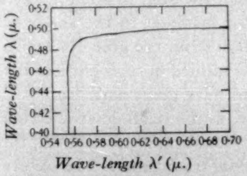

Figure 40. Relation between complementary wave-lengths λ and λ′, for observer E.

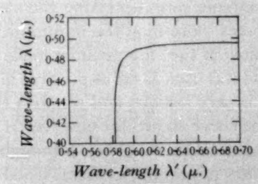

Figure 41. Relation between complementary wave-lengths λ and λ′, for observer F.

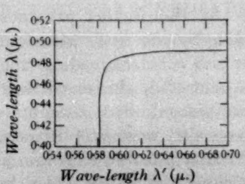

Figure 42. Relation between complementary wave-lengths λ and λ′, for observer L.

the hue-discrimination curve shown. This curve is especially interesting, however, as it is probably by far the most accurate of the curves showing very poor discrimination, since the observer was very careful in making his observations. At this point it is convenient to point out that curves showing very poor discrimination and very rapid changes in the value of the difference limen cannot be obtained with any high degree of accuracy. Suppose, for example, that the observer G is taking a step towards the red, which in reality ends at 0·56 μ.; now at 0·56 μ. the limen is rising rapidly, and thus the change in colour is small and becoming smaller, and therefore it is very easy to pass to a place beyond the maximum, say at 0·60 μ., where the limen is decreasing and thus the step is more easily determined. As can be seen this would add 0·04 μ. to the value of the step. It is possible to ensure against this type of error to a certain extent by repetition of the results, when those which are not consistent must not be included; the safest method is, however, for the observer to take extreme care in making the step, and to make the step in such a way that he never sees more than the minimum difference; for instance, in the above example, the whole of the step must be made in the direction from the green to 0·56 μ. This method was used as far as possible in making observations in such parts of the curve, but it is very tedious and requires the observer to have great patience.

Table 4

Characteristic	Group I	Group II	Group III
Trichromatic coefficients	A, D, F	B, C, E	
Hue-discrimination	A, D	B, C, E	
Mixture curves	A, D, F	C, E	B
Saturation disc	B	D, E	
Colour-triangle	A, C	B, D, E, F	
Complementary wave-lengths	A, D, F	B, E	C

The curve shown for observer H is incomplete, as the readings in the violet have only been taken roughly. Although that part of the curve is not shown, there is a secondary minimum, as seems usual with the normal trichromat. The observer was to all intents normal, the rise in the yellow region being only from the normal value of 0·0010 to 0·0015 μ.; his position on the Nagel distribution curve was, however, on the extreme of the normal towards the deuteranomalous.

Observations were taken by two further protanomalous observers. A large number of results were taken by the first, who found colour-matching rather difficult in that he could not give constant readings for the proportion of the red-green and blue constituents, and could do so still less for the luminosity values. Before the observations were discontinued, attempts were made to obtain hue-discrimination readings; these also were very inconsistent. In the case of the second observer, M, it was found possible to obtain a hue-discrimination curve. The curve shows a high discrimination in the violet, but no secondary minimum. In the case of the coefficients the values of the proportions of the constituents were quite constant, but the luminosity values varied widely, two consecutive readings differing by as much as 100 per cent. Several attempts were made to obtain accurate settings before the readings were discontinued. It seems worth recording that such an effect was not found in the case of any of the deuteranomalous observers, or in the case of observer L. Any difficulties found in the case of the deuteranomalous luminosity curves were generally definite errors, which appeared also in the values of the coefficients.

One observer was found and classed as deuteranomalous from his Nagel reading; this classification was borne out by his luminosity readings, but his hue-discrimination showed only about two colour steps between 0·54 and 0·65 μ., and it was impossible to obtain any coefficients in the yellow region. Measurements were then taken with the blue and green primaries alone, as if the observer had been a deuteranope, and in the region between 0·46 and 0·59 μ. satisfactory matches were obtainable, but it was found impossible to obtain a match at 0·65 μ. No results are given for this observer; the coefficients between 0·46 and 0·53 μ. are similar to those given by Pitt for a deuteranope. Clearly in the case of the coefficients in the yellow region some special convention would have to be adopted, owing to the large tolerances by which a match must be defined for this type of observer.

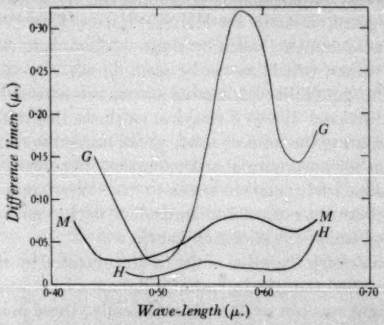

Figure 43. Hue-discrimination curves. Observers G, H, M.

§7. PREVIOUS INVESTIGATIONS

As regards the statistical survey, there have already been several very full sets of results for the percentage of colour anomalies occurring. Those of Schmidt(7), Waaler(11) and von Planta(12) have been referred to and comparison has been made. In his paper von Planta gives a survey of a large number of sets of statistics, and discusses the possibility of racial differences. However, while these workers used the anomaloscope, they do not publish a curve or table showing the variation of the red-to-green ratio needed in the match for different observers, although such a curve is given by Houston(18). For the author's purpose a repetition of the results was in any case necessary, for it was desirable to know the position on the distribution curve of the anomalous observers examined, and if possible to select a wide range of observers. In practice it was necessary to select the observers for their reliability rather than for their position on the distribution curve, although, as can be seen from table 3, the range also is satisfactory.

The results obtained by Schmidt, Waaler and von Planta show that a large number of women were examined; in the author's examination men were chosen in preference to women owing to the relatively greater chance of finding observers with defective colour-vision.

After the discovery of anomalous trichromatism by Lord Rayleigh(2), many cases were investigated, notably by Hering(13), von Kries(14), and Abney and Watson(15). The measurements taken by these workers were mainly concentrated on the luminosity values, which, as can be seen, do not vary as much as the other characteristics. The possibility of anomalous trichromatism being caused by a colour pigment is discussed by von Kries, and he shows that this explanation is unsatisfactory by comparing the ratio of red to green needed to match various colours in the yellow region for both normal and anomalous observers. Much of Abney's research on anomalous trichromatism seems to have been based on the assumption that the difference between normal and anomalous trichromatism was caused by a reduction or shift of one of the sensation curves.

In the main, in assessing the value of the results obtained by earlier investigators, it must be borne in mind that the intensity of light available was very low, and the question of stray light was not dealt with sufficiently; these points are if anything of more importance in the investigation of anomalous than of normal observers, since the tolerances for a match in the yellow region are often very large, and ease of observation will tend to reduce these tolerances to a minimum.

In the measurement of the hue-discrimination limen the necessity of equating the intensities of the two halves of the field throughout the observation was not realized until quite recently. In general the two halves were made equal in intensity when the wave-lengths were the same, and then one wave-length was changed until the smallest detectable difference between the two halves was found. Clearly, in view of the variation of luminosity with wave-length, the limen found by this method will be due to differences partly of colour and partly of intensity.

Steindler(16) gives the hue-discrimination curves for normal trichromats and for dichromats, but the precaution of keeping the two halves of the field at the same intensity was not taken, and so the results are not comparable with other measurements. It is, however, worth noting that the curve given as for a protanope shows discrimination in the yellow region of the spectrum, and may therefore have been for a protanomalous observer. As, however, the limen in which the results are expressed is a complex mixture of intensity and colour, this is by no means certain.

The importance of eliminating stray light in hue-discrimination measurements cannot be over-estimated. For example, during a series of observations in the violet region for observer A the apparatus was found to be out of adjustment in such a way as to allow a small quantity of stray light to enter, and the results bore no relation to those obtained immediately after the apparatus had been readjusted.

The results obtained by Pitt were taken with the apparatus used by the author, so that the necessary precautions as to stray light and the convenience of observation were those fully detailed by Wright in his paper describing the apparatus. Reference to Pitt's paper will show that luminosity, spectral-mixture, and hue-discrimination curves for three deuteranomalous observers W. F. T., E. H. B. M., D. H. K. L. are given. These observers can be seen to belong to the same type as the author's observers A and D; it is in this respect that the results obtained by the author differ from those obtained by Pitt, for although there are not many more observers they vary considerably in type. In the case of observers W. F. T. and D. H. K. L. the point of maximum luminosity has been moved to the red more than in the case of observers A and D, being at about $0{\cdot}57\mu$. The curves for W. F. T. are somewhat different from the rest both of Pitt's and of the author's observers, the blue-mixture curve being more comparable with the normal in size, but having its maximum moved to the violet, while the red-mixture curve has its maximum moved to the red. This displacement is accompanied by an extension of the hue-discrimination curve into both the red and the violet regions far beyond the normal. A further point of interest is a comparison between the green-mixture curves of observers D. H. K. L., E and B, there being a general similarity of shape in the neighbourhood of $0{\cdot}56\mu$. in all three cases, notwithstanding the fact that the characteristics as a whole are different.

§ 8. THEORETICAL CONSIDERATIONS

Since the anomalous trichromat has a trichromatic system of colour-vision, each match is unique, although in practice it may be difficult to determine the exact constituents of the match. Owing to the poor hue-discrimination in the yellow region it will be possible to select two colour mixtures, both of which match the same spectral colour for the anomalous trichromat. These same two mixtures would of course be different for the normal trichromat and may perhaps both fail to match the spectral colour. Such a state of affairs must not be considered to mean that the match for the anomalous trichromat is not unique, since it is merely caused by unusually large tolerances that this type of observer gives to a colour match. In applying the term "unique" to the anomalous match, or for that matter to the normal match, a range of mixtures, the size of which is determined by the hue-discrimination, must be considered as satisfying the match, but outside this range there is no other range that would do so. Further, it is necessary to consider that the hue-discrimination has a definite finite value in the region; for instance if a dichromat is asked to make a match in the yellow region using red, green, and blue primaries, then the settings for the red and green readings cannot be unique if the primaries are such that he can obtain a perfect colour-match between the red and green primaries.

The match given by the anomalous trichromat is not the same as that given by the normal trichromat, and conversely the normal match is not valid for the anomalous observer, as it is in the case of the dichromat. From the statement that the normal match is not valid for the anomalous observer, the limiting type of observer mentioned at the end of § 5 must be excepted, since for him the normal match is satisfactory as a result of the large tolerances allowed for a match by this type of observer. The importance of the fact that the normal and anomalous matches are different and that the normal match is not satisfactory for the anomalous observer cannot be stressed too highly, and in any attempt to correlate normal and anomalous trichromatism it makes any uniform reduction of one of the hypothetical fundamental sensation curves invalid as an explanation(1).

An examination of the Nagel distribution curve is the most natural beginning in a discussion of the nature of the relation between normal and anomalous trichromatism. To the question whether the anomalous trichromats are an intermediate stage between normal trichromats and dichromats, the continuous form of the Nagel curve would suggest an affirmative answer. But if this question is modified and we wish to know whether there is a continuous gradation between normal and dichromatic vision, the curve gives a modified answer. On the protanomalous side of the curve we find a continuous gradation from the normal to the dichromat; owing to the fact that the number of observers examined was not very large, any small irregularities which might be present would not be evident, but if they exist they must be smaller than the maximum found for the deuteranomalous. On the other hand, on the side of the deuteranomalous observers we find a secondary maximum in the curve, showing that while there may be observers at any point between the normal and the deuteranope there is one place at which the formation of anomalous trichromatism is more likely than elsewhere.

Suppose we consider the evolutionary development suggested by McDougall(17) on the basis of the trichromatic theory. According to this theory, from the monochromatic state the blue and yellow sensations are supposed to have developed first, and later the yellow is supposed to have split up into red and green. The type of curve to be expected from this theory would be a central maximum with the sides sloping away to the protanopes and the deuteranopes, and the rates of falling off would be in some way proportional to the numbers of protanopes and deuteranopes respectively. Alternatively, purely on the grounds of probability, the type of curve to be expected would have a sharp central maximum and fall away equally on each side. In practice, on the protanomalous side there is a uniform rate of falling away, but the number of observers found at a distance from the central maximum is perhaps greater than would be expected purely on the grounds of probability. On the side of the deuteranomalous observers, on the other hand, there is a secondary maximum reaching a height of about 1/25 of the main maximum, and being much flatter it spreads over about the same range on a logarithmic scale as the main maximum. The existence of this maximum shows that in some way the deuteranomalous state is peculiar and is to be distinguished from other forms of colour deficiency. From the point of view of evolutionary development, the existence of so many deuteranomalous observers and their particular distribution would indicate that the state was evolutionarily stable as compared with the protanomalous state. This might be taken to mean that in the splitting of the yellow sensation, as visualized by McDougall, two stages are necessary for the complete process in the transition between the deuteranope and the normal. Alternatively in view of the fact that Schmidt⁽⁷⁾ finds a definite gap between the normal and deuteranomalous observers in the Nagel distribution curve, it may be that there are two alternative ways in which the deuteranopic state may develop, the most usual being a development to the normal, and the secondary being a development to the deuteranomalous state. While the latter arrangement should be considered as possible, it would seem to be unlikely since it would imply that there were two distinct forms of deuteranope and that, further, in the most usual change (between the deuteranope and the normal) there were no intermediate stages as there are in the case of the protanomalous observers, although the existence of observers throughout the whole range in the case of the author's results would supply this deficiency. Further, the symmetrical shape of the deuteranomalous maximum would seem to support the idea of a continuous transition between the deuteranope and the normal, with a preferential state corresponding to the deuteranomalous maximum.

Before considering the mechanism by which these changes may be produced, it is convenient to discuss the characteristics of the anomalous trichromats in a general way and to compare them with those of the normal trichromat. The general form of the curves for the anomalous trichromat is similar to that for the normal trichromat, but in the hue-discrimination curves we find a definite shift of the salient points towards the red end of the spectrum for both protanomalous and deuteranomalous observers. Moreover this shift is not limited to the yellow region, but in the case of observers A and B, where there is a point of maximum discrimination in the violet region, this is also moved towards the red. In the case of two of Pitt's observers this shift towards the red only holds in the yellow region, the blue-green point of maximum discrimination being moved towards the violet.

In an appendix to Pitt's report on dichromatism⁽¹⁾, W. D. Wright gives a theoretical discussion, and points out that if an observer is asked to point to the colour in the spectrum between red and green, which has the properties of neither red nor green, then most observers will point to very nearly the same place.

During the investigations each of the anomalous observers was asked to point to this "pure yellow," and when a ground glass screen was placed in the spectrum it was found that the observers were very definite about the position of the yellow, which was slightly to the green side of the normal in the case of the protanomalous and to the red in the case of the deuteranomalous. When the observers were asked to set the test colour of the colorimeter, however, it was not generally possible to get concordant results. The results for observer C were sufficiently good to enable a mean to be taken, and a value of $0{\cdot}595\,\mu$. was found, as compared with approximately $0{\cdot}580\,\mu$. for the normal. In the movement of the colour which the observer calls "pure yellow", we find a movement one way for the protanomalous and the other way for the deuteranomalous, while in the characteristic points of the hue-discrimination curve both protanomalous and deuteranomalous are moved in the same direction.

If the differences between the normal and anomalous hue-discrimination curves are taken as a measure of the degree of deficiency of the observer, then it can be seen that the other characteristics cannot always be treated as an obvious guide to the extent of the defect. The mixture curves should to some extent be excepted from this, as in a general way they show the sensitivity of the observer to changes in hue. In the case of the protanomalous observer the evidence of his relatively high hue-discrimination in the red would not seem to be present; however it is at the ends of the spectrum that the difference between theory and practice becomes most evident in the theoretical curves given by von Helmholtz(9) and Schrödinger. If a relation is found between the difference limen and the differential coefficients of the proportions of the fundamental sensations with respect to the wave-length, or, more generally, between the difference limen and some function of the fundamental sensations, it must apply equally to all forms of colour-vision. In fact the true relation would only require that the appropriate fundamental sensations should be used, when it would be equally applicable to the normal, the anomalous trichromat, and the dichromat. In fact the most thorough test of such a relation, when it has been worked out for a normal trichromat, would be its application to the characteristics of an anomalous trichromat. This apparent discrepancy between the various characteristics is particularly noticeable as regards the position on the Nagel distribution curve. For example in the case of observers A and D (see tables 3 and 4)

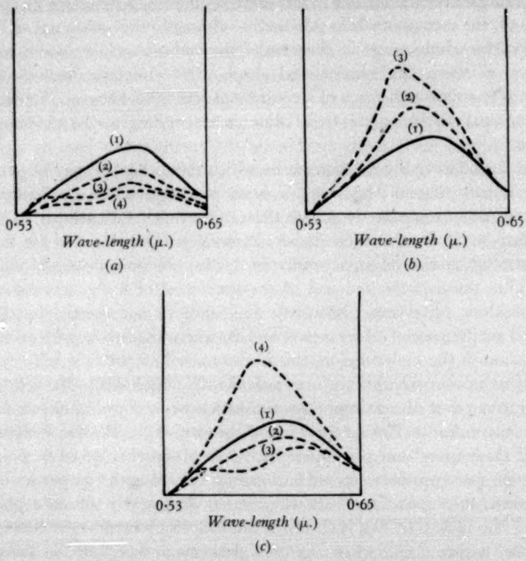

Figure 44. Showing the possible changes in the red luminosity curve between the normal and the dichromat.

A is farther from the normal than D on the Nagel curve, but his hue-discrimination is the more nearly normal. To some extent this can be accounted for by the differences in relative luminosity, as can be seen by a comparison of the luminosity curves in the regions of 0·535 and 0·65 μ. Thus the individual characteristics cannot be regarded as a continuous series of states between normal trichromatism and dichromatism.

The changes between normal and anomalous observers shown in the mixture curves appear to be of a complex nature. The problem is complicated by the form of the red curve in the cases of observers C and E. From the point of view of the mixture curves, there seem to be three possible ways through which a series of changes between normal and dichromat could be made. These can be best shown by means of figures; in figures (44*a*) and (44*b*) we have the changes shown as two entirely separate mechanisms, which must both exist together. In (*a*) the change is obtained by a transformation from the normal through the types represented by observers C and E and the final disappearance of the red curve into insignificance. In the case of method (*b*) the changes are given an alternative path passing from the normal to the type represented by observer B, the red curve finally merging into the green curve. The third possibility is in reality a combination of the former two, and is shown in figure (44*c*). In this case the changes are supposed to take place, from the normal, through the types represented by observers A and C and finally instead of the red curve disappearing, the point of inflection is moved higher up the curve, giving the type represented by observer B, and the red curve joins up with the green curve as in case (*b*).

The idea of there being two evolutionary modes in the case of the deuteranomalous was introduced previously (page 687) and in this case the possibility of the deuteranomalous as an alternative final state was suggested. This might be modified to include two types of change, the first, similar to the protanomalous, being continuous between normal and deuteranope, and the second series having a preferential state through which it must pass or at which it must remain, corresponding to the maximum in the deuteranomalous region.

The actual mechanism by which such changes may be produced are clearly complex, and will probably not rest entirely in the photochemical changes or in the subsequent analysis. While the possibility of some differences between the photochemical substance in the retina of the normal and anomalous observers might be considered, further evidence from adaptation phenomena and the physiology of the anomalous eye is necessary.

§9. ACKNOWLEDGEMENTS

The author wishes to express his gratitude to Dr W. D. Wright for his help and interest both in the carrying out and the presentation of this work. The author's thanks are also due to all those who made the observations, to the Physical Society and to the Staff of the Fulham Labour Exchange for facilities for parts of the statistical survey (and in particular to Mr P. Rainsford Hannay for his help in this part of the work), and to the Medical Research Council for their financial assistance.

REFERENCES

(1) Pitt, F. H. G. *Spec. Rep. Ser. Med. Res. Coun., Lond.*, No. 200 (1935).
(2) Lord Rayleigh. *Nature, Lond.*, **25**, 64 (1882).
(3) Wright, W. D. *Trans. Opt. Soc. Lond.* **29**, 225 (1927–8).
(4) Smith, T. and Guild, J. *Trans. Opt. Soc. Lond.* **33**, 73 (1931–2).
(5) Wright, W. D. *Spec. Rep. Ser. Med. Res. Coun., Lond.*, No. 139 (1929).
(6) Trendelenburg, W. *Klin. Mbl. Augenheilk.* **83**, 721–32 (1929).
(7) Schmidt, I. *Z. Bahnärzt.* **2** (1936).
(8) Judd, D. B. *J. Opt. Soc. Amer.* **23**, 359 (1933).
(9) von Helmholtz, H. *Handbuch der Physiologischen Optik*, 2. Auflage, p. 455.
(10) Schrödinger, E. *Ann. Phys., Lpz.*, **63**, 483 (1920).
(11) Waaler, G. H. M. *Acta Ophthal., Kbh.*, **5**, 301–45 (1927) and *Z. indukt. Abstamm.- u. VererbLehre*, **45**, 270 (1927).
(12) von Planta, P. *Arch. Ophthal., Kbh.*, **120**, 255 (1928).
(13) Hering. *Lotos*, **6** (1885).
(14) von Kries, J. *Z. Psychol. Physiol. Sinnesorg.* **19**, 64 (1899).
(15) Abney, Sir W. de W. *Researches in Colour Vision*, p. 293. (London, 1913.)
(16) Steindler, O. *S.B. Akad. Wiss. Wien*, Abt. II *a*, **115**, 39 (1906).
(17) McDougall, W. *Mind*, N.S., **10**, 212–4 (1901).
(18) Houston, H. A. *Vision and Colour Vision* (London, 1932).

Table 5. Characteristics for observer A

Wave-length λ (μ.)	Relative luminosity of equal-energy spectrum	Trichromatic coefficients J.H.N. (1) units			Mixture curves for equal-energy spectrum			Complementary wave-lengths (μ.)		Hue-discrimination; just-noticeable wave-length differences (μ.)	Saturation-discrimination log $\frac{L_W+L_S}{L_S}$	Wave-length λ (μ.)
		B (0·46μ.)	G (0·53μ.)	R (0·65μ.)	L_B	L_G	L_R	λ	λ'			
0·41	0·0060	1·032	−0·050	0·018	0·0096	−0·0055	0·0019	0·41	0·5820	—	—	0·41
0·43	0·0120	1·024	−0·037	0·013	0·0167	−0·0071	0·0024	0·43	0·5825	0·0048 (0·44)	—	0·43
0·45	0·0286	1·016	−0·021	0·005	0·0351	−0·0085	0·002	0·45	0·5836	0·0033	—	0·45
0·46	0·050	1·000	0·000	0·000	0·050	0·000	0·000	0·46	0·5842	0·0025	—	0·46
0·47	0·073	0·951	0·057	−0·008	0·045	0·032	−0·004	0·47	0·5858	0·0029	—	0·47
0·48	0·100	0·849	0·178	−0·027	0·032	0·080	−0·012	0·48	0·5888	0·0023	—	0·48
0·49	0·140	0·651	0·410	−0·061	0·019	0·141	−0·020	0·49	0·5997	0·0017	—	0·49
0·50	0·234	0·393	0·690	−0·083	0·012	0·251	−0·029	—	—	0·0016	—	0·50
0·51	0·438	0·171	0·896	−0·067	0·008	0·463	−0·033	—	—	0·0017	—	0·51
0·52	0·683	0·033	1·001	−0·034	0·002	0·704	−0·023	—	—	0·0024	—	0·52
0·53	0·828	0·000	1·000	0·000	0·000	0·828	0·000	—	—	0·0036	—	0·53
0·54	0·919	−0·015	0·992	0·023	0·000	0·899	0·020	—	—	0·0054	—	0·54
0·55	0·974	−0·020	0·970	0·050	0·000	0·929	0·045	—	—	0·0072	—	0·55
0·56	1·000	−0·022	0·934	0·086	0·000	0·918	0·082	—	—	0·0079	—	0·56
0·57	0·976	−0·020	0·886	0·134	0·000	0·853	0·123	—	—	0·0065	—	0·57
0·58	0·918	−0·018	0·821	0·197	0·000	0·743	0·175	—	—	0·0048	—	0·58
0·59	0·830	−0·015	0·740	0·275	0·000	0·612	0·218	0·4811	0·59	0·0039	—	0·59
0·60	0·692	−0·012	0·627	0·385	0·000	0·435	0·251	0·4902	0·60	0·0036	—	0·60
0·61	0·547	−0·010	0·505	0·505	0·000	0·279	0·268	0·4936	0·61	0·0037	—	0·61
0·62	0·408	−0·008	0·360	0·648	0·000	0·150	0·258	0·4957	0·62	0·0040	—	0·62
0·63	0·289	−0·005	0·195	0·810	0·000	0·058	0·231	0·4973	0·63	0·0046	—	0·63
0·64	0·183	−0·003	0·072	0·931	0·000	0·014	0·169	0·4981	0·64	0·0058	—	0·64
0·65	0·110	0·000	0·000	1·000	0·000	0·000	0·110	0·4984	0·65	0·0073	—	0·65
0·67	0·0316	0·000	−0·077	1·077	0·000	−0·0025	0·0341	—	—	—	—	0·67
0·70	0·0056	0·000	−0·120	1·120	0·000	−0·0007	0·0063	0·4989	0·70	—	—	0·70
1931 C.I.E. S_B source		0·343	0·511	0·146	Relative luminosities of trichromatic units of primaries							
λ=0·61μ.		−0·010	0·505	0·505	0·46μ.	0·53μ.	0·65μ.					
λ=0·5825μ.		−0·017	0·803	0·214								
λ=0·4940μ.		0·537	0·537	−0·074	0·085	1·000	0·959					

Table 6. Characteristics for observer B

Wave-length λ (μ.)	Relative luminosity of equal-energy spectrum	Trichromatic coefficients J.H.N. (1) units			Mixture curves for equal-energy spectrum			Complementary wave-lengths (μ.)		Hue-discrimination; just-noticeable wave-length differences (μ.)	Saturation-discrimination log $\frac{L_W+L_S}{L_S}$	Wave-length λ (μ.)
		B (0·46μ.)	G (0·53μ.)	R (0·65μ.)	L_B	L_G	L_R	λ	λ′			
0·41	0·005	1·014	−0·019	0·005	0·0070	−0·0033	0·0013	0·41	0·5453	—	—	0·41
0·43	0·010	1·010	−0·013	0·003	0·0128	−0·0042	0·0014	0·43	0·5454	0·0146	—	0·43
0·45	0·012	1·008	−0·009	0·001	0·0148	−0·0034	0·0006	0·45	0·5456	0·0052	—	0·45
0·46	0·023	1·000	0·000	0·000	0·023	0·000	0·000	0·46	0·5457	0·0032	—	0·46
0·47	0·040	0·907	0·105	−0·012	0·012	0·034	−0·006	0·47	0·5470	0·0028	1·700	0·47
0·48	0·060	0·798	0·220	−0·018	0·008	0·059	−0·007	0·48	0·5480	0·0020	—	0·48
0·49	0·082	0·630	0·395	−0·025	0·005	0·085	−0·008	0·49	0·5513	0·0013	1·120	0·49
0·50	0·166	0·330	0·700	−0·030	0·003	0·174	−0·011	0·50	0·6235	0·0011	—	0·50
0·51	0·323	0·145	0·880	−0·025	0·002	0·335	−0·014	—	—	0·0013	0·845	0·51
0·52	0·526	0·020	0·998	−0·018	0·001	0·540	−0·015	—	—	0·0023	—	0·52
0·53	0·730	0·000	1·000	0·000	0·000	0·730	0·000	—	—	0·0048	0·705	0·53
0·54	0·878	−0·004	0·883	0·121	0·000	0·729	0·149	—	—	0·0094	—	0·54
0·55	0·960	−0·008	0·735	0·273	0·000	0·640	0·324	0·4877	0·55	0·0150	0·635	0·55
0·56	1·000	−0·009	0·661	0·348	0·000	0·561	0·439	0·4945	0·56	0·0220	—	0·56
0·57	0·967	−0·008	0·605	0·403	0·000	0·486	0·481	0·4959	0·57	0·0252	0·620	0·57
0·58	0·900	−0·006	0·568	0·438	0·000	0·419	0·481	0·4970	0·58	0·0268	—	0·58
0·59	0·793	−0·005	0·553	0·452	0·000	0·355	0·438	0·4972	0·59	0·0276	0·640	0·59
0·60	0·682	−0·004	0·532	0·472	0·000	0·294	0·388	0·4980	0·60	0·0278	—	0·60
0·61	0·555	−0·003	0·5015	0·5015	0·000	0·223	0·332	0·4983	0·61	0·0268	0·680	0·61
0·62	0·431	−0·002	0·408	0·594	0·000	0·136	0·295	0·4995	0·62	0·0242	—	0·62
0·63	0·299	−0·001	0·250	0·751	0·000	0·055	0·244	0·5009	0·63	0·0252	0·730	0·63
0·64	0·194	−0·001	0·100	0·901	0·000	0·013	0·181	0·5015	0·64	0·0280	—	0·64
0·65	0·1144	0·000	0·000	1·000	0·000	0·000	0·1144	0·5020	0·65	0·0330	0·780	0·65
0·67	0·0389	—	—	—	—	—	—	—	—	—	—	0·67
0·70	0·00638	—	—	—	—	—	—	—	—	—	—	0·70
1931 C.I.E. S_B source		0·230	0·599	0·171	Relative luminosities of trichromatic units of primaries							
$\mathring{\lambda}=0·61\mu$. $\lambda=0·5825\mu$. $\lambda=0·4940\mu$.		−0·003 −0·006 0·5135	0·5015 0·564 0·5135	0·5015 0·442 −0·027	0·46μ. 0·0393	0·53μ. 1·000	0·65μ. 1·49					

Table 7. Characteristics for observer C

Wave-length λ (μ.)	Relative luminosity of equal-energy spectrum	Trichromatic coefficients J.H.N. (1) units			Mixture curves for equal-energy spectrum			Complementary wave-lengths (μ.)		Hue-discrimination; just-noticeable wave-length differences (μ.)	Saturation-discrimination log $\frac{L_W+L_S}{L_S}$	Wave-length λ (μ.)
		B (0·46μ.)	G (0·53μ.)	R (0·65μ.)	L_B	L_G	L_R	λ	λ'			
0·41	0·00278	1·006	−0·010	0·004	0·00298	−0·0004	0·0002	0·41	0·5969	—	—	0·41
0·43	0·0126	1·004	−0·006	0·002	0·0133	−0·0011	0·0004	0·43	0·5970	—	—	0·43
0·45	0·0241	1·001	−0·002	0·001	0·0245	−0·0007	0·0003	0·45	0·5972	0·0164	—	0·45
0·46	0·0407	1·000	0·000	0·000	0·0407	0·000	0·000	0·46	0·5973	0·0104	—	0·46
0·47	0·075	0·933	0·082	−0·015	0·039	0·046	−0·010	0·47	0·5988	0·0066	—	0·47
0·48	0·102	0·794	0·252	−0·046	0·024	0·101	−0·022	0·48	0·6060	0·0046	—	0·48
0·49	0·148	0·611	0·449	−0·060	0·016	0·157	−0·025	0·49	0·6328	0·0032	—	0·49
0·50	0·220	0·399	0·656	−0·055	0·0106	0·2326	−0·0232	—	—	0·0025	—	0·50
0·51	0·429	0·189	0·850	−0·039	0·0074	0·446	−0·0244	—	—	0·0023	—	0·51
0·52	0·603	0·045	0·967	−0·012	0·002	0·610	−0·009	—	—	0·0032	—	0·52
0·53	0·765	0·000	1·000	0·000	0·000	0·765	0·000	—	—	0·0054	—	0·53
0·54	0·917	−0·015	0·900	0·115	0·000	0·797	0·121	—	—	0·0093	—	0·54
0·55	0·974	−0·020	0·865	0·155	0·000	0·804	0·171	—	—	0·0164	—	0·55
0·56	0·999	−0·018	0·858	0·160	0·000	0·819	0·181	—	—	0·0208	—	0·56
0·57	0·968	−0·016	0·846	0·170	0·000	0·782	0·187	—	—	0·0212	—	0·57
0·58	0·913	−0·014	0·817	0·197	0·000	0·710	0·203	—	—	0·0184	—	0·58
0·59	0·818	−0·012	0·758	0·254	0·000	0·585	0·233	—	—	0·0143	—	0·59
0·60	0·702	−0·010	0·600	0·410	0·000	0·387	0·315	0·4735	0·60	0·0105	—	0·60
0·61	0·575	−0·008	0·504	0·504	0·000	0·262	0·313	0·4820	0·61	0·0077	—	0·61
0·62	0·462	−0·006	0·442	0·564	0·000	0·183	0·279	0·4850	0·62	0·0077	—	0·62
0·63	0·316	−0·004	0·351	0·653	0·000	0·098	0·218	0·4882	0·63	0·0097	—	0·63
0·64	0·194	−0·002	0·141	0·861	0·000	0·023	0·171	0·4930	0·64	0·0144	—	0·64
0·65	0·116	0·000	0·000	1·000	0·000	0·000	0·116	0·4940	0·65	0·0226	—	0·65
0·67	0·0324	—	—	—	—	—	—	—	—	—	—	0·67
0·70	0·00502	—	—	—	—	—	—	—	—	—	—	0·70
1931 C.I.E. S_B source		0·390	0·396	0·214	Relative luminosities of trichromatic units of primaries							
λ=0·61μ. λ=0·5825μ.		−0·008 −0·013	0·504 0·806	0·504 0·207	0·46μ.	0·53μ.	0·65μ.					
λ=0·4940μ.		0·530	0·530	−0·060	0·0746	1·000	1·19					

Table 8. Characteristics for observer D

Wave-length λ (μ.)	Relative luminosity of equal-energy spectrum	Trichromatic coefficients J.H.N. (1) units			Mixture curves for equal-energy spectrum			Complementary wave-lengths (μ.)		Hue-discrimination; just-noticeable wave-length differences (μ.)	Saturation-discrimination log $\frac{L_W+L_S}{L_S}$	Wave-length λ (μ.)
		B (0·46μ.)	G (0·53μ.)	R (0·65μ.)	L_B	L_G	L_R	λ	λ'			
0·41	0·00968	1·023	−0·035	0·012	0·01725	−0·01059	0·00302	0·41	0·5933	—	—	0·41
0·43	0·0263	1·020	−0·028	0·008	0·0416	−0·0204	0·0051	0·43	0·5936	0·006 (0·44)	—	0·43
0·45	0·0412	1·012	−0·016	0·004	0·0534	−0·015	0·0028	0·45	0·5940	0·0041	—	0·45
0·46	0·060	1·000	0·000	0·000	0·060	0·000	0·000	0·46	0·5944	0·00295	—	0·46
0·47	0·0805	0·956	0·056	−0·012	0·0435	0·045	−0·008	0·47	0·5955	0·00215	1·160	0·47
0·48	0·121	0·850	0·185	−0·035	0·028	0·110	−0·017	0·48	0·5993	0·0016	—	0·48
0·49	0·192	0·660	0·405	−0·065	0·018	0·201	−0·027	0·49	0·6097	0·0013	0·750	0·49
0·50	0·331	0·420	0·675	−0·095	0·013	0·360	−0·042	—	—	0·0014	—	0·50
0·51	0·515	0·193	0·865	−0·058	0·007	0·538	−0·030	—	—	0·0020	0·570	0·51
0·52	0·719	0·048	0·974	−0·022	0·002	0·731	−0·014	—	—	0·00265	—	0·52
0·53	0·851	0·000	1·000	0·000	0·000	0·851	0·000	—	—	0·0036	0·520	0·53
0·54	0·945	−0·023	0·973	0·050	0·000	0·908	0·038	—	—	0·0050	—	0·54
0·55	0·992	−0·022	0·927	0·095	0·000	0·916	0·077	—	—	0·0065	0·490	0·55
0·56	0·996	−0·021	0·891	0·130	0·000	0·892	0·107	—	—	0·0085	—	0·56
0·57	0·972	−0·020	0·855	0·165	0·000	0·839	0·134	—	—	0·0098	0·520	0·57
0·58	0·922	−0·018	0·817	0·201	0·000	0·758	0·165	—	—	0·0103	—	0·58
0·59	0·836	−0·016	0·742	0·274	0·000	0·642	0·195	—	—	0·0089	0·560	0·59
0·60	0·726	−0·013	0·636	0·377	0·000	0·488	0·238	0·4812	0·60	0·0065	—	0·60
0·61	0·568	−0·010	0·505	0·505	0·000	0·312	0·256	0·4903	0·61	0·0044	0·620	0·61
0·62	0·420	−0·008	0·328	0·680	0·000	0·155	0·265	0·4938	0·62	0·0037	—	0·62
0·63	0·287	−0·005	0·185	0·820	0·000	0·062	0·225	0·4957	0·63	0·0043	0·670	0·63
0·64	0·188	−0·002	0·079	0·923	0·000	0·016	0·172	0·4970	0·64	0·0060	—	0·64
0·65	0·122	0·000	0·000	1·000	0·000	0·000	0·122	0·4985	0·65	0·0085	0·730	0·65
0·67	0·0370	0·000	−0·020	1·020	0·000	−0·0009	0·0379	—	—	—	0·810	0·67
0·70	0·00453	0·000	−0·030	1·030	0·000	−0·00017	0·00470	0·4987	0·70	—	0·920	0·70
1931 C.I.E. S_B source		0·336	0·457	0·207	Relative luminosities of trichromatic units of primaries							
λ=0·61μ.		−0·010	0·505	0·505	0·46μ.	0·53μ.	0·65μ.					
λ=0·5825μ.		−0·018	0·800	0·218								
λ=0·4940μ.		0·545	0·545	−0·090	0·056	1·000	0·824					

Table 9. Characteristics for observer E

Wave-length λ (μ.)	Relative luminosity of equal-energy spectrum	Trichromatic coefficients J.H.N. (1) units			Mixture curves for equal-energy spectrum			Complementary wave-lengths (μ.)		Hue-discrimination; just-noticeable wave-length differences (μ.)	Saturation-discrimination log $\frac{L_W+L_S}{L_S}$	Wave-length λ (μ.)
		B (0·46μ.)	G (0·53μ.)	R (0·65μ.)	L_B	L_G	L_R	λ	λ'			
0·41	0·00845	—	—	—	—	—	—	—	—	—	—	0·41
0·43	0·0166	—	—	—	—	—	—	—	—	—	—	0·43
0·45	0·0286	—	—	—	—	—	—	—	—	—	—	0·45
0·46	0·0432	1·000	0·000	0·000	0·0432	0·000	0·000	0·46	0·5548	0·0140	1·125	0·46
0·47	0·073	0·969	0·031	0·000	0·043	0·030	0·000	0·47	0·5550	0·0088	—	0·47
0·48	0·115	0·820	0·180	0·000	0·020	0·095	0·000	0·48	0·5580	0·0054	0·730	0·48
0·49	0·166	0·621	0·379	0·000	0·012	0·154	0·000	0·49	0·5671	0·0038	—	0·49
0·50	0·262	0·335	0·665	0·000	0·006	0·256	0·000	—	—	0·0034	0·585	0·50
0·51	0·456	0·119	0·881	0·000	0·003	0·453	0·000	—	—	0·0048	—	0·51
0·52	0·691	0·020	0·980	0·000	0·001	0·690	0·000	—	—	0·0078	0·555	0·52
0·53	0·845	0·000	1·000	0·000	0·000	0·845	0·000	—	—	0·0117	—	0·53
0·54	0·954	−0·012	0·988	0·024	0·000	0·933	0·021	—	—	0·0175	0·565	0·54
0·55	0·992	−0·020	0·900	0·120	0·000	0·882	0·110	—	—	0·0262	—	0·55
0·56	0·996	−0·018	0·828	0·190	0·000	0·821	0·175	0·4834	0·56	0·0303	0·600	0·56
0·57	0·970	−0·016	0·770	0·246	0·000	0·748	0·222	0·4913	0·57	0·0297	—	0·57
0·58	0·919	−0·014	0·736	0·278	0·000	0·681	0·238	0·4928	0·58	0·0264	0·630	0·58
0·59	0·800	−0·011	0·695	0·316	0·000	0·562	0·238	0·4943	0·59	0·0212	—	0·59
0·60	0·666	−0·009	0·614	0·395	0·000	0·416	0·250	0·4954	0·60	0·0166	0·680	0·60
0·61	0·521	−0·007	0·5035	0·5035	0·000	0·269	0·252	0·4969	0·61	0·0152	—	0·61
0·62	0·380	−0·005	0·416	0·588	0·000	0·164	0·216	0·4974	0·62	0·0155	0·720	0·62
0·63	0·256	−0·002	0·284	0·718	0·000	0·076	0·180	0·4980	0·63	0·0167	—	0·63
0·64	0·160	−0·001	0·070	0·931	0·000	0·012	0·148	0·4987	0·64	0·0188	0·750	0·64
0·65	0·0938	0·000	0·000	1·000	0·000	0·000	0·0938	0·4987	0·65	0·0220	—	0·65
0·67	0·0289	—	—	—	—	—	—	—	—	—	0·785 (0·66μ.)	0·67
0·70	0·00307	—	—	—	—	—	—	—	—	—	—	0·70
1931 C.I.E. S_B source		0·332	0·566	0·102	Relative luminosities of trichromatic units of primaries							
λ=0·61μ.		−0·007	0·5035	0·5035	0·46μ.	0·53μ.	0·65μ.					
λ=0·5825μ.		−0·013	0·727	0·286								
λ=0·4940μ.		0·500	0·500	0·000	0·046	1·000	0·931					

Table 10. Characteristics for observer F

Wave-length λ (μ.)	Relative luminosity of equal-energy spectrum	Trichromatic coefficients J. H. N. (1) units			Mixture curves for equal-energy spectrum			Complementary wave-lengths (μ.)		Hue-discrimination; just-noticeable wave-length differences (μ.)	Saturation-discrimination log $\frac{L_W+L_S}{L_S}$	Wave-length λ (μ.)
		B (0·46μ.)	G (0·53μ.)	R (0·65μ.)	L_B	L_G	L_R	λ	λ′			
0·41	0·013	1·024	−0·042	0·018	0·025	−0·019	0·007	0·41	0·5826	—	—	0·41
0·43	0·022	1·023	−0·038	0·015	0·040	−0·028	0·010	0·43	0·5828	—	—	0·43
0·45	0·037	1·020	−0·023	0·003	0·059	−0·025	0·003	0·45	0·5833	—	—	0·45
0·46	0·051	1·000	0·000	0·000	0·051	0·000	0·000	0·46	0·5842	—	—	0·46
0·47	0·062	0·957	0·058	−0·015	0·033	0·038	−0·009	0·47	0·5864	—	—	0·47
0·48	0·095	0·864	0·162	−0·024	0·024	0·083	−0·011	0·48	0·5902	—	—	0·48
0·49	0·157	0·662	0·400	−0·062	0·014	0·166	−0·023	0·49	0·6082	—	—	0·49
0·50	0·261	0·340	0·738	−0·078	0·007	0·281	−0·027	—	—	—	—	0·50
0·51	0·420	0·135	0·915	−0·050	0·003	0·439	−0·022	—	—	—	—	0·51
0·52	0·611	0·032	0·988	−0·020	0·001	0·621	−0·011	—	—	—	—	0·52
0·53	0·770	0·000	1·000	0·000	0·000	0·770	0·000	—	—	—	—	0·53
0·54	0·906	−0·019	0·960	0·059	0·000	0·859	0·047	—	—	—	—	0·54
0·55	0·972	−0·021	0·918	0·103	0·000	0·882	0·090	—	—	—	—	0·55
0·56	0·999	−0·019	0·880	0·139	0·000	0·874	0·125	—	—	—	—	0·56
0·57	0·966	−0·016	0·841	0·175	0·000	0·813	0·153	—	—	—	—	0·57
0·58	0·900	−0·013	0·807	0·206	0·000	0·731	0·169	—	—	—	—	0·58
0·59	0·788	−0·010	0·725	0·285	0·000	0·581	0·207	0·4790	0·59	—	—	0·59
0·60	0·641	−0·008	0·619	0·389	0·000	0·409	0·232	0·4875	0·60	—	—	0·60
0·61	0·495	−0·006	0·503	0·503	0·000	0·260	0·235	0·4907	0·61	—	—	0·61
0·62	0·361	−0·004	0·317	0·687	0·000	0·122	0·239	0·4929	0·62	—	—	0·62
0·63	0·244	−0·002	0·201	0·801	0·000	0·053	0·191	0·4937	0·63	—	—	0·63
0·64	0·153	−0·001	0·100	0·901	0·000	0·017	0·136	0·4941	0·64	—	—	0·64
0·65	0·096	0·000	0·000	1·000	0·000	0·000	0·096	0·4948	0·65	—	—	0·65
0·67	0·0347	—	—	—	—	—	—	—	—	—	—	0·67
0·70	0·00318	—	—	—	—	—	—	—	—	—	—	0·70
1931 C.I.E. S_B source		0·423	0·443	0·134	Relative luminosities of trichromatic units of primaries							
λ=0·61μ.		−0·006	0·503	0·503	0·46μ.	0·53μ.	0·65μ.					
λ=0·5825μ.		−0·012	0·796	0·216								
λ=0·4940μ.		0·540	0·540	−0·080	0·053	1·000	0·904					

Table 11. Characteristics for observer L

Wave-length λ (μ.)	Relative luminosity of equal-energy spectrum	Trichromatic coefficients J.H.N. (2) units			Mixture curves for equal-energy spectrum			Complementary wave-lengths (μ.)		Hue-discrimination; just-noticeable wave-length differences (μ.)	Saturation-discrimination log $\frac{L_W+L_S}{L_S}$	Wave-length λ (μ.)
		B (0·46μ.)	G (0·53μ.)	R (0·65μ.)	L_B	L_G	L_R	λ	λ′			
0·41	0·011	1·040	−0·055	0·015	0·023	−0·012	0·000	0·41	0·5819	—	—	0·41
0·43	0·035	1·026	−0·035	0·009	0·055	−0·020	0·000	0·43	0·5823	0·0100 (0·44)	—	0·43
0·45	0·0624	1·014	−0·017	0·003	0·0764	−0·014	0·000	0·45	0·5827	0·0081	—	0·45
0·46	0·0994	1·000	0·000	0·000	0·0994	0·000	0·000	0·46	0·5830	0·0063	—	0·46
0·47	0·145	0·960	0·065	−0·025	0·085	0·063	−0·003	0·47	0·5852	0·0046	—	0·47
0·48	0·176	0·890	0·195	−0·085	0·054	0·128	−0·006	0·48	0·5913	0·0031	—	0·48
0·49	0·218	0·735	0·515	−0·250	0·026	0·202	−0·010	0·49	0·6350	0·0018	—	0·49
0·50	0·312	0·430	0·870	−0·300	0·014	0·309	−0·011	—	—	0·0013	—	0·50
0·51	0·508	0·170	1·030	−0·200	0·008	0·510	−0·010	—	—	0·0013	—	0·51
0·52	0·723	0·055	1·045	−0·100	0·004	0·726	−0·007	—	—	0·0018	—	0·52
0·53	0·890	0·000	1·000	0·000	0·000	0·890	0·000	—	—	0·0036	—	0·53
0·54	0·991	−0·010	0·920	0·090	0·000	0·981	0·010	—	—	0·0062	—	0·54
0·55	0·988	−0·014	0·786	0·228	0·000	0·960	0·028	—	—	0·0090	—	0·55
0·56	0·945	−0·012	0·600	0·412	0·000	0·884	0·061	—	—	0·0112	—	0·56
0·57	0·815	−0·011	0·411	0·600	0·000	0·711	0·104	—	—	0·0120	—	0·57
0·58	0·641	−0·010	0·300	0·710	0·000	0·518	0·123	—	—	0·0106	—	0·58
0·59	0·448	−0·008	0·204	0·804	0·000	0·321	0·127	0·4783	0·59	0·0071	—	0·59
0·60	0·281	−0·007	0·142	0·865	0·000	0·175	0·106	0·4838	0·60	0·0052	—	0·60
0·61	0·178	−0·006	0·091	0·915	0·000	0·089	0·089	0·4870	0·61	0·0043	—	0·61
0·62	0·0991	−0·004	0·046	0·958	0·000	0·0316	0·0675	0·4887	0·62	0·0036	—	0·62
0·63	0·0529	−0·002	0·015	0·987	0·000	0·0053	0·0476	0·4898	0·63	0·0034	—	0·63
0·64	0·0298	−0·001	0·005	0·996	0·000	0·0014	0·0284	0·4902	0·64	0·0040	—	0·64
0·65	0·0131	0·000	0·000	1·000	0·000	0·000	0·0131	0·4904	0·65	0·0058	—	0·65
0·67	0·00318	0·000	−0·003	1·003	0·000	−0·00009	0·00327	—	—	—	—	0·67
0·70	0·00041	0·000	−0·004	1·004	0·000	−0·00002	0·00043	0·4907	0·70	—	—	0·70
1931 C.I.E. S_B source		0·264	0·194	0·542	Relative luminosities of trichromatic units of primaries							
λ=0·61μ.		−0·006	0·091	0·915	0·46μ.	0·53μ.	0·65μ.					
λ=0·5825μ.		−0·010	0·275	0·735								
λ=0·4940μ.		0·658	0·658	−0·316	0·095	1·000	0·100					

DISCUSSION

Dr W. D. **Wright**. This paper provides the most exhaustive analysis of anomalous trichromatism that has yet been reported. Moreover, the Physical Society has been well advised in waiving its usual practice so far as to publish both diagrams and tables for the characteristics of each observer. For any quantitative examination of the results the tables are essential, but the diagrams are equally valuable for a more general discussion of the various types of observer that are found.

The results on saturation-discrimination are of special interest, for I believe that they are the first measurements on anomalous trichromats to have been published. The value of the data as a whole is twofold. In the first place the results are of theoretical interest and importance as showing precisely the variations from normal vision that do occur, and this knowledge should lead to a further elucidation of the visual processes. In particular, theoretical attempts to relate one characteristic to another, for instance the hue-discrimination curve and the mixture curves, can now be applied to a number of different visual mechanisms, and any theory can now be put to a correspondingly more stringent test. In this connexion it should be realized that the theoretical manipulation of the data is not likely to yield results of any importance unless they are expressed in terms of some fundamental primaries or responses. At present the values have been tabulated in terms of the instrument primaries that were used. I should like to ask the author whether he would expect some of the rather irregular bumps that occur on the mixture curves to disappear if the results were transformed to a new set of primaries, or whether they are an inherent part of the curves.

The second general use to which the results can be put is the practical evaluation of the degree of deficiency to which an observer is subject and the consequent extent to which his activities should be limited. The anomalous-trichromat group is especially important because it includes the borderline cases between the normal and the abnormal, and they are the persons who might be liable to be rejected from certain occupations when in practice their inclusion would be quite safe or, alternatively, they might be included when they should have been excluded. The recognition and elimination of dichromats is comparatively easy, but the decision whether a person is merely an extreme variation from the normal, or actually slightly anomalous, may be very difficult.

To understand what is involved, it would be of very material aid if some picture could be obtained of the sensations which the colour-blind person perceived in terms of those of which the normal person is conscious. Suppose, for instance, we were prepared to assume that the blue and yellow radiations produced the same sensation for both types of observer, then it should be possible to relate all the colour sensations of the anomalous observer with those of the normal observer, by stepping off the discrimination steps from the blue and the yellow. It should, in fact, be possible to plot the spectrum locus for the anomalous observer in the normal colour triangle, and in the limit this locus would reduce to the straight line that is found for the dichromat. This would provide a very convenient way of demonstrating the gradation from one form of colour-vision to another, and would be of value in estimating the degree of abnormality exhibited by an observer. If, in addition, it were found that the spectrum locus as derived from discrimination data also represented the colour-mixture results to a reasonable degree of accuracy, it would be a fact of very considerable theoretical importance. It would be interesting to know whether the author has attempted any calculations on these lines, and if so, the extent to which he has been successful.

AUTHOR's reply. As regards the irregularities in the mixture curves, I think that those just by a primary would be affected by a change of primaries, but not those removed from a primary. The mixture curves for observer C have been referred to the fundamental responses given by Dr Wright,* and the irregularity at $0{\cdot}69\,\mu$. still persists. However, without some experimental evidence it does not seem justifiable to assume that these fundamental responses are applicable to an anomalous observer.

The existence of the irregularities in the relation between the complementary wave-lengths in the case of observer C would lead one to suspect that they are of a fundamental nature.

With regard to Dr Wright's suggestion as to finding some relation between the normal and anomalous sensations, some tentative work was done on these lines. From the saturation-discrimination data obtained for observers B, C, and D, it was seen that the spectrum colours in the red-yellow-green region appeared very desaturated in comparison with the normal, and that the saturation corresponded approximately to the minimum for the normal in the region. This is clearly in agreement with the hue-discrimination data, and may be taken to confirm the suggestion put forward by Wright in Pitt's report(1), that the anomalous observer sees red and green as desaturated orange and yellow-green respectively. Working from this fact an attempt has been made to obtain a picture of the appearance of the spectrum to the anomalous observer in terms of normal sensations. The area of the colour-triangle for the normal observer represents a definite number of distinguishable colours, while the straight line to which the colour triangle for the dichromat reduces also represents a certain smaller number of distinguishable colours. Now the anomalous trichromat can see more colours than the dichromat, but fewer than the normal. Hence, to give a subjective representation of the number of colours, the anomalous trichromat should have a colour triangle smaller than the normal and yet larger than the dichromat. If, however, the anomalous colour triangles are plotted relative to the same physical stimuli as the normal, it is clear that the triangles must always be of the same order of size. It is therefore necessary to devise some method by which the triangles may be expressed in terms of the same subjective stimuli as the normal. We have seen above that it is reasonable to suppose that the anomalous trichromat sees red and green as desaturated orange and yellow-green. Now if we extend this by saying that the sensation of yellow is the same for both normal and anomalous trichromat, then there is one point at which we may fix the anomalous subjective colour triangle relative to the normal. If at the same time we assume, as in McDougall's evolutionary theory, that the blue sensations are the same in each case, then we can say that the straight line of

* Wright, W. D. *Proc. Roy. Soc.* B, **115**, 49–87 (1934).

the dichromat should be drawn between the blue and the yellow of the normal triangle, and that the anomalous triangles should be drawn about this line and between it and the normal triangle.

If now, starting from the yellow and working towards either the red or the green, we suppose that one hue-discrimination step will produce the same change in colour, whether it is for the normal or for the anomalous trichromat, then by finding the number of steps for the anomalous trichromat between the yellow and $0{\cdot}65\,\mu$., we may say that this corresponds in colour sensation to a colour distant from the yellow, in the normal case, by the same number of hue-discrimination steps. In this way it is possible to obtain two wave-lengths in the normal spectrum to which $0{\cdot}65\,\mu$. and $0{\cdot}53\,\mu$. in the anomalous spectrum correspond in colour. In the yellow region the assumptions involved in the above procedure would seem to be justified, at least as a first approximation. It is, however, necessary to make the further assumption that the changes which have been made are also applicable in the blue-green region.

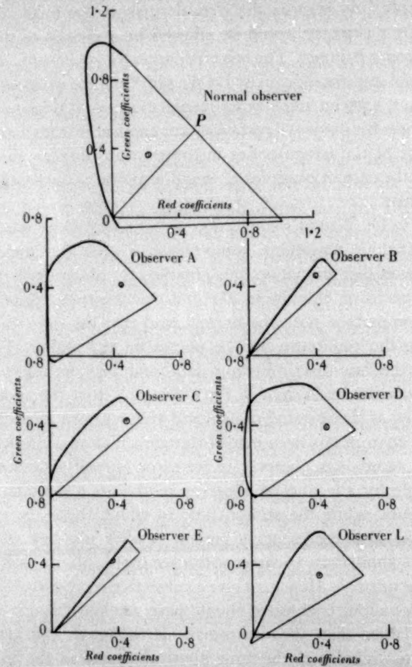

Reduced colour triangles for Observers A, B, C, D, E and L compared with normal.
$\odot = S_B$: OP = Straight line for dichromat.

For convenience the yellow chosen was at 0·5825μ. and the colour triangles of all the anomalous observers were referred to the W.D.W. system. In each case the numbers of colour steps between 0·5825μ. and 0·53μ. and 0·65μ. were determined from the hue-discrimination curve for the observer. From this latter, and from the characteristics of the normal observer, the coefficients of the colours in the normal triangle corresponding to 0·53μ. and 0·65μ. in the anomalous triangle, were found. This gave the new coefficients for the red and the green primaries, and the modified coefficients for the remaining wave-lengths were determined by the appropriate transformations.

The transformation is in reality equivalent to referring the anomalous triangles to a set of primaries R_A, G_A and B_A. If the normal primaries are R_N, G_N and B_N, then from the hue-discrimination we have

$$\left.\begin{aligned} C_{A\,0\cdot65\mu.} &= C_N = aR_N + bG_N \\ C_{A\,0\cdot53\mu.} &= C_N = a'R_N + b'R_N \end{aligned}\right\},$$

where C_A is the colour for the anomalous and C_N for the normal.

Then the new primaries R_A and G_A are chosen so that

$$C_{N\,0\cdot65\mu.} = aR_A + bG_A = R_N,$$
$$C_{N\,0\cdot53\mu.} = a'R_A + b'G_A = G_N.$$

Further we say $$C_{A\,0\cdot5825\mu.} = C_{N\,0\cdot5825\mu.}$$
and $$0\cdot5R_A + 0\cdot5G_A = 0\cdot5R_N + 0\cdot5G_N;$$
also $$B_N = B_A.$$

For example, in the case of observer A, the number of steps between 0·5825μ. and 0·65μ. is 15·52, and that between 0·5825μ. and 0·53μ. is 8·92, as compared with the normal values of 48·64 and 30·67.

From the curves we find

$$C_{A\,0\cdot65\mu.} = C_{N\,0\cdot5963\mu.} = 0\cdot662R_N + 0\cdot338G_N \quad \text{(the blue being neglected)},$$
$$C_{A\,0\cdot53\mu.} = C_{N\,0\cdot5716\mu.} = 0\cdot366R_N + 0\cdot634G_N.$$

From this we choose the primaries so that

$$C_{N\,0\cdot65\mu.} = 0\cdot662R_A + 0\cdot338G_A = R_N,$$
$$C_{N\,0\cdot53\mu.} = 0\cdot366R_A + 0\cdot634G_A = G_N,$$

and solving for R_A and G_A we find that the anomalous primaries are

$$R_A = 2\cdot142R_N - 1\cdot142G_N,$$
$$G_A = -1\cdot237R_N + 2\cdot237G_N,$$
$$B_A = B_N.$$

As such, the triangles are a perfectly legitimate means of expressing the coefficients of the anomalous observers. If, however, the triangles are to be considered as a subjective representation of the colour sensations of the anomalous trichromat in comparison with the normal, then it is necessary to consider the assumptions made in deriving them. These assumptions are: (1) that the sensation of yellow is the same for both normal and anomalous trichromats; (2) that the yellow occurs in the same place in the spectrum for all observers, and is at $0{\cdot}5825\mu$.; (3) that one hue-discrimination step will correspond to the same change in sensation, whether it is for the normal or for the anomalous trichromat; and (4) that the sole differences between normal and anomalous trichromats are due to change in the red and green sensations, and that the blue is the same for both.

Examining these assumptions, we note that the first necessitates that the sensations experienced by the normal and anomalous trichromats shall be comparable. This type of assumption cannot be proved or disproved, and it is only possible to consider the probability of its being true. The second assumption is definitely only a first approximation, since it was seen that the positions of the pure yellow differed slightly for normal and anomalous trichromats. The use of $0{\cdot}5825\mu$. is again an approximation, the value being chosen merely for convenience. The assumption that a hue-discrimination step means the same change in sensation for both normal and anomalous trichromats is of the same type as the first, but if the first may be made this assumption should not introduce any large error, at least in the yellow region. The last assumption is probably the largest source of error in deriving the triangles. The characteristics have shown that the differences between normal and anomalous trichromats are not confined to the yellow region nor yet to the red and green sensations entirely. For example, if they were so confined, the hue-discrimination in the blue-green region for observer B should be poor, while in fact it is comparable with the normal.

The reduced triangles must therefore be considered only as representing the anomalous sensations in terms of the normal within the limitations imposed by the assumptions.

A rigorous test of the validity of the triangles, assuming the sensations to be comparable, would necessitate a large amount of saturation-discrimination data. If, however, we compare the saturation-discrimination of the normal and observer D in the blue-green region with the distance between the white point and the spectral locus, we can see that an approximately proportionate reduction has taken place. On the other hand, in the case of observer B, where the saturation-discrimination is nearly normal, the reduced triangle is very narrow and in consequence the agreement is poor. The suggestion that the reduced triangles represent the anomalous sensations in terms of the normal, or that it is possible to draw such triangles by any similar method, implies that the anomalous trichromats have different fundamental sensations and yet the same physiological mechanism as the normal. Thus, in the case of observer D, where the saturation-discrimination supplies a favourable test, it can be said that the assumptions are to some extent justified; on the other hand, in the case of observer B, where the agreement is poor, it can definitely be said that the assumptions are not justified, and similar considerations would apply to observer E. The possibility of there being two mechanisms, either coexistent or alternative, has been present throughout, and while, as has been stressed, the reduced triangles must not be used as theoretical proof, they do in this case offer at least a feasible theory as to the nature of the two mechanisms, namely, a change in fundamental sensations, and a change in the physiological perception mechanism.

HEAT-CONDUCTION IN A MEDIUM HAVING THERMAL PROPERTIES DEPENDING ON THE TEMPERATURE

By M. R. HOPKINS, M.Sc.

Communicated by Prof. E. J. Evans, 25 March 1938. Read in title 24 June 1938

ABSTRACT. Typical standard calculations in the theory of heat-conduction are modified to allow for the variation of the thermal properties of the medium with temperature.

We consider a region V of the medium, either extending to infinity or confined by given boundaries. Let $h(x, y, z)$ be the initial temperature of the medium, $H(x, y, z, t)$ the temperature of the boundaries, if any, and $Q(x, y, z, t)$ the rate of generation of heat per unit volume. If we write k for the conductivity and c for the product of the specific heat and density, the equation is

$$c\dot{\theta} - \text{div}\,\{k \text{ grad } \theta\} = Q \qquad \text{......(1)},$$

where θ is the temperature and $\dot{\theta}$ means $\partial\theta/\partial t$.

Let $\Theta(x, y, z, t)$ be the solution of the problem obtained by assuming that c and k have constant values c_0 and k_0, the equation thus reducing to

$$L[\theta] = Q \qquad \text{......(2)},$$

where

$$L = c_0 \frac{\partial}{\partial t} - k_0 \text{ div grad}.$$

Θ is, of course, the standard solution, worked out for a variety of cases in the textbooks on heat-conduction.

Provided c/k is independent of temperature the solution of (1) can be obtained at once by the methods used to determine Θ; for if $c/c_0 = k/k_0 = p(\theta)$, say, where c_0 and k_0 are the values at any arbitrary temperature, and if we write

$$\phi = \int_{\theta_0}^{\theta} p(\theta)\, d\theta,$$

where θ_0 is any arbitrary temperature, then the initial and boundary values of ϕ, say $h'(x, y, z)$ and $H'(x, y, z, t)$, are obtained by setting h and H as the upper limit of the integral; moreover one can easily show that the equation satisfied by ϕ is obtained from (2) on replacing θ by ϕ. Thus from the expression for Θ in terms of h, H, and Q, we obtain ϕ on replacing h and H by h' and H'.

Though we shall find this result useful, we must, for practical purposes, assume no such relationship between c and k. Let us write

$$c = c_0\{1 + \mu f(\theta)\} \quad \text{and} \quad k = k_0\{1 + \mu F(\theta)\}.$$

Then the equation is

$$L\,[\theta]=Q+\mu\,[k_0 \operatorname{div}\{F(\theta)\operatorname{grad}\theta\}-c_0 f(\theta)\,\dot{\theta}] \qquad \ldots\ldots(3).$$

If we think of the whole expression in the bracket as $G(x, y, z, t)$, we may note that the same equation would arise if heat were generated at the rate $Q+\mu G$ per unit volume in a medium in which c and k had the values c_0 and k_0. In the latter medium let $g(x, y, z, x', y', z', t-\tau)$ be the Green's function for zero boundary temperature, that is, the temperature at co-ordinates x, y, z and time t due to the generation of unit quantity of heat at x', y', z' and τ, the boundaries being kept at temperature zero. Then the required solution is evidently

$$\Theta+\mu\int_V\int_0^t g\,.\,G(x', y', z', \tau)\,dx'\,dy'\,dz'\,d\tau \qquad \ldots\ldots(4).$$

Regarding the term in μ as a correction effect, we evaluate it approximately by writing the known function Θ instead of θ in G. It is to be noted that g is a known function which, even if Q is zero, will have arisen in the calculation of Θ. If, owing to symmetry, only an integral of g with respect to the dashed co-ordinates (perhaps over a plane or a spherical shell) has arisen in the calculation of Θ, the same integral will suffice for calculating the correction term.

If we think of the solution as a power series in μ, the coefficients of the higher powers can be evaluated similarly by the aid of the Green's function. At every stage of the approximation the initial and boundary values will be those of the principal term Θ, and these are the values prescribed. In a few very simple cases the equations determining the coefficients of the powers of μ can be solved directly, without the aid of a Green's function.

In many cases it will be sufficiently accurate to regard c and k as linear in the temperature, so that we can write $\mu f(\theta)=\mu_1\theta$ and $\mu F(\theta)=\mu_2\theta$. The solution as far as the first power of the μ's will then be of the form $\Theta+\mu_1\psi_1+\mu_2\psi_2$. It will sometimes be quicker to evaluate only one of the two functions ψ_1 and ψ_2 by the above method; the other can then be deduced, since the sum of the two is readily obtained by setting $\mu_1=\mu_2$, thus obtaining a medium in which c/k is independent of temperature, for which the exact solution, and hence $\psi_1+\psi_2$, is given by the theorem stated earlier in the paper.

We turn now to some typical applications. The results only will be given, since the calculations are straightforward and of little interest.

(1) A sheet of infinite area, bounded by the planes $x=0$ and $x=d$, is at temperature θ_0 at time zero, and its surfaces are kept always at temperature zero. We take the linear form mentioned above for c and k, and we assume that $\mu_1\theta_0$ and $\mu_2\theta_0$ are not large fractions. We then apply equation (4), and for the calculation we require, not, of course, the Green's function itself, but only the solution for an instantaneous plane source with boundary temperature zero. Putting $\kappa^2=k_0/c_0$, we find for the temperature at x and t

$$\sum_{n, m, p=0}^{\infty} 4\theta_0 \sin n_1 x\left\{\frac{e^{-n_1^2\kappa^2 t}}{n_1 d}-\frac{16\theta_0 n_1\,[\mu_1(m_1^2+p_1^2)-\mu_2 n_1^2]\,[e^{-(m_1^2+p_1^2)\kappa^2 t}-e^{-n_1^2\kappa^2 t}]}{d^3\,[(m_1+p_1)^2-n_1^2]\,[(m_1-p_1)^2-n_1^2]\,[m_1^2+p_1^2-n_1^2]}\right\}.$$

Here $n_1 = (2n+1)\,\pi/d$, and m_1 and p_1 are similarly defined in terms of m and p. When t is very great the temperature is practically the same as if c and k had the values c_0 and k_0 and either the initial conditions were established at a time differing somewhat from zero or the initial temperature differed somewhat from θ_0.

(2) As an example, using non-linear expressions for c and k we will take the case of a semi-infinite medium initially at uniform temperature θ_0 and having the boundary kept at zero temperature. This case is the subject of a paper by J. H. Awbery(1), who shows that the solution will contain x and t only in the form $x/\sqrt{t}$, the partial differential equation of heat-conduction thus reducing in this case to an ordinary differential equation. Except in the case when c/k is constant his solution of this equation is, however, open to a criticism as regards its utility, for it contains, not the initial temperature, but a parameter the value of which in terms of the initial temperature and the thermal coefficients remains unspecified, owing to the solution, which contains a power series in $x/\sqrt{t}$, failing at large values of the variable and hence at the initial state. Our method, which here reduces to a direct integration without the aid of a Green's function, gives

$$\begin{aligned}\theta = \theta_0 I + \mu\theta_0^2\,[\tfrac{1}{2}\beta\,(I - I^2) + \gamma\,(1 - E^2 - I - yEI)]&\\ + \mu^2\theta_0^3\,[\tfrac{1}{2}\beta^2\,(I^3 - I^2) + \beta\gamma F + \gamma^2 G + \tfrac{1}{3}\beta_1\,(I - I^3) + \gamma_1 H]&,\end{aligned}$$

where $y = x\sqrt{\pi}/2\kappa\sqrt{t}$; $c = c_0\,(1 + \mu\alpha\theta + \mu^2\alpha_1\theta^2)$; $k = k_0\,(1 + \mu\beta\theta + \mu^2\beta_1\theta^2)$;

$$\gamma = (\beta - \alpha)/\pi; \quad \gamma_1 = (\beta_1 - \alpha_1)/\pi; \quad E = e^{-y^2/\pi};$$

$$F = 1 - E^2 - (2 + yE - 4E^2)\,I + (1 + \tfrac{5}{2}yE)\,I^2 - 3\sqrt{3}\,(I_1 - I)/2;$$

$$\begin{aligned}G = -2\,(1 - E^2) - y\,(E + \tfrac{1}{2}E^3) + \{2 + 2yE - (\pi + y^2)\,E^2\}\,I - \tfrac{1}{4}\,(\pi + 2y^2)\,yEI^2&\\ + \tfrac{3}{4}\sqrt{3\pi}\,(I_1 - I)&;\end{aligned}$$

$$H = -2E^2 I - yEI^2 + \sqrt{3}\,(I_1 - I).$$

I signifies $I(y/\sqrt{\pi})$ defined as $\dfrac{2}{\sqrt{\pi}}\displaystyle\int_0^{y/\sqrt{\pi}} e^{-u^2}\,du$ and I_1 is $I\left(y\sqrt{\dfrac{3}{\pi}}\right)$. The calculation is carried as far as the terms in μ^2.

(3) For the next example let us create an artificial difficulty by choosing a case of a hypothetical nature having initially an infinite temperature in an infinitesimal region; such a case may evidently give rise to difficulties of convergence. We shall take, in fact, the instantaneous plane source generating suddenly, at time zero, in an infinite medium at temperature zero, a quantity of heat Q per unit area of the plane $x = 0$, thus producing instantaneously an infinite temperature there. If we use the linear form for c and k, the calculation as far as the first power of the μ's gives

$$\theta = At^{-\frac{1}{2}}\,E\,[1 + \tfrac{1}{2}At^{-\frac{1}{2}}\,\{(\mu_2 - \mu_1)\,yI - \mu_2 E\}],$$

where E and I are as in the previous example and A is $Q/2\kappa c_0\sqrt{\pi}$. For small values of the μ's the correction term is only a small fraction of the whole throughout a certain range of x and t, and the approximation there is probably a good one; it certainly is if $\mu_1 = \mu_2$, as is easily shown by writing down the exact solution for that case. The infinite initial temperature does not arise, of course, in any real physical problem.

(4) In conclusion a case in which the surface temperature is varied with time has been considered. The calculations are found to give no particular difficulty, but the expression obtained is naturally rather cumbrous and is hardly of sufficient interest to be given here.

I am indebted to Dr P. M. Davidson for supplying me with the general method described above, together with the calculations for a typical case, the cooling of a sphere, which had arisen in some experimental work.

REFERENCE

(1) AWBERY, J. H. *Proc. Phys. Soc.* **48**, 118 (1936).

THE PRINCIPAL PARAMAGNETIC SUSCEPTIBILITIES OF POTASSIUM FERRICYANIDE AT LOW TEMPERATURES

By L. C. JACKSON

H. H. Wills Physical Laboratory, University of Bristol

Received 9 *May* 1938. *Read in title* 24 *June* 1938

ABSTRACT. The author's previous measurements of the principal magnetic susceptibilities of potassium ferricyanide have been repeated and extended to a temperature of 14·2° K. Two of the principal susceptibilities are approximately equal throughout the whole temperature range from 290 to 14° K., but that along the third principal axis is considerably smaller. The anisotropy is almost 400 per cent at 14° K. and is still increasing as the temperature falls. A brief comparison with Howard's theory of the magnetic properties of $K_3\,[Fe\,(CN)_6]$ is made.

---

§1. INTRODUCTION

In 1933 some measurements were published of the principal susceptibilities of the paramagnetic crystal, potassium ferricyanide, over the temperature range from 290 to 75° K.(1). The main features of the results, the low magnetic moment and the high anisotropy of the crystal, later received a very satisfactory explanation at the hands of J. B. Howard(2). It seemed of considerable interest to extend the measurements to lower temperatures as opportunity permitted and to compare them with the theory. The results for the temperature range from 290 to 14° K. are presented below.

§2. EXPERIMENTAL PROCEDURE AND RESULTS

The susceptibilities were determined with the aid of the same apparatus as before, a Sucksmith magnetic balance adapted for use at low temperatures. These temperatures were obtained with suitable liquefied gases boiling under atmospheric or reduced pressure, viz. methyl chloride, ethylene, oxygen and hydrogen. Since the crystals of potassium ferricyanide, though actually monoclinic, are very nearly orthorhombic ($\beta = 90^\circ\,6'$) and since the previous determinations had shown that the magnetic properties also are in agreement with this fact, measurements were made in the work now described of the susceptibilities along three mutually perpendicular directions in the crystal, one perpendicular to the plane (100), another perpendicular to the plane (010), and one parallel to the *c* axis. These susceptibilities will then represent the three principal susceptibilities of the crystal with an accuracy of 1 or 2 per cent, which is quite adequate for the present results.

The results of the measurements are given in tables 1, 2 and 3.

Table 1. χ_1, viz. χ perpendicular to the (100) plane

T (° K.)	$\chi_1 \times 10^6$	χ'_{1m}	$1/\chi'_{1m}$	μ^2_{1B}
289·7	$7{\cdot}4_7$	0·00260	385	6·07
248·9	$8{\cdot}5_1$	0·00294	340	5·90
208·0	$10{\cdot}0_4$	0·00344	291	5·77
169·7	$12{\cdot}2_1$	0·00416	240	5·69
117·9	$16{\cdot}4_4$	0·00555	180	5·28
90·1	$20{\cdot}2_3$	0·00680	147	4·94
74·3	$23{\cdot}0_4$	0·00772	130	4·73
63·9	$26{\cdot}5_3$	0·00887	113	4·57
20·5	$72{\cdot}7_8$	0·02408	41·5	3·97
17·0	$85{\cdot}3_7$	0·02824	35·4	3·87
14·6	$97{\cdot}2_3$	0·03214	31·1	3·78

Table 2. χ_2, viz. χ parallel to the *c* axis

T (° K.)	$\chi_2 \times 10^6$	χ'_{2m}	$1/\chi'_{2m}$	μ^2_{2B}
291·9	$6{\cdot}3_1$	0·00222	450	5·22
273·2	$6{\cdot}6_8$	0·00234	427	5·15
248·8	$7{\cdot}0_0$	0·00244	410	4·90
221·2	$7{\cdot}5_6$	0·00263	380	4·69
179·2	$8{\cdot}4_5$	0·00292	342	4·22
169·6	$8{\cdot}7_0$	0·00300	333	4·10
144·0	$9{\cdot}4_7$	0·00326	307	3·78
117·0	$10{\cdot}3_4$	0·00354	282	3·35
90·2	$11{\cdot}3_5$	0·00388	258	2·82
75·5	$12{\cdot}0_0$	0·00409	244	2·48
63·8	$12{\cdot}5_4$	0·00428	234	2·20
20·4	$21{\cdot}1_1$	0·00709	141	1·16
17·0	$23{\cdot}8_9$	0·00800	125	1·09
14·2	$27{\cdot}0_4$	0·00904	111	1·03

Table 3. χ_3, viz. χ perpendicular to the (010) plane

T (° K.)	$\chi_3 \times 10^6$	χ'_{3m}	$1/\chi'_{3m}$	μ^2_{3B}
289·5	$7{\cdot}0_0$	0·00244	410	5·69
248·9	$8{\cdot}0_3$	0·00278	360	5·58
217·8	$9{\cdot}0_7$	0·00313	320	5·49
195·8	$9{\cdot}9_6$	0·00342	292	5·39
169·3	$11{\cdot}4_3$	0·00390	256	5·32
120·7	$15{\cdot}2_1$	0·00515	194	5·01
90·1	$19{\cdot}8_9$	0·00669	149	4·86
76·2	$23{\cdot}1_0$	0·00774	129	4·75
64·1	$26{\cdot}3_7$	0·00882	113	4·56
20·4	$75{\cdot}6_4$	0·02503	40·0	4·11
17·1	$89{\cdot}5_0$	0·02959	33·8	4·08
14·0	107·9	0·03565	28·0	4·02

In the above tables χ_1, in accordance with the usual convention, is the larger of the principal susceptibilities in the *ac* plane and χ_3 is the one along the axis of symmetry. χ'_m is the molecular susceptibility corrected for the diamagnetism of the molecule.* μ_B is the effective Bohr magneton number calculated from $\mu_B = 2{\cdot}839\,\sqrt{(\chi'_m T)}$.

---

* The correction applied for the diamagnetic properties of the molecule was 140×10^{-6}, obtained from $K^+ = -18{\cdot}5 \times 10^{-6}$, $CN^- = -10{\cdot}8 \times 10^{-6}$, $Fe^{+++} = -20 \times 10^{-6}$. See E. C. Stoner, *Magnetism and Matter*, p. 470.

§ 3. DISCUSSION

The present results are in good agreement with those of the previous measurements, this being all the more satisfactory since the new determinations were made on a crystal grown from another specimen of the salt of different origin. (The kink previously suspected in the χ_2 curve eventually proved to be spurious.)

It will be seen that χ_1 and χ_3 are almost equal throughout the whole temperature range and that the $\{1/\chi, T\}$ curves for these quantities cross between 60° and 70° K. On the other hand, χ_2 diverges more and more from χ_1 and χ_3 as the temperature falls. In other words the anisotropy of the crystal becomes more pronounced at low temperatures, reaching the surprisingly large value of 400 per cent at 14·2° K. The crystal is thus almost uniaxial at the lowest temperatures.

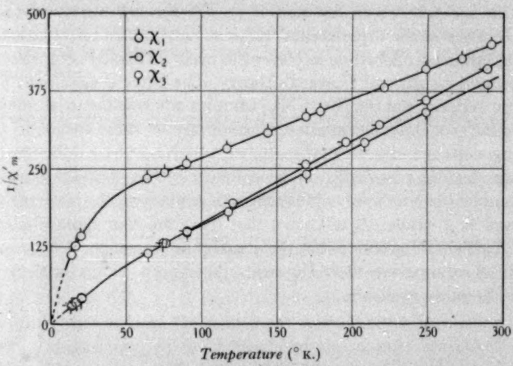

Figure 1. The principal susceptibilities of potassium ferricyanide.

Howard's theory of the author's earlier results for potassium ferricyanide may be summarized as follows. The Fe^{+++} ion is regarded as being situated in a very high electrostatic field of cubic symmetry (due to the CN groups) on which is superposed a smaller field of rhombic, almost axial, symmetry. Under the action of the cubic field the coupling of the individual l's of the five electrons of Fe^{+++} to a resultant orbital angular momentum L is destroyed, and the lowest level of the unperturbed ion (electron spin being neglected) splits into a triply degenerate level d_ϵ and a doubly degenerate level d_γ. For an octahedral arrangement of the CN groups, the d_ϵ level will lie lower. Further, it is assumed that the d_γ level will be situated so high that its contribution to the susceptibility can be neglected. The rhombic field now splits the d_ϵ level into three levels which, on the introduction of the electron spin, are all doubly degenerate. There are five electrons to fit into these three levels so that two will be doubly occupied and, by the Pauli principle, will contribute nothing to the susceptibility. The fifth electron has a free spin so that the magnetic properties will correspond to $S=\frac{1}{2}$ if one can neglect orbital contributions to the susceptibility. Howard, however, shows that the latter cannot be wholly neglected and introduces a coupling coefficient between l and s to allow for this fact. A knowledge of the positions of the six levels which exist in the presence of a magnetic field then enables one to calculate the susceptibility. The low value of the magnetic moment and the high magnetic anisotropy are satisfactorily explained by a suitable choice of the coupling coefficient and the coefficients of the rhombic field.

Howard's published curves for μ_B^2 against T only extend to 75° K. A continuation of his calculations to lower temperatures shows that the value of μ_B^2 for both χ_1 and χ_3 at the absolute zero is about 4·0. A comparison with the values given in the present tables shows that Howard's theoretical curves are in reasonable agreement with the experimental results over the whole temperature range yet covered. This is not, however, the case for χ_2. The theoretical value for μ_B^2 at 0° K. is about 2·0, whereas the experimental value at 14·2° K. is already as low as 1·0.

It is not, however, opportune at present to make a detailed comparison between the experimental results and Howard's theory. The latter is essentially a theory of the magnetic behaviour of the $[Fe(CN)_6]$ complex whereas the experimental results for the crystal give only the minimum anisotropy of these magnetic units. The $[Fe(CN)_6]$ groups may be variously situated relative to each other in the crystal lattice, and a detailed knowledge of the structure of the crystal is required before one can calculate the anisotropy of the magnetic units from the observed anisotropy of the crystal as a whole. It is known that there are four molecules in the unit cell of the $K_3[Fe(CN)_6]$ lattice, but the actual positions of the CN groups are not yet known. A comparison with Howard's theory can be undertaken when this information becomes available.

REFERENCES

(1) Jackson, L. C. *Proc. Roy. Soc.* A, **140**, 695 (1933).
(2) Howard, J. B. *J. Chem. Phys.* **3**, 813 (1935).

A NOTE ON THE SPECTRUM OF CADMIUM FLUORIDE, CdF

By R. W. B. PEARSE, Ph.D.
Lecturer in Physics, Imperial College of Science and Technology
AND
A. G. GAYDON, Ph.D.
Beit Scientific Research Scholar, Imperial College of Science and Technology

Received 9 *May* 1938. *Read in title* 24 *June* 1938

ABSTRACT. The spectrum observed by Asundi, Samuel and Zaki-uddin and attributed by them to cadmium fluoride, CdF, has been identified with the known spectrum of calcium fluoride, CaF. New experimental work with cadmium fluoride is briefly described. Mention is also made of absorption bands incorrectly attributed to cadmium bromide and cadmium iodide.

---

§ 1. PREVIOUS WORK ON THE SPECTRUM OF CADMIUM FLUORIDE

Two emission band systems, in the yellow-green and orange regions of the spectrum, have been observed by Asundi, Samuel and Zaki-uddin⁽¹⁾ in an arc containing cadmium fluoride. These bands were analysed and attributed to the molecule CdF.

During the course of other investigations, we noticed that the head of the strongest sequence of the orange system was coincident with that of the calcium-fluoride spectrum, at 6064 A. A closer investigation revealed that the two spectra were very probably identical. In table 1 the wave-lengths, intensities and analysis of the two strongest sequences of bands in the orange attributed to CdF by Asundi, Samuel and Zaki-uddin are compared with the corresponding heads in

Table 1

CdF			CaF		
λ	Intensity	v', v''	λ	Intensity	v', v''
6064·3	4	0, 0 Q_1	6064·4	10	0, 0 Q_{12}
6061·8	4	1, 1 Q_1	6062·3	9	1, 1 Q_{12}
6060·0	5	2, 2 Q_1	6060·4	8	2, 2 Q_{12}
6058·8	3	3, 3 Q_1	6058·6	7	3, 3 Q_{12}
6057·6	5	4, 4 Q_1	6057·0	6	4, 4 Q_{12}
6056·0	3	5, 5 Q_1	6055·5	5	5, 5 Q_{12}
6054·7	3	6, 6 Q_1	6054·0	5	6, 6 Q_{12}
6053·3	1	0, 0 P_2	6052·8	4	7, 7 Q_{12}
6036·9	4	0, 0 Q_2	6036·9	6	0, 0 Q_2
6034·6	3	1, 1 Q_2	6034·8	6	1, 1 Q_2
6032·5	3	2, 2 Q_2	6032·9	5	2, 2 Q_2
6031·0	2	3, 3 Q_2	6031·1	5	3, 3 Q_2
6029·3	1	4, 4 Q_2	6029·3	4	4, 4 Q_2
6027·9	1?	5, 5 Q_2	6027·8	4	5, 5 Q_2

the calcium-fluoride spectrum as measured by Johnson(2); the wave-lengths given by the latter are only reproduced here to the nearest 0·1 A.; the analysis is that proposed by Harvey(3).

It will be seen that the wave-lengths agree closely; for the weaker bands the agreement is slightly less close but still quite convincing. The general intensity-distribution throughout the two systems is also in satisfactory agreement. The analysis proposed for the bands attributed to CdF is similar to the accepted analysis for CaF but differs in detail.

The agreement between the wave-lengths of the yellow-green bands reported by Asundi, Samuel and Zaki-uddin and those for calcium fluoride is not nearly so complete, but as the characteristic groups of calcium lines at λλ5602·8, 5601·3, 5598·5, 5594·5, 5590·1, 5588·7, 5582·0 and λλ5270·3, 5265·5, 5264·2, 5262·3, 5261·7 appear in the reproduction of their photograph showing the yellow-green bands, it seemed desirable to check these experimentally.*

§2. EXPERIMENTAL OBSERVATIONS

Using a glass prism spectrograph giving the visible spectrum on a 12 in. plate, and a Hilger E. 1 quartz spectrograph, we have photographed spectra obtained by introducing cadmium fluoride into an arc between cadmium electrodes, and calcium fluoride into an arc between graphite electrodes. An arc between graphite electrodes fed with cadmium fluoride has also been photographed in the green with a 20-ft. concave grating spectrograph giving a dispersion of 3·8 A./mm. in the first order.

The CaF bands in the orange and yellow-green appeared on all the spectrograms of the cadmium-fluoride arcs, although the calcium lines were less intense on our plates than in the reproduction of the yellow-green bands shown by Asundi, Samuel and Zaki-uddin. Direct comparison of the spectra obtained with the fluorides of calcium and cadmium showed that there were no other bands in the yellow-green or orange that could be assigned to a fluoride of cadmium.

No strong well-developed system of bands which could be attributed to CdF appeared on our plates between 6800 A. and 2400 A., but a few rather weak bands were observed in the region 3000–2800 A. The approximate wave-lengths and intensities of these are listed in table 2; the letters *R* and *V* indicate that the band is degraded to longer or shorter wave-lengths respectively.

Table 2

λ	Degraded to	Intensity
3005	*R*	5
2961·5	*V*	5
2908	*R*	2
2904	*R*	1
2862	*V*	5
2819	*V*	3

---

* Subsequently we discussed the identity of these spectra with Prof. Samuel, who since informs us that Dr Asundi has re-examined the plates and verified our conclusions.

We have not succeeded in identifying these bands, but in view of their rather inconsistent behaviour we hesitate to attribute them to CdF. In addition to calcium, thallium was present as an impurity in our cadmium; the spectrum of thallium fluoride⁽⁴⁾ lies in the same region as the bands listed above, but the wave-lengths of the individual bands do not agree. The emission spectra of cadmium chloride, bromide and iodide observed by Wieland⁽⁵⁾ all lie in the region 3500 to 3000 A., and hence the bands listed in table 2 seem to be in quite a likely part of the spectrum for CdF.

§3. ABSORPTION BANDS ATTRIBUTED TO CADMIUM BROMIDE AND IODIDE

Walter and Barratt⁽⁶⁾, Barratt⁽⁷⁾, and Barratt and Bonar⁽⁸⁾ have studied the absorption band spectra produced by various cadmium compounds and by various impurities which occur in cadmium; various band systems observed by earlier workers and attributed to Cd_2, CdO and InCd were identified with CdCl, TlCl and Bi_2. Walter and Barratt tabulate some absorption bands which they attribute to cadmium bromide and cadmium iodide; these bands were not observed by Wieland⁽⁵⁾ in emission. We have noticed that the absorption bands attributed to cadmium bromide agree within the limits of measurement with the band system of thallium bromide observed by Butkow⁽⁹⁾ and that of those attributed to cadmium iodide some agree with bands of thallium iodide⁽⁹⁾ and the remainder with bands of bismuth iodide⁽¹⁰⁾.

REFERENCES

(1) Asundi, R. K., Samuel, R. and Zaki-uddin, M. *Proc. Phys. Soc.* **47**, 235 (1935).
(2) Johnson, R. C. *Proc. Roy. Soc.* A, **122**, 161 (1929).
(3) Harvey, A. *Proc. Roy. Soc.* A, **133**, 336 (1931).
(4) Howell, H. G. *Proc. Roy. Soc.* A, **160**, 242 (1937).
(5) Wieland, K. *Helv. Phys. Acta*, **2**, 42 (1929).
(6) Walter, J. M. and Barratt, S. *Proc. Roy. Soc.* A, **122**, 201 (1929).
(7) Barratt, S. *Trans. Faraday Soc.* **25**, 758 (1929).
(8) Barratt, S. and Bonar, A. R. *Phil. Mag.* **9**, 519 (1930).
(9) Butkow, K. *Z. Phys.* **58**, 232 (1929).
(10) Morgan, F. *Phys. Rev.* **49**, 41 (1936).

COLOUR SENSATIONS PRODUCED BY ULTRA-VIOLET LIGHT

By A. G. GAYDON, Ph.D., A.Inst.P.
Beit Scientific Research Scholar, Imperial College, London, S.W. 7

Received 28 *January* 1938. *Read* 2 *June* 1938

ABSTRACT. The crystalline lens of the author's left eye has, as the result of an accident, been destroyed. The eye is now sensitive to ultra-violet light of quite low intensity. The sensation between 3600 and 3100 A. is blue, not violet. The sensations produced by extremely faint ultra-violet light on the dark-adapted retina are discussed; the behaviour is essentially similar to that in normal scotopic vision, the light appearing colourless and the peripheral region being more sensitive than the fovea.

§ 1. INTRODUCTION

It has been reported by Saidman(1) that young people with normal sight can see ultra-violet light of high intensity as far as 3341 A. He says there is a focused image on the retina which produces a blue sensation, and a violet halo surrounding this image due to fluorescence of the lens of the eye. The ability to see beyond about 3800 A. is, however, lost with advancing age. It has also been recorded that people who have had an operation for cataract, involving removal of the crystalline lens, are able to see down to 3020 A. Similar observations have been made by de Groot(2). Nevertheless it does not seem to be common knowledge that ultra-violet light produces a blue sensation; moreover I have been unable to find a record of any observations on scotopic vision for ultra-violet light. It therefore seems desirable to record in some detail the sensations that are produced by light between 4000 and 3100 A. now that the lens of my eye has been destroyed.

§ 2. THE HISTORY OF THE EYE

Before the accident my colour vision was quite normal. In 1933 it was tested by Mr F. H. G. Pitt at the Royal College of Science and my colour-matching and hue-discrimination were not in any way abnormal.

In January 1936, while distilling some di-iso-propyl ether* at the British Cotton Industry Research Association, I was involved in a very severe explosion. My right eye had to be removed and my left eye was badly cut by flying glass; the crystalline lens was punctured and formed a cataract. This cataract has now to a large extent absorbed. The remains of the capsule of the lens and the cuts in the cornea interfere with the sight, but by using a small stop I can obtain almost perfect definition and it seems that the retina is normal and healthy.

---

* Details of the explosion have been published in *Chemistry and Industry*, **55**, 421 (1936).

I noticed as sight returned that dark spectacles which most people described as of neutral colour appeared to me to be violet; I have since observed that these spectacles, which are of a very common type, although absorbing fairly uniformly throughout the visible spectrum, are much more transparent to near ultra-violet light. As soon as I was able to resume spectroscopic research work I therefore examined my colour vision, and was surprised to find that I could see quite easily down to 3300 A. with glass spectacles on, and a little farther with quartz lenses.

My colour vision between 4400 A. and the red appears to be still fairly normal, although settings with a Nagel anomaloscope show that I am relatively less sensitive to red light, my setting being on the protanomalous side of the average, but well within the range of settings made by various normal observers.

In view of the effect of age on ultra-violet sensitivity it seems relevant to record that I am aged 26.

§ 3. OBSERVATIONS WITH LIGHT OF MODERATE INTENSITY

An iron arc has been used as a source for most of the observations; I am familiar with the wave-lengths of the principal groups of lines in the spectrum of this arc and could thus dispense with a wave-length scale. I have viewed the spectrum of the arc on several spectrographs and am able to see down to 3100 A. even on instruments of large dispersion. Some idea of my abnormal sensitivity may be gained from the fact that I find it easier to focus and adjust the slit-width of a 20-ft. concave grating spectrograph by observing second-order 3400 A. than by using the first-order 6800 A.

The colour sensations produced by the iron arc spectrum as obtained in a Hilger medium quartz spectrograph (E 2) using a quartz eye-piece are listed in table 1.

Table 1

Wave-lengths (A.)	Remarks
7000 to 4600	Normal; intensity maximum in the green
4500	Blue
4400 to 4300	Blue-violet
4200 to 3900	Violet, but much stronger than as observed previously
3800 to 3700	Very strong whitish violet. The spectrum between 3850 and 3800 A. is very intense and is almost comparable in apparent brightness with the green maximum, the light being unbearably bright if the slit is opened to a width of about 0·1 mm. This intensity is probably largely accounted for by the strength of the iron arc spectrum in this region
3650	Strong whitish blue-violet
3600 to 3150	Strong blue
3100	Blue. There is some indication that the 3100 A. iron triplet is a slightly more violet shade of blue, but this may be only a contrast effect due to the strong blue sensation produced by the neighbouring light
3091	Only just visible with normal slit width
3083	Invisible

I was at first of the opinion that the sensation produced by light between 3600 and 3300 A. was a rather whiter blue than ordinary spectrum blue. I set up a small spectrometer in such a way as to obtain two spectra of the iron arc, one above the other and relatively displaced along the spectrum. By moving the two spectra with respect to each other I was able to make a direct comparison of the colour of the ultra-violet light against the visible spectrum. Some slight difficulty was experienced because of the different focusing of the lenses for visible and ultra-violet light. The spectrum between 3300 and 3600 A. was found to make an almost perfect colour-match with the small group of iron lines at 4530 A., i.e. quite a true blue and apparently free from any sensation of white. The iron arc spectrum between 4600 and 4400 A. as observed with prismatic dispersion appeared of similar intensity to that between 3600 and 3300 A., the ultra-violet being if anything a little stronger; the iron arc of course is also rather stronger in this region as observed photographically.

Some observations have also been made after the eye has been fatigued to light of various colours. After fatiguing to red light the violet region between 4300 and 3700 A. appears less violet and the sensation is then blue from 4700 right down to 3100 A. If the eye is first fatigued to blue light, then the violet patch is more noticeable and appears redder. It therefore seems that the red sensation, in addition to the strong maximum around 6000 A., has a second weak maximum around 3950 A. and then falls to zero at about 3600 A. The blue sensation as recorded by the retina, unlike that obtained by a normal eye with its absorbing lens as well, appears to be stimulated by light between 4800 and 3100 A., where the limit is possibly set by the absorption of the cornea.

§4. DISCUSSION OF THE FOREGOING OBSERVATIONS

Several people have suggested that my sensitivity to ultra-violet light, now that the absorbing material of the lens has been destroyed, is due to fluorescence of the retina. I am of the opinion that this is not so. Firstly, the visual acuity for ultra-violet light and for light in the visible spectrum is the same, while judging by the behaviour of oiled photographic plates used for photography in the far ultra-violet, I should expect a deterioration in the visual acuity for a fluorescence effect. Secondly, the sensitivity seems to be much about the same from 4300 to 3100 A.; since for fluorescence the light must presumably be first absorbed by some substance in the retina and then re-emitted in all directions, I should expect a relatively much lower efficiency for fluorescence than for the normal process of sight. Thirdly, the fluorescent light emitted by most, though of course not all, organic compounds consists of a rather extensive continuous or banded region of the spectrum; light of wave-lengths between 3600 and 3100 A. seems to me to make an almost perfect colour-match with $\lambda 4530$, in which region only the blue sensation is stimulated at all strongly; if the sensation of light was being produced by fluorescence over a broad region of the spectrum, the saturation of the colour observed would be low and an admixture of white with the blue would be required to make a good match against the ultra-violet light. Taken individually none of the above reasons is conclusive evidence that the sensation produced by ultra-violet light is not caused by fluorescence of the retina, but taken collectively the three reasons must be considered as very strong. Moreover, since all the sensations observed for ultra-violet light are qualitatively, and roughly quantitatively, the same as those produced by light in the visible spectrum, it seems quite unnecessary to postulate any mechanism alternative to that for ordinary sight.

It seems that it should now be possible to draw three-colour mixture curves of the type drawn by Wright and Pitt(3) for the retina itself between 7000 and 3100 A.; these curves will differ from those for a normal eye because the latter are modified by absorption of light by the crystalline lens, which reduces the intensity of the violet light falling on the retina and cuts off all but a very small fraction of the light below 3800 A. Any attempt to draw these colour-mixture curves quantitatively would necessitate erecting special apparatus and calibrating light sources for the ultra-violet; this I have so far made no attempt to do. I have however sketched out the probable trend of my *sensation* curves in figure 1; the curves have been drawn from

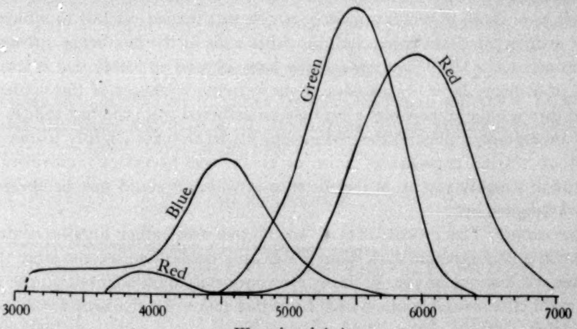

Wave-length (A.)

Figure 1.

visual observation of the spectrum assisted by the fatigue-experiments already described, by my photopic luminosity curve, which has been roughly measured between 4800 and 4000 A., and by a qualitative estimate of my hue-discrimination, which shows a minimum of sensitivity around 4000 to 3900 A., a comparatively high sensitivity around 3700 to 3650 A., and practically zero sensitivity below 3600 A. These sensation curves, which are of the type drawn by König and others, are of course purely qualitative, and cannot be considered as more than careful guesses. Blue light has of course a very small luminosity compared with the green, and in order to show the interesting features of the blue sensation below 4300 A. I have had to draw the blue sensation curve to a larger scale than the others.

The colour-mixture curves published by Wright and Pitt show a rise of the red coefficient to a very flat maximum around 4200 A. The red maximum which I observe between 4000 and 3900 A. is quite definite, and the change in the appearance of this region of the spectrum produced by fatiguing the eye to red light is almost startling. It is difficult to compare the intensities of the sensations produced by widely different regions of the spectrum, as no allowance can readily be made for the intensity-distribution of the light from the source, so the relative heights of the two red maxima are rather indeterminate.

§ 5. SCOTOPIC VISION

Source. For examination of the sensitivity of the dark-adapted eye to very weak ultra-violet light, a very weak source which is relatively rich in ultra-violet light is necessary. A neon lamp run through an extremely small capacity glows feebly, and as the neon spectrum has several fairly strong lines between 3800 and 3300 A. this seemed suitable as a source. It was used in conjunction with an ultra-violet filter which transmitted between 3830 and about 3300 A. This filter appeared almost black to people with normal sight, the filament of an electric lamp being only just visible when held right up against the filter. The neon lamp was run from the 230-volt a.-c. mains through a switch, which was turned off but to which about 4 ft. of ordinary flex was connected, the other ends of the flex being unconnected; this flex acted as a small capacity and the lamp glowed so feebly that it was barely visible in ordinary light. Some idea of the extreme weakness of this source when viewed through the ultra-violet filter may be gathered from the fact that to darken a fast photographic plate (Ilford Monarch, H. & D. 525) slightly (to an optical density of 0·2) an exposure of 2 hr. at 10 in. was necessary, equivalent to an exposure of roughly 100 hr. at the distance at which it could just be observed by the dark-adapted eye.

Observations. The process of dark-adaptation took rather long, and after half an hour in a photographic dark room it was only possible to see the lamp through the filter at a distance of 3 ft. With my eye completely dark-adapted (in the middle of the night after several hours in bed) I was just able to see the lamp at a distance of roughly 6 ft.

The sensation produced by such faint light was of course quite colourless. It was also noticed that the lamp was most easily observed by looking slightly to one side so that the image fell not on the fovea but on the outer part of the retina. This is of course also the case for scotopic vision with light of other colours, and in fact the observations for ultra-violet light and visible light seem to be in all ways at least qualitatively the same. The degree of dark-adaptation and the sensitivity of the retina to faint ultra-violet light are high.

Discussion of the observations. In view of the preliminary nature of the observations recorded above, and as I have so far not been able to measure my scotopic luminosity curve, it would be unprofitable to discuss existing theories of scotopic vision or to make any suggestions to account for the apparently high sensitivity of the dark-adapted retina to light below 3800 A. The scotopic luminosity curve for a normal eye has a maximum in the green(4) and falls off sharply on the short-wavelength side at about 4500 A. The visible absorption band of visual purple(5) agrees very closely with the scotopic luminosity curve, and photochemical bleaching of thin films of visual purple varies with wave-length in much the same way, the similarity of these three curves being in fact the basis on which visual purple is assumed to be intimately connected with scotopic vision. Recently Dartnall and Goodeve(6) have pointed out that the absorption of visual purple is higher in the violet than that indicated by a luminosity curve drawn so that the maxima of the curves coincide, and have attempted to correct the luminosity curve for absorption by yellow pigmentation of the retina and absorption of the lens. A quantitative comparison of my scotopic luminosity curve with the absorption by visual purple down to 3100 A. would be very interesting.

§6. CONCLUSION

It seems that measurements of the colour-vision and scotopic-luminosity curves of subjects who have had an operation for cataract, and who are thereby sensitive to ultra-violet light, might considerably extend our knowledge of the very complex problems associated with vision, and that the region of the spectrum between 4000 and 3100 A. would well repay a more thorough study than it has so far received.

§7. ACKNOWLEDGEMENTS

I should like to express my thanks to Dr R. W. B. Pearse and Dr W. D. Wright for helpful discussion, and to Miss W. M. McKeon for co-operation in measuring my photopic luminosity curve in the blue.

REFERENCES

(1) Saidman, J. *C.R. Acad. Sci., Paris*, **196**, 1537 (1933).
(2) Groot, W. de. *Nature, Lond.*, **134**, 494 (1934).
(3) Wright, W. D. and Pitt, F. H. G. *Proc. Phys. Soc.* **47**, 205 (1935).
(4) Hecht, S. and Williams, R. E. *J. Gen. Physiol.* **5**, 1 (1922).
(5) Houstoun, R. A. *Vision and Colour Vision* (1932).
(6) Dartnall, H. J. A. and Goodeve, C. F. *Nature, Lond.*, **139**, 409 (1937).

DISCUSSION

Prof. Allan Ferguson. I have had the lens of my left eye removed as the result of the development of a simple cataract, but I have not, as yet, made any quantitative investigations of the type described by Dr Gaydon. Qualitatively I notice that mercury-vapour lamps appear as surrounded by a vivid violet aura, and that, after a day spent in brilliant sunshine, I observe the late afternoon sky as very rich in reddish-purple hues, the psychological effect being oddly unnatural. Further, at any period, acuity of vision falls off very rapidly as darkness comes on. I cannot resist taking this opportunity to congratulate the author on the courage and pertinacity which has enabled him to obtain so much of good from a misfortune so serious.

Dr W. D. Wright. This paper is of very considerable interest and should prove of value in furthering our knowledge of the visual processes. My main regret is that our colorimeter, on which the author took certain of his observations, was not designed to extend into the ultra-violet and so did not enable him to record any quantitative observations on colour-mixture and hue-discrimination. I tried to persuade Dr Gaydon to guess his hue-discrimination curve, but could not induce him to be so rash. It would appear, however, that on the assumption that a minimum in the curve occurs where the hue is at a point of change between two main sensations, for instance at the blue-green, an extra minimum should occur at about 3800 A., where the hue is changing back from purple to blue. The main value of the results will no doubt be found in relating them to the photo-chemical processes occurring in the retina. It would, of course, have been very exciting if Dr Gaydon had experienced a new sensation altogether in the ultra-violet.

Dr F. H. G. PITT. The author has remarked that persons who have had an operation for cataract, involving removal of the crystalline lens, are able to see down to 3020 A. I know one who has had a cataract removed from his left eye and he, too, can see well down into the ultra-violet, and like Dr Gaydon sees this as a blue sensation. He can also see weak light-sources through an ultra-violet filter (Wratten No. 18*a*).

AUTHOR'S REPLY. I also have noticed the purple effect after sunset remarked on by Prof. Ferguson, the colour being particularly noticeable if seen in contrast with artificial light.

In reply to Dr Wright, I have stated in the paper that my hue-discrimination has a maximum of sensitivity (i.e. the curve shows a minimum) around 3700 or 3650 A.; the sensitivity here is probably about 10 to 20 A., but as the colour of the light appears to change slightly with intensity, being relatively blue for strong light and violet for light of low intensity, it is not easy to draw a quantitative hue-discrimination curve.

I am very interested to hear that Dr Pitt's friend confirms my observations.

Recent measurements made by Dr C. F. Goodeve at University College indicate that my eye, when dark-adapted, is roughly 1000 times as sensitive, compared with the green maximum, as a normal eye to light of wave-length 3650 A. For this wave-length the sensation is blue for light of high intensity, violet for light of low intensity and colourless for very weak light.

THE DISSIPATION OF ENERGY BY A PENDULUM SWINGING IN AIR

By E. C. ATKINSON, M.A.

Received 17 *February* 1938. *Read* 24 *June* 1938

ABSTRACT. The decrement of a pendulum falls slowly with the amplitude: hence the need for determinations based on small changes of angle. The resulting errors of observation lead to erratic values but not to systematic error. The result of measurements with a seconds pendulum enclosed in a case is shown by a smoothed curve, the departure from observed times being expressed by *smoothing fractions*, and a *smoothing figure* is a measure of this departure for the whole or part of the experiment. From the decrement the rate of loss of energy is calculated. This 7 kg. pendulum with amplitude 53′ dissipates a Board of Trade Unit (which serves a 70 W. lamp for 14 hours) in rather over 100,000 years. Experiments with different pendulums are described by which the component losses due to suspension, rod, and bob are found. Suspension springs made from thin strip clamped in chaps dissipate large and variable amounts of energy compared with springs made from thick strip ground thin in the middle. The variable losses are associated with variable rates of the pendulum. The cylindrical case adds considerably to the air resistance. The measured loss due to a gravity impulse lever is little in excess of the computed loss from collision with the pendulum: for a seconds pendulum 1/2000 part of the free pendulum loss.

§ 1. DECREMENT AND ENERGY DISSIPATION

SUPPOSE a pendulum encounters at each moment a resistance proportional to its velocity, producing an acceleration $2\delta\dot{\theta}$ radian/sec.^{2} when the pendulum makes an angle θ with its position of rest. The equation of motion is then

$$\ddot{\theta}+2\delta\dot{\theta}+dg\theta/K^2=0 \qquad \text{......(1)},$$

d being the distance of the centre of gravity below the turning point and MK^2 being the moment of inertia of the pendulum of mass M g. about this point in C.G.S. units. It follows that

$$\theta=\alpha_0 e^{-\delta t}\sin nt$$

t seconds after the moment when θ was 0 and the amplitude α had its initial value α_0, amplitude being the semi-arc, and

$$n=\sqrt{\frac{dg}{K^2}}=2\pi \text{ times the frequency of oscillation.}$$

Thus $\alpha=\alpha_0 e^{-\delta t}$ and δ is found from t_1 and t_2 for α_1 and α_2 respectively from

$$\delta=(\log_e\alpha_1-\log_e\alpha_2)/(t_2-t_1) \qquad \text{......(2).}$$

I call δ the *decrement*.* Then,

$$\delta = -\frac{1}{\alpha}\frac{d\alpha}{dt}$$

$$\text{i.e.}\quad = -\frac{\Delta\alpha}{\alpha}\ \text{per second.}$$

Logarithmic decrement is defined as $-\Delta\alpha/\alpha$ per cycle and is equal to $2\pi\delta/n$.

The energy of the pendulum $= \frac{1}{2}MK^2n^2\alpha^2$,

$$\text{hence the loss of energy}\quad = MK^2n^2\alpha\Delta\alpha$$

$$= 2\pi n\delta MK^2\alpha^2\ \text{erg/c.} \qquad \text{......(3).}$$

§ 2. OBSERVATIONS FOR DECREMENT

The decrement in an electrical circuit consisting of a condenser in series with an air-cored inductance is independent of the current-amplitude, provided Ohm's law holds good. With a pendulum, on the other hand, δ decreases slowly with α and must be determined by observations of t for successive values of α differing, say, by $2{\cdot}5'$. In an investigation of the relation between rate and arc(1) δ was needed for calculating the effect of maintenance. Comments which I made on these measurements did not, apparently, distinguish clearly between erratic values and systematic error.† I will, therefore, describe an observation.

The micrometer eyepiece is adjusted so that a line on the moving scale fixed to the pendulum comes to rest beyond the index, whilst another line travels to an equal distance beyond it at the other end of the swing. As the amplitude falls these stationary positions approach the index, and the moment is recorded when a line appears to coincide with the index, the other line doing so half a cycle later.

An error of observation consists in ante-dating or post-dating the event, i.e. in recording a moment when the lines do not coincide with the index.

§ 3. EFFECT OF ERRORS OF OBSERVATION. SCALE-CALIBRATION

In table 1 α becomes $82{\cdot}14'$ (column 1), 1275 sec. (column 6) from the start. Suppose the true time is 1272. The error has made the preceding interval 446 sec. instead of 443 (making $10^7\,\delta$ too small by 4·6 units) and the succeeding interval 454 instead of 457 (making $10^7\,\delta$ too large by 4·4 units). The error makes a difference of 9 units in the drop from one value of δ to the next, but its effect on the average value is quite inappreciable, i.e. it does not introduce systematic error.

The angular errors in estimating coincidences of lines with index are probably about the same for all amplitudes; possibly better observations are obtained with large amplitudes when the glimpse of the line in its stationary position is more

---

* In a previous paper(1) I described δ as logarithmic decrement in error.

† Prof. R. A. Sampson(2) supposed that the values used might be systematically too large by 10 per cent or even by 24 per cent.

Table 1. Decrement of E_{14} in cylindrical case. (Barometer 540 mm.)

1	2	3	4	5	6	7	8	9	10	11	12
a	$\Delta \log_e a$	Seconds observed				δ_{10} $\times 10^7$	δ smoothed $\times 10^7$	Seconds calc.	Seconds calc. − obs.	Smoothing fraction $\times 10^4$	Square $\times 10^8$
		Oct.	Nov	Mean	Total						
89·60	0·02768	396	412	404			690	402	+3	75	56
87·15	0·02932	430	421	425	404	687	685	427	+1	25	06
84·62	0·02992	446	446	446	829	681	679	440	+3	69	48
82·14	0·03088	456	451	454	1,275	675	672	460	−3	66	44
79·65	0·03184	481	483	482	1,729	666	663	480	+3	64	41
77·15	0·03289	501	510	505	2,211	658	654	502	+1	20	04
74·65	0·03441	531	533	532	2,716	648	645	534	−2	39	15
72·13	0·03508	546	546	551	3,248	640	636	552	0	0	0
69·64	0·03640	574	586	580	3,799	631	627	581	+1	17	03
67·15	0·03846	630	625	628	4,379	620	619	622	+2	33	11
64·62	0·03907	651	637	644	5,007	615	615	646	−4	63	40
62·14	0·04022	647	659	653	5,651	612	612	658	−2	31	09
59·69	0·04166	685	681	683	6,304	610	608	685	+3	45	20
57·26	0·04461	740	737	739	6,987	605	604	739	+5	70	49
54·76	0·04654	789	782	785	7,726	597	598	780	+5	66	43
52·27	0·04863	834	834	834	8,511	592	589	825	0	0	0
49·79	0·05190	881	876	879	9,345	581	580	895	−9	104	108
47·27	0·05436	964	976	970	10,224	573	570	954	+7	75	56
44·77	0·05817	1047	1,031	1039	11,194	568	562	1033	−9	90	81
42·24	0·06106	1073	1,080	1076	12,233	563	558	1093	−15	141	199
39·74	0·06388	1134	1,143	1139	13,309	558	554	1152	+2	19	04
37·28	0·06858	1269	1,264	1266	14,448	552	549	1250	+15	125	157
34·81	0·07416	1375	1,364	1370	15,714	545	543	1364	−1	08	01
32·32	0·07950	1503	1,464	1483	17,084	538	537	1481	−7	49	24
29·85	0·08663	1638	1,610	1624	18,567	535	531	1631	−9	57	33
27·37	0·04770		8,940		20,191		(534)		−2	10	01
16·99	1·250		24,300				(515)				1053
4·87											

Smoothing figures: $\sqrt{(1053\times 10^{-6}/26)}$, equal to 0·00637 for whole series; $\sqrt{(605\times 10^{-6}/6)}$, equal to 0·01005 for 50′ to 35′; $\sqrt{(448\times 10^{-6}/20)}$, equal to 0·00473 for remainder. October times have been increased 1·1 per cent to correct for higher pressure. First and last figures in column 7 relate to 5′ intervals.

momentary. Thus the fraction (error in seconds/interval for 2·5′) measures the proportional error in δ and also, being proportional to the angular error, may be taken as a measure of the unreliableness of observation.

Unequal spacing of scale divisions is another source of error. The scale used with pendulum E since 1931 was ruled on ivory by a firm of opticians to replace my amateur effort, yet in this the largest space exceeds the smallest by 4 per cent. I have recently recalibrated it, using the micrometer eyepiece arranged to give a magnification such that 500 divisions on the micrometer head correspond to the 2·5′ space.

§4. DECREMENT-DETERMINATIONS IN 1934 AND 1937

The δ values already referred to were obtained in 1934 from two runs, but for half the intervals observations from one run only were available. From such meagre material, a spread of points on the graph was to be expected, but two especially low points near 50′, not balanced by high points on either side, suggested that some resonant effect due to the cylindrical case might exist for this angle.

In October and November 1937 I made observations with pendulum E_{14} (similar to E_{11} but for a larger bob for which $M=7\cdot2$ kg. as compared with 6·2 for E_{11}) in the same enclosure. Two runs were used from each month. Between the experiments, I made two changes in the micrometer which experience shows to have improved the observing, but I have assigned equal weight to October and November.

Table 1 will make clear the way in which I have used this material. Values for δ are calculated from time intervals for 10′, e.g. from 89·60′ to 79·65′ and next from 87·15′ to 77·15′; all amplitudes are corrected by calibration and reduced to true minutes of arc (column 7). These values have been used as a guide to obtain smoothed values (column 8), for the original 2·5′ intervals. With any smoothed value there is associated a time interval derived from equation (2) which is entered in column 9, and from this column 10 is built step by step giving a calculated time for reaching each angle and thence the difference between calculated and observed times. For example, $\alpha=64\cdot62$ is entered as being reached 5007 seconds from the start. The calculated time is 5003 (assuming that 89·60 occurred 3 seconds later than recorded). The smoothing process consists in reconciling so far as possible regularity in change of δ with agreement between computed and observed times. It should be remembered that an observation is not an interval of time but the start or finish of such, and column 10 shows to what extent an arbitrary manipulation of figures involves departure from the observed times. The *smoothing fraction* in the above case $=-4/\{(622+646)/2\}=0\cdot0063$ (cf. § 3). The root mean square of a series of such fractions may be called the *smoothing figure* for the series, and its smallness is an indication of the confidence which may be placed in the result.

§ 5. THE DECREMENT CURVE

The 1937 result is shown on a large scale (for the zero line is far below the figure in *A* of figure 1. The smoothing figure is 0·0064 (the factors at the heads of columns 7, 8, 11 and 12 of table 1 should be noticed), as compared with 0·0118 for the 1934 curve obtained in the same way. If we bear in mind the time and care expended to obtain the later results compared with the earlier, the smaller smoothing figure is not surprising.

It will be noticed in column 11 that the smoothing fraction reaches 0·01 in three cases, all of them in the region $\alpha=50'$ to 35′. For this region the smoothing figure is 0·0100, and it is 0·0046 for the rest of the curve. On comparing the October figures with those obtained in November, I find that the irregularities of δ in this region are strikingly similar in the two cases. This would result from faulty calibration of the scale, but the deviations are five times as large as any that can come about in this way since the latest calibration.

I think that the curve represents the truth fairly closely, but it may have been simplified too much between 50′ and 30′. It lends no support to the 1934 observations of low values around 50′. The hump between 45 and 65 is real. I suppose the shape of the curve is largely due to the 20 cm. cylindrical case: I cannot see how the two regions of relatively low values would occur with a pendulum swinging in the open.

Study of these large-scale curves tends to give an exaggerated idea both of the amount and of the irregularity of change of δ. I have therefore added curve *B*, which is the same as *A* but on a smaller scale so that the zero line also appears.

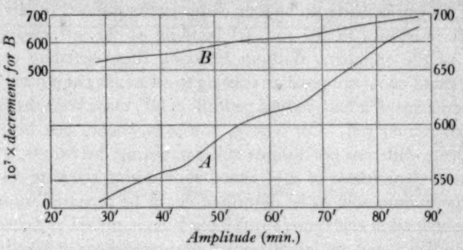

Figure 1. Decrement of seconds pendulum E_{14} in cylindrical case at 540 mm.

§6. ENERGY-DISSIPATION. CHANGES IN δ

The loss of energy at any amplitude can be obtained from equation (3) when the moment of inertia ($6{\cdot}9 \times 10^7$ g.-cm.^{2} for E_{14}) is known.

Taking $\alpha = 53'$, for example, table 1 gives $\delta = 596 \times 10^{-7}$, $n = \pi$ (seconds pendulum). The loss $= 2\pi^2 \times 596 \times 6{\cdot}9\ (53/3438)^2 = 19{\cdot}3$ erg/c. This loss (9·6 ergs per second) may sound a large amount, and it is enormous compared with the flow of energy needed for radio reception. On the other hand, a Board of Trade Unit (which serves a 70 watt lamp for 14 hours) is $3{\cdot}6 \times 10^{13}$ ergs, so that the pendulum loses this amount of energy in 118,000 years.

When a pendulum is maintained at a steady amplitude, the input, of course, balances the loss. When the supply is (1) very steady as it is with my gravity impulse and is (2) independent of amplitude, change in δ due to change in air-density, for example, can be measured indirectly without disturbing the clock, by noting the change of amplitude, for in this case the loss remains constant; hence

$$\frac{\Delta\delta}{\delta} + \frac{2\Delta\alpha}{\alpha} = 0 \qquad \text{......(4).}$$

I find that when air pressure is changed from 532 mm. to 586 mm., α falls from $68{\cdot}49'$ to $66{\cdot}91'$. From table 1, $10^7\delta = 627$ at $68{\cdot}4'$ and falls $8 \times 1{\cdot}58/2{\cdot}5 = 5$ with amplitude. With increased pressure $10^7\Delta\delta = 627 \times 2 \times 1{\cdot}58/68{\cdot}4 = 29$, equation (4). Thus the new $10^7\delta$ is $627 + 29$ at $66{\cdot}91'$ and $627 + 29 + 5$ at $68{\cdot}49'$, an increase of 34 for 54 mm., just 1 per cent per cm.

The gravity impulse fulfils the second condition that supply is independent of amplitude. Where inertia of the impulsing mechanism plays a part, the energy supplied falls off with amplitude. This happens with a Graham escapement in the early part of the impulse. In the Shortt clock the important part of the impulse—the last part—falls rapidly with increasing amplitude. This aids in restoring a disturbed amplitude and also counteracts circular error to some extent when the impulse is timed so that it finishes after the pendulum has passed the central position.

§ 7. THE DISSIPATION COMPONENTS

The loss of energy is made up of four components due to: (*a*) air resistance to the bob, (*b*) air resistance to the rod, (*c*) bending of the suspension spring and (*d*) movement of the support. Without knowing these separate components, I realized in 1931 that I could not use data relating to a seconds pendulum (*S*) to predict the loss and decrement of a half-second pendulum (*H*) made with the same bob and spring and a shortened rod. Conversely, the components can be measured by experimenting with different pendulums and combining the results.

The decrement experiment of 1937 aimed at obtaining accurate results. On the other hand, experiments now to be described could be repeated more accurately, some data not obtained at the time (1932) have been supplied as far as possible by more recent experience, and, in one particular, uncertainty could have been removed by modifying the experiment. Moreover, the theory is approximate only, but the experiments seem to justify its use. However, results follow which are fairly accurate, and which, so far as I know, have not been obtained by other means.

§ 8. EXPERIMENTS TO MEASURE COMPONENTS

The loss per cycle is found by decrement experiments for several pendulums all supported by the same brackets through the same suspension spring *D*. All rods are of the same diameter ($\frac{5}{16}$ in.) and *S* and *H* have the same bob. For all pendulums the loss is found for $\alpha = 53'$ and also for *S* at $\alpha = 26{\cdot}5'$.

Besides *S* and *H*, bobless pendulums were used consisting of rods of different lengths attached to the spring. The experiments do not distinguish between (*c*) and (*d*), and their combined effect is called *suspension loss*.

Six rod pendulums ranging in length from 90 to 15 cm. were experimented with (§ 9) and the constant suspension loss (§ 13) was separated from the variable air resistance loss which depends on length and frequency. From these results, the rod losses for *S* and *H* are obtained, and thus the sum of the suspension and bob losses is found for *S* and *H*. The former is nearly the same for the two (by compensating for the reduced rod-weight of *H* it would be made the same, § 13), whilst the bob loss for *S* is 10·0 times that for *H*. In actual fact the theory is not quite so simple as this, hence the need for allowing for the *S* loss at 26·5′ (§ 10). The separation of bob loss from suspension loss is reduced to solving simultaneous equations.

§ 9. EXPERIMENTS WITH ROD PENDULUMS

To find how the observed losses *E* of the different rods are related to one another and to the rod losses of *S* and *H*, the hypothesis of § 1 is extended to the supposition that each cm. of rod meets with a resistance proportional to its linear

Table 2. Losses by rod pendulums. Rod losses by *S* and *H*

Rod	1	2	3	4	5	6	7	8
L (cm.)	90·5	70·0	49·9	34·7	24·7	15·1	43·0	I.L. in action
M (g.)	353·5	273·2	194·9	135·5	96·7	59·4	168	
n (computed, § 20)	4·10	4·72	5·75	7·27	9·34	13·79	6·31	
n (observed)	4·07	4·72	5·77	7·30	9·40	13·80	6·32	
Seconds 70/30	1021	981	902	800	622	377	893	855
$\delta \times 10^4$	8·41	8·66	9·42	10·62	13·66	22·5	Diff.	0·42
$MK^2 \times 10^{-3}$	994	463	172	60	23·0	6·52	111	
Erg/c. ($\alpha = 53'$)	5·025	2·824	1·397	0·692	0·441	0·303	I. L. loss 0·045	
Air loss/c. (suspension = 0·182)	4·84	2·64	1·21	0·510	0·259	0·121	(See § 22)	
$[(L+0{\cdot}9)^3+1850] \times 10^{-5}$	7·65	3·58	1·33	0·470	0·186	0·0594		
κ	740	402	182·1	81·5	41·6	19·5	}	
$\sigma \times 10^5$	655	657	667	626	622	621		

S $\alpha = 53'$, $\kappa = 603{\cdot}8$, therefore $\sigma = 656$. Rod loss = 3·96 erg/c.
26·5 151·0 644 0·97
H 53 15·31 621 0·095

velocity. A rod-length L cm. starts at 0·9 cm. from the turning point and the air-resistance loss takes the form $\sigma n \alpha^2 \left[x^3\right]_{0\cdot 9}^{L+0\cdot 9}$ erg/c. A platform at 15·4 cm. carries the scale. As these move in their own plane, I reckon the resistance as half that for an equal surface of rod. If s is the suspension loss for the mean angle 53′ (§ 12),

$$\begin{aligned} E - s &= \sigma n\,[(L+0{\cdot}9)^3 + 1850]\,(53/3438)^2 \\ &= \sigma\kappa \text{ erg/c.} \end{aligned} \qquad \ldots\ldots(5),$$

where 1850 is the platform term. σ, like δ, grows slowly with speed and so with κ. Each point on A figure 2 represents E for a rod (ordinate), with κ as abscissa. The graph through these points extended to the y axis will cut this in C at height s erg/c. The line A is supposed to be the tangent at C to the graph, passing very nearly through points 6 and 5. Line B represents the lower end of A on a ten-fold scale, and shows that the constant (§ 13) s is about 0·18 erg/c. The value 0·182 is found by trial so as to make σ for rod 6 just less than σ for rod 5.

Equation (5) shows that if the line joining C to 3 (say) makes angle θ_3 with the horizontal, then $\sigma_3 \times 10^2 = \tan\theta_3$ (account being taken of the scales used for the co-ordinates). Thus, the fact that the points for the longer rods stand above the line which passes nearly through 5 and 6 indicates that σ grows with κ.

The three arrows show values of κ for H and the two cases of S for which we need to know the resistance (in calculating κ for these, there is no platform term).

κ ranges from 20 to 740, and the comparatively small change in $10^5\sigma$ from 620 to 660 suggests that the values chosen for S and H will not be far wrong. The worst determination of E appears to be the one for rod 3.

The observed results and calculations are shown in table 2. Columns 7 and 8 refer to impulse lever losses (§ 22). The computed value of n (§ 20) is not used in finding the losses. "Seconds 70/30" means the time interval between $\alpha = 70$ scale divisions and $\alpha = 30$. The relation between this range and 53′ is discussed in § 12.

All experiments were made in the open air. Records were made of pressure and temperature, but no corrections were applied for the small changes. M is the weight of the rod. In addition there is 5 g. at 15·4 cm. for platform and scale. For S and H the values of κ are calculated and these give the appropriate values of σ and, finally, the air resistance for the rods is $\sigma\kappa$.

The suspension loss 0·182 erg/c. is an interesting quantity (§ 21). It relates to light pendulums only and must not be confused with the much heavier loss with S and H.

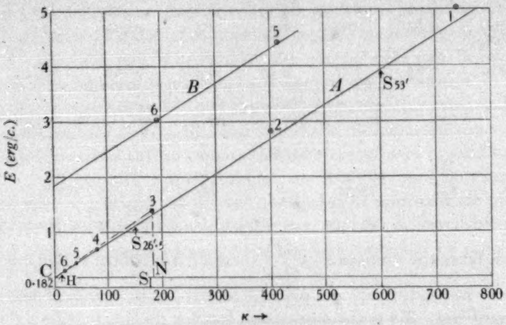

Figure 2. Loss of energy by rod pendulums. In open at 750 mm.

§ 10. CALCULATION OF COMPONENTS FOR *S* AND *H*

To find the ratio of the bob losses, the same principle is applied as before. If the flat ends of the cylindrical bob are at L_1 and L_2 cm. from the turning point, the resistance to the curved surface produces a loss which may be written

$$3\sigma n\alpha^2\int_{L_1}^{L_2} x^2\,dx.$$

The surface πr^2 of each end has the same area as $\frac{1}{2}r$ cm. of the curved surface, but as these ends move in their own planes σ is reduced to $\rho\sigma$, say where $1 > \rho > 0$, so the whole loss is

$$3\sigma n\alpha^2\left[\int_{L_1}^{L_2} x^2\,dx + \rho r\,(L_1^2 + L_2^2)/2\right].$$

Using σ for S and σ' for H and inserting the numerical values of L_1, L_2 and r, we have

$$\frac{H \text{ bob loss}}{S \text{ bob loss}} = \frac{\sigma}{\sigma'}\,\frac{4970 + 1186\rho}{580 + 148{\cdot}5\rho}.$$

The coefficient of $\sigma/\sigma' > 8{\cdot}45$ $(\rho = 1) < 8{\cdot}57$ $(\rho = 0)$. For want of better knowledge, I put $\frac{1}{2}$ for ρ as in § 9 and then the ratio is $8{\cdot}50\,\sigma/\sigma'$.

With its longer rod S is heavier than H and the suspension loss is greater for S than H by an unknown amount. If this is y erg/c. for H, I give one solution for the case in which the S loss is $1{\cdot}04y$ and another for $1{\cdot}08y$ (§ 13). The bob loss for H being x erg/c., that for S at same amplitude (53′) is $8{\cdot}50x \times \sigma/\sigma'$. It would, therefore, be just $8{\cdot}50x$ if the change in σ due to the change in range of velocities were neglected. Now, S with α equal to 26·5′ has the same range of bob velocities (strictly for mid-bob only) as H has at 53′, and the transition to S at 53′ *neglecting change* in σ is in the ratio of squares of linear amplitudes, i.e. 4 : 1.

Table 3 shows the steps in calculation. Total losses are observed quantities, rod losses come from § 9, and suspension losses are expressed as above in terms of y; $1{\cdot}04y/4$ for S 26·5′ assumes that the loss $\propto \alpha^2$. This should be true for bracketing and it is so for an unloaded spring. I think that it is probably not exactly true for a spring supporting a heavy pendulum. Bob losses expressed as remainders contain y and they can also be expressed in terms of x according to reasoning which I have just given (and which is not perhaps self-evident at first sight). Hence values for x, y and σ/σ'.

Table 3. Components of loss for S and H (ergs per cycle)

	Suspension loss for $S=$					
	(1) $1{\cdot}04y$			(2) $1{\cdot}08y$		
Amplitude	H 53′	S 53′	S 26·5′	H 53′	S 53′	S 26·5′
Total loss	2·658	19·37	4·257		As in (1)	
Rod	0·095	3·96	0·97		As in (1)	
Suspension	y	$1{\cdot}04y$	$1{\cdot}04y/4$	y	$1{\cdot}08y$	$1{\cdot}08y/4$
Bob	2·563 $-y$ x	15·41 $-1{\cdot}04y$ $8{\cdot}5x\sigma/\sigma'$	3·305 $-1{\cdot}04y/4$ $8{\cdot}5x/4$	2·563 $-y$	15·41 $-1{\cdot}08y$	3·305 $-1{\cdot}08y/4$
	$x=1{\cdot}415$, $y=1{\cdot}148$, $8{\cdot}5\sigma/\sigma'=10{\cdot}05$			$x=1{\cdot}408$, $y=1{\cdot}155$, $8{\cdot}5\sigma/\sigma'=10{\cdot}05$		
	Results					
	(1) $1{\cdot}04y$			(2) $1{\cdot}08y$		
Amplitude	H 53′	S 53′	S 26·5′	H 53′	S 53′	S 26·5′
Bob	1·41	14·22	3·01	1·41	14·16	3·00
Rod	0·09	3·96	0·97	0·09	3·96	0·97
Suspension	1·15	1·19	0·30	1·15	1·25	0·31
Impulse	0·04	0·01 to 0·02	—	0·04	0·01 to 0·02	—
	2·69	19·38	4·28	2·69	19·38	4·28

Bob dimensions: 16·5 cm. long × 7·8 cm. in diameter. Rod 0·79 cm. in diameter. Pendulums swinging in open air at about 750 mm.

The second part of the table gives final results. For solving the equations I have worked to three places of decimals, but the experimental work does not justify the retention of more than two. I have added impulse lever losses (§ 22) for completeness.

§ 11. VALUES OF THE COMPONENTS

I repeat that these values relate to pendulums swinging in the open air at atmospheric pressure. Bob losses are higher (§ 23) when the pendulums are inside cases. Perfect suspension would not materially reduce the spring and bracketing losses (§§ 13, 21).

Faulty design of the experiments is unfortunate, but comparison of the two solutions shows that the uncertainty introduced thereby is not very serious.

Whilst with *S* suspension loss forms about 6 per cent of the whole, it amounts to 43 per cent with *H*. W. H. Shortt(3) in 1928 estimated the spring loss at 2 to 4 erg/c. He does not say how this figure was obtained, but it seems far too large for the suspension spring of the master pendulum.

In *H*, 2 cm. of rod projecting beyond the bottom of the bob adds needlessly to the rod resistance.

For equal speeds a square centimetre of rod dissipates just about twice as much energy as an equal area of bob.

Nearly $\frac{3}{4}$ of the energy lost by *S* is due to the bob. When low losses are desired, reductions can be made by working in low pressures and also by replacing air by hydrogen.

The size and shape of the bob, too, affects the resistance. At the amplitudes used for precision clocks the air movement is not turbulent, and the important element affecting resistance is skin friction. In such a case shape is of less importance than surface area. The bob used in these experiments is not ideal in this respect. It is made of a bronze of density 8·7, as compared with 11·4 for lead. Its height is 2·1 times its diameter, whereas the right circular cylinder of least surface for given volume has its height equal to its diameter. Actually, the difference is remarkably small—$5\frac{1}{2}$ per cent.

Some ten years ago A. W. Hirst experimented at Bristol on a pendulum fitted first with a long bob of circular section, and later with one of elliptical section having the major axis about three times the minor. Results were published by Prof. David Robertson.(4) Air pressures ranged from 250 mm. to 1275 and amplitudes from 100′ to 300′. With these large arcs turbulent motion is present and the oval bob has the advantage, especially with high pressures and the larger arcs. With small angles, however, the oval bob is at a disadvantage owing to its larger surface and the circular cylinder encounters the smaller resistance.

I did not realize in 1932 the need for the value of *E* for *S* at half amplitude. This I have supplied by using the ratio of decrements obtained from table 1.

§ 12. RHEINBERG SCALE AND THE MEAN ANGLE

The observations with rod pendulums and for *H* were made by means of a Rheinberg scale with 0·1 mm. spaces. At a distance of 15 cm. from the turning point this space subtends an arc of 2·292′ representing amplitude 1·146′. The scale is a photographic negative with transparent lines on a dark ground. A beam of light is reflected by mirrors through the scale to the micrometer eyepiece. This scheme proved valuable in finding the short intervals of time with accuracy. Instead of observing coincidences with the index (§ 2), the overlapping lines only are observed. These produce a characteristic flicker after true coincidence. When this ceases the dark space between them appears quite suddenly, so that I think the moment at which the edges of the lines just touch can be observed to the nearest second. I estimate that the allowance for reading on the edge of the line is 0·1′. Thus, "70 divisions" means that $\alpha = 69{\cdot}9 \times 1{\cdot}146$ arc minutes.

δ, then, is found from the interval between $\alpha = 80{\cdot}1$ and 34·3, and equation 3 is true for the α for which this is the decrement. In 1932 I was satisfied to take 57′, the average angle, but δ is a mean with regard to *time* (and not *amplitude*) and the correct amplitude depends on the shape of the δ graph.

In 1932, readings were taken for each 5 divisions fall of α and I have combined all the observations to find this shape, which is definitely steepest in the middle, easing off at each end: a result which clearly gives no true information about changes in δ and shows that the Rheinberg scale needs calibrating. As this cannot be done whilst the scale is in use, I have adopted the angle 53′ which would be right if the graph were straight.

These half-second pendulums with heavy bobs are stumpy in appearance, since the bobs are longer than the exposed parts of the rods.

§ 13. SUSPENSION LOSSES

The combined loss due to strain of the bracketing, and bending of the spring could be found by measurements made with the pendulum in vacuo, for then these are the only losses remaining. Unfortunately for this method, the air resistance does not become negligible until the pressure has fallen far below what I could reach or measure. Air viscosity remains practically constant, whilst pressure is reduced from 760 mm. to 1 mm. Referring to experiments with a light half-second pendulum mounted on knife edges, A. L. Loomis wrote in 1933 that "the decrement was cut in half by reducing the gas pressure from 0·025 mm. to 0·001 mm." What fraction of the total loss is still due to air resistance even at 0·001 mm.?

My experiments do not distinguish between bracketing and spring losses, although it seems clear (see below and § 21) that the first is negligible for the light pendulums. When a pendulum is supported on a wooden case, as in a grandfather clock, the bracketing loss is frequently much larger than all the others combined. For a precision clock a sturdy support is important. The experiments were made on brackets attached to a 14 in. house wall. Brickwork was removed and replaced by 2 cwt. of concrete well keyed to the bricks (a tedious job). Long bolts, fixed at the back to an iron plate, were buried in the concrete and care was taken to make a rigid structure of special brackets, the top plate of the case and the *L* girder for carrying the suspension spring.

The experiments show that suspension loss increases from 0·18 erg/c. for the lightest rod (59 g.) to about 1·2 for the heaviest pendulum (7290 g.).

The bracketing part of this increases as the square of the maximum horizontal stress and so, for constant amplitude, as the square of the pendulum weight. Thus, if 1·2 ergs were entirely bracketing loss, this would correspond to 0·004 erg for the heaviest rod and I conclude that the suspension loss for the rods is practically pure spring loss, which is very nearly the same for all the rods (§ 21).

Owing to its longer rod, S is 300 g. heavier than H (6990 g.). This increases the bracketing loss by 8·7 per cent and the spring loss to an unknown (probably very small) extent. Thus the first solution in table 3 supposes the suspension loss shared fairly equally between brackets and spring, and the second assumes that the brackets are responsible for nearly all the loss (which I regard as improbable). All ambiguity could have been avoided by adding a piece of bob to H which would be replaced by another on S of the same size and shape but 300 g. lighter.

It would be very interesting to know the value of the spring loss alone. Four years ago A. L. Loomis was studying this matter and succeeded in observing the motion of the support with an interferometer. I do not know that he has published any results.

The term *bracketing loss* is intended, of course, to include losses in walls (or pillars) and beyond.

§ 14. THE GROUND SPRING

I have asserted that the suspension losses shown in table 3 could not be much reduced and have described precautions taken to keep the bracketing part small. The suspension spring used in the experiments was first tried in 1931. This trial ended a disappointing stage in the search for precision time-keeping. I had been troubled with a pendulum which would not hold its rate. One part after another was replaced but still both rate and amplitude increased with time. Experiments in 1931 showed clearly that changes in the spring could produce such results (§ 16) and I consulted Dr A. A. Griffith, who reported that he had experienced similar behaviour in springs used for other purposes and recommended the formation of a spring by grinding away the central part from a strip of thick metal, leaving the thick ends for gripping. In this way, hardening of the metal by the cold working, where a thin strip is clamped in chaps, is avoided. This steel spring was the first one which I made in this way. More details are given later; it will suffice for the moment to say that it proved a success and was soon replaced by a ground elinvar spring (which is still in use on pendulum E) and so left free for the experiments I have described.

Ground springs are not a new feature in pendulum building. Keelhoff⁽⁶⁾ in 1906 takes it for granted that such springs will be used for "pendules d'observation"—by which he means those used when one seeks the greatest precision, regardless of cost. Shortt adopted them in 1921 for suspending the master pendulums of his clocks. I have recently measured one at Langleybury Church, Herts, on a turret clock built in 1879.

§ 15. CLAMPED SPRINGS

In 1923 I made a light pendulum for a grandfather clock which led to an unexpected improvement in time-keeping, mainly because it was supported by the wall instead of the clock case⁽⁵⁾. The regulation is done by weights placed on a shelf midway up the pendulum rod in the usual way. A record of the weights used shows that there has been no secular change in rate during 14 years although this rate is erratic. The suspension spring consists of a strip of thin invar (such was my ignorance) gripped in chaps. Its good behaviour in supporting the light (1·4 kg.) bob did not prepare me for difficulties with 7 kg. pendulums.

When I found these heavier pendulums accelerating in rate, I suspected the springs of an increase of elasticity over the whole length. To account for the changes observed in this way, so large a change in e would be needed that I was told fracture must follow in a few million vibrations and I sought elsewhere for a cause. (Cf. the local hardening referred to above).

In 1931 I tried the effect of gently annealing an elinvar spring with astonishing results. The impulse which had kept α at about 38′ now only sufficed for 25′, but in only 18 hours matters had much improved. Further annealing showed that the bending of the metal involved heavy losses of energy and that the cold working due to the running of the pendulum rapidly hardened the elinvar.

Then I made a steel spring of 0·019 cm. strip clamped in chaps and took numerous observations for 6 weeks on a pendulum supported by it, both by taking rough decrement measures and also by making amplitude observations (§ 6) which gave more exact information. Changes in rate were observed at the same time. The amplitude was still growing at the end of the 6 weeks when the clamped spring was replaced by the ground one.

§ 16. LOSSES WITH CLAMPED SPRINGS

Table 4 shows how the decreasing loss in this clamped spring has been compared with the loss in the ground spring. I have supposed that the suspension loss (table 3) is entirely due to the ground spring: if it is partly due to bracketing, the contrast between the springs is greater still. In passing from 53′ to 36′ and back I have assumed that the loss $\propto \alpha^2$, which is probably not strictly true (§ 10). The first two amplitudes were observed when the pendulum was in the open, the rest with it

Table 4. Clamped and ground steel springs

Seconds pendulum. Energy loss in ergs per cycle. The maintenance supplies 11·1 erg/c.

1931	Spring	Barometer (in.)	α with 11·1 erg	Ergs with $\alpha = 36'$	Suspension loss	
					36′	53′
Mar. 22	Clamped steel	29·57	33·53′	12·8 in open	4·5	9·8
April 2	,,	(29·21)	35·17′	11·6 in open	3·3	7·2
7	,,	23·95	33·80′	12·6 in case	3·15	6·8
27	,,	23·95	34·62′	12·0 in case	2·55	5·5
May 1	Ground steel (*d*)	(23·52)	38·60′	10·0 in case	0·55	1·2 from table 3

When pressure is in brackets, the observed α has been reduced to that for the pressure shown in the line above.

in the case. The argument proceeds ***upwards***: 1·2 erg/c. at 53′ (table 3) for the ground spring ≡ 0·55 at 36′ out of a total of 10·0 with barometer at 23·95″. The amplitude was read at 23·52″ but this figure has been enclosed in brackets to indicate that 38·60′ is the amplitude corresponding to 23·95″ obtained by applying a correction for 0·43″ to the observed reading. Thus 11·1 erg/c. maintains α at 38·60. The loss 10·0 for $\alpha = 36'$ is obtained by neglecting any change in δ for the small change of α, so that ergs vary simply as α^2.

Similarly, on April 27 the loss with the clamped spring would have been 12·0 at 36′, i.e. 2·0 more than with the ground spring, and this change is due solely to the spring: 0·55 erg/c. for the ground spring changes to 2·55 for the clamped one. The result for April 7 is obtained in the same way.

On April 2, the air losses are different and I have assumed that from April 2 to April 7 the spring loss fell off at the same rate as during the next period—hence 3·3 for April 2. The next step backwards is from 11·6 to 12·8 calculated as before, an increase again due solely to the spring.

At the start, then, the loss in the clamped spring is 8 times that of the ground spring. After 5 weeks the loss is only 56 per cent of its initial value.

The decrease in loss of energy was accompanied by a rapid increase in clock rate; towards the end of the 5 weeks it still amounted to 0·01 sec./day^2.

The annealed elinvar spring when started up showed a loss which would have been about 30 erg/c. at 53′ and as has already been stated a large part of the rate of loss had disappeared after the pendulum had been swinging for 18 hours.

With ground springs, on the other hand, the amplitude remained unchanged from the first day of use and there was corresponding stability of rate.

§ 17. THE UNIFORM SPRING

The theory of the suspension spring has been dealt with by various writers(6, 7, 8). About its behaviour when in use, on the other hand, I have found very little.

With a uniform spring the top end is the troublesome part, because curvature increases rapidly from the middle to the top, especially with springs which are otherwise of suitable dimensions for a precision pendulum. This is shown in figure 3 relating to springs of which details are given in table 5. The first of these is the uniform counterpart of the 1931 ground-steel spring (so far as it can correspond to a non-uniform spring). The thickness (nearly 0·006″) is reasonable and the spring is certainly not too short. Its shape in use is shown as curve *A* where the amplitude is pictured as about 33° (!). Notice how nearly straight the bottom half of the spring remains and how much of the bend is taken at the top. This is shown more clearly by curve *B* which shows the curvature for all parts. The greatest curvature, 0·048, at the top falls to half value at 0·2 of the way down and to one-tenth at the lower end—the values relate to the reasonable amplitude of 53′.

The weight of the pendulum subjects the spring to a nearly constant stress Mg/ew dyne/cm^2 (for the meaning of the symbols, see table 5) through the whole of the spring.

There is an alternating stress due to the bending of the spring which reaches its largest (positive or negative) value for each part of the spring at full amplitude. This peak value is largest on the surface of the spring just at the top, viz. $ec/2\rho_0$.

Consider first a spring consisting of one piece of metal forming both spring and ends. Uniformity involves an abrupt change of section at each end, as in *A* of figure 3 and *b* of figure 4. It is well known that abnormal stresses occur in the region of a discontinuity of this kind, but the analysis which provides the figures in table 5 takes no account of these abnormal stresses. Theorists tend to lose sight of them. Thus Keelhoff, in referring to the ground spring, urges that the rounding off between the spring and the thick end should be made very short lest it should invalidate the calculations, "le contraire n'aurait d'ailleurs aucune utilité."*

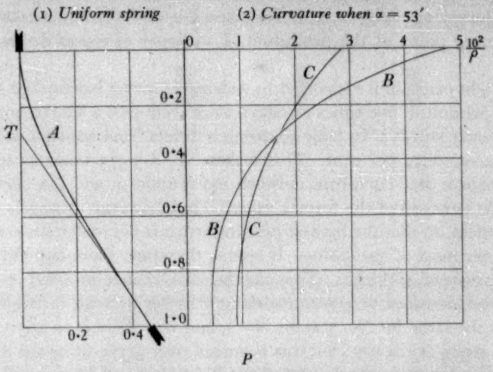

Figure 3. Shape and curvature of uniform suspension spring. *A*, Shape of spring at large amplitude, $\lambda=3{\cdot}28$; *B*, curvature of this spring, $\alpha=53'$; *C*, curvature of spring 50 per cent thicker than *A* when $\alpha=53'$, $\lambda=1{\cdot}89$.

Table 5. Uniform springs

Seconds pendulum	e dyne/cm²	l	Spring	w	c	$\frac{1}{\rho_0}$	Stresses dyne/cm² × 10⁸		λ
							Loading	Bending	
$M=7290$ g.	$2{\cdot}13\times10^{12}$	1·05	1	1·27	0·0148	0·0473	3·80	7·47	3·28
$k^2\dagger=195$ cm²			2	1·27	0·0222	0·0286	2·53	6·78	1·89
			3	4·30	0·0148	0·0286	1·12	4·52	1·89

Spring dimensions: *l*, length; *w*, width; *c*, thickness; all in cm. Young's Modulus, *e*. The bending stress is the largest one, viz. that on the surface at the top when $\alpha=53'$. Spring properties (shape, effect on rate etc.) are expressed in terms of λ and its hyperbolic functions, where $\lambda=l\sqrt{(12Mg/ec^3w)}$. † About centre of mass.

---

* *Suspension à Ressort*, p. 16.(6)

The top extremity, then, of this spring is a region of especially heavy stresses at the outside layers. When the spring consists of a thin strip gripped in chaps matters are worse still, because there is movement within the jaws (§ 21) and this cold working will lead to hardening of the metal. The slipping to and fro of the spring surfaces within the chaps accounts for some at least of the losses observed. As the metal hardens there the movement will decrease and so will the loss of energy. Moreover, the spring ceases to be uniform and less of the bending takes place at the top, the turning point of the pendulum (T in figure 3) moves down and the rate increases.

Since a light pendulum supported by a clamped spring has worked satisfactorily, could not a pendulum five times as heavy work well with a similar spring if this is made sufficiently sturdy? In table 5, spring 2 differs from spring 1 only in c which has been increased 50 per cent. This makes No. 2 3·375 times as stiff as No. 1. Figure 3C shows that curvature is much more uniform and the curvature at the top is only 60 per cent of the former value. This, however, is largely offset by the greater thickness, so that the highest bending stress is not materially reduced, and it is increased for most of the spring. It seems, therefore, more hopeful to make the spring wider instead of thicker. To make the same change in λ and in stiffness, the width must be increased to 4·3 cm., making it rather difficult to house the spring. Curvature is the same for No. 3 as for No. 2, and now there is an appreciable fall in the bending stress at the top; but this is spread over 3·375 times the distance. If a clamped spring can avoid secular change with a 7 kg. pendulum, it will, apparently, be a very stiff one and the ground spring, which need not be so stiff, is the more attractive choice.

§ 18. THE NON-UNIFORM GROUND SPRING

In figure 4 four stages are indicated in the development of the suspension spring. The change from the clamped spring (*a*) to the all-one-piece spring (*b*) cuts out the working within the chaps. This could probably be effected by soldering the spring in the chaps as Sir Charles Boys has done. There still remains the abrupt change of section which gives rise to abnormal stresses.

When the spring is ground out of the solid (*c*) the easy transition from uniform spring to rigid end will occur even when the maker does not know that this is an important result.

So long as the rest of the spring is uniform, the top part has the heavy share of bend and stress shown in table 5. The last step, then, is to make the spring non-uniform (*d*) and leave it somewhat thicker towards the top, so as to make the curvature more uniform.

The theory of the non-uniform spring is difficult compared with that of the uniform spring. J. Haag has stated the general theory fully—the differential equations are there but, except in trivial cases, they have not been solved. In order to obtain information about a suitable section for a spring, it is useless to try to find the shape which a spring of given section will assume as the pendulum swings, because the differential equation stands in the way. If, however, the shape is given, then the section can be found, for the equation has ceased to be differential. A section can be found, for example, which makes the spring bend into a circular arc. This would not be adopted in practice because the central part of this spring is unnecessarily thick. I have obtained various other solutions, which seem reasonable, based on equalizing the stresses on the surface of the spring rather than the curvature. I do not think that any special form will lead to a perfect spring, but theory can help in deciding how much thickening-up is to be desired towards the top of the spring.

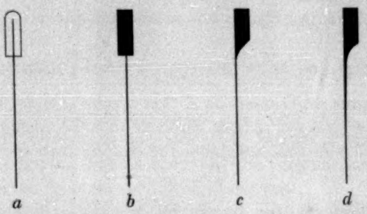

Figure 4. Suspension springs: *a*, uniform spring clamped in chaps; *b*, ends and spring all one piece, abrupt change of section; *c*, ground uniform spring, change of section eased off; *d*, ground non-uniform spring for more uniform curvature.

§ 19. ELINVAR VERSUS STEEL SPRINGS

I was able to use spring *d* for the experiments on component losses because I replaced it on pendulum *E* by a ground elinvar spring. It is not so easy to make a good spring from this as from steel. An alloy called "Isoelastic" is used in America for the coiled springs of weighing machines. Prof. A. W. Price of Toronto has kindly sent me a strip of this material, from which I hope to fashion a suspension spring. Isoelastic may prove more suitable than elinvar for this purpose. At Greenwich the elinvar spring of *SH*, No. 3, has been replaced by a steel one(9) in order, I suppose, to test whether the secular change of rate can be reduced in this way.

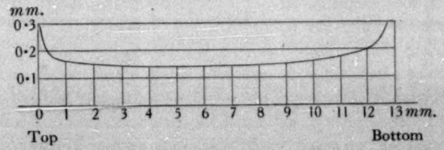

Figure 5. The ground steel spring *d*. Notice easing off into thick ends. The growth in thickness towards the top is desirable. That towards the bottom is detrimental.

This raises the question whether it is important to secure a zero elasticity coefficient for the spring, when changes can be compensated at the bob and when temperature-control should make even this unnecessary. I think that control is always imperfect because this relates to air-temperature, which settles bob-temperature, whereas spring-temperature depends partly on the wall (or pillar) temperature where the pendulum is supported. For my clock *F*, which is kept at constant temperature, I have followed the example of the National Physical Laboratory by using auxiliary heating for the brackets, which helps also to maintain a constant temperature-gradient in the sealed case.

Figure 5 shows the contour of spring *d*. The increase of thickness towards the bottom is quite wrong (§ 18). Towards the top end the increase is, I think, insufficient.

§ 20. SPRING *d*. YOUNG'S MODULUS AND PENDULUM RATE

I found by a simple experiment on *d* that a pure couple $8{\cdot}52 \times 10^4$ cm.-dyne bends the spring through 0·128 radian. Suppose that the spring at x cm. from one end makes an angle θ with this end under the couple, then the couple is

$$\frac{ec^3w}{12}\frac{d\theta}{dx},$$

whence

$$\theta_l = \frac{12 \times \text{couple}}{ew} \int_0^l \frac{dx}{c^3} \qquad \text{......(6).}$$

The measurements used for figure 5 show that the integral $= 3{\cdot}38 \times 10^5$. It follows that $e = 2{\cdot}13 \times 10^{12}$, indicating a good quality of steel. A uniform spring of length 1·05 cm., of equal flexibility, and of the same width and material has $1{\cdot}05/c^3$ equal to $3{\cdot}38 \times 10^5$, so that $c = 0{\cdot}0146$ cm. On the other hand, the uniform spring giving the observed frequency with the shortest of the rods suspended from it would be 0·0148 cm. thick and the difference between the two values is a hint that no uniform spring is equivalent to a non-uniform one. The formula giving n for a pendulum suspended from a uniform spring is shown in table 6.

Table 6

	S, $\lambda = 3{\cdot}28$	Rod, 15 cm., $\lambda = 0{\cdot}309$
$\dfrac{n^2}{g} = \dfrac{d + l/\lambda \tanh \lambda}{d^2 + k^2 + dl}$	$\dfrac{96{\cdot}72 + 0{\cdot}32}{9355 + 195 + 101}$	$\dfrac{8{\cdot}46 + 11{\cdot}32}{71{\cdot}57 + 21{\cdot}13 + 8{\cdot}88}$
	$n = \pi$	$n = 13{\cdot}8$

The centre of mass of the pendulum is *d* cm. below the bottom of the spring. *k* is the radius of gyration about the centre of mass. λ is defined in table 5.

I have given numerical values for the different terms in the formula for the largest and for the smallest of the pendulums used in the experiments. With an ordinary pendulum the second term in the numerator forms a small correction to the main term *d*, but for the short rod it has become the principal term. It is interesting to find how well the formula fits so large a range of cases. For this reason, I have given the computed values of *n* above the observed ones in table 2, but the latter have been used in connection with the experiments.

§ 21. ROD PENDULUMS: SPRING LOSS

In a suspension spring the alternating stress due to bending is combined with the constant stress due to weight and it is not to be expected that a formula which is true in the absence of the latter stress will also apply when it is there. Kimball and Lovell(10) showed that, when an element of volume dV of an elastic body is subjected to an alternating stress whose peak value is S_m, the energy dissipated will be $\xi \times S_m{}^2 dV$ erg/c. ξ is a constant depending on the material.

Taking the case of a uniform spring and integrating for the whole volume,

$$\text{Loss} = \frac{\xi e l M g \alpha^2}{2}\left(\frac{1}{\lambda \tanh \lambda} + \frac{1}{\sinh^2 \lambda} - \epsilon\right) \text{erg/c.} \qquad \ldots\ldots(7).$$

Here ϵ represents terms aggregating about 3 per cent of the whole for a seconds pendulum, to which the formula does not apply, but for all the rod pendulums the terms are quite negligible. For all the rods, the constant stress is comparatively small and for these the formula should be nearly true.

Here λ is a proper fraction and the formula can be simplified to

$$\text{Loss} = \frac{\xi e^2 w c^3 \alpha^2}{12 l}\left(1 + \frac{\lambda^4}{45} - 0{\cdot}004\lambda^6\right) \text{erg/c.} \qquad (8).$$

Replacing the non-uniform spring *d* by the uniform spring of equal flexibility, I find $\lambda = 0{\cdot}32$ for the shortest rod and 0·75 for the longest. Hence the loss is $\xi \times 3{\cdot}36 \times 10^{14} \times 1{\cdot}0002$ for the short rod whilst the last factor is 1·006 for the long one. The greatest loss, then, is only 0·6 per cent larger than that due to a pure couple. Thus the spring loss is practically the same for all the rod pendulums, as has been assumed in § 13.

Assuming that the whole of the observed suspension loss is due to the spring, we have $3{\cdot}36 \times 10^{14}\xi = 0{\cdot}182$, or $\xi = 0{\cdot}55 \times 10^{-15}$. In Kimball and Lovell's list the smallest value of ξ is $0{\cdot}306 \times 10^{-15}$ for hard rolled phosphor bronze. Next to this comes $1{\cdot}10 \times 10^{-15}$ for swaged nickel ($3\frac{1}{2}$ per cent) steel. Thus, the steel of *d* comes between these two substances with smallest losses. This seems to confirm the conclusion that for the rod pendulums there is no appreciable bracketing loss.

Kimball and Lovell experimented with flexible rotating bars. They also experimented with springs and make a statement which bears out the conclusions arrived at regarding clamped springs. They say that the vibration tests gave values 2 or 3 times as high as those obtained by the other method: "*considerable energy was dissipated by surface friction in the clamps*."

§ 22. IMPULSE-LEVER LOSS

The impulse levers for pendulums *E* and *F* consist of three arms mutually at right angles, one of which carries the needle points forming the axis, which is placed in line with the axis about which the pendulum turns. The other horizontal arm is weighted and produces a clockwise moment about the axis causing the lower end of the vertical arm to press towards the left against the pendulum rod or else against the armature lever which moves between two stops. When the pendulum, moving towards the right hand, reaches an angle θ beyond the vertical, it picks up the impulse lever and the two move together to the full amplitude and back again to angle θ on the left hand of the vertical. During this extra (2θ) left-hand movement, the energy necessary for maintenance is supplied to the pendulum.

Observations for decrement may be made (*a*) with the impulse lever entirely out of action, clear of the pendulum, or (*b*) with the armature lever stationary against its right-hand stop and impulse lever in position, the pendulum picks it up as usual at $+\theta$ but, after passing full amplitude, drops it again at $+\theta$, no energy being supplied to the pendulum, or else (*c*) with the armature lever to the left so that the impulse lever moves through the range $-\theta$ to $+\alpha$ and back to $-\theta$.

In (*a*) decrement is due entirely to loss of energy by the free pendulum. In (*b*) there is in addition loss due to the impulse lever, this being less than the loss when the lever is impulsing, and in (*c*) the additional loss is greater than this latter loss by an equal amount.

In order to find the lever loss, then, the decrement for (*a*) is subtracted from the mean of the decrements for (*b*) and (*c*). The lever loss is, however, so small compared with the pendulum loss that it cannot be observed with an ordinary pendulum which the lever is intended to impulse. The losses with rod pendulums being smaller, I made one of these which beat nearly half seconds and obtained the results shown in columns 7 and 8 of table 2, showing a loss due to the lever of 0·045 erg/c.

Apart from frictional losses there is loss of energy due to the inelastic collision when the pendulum meets the lever. This collision imparts energy to the lever, which is lost when the lever is arrested at $-\theta$, and there is further loss of energy as heat. When mk^2 for the lever is very small compared with MK^2 for the pendulum, the equation resulting from the principle of conservatum of angular momentum shows that these two amounts of energy are virtually equal and that their sum $= mk^2\dot{\theta}^2 = mk^2n^2\alpha^2\cos^2\tau$, $\theta/\alpha = \sin\tau$. With $\theta = 25'$ and $\alpha = 53'$, the loss due to collision is 0·037 erg/c.

Turning again to the experimental result, comparing the larger amplitudes with the smaller ones I find that the loss for the former is too small compared with that for the latter. To get an accurate value for so small a quantity, it would have been necessary to repeat the experiment many times. I feel justified, however, in concluding that the total loss is not greatly in excess of that due to the collision and, for want of more exact information I think it best to adopt this calculated value for the impulse lever loss. Hence the value 0·04 erg/c. for H given in table 3.

For S ($n = \pi$ as compared with 2π for H) the collision loss is reduced to 0·01 erg/c., which is the figure I have inserted in table 3. I suppose that the total lever loss is at most less than 0·02, which is about one-thousandth part of the pendulum loss.

Prof. Sampson says of Cottingham's lever that its loss "appears to amount to one-tenth of what is required for free maintenance." I have not seen this clock, but in making my lever I was following Sampson's description of Cottingham's. I cannot suppose that any lever could dispose of 2 erg/c.

My lever weighed 2·93 g. The horizontal arm from axis to centre of gravity is small. In order to increase this arm and thus the constancy of impulse, I have reduced the weight of the lever to 0·7 g., of which nearly one-third is at the solid end of the horizontal arm. This lighter lever has, however, a moment of inertia larger than that of the old lever. For these new levers, I sought in vain for tubes with thin walls and had to make these myself out of 0·001-in. german-silver foil with silver-soldered seams.

§ 23. EFFECT OF ENCLOSING PENDULUM IN CASE

H is normally enclosed in an inverted propagating glass with the bob about half way up. This case adds about 16 per cent to the total loss and so about 30 per cent to the resistance experienced by the bob. When the air pressure is reduced by 200 mm. the loss is about the same as at full pressure in the open. *S* is housed in a glass cylinder 122 cm. long and 20 cm. in diameter. This adds somewhat less than 20 per cent to the decrement and again reduction to about 550 mm. restores the open-air amplitude.

I have no experience with pendulums working in gas at low pressures.

I have not found the opportunity for repeating the experiments on loss components with greater precision. In the hope that another investigator will do so, I have taken care to point out the short-comings of these experiments.

REFERENCES

(1) Atkinson, E. C. *Proc. Phys. Soc.* **48**, 613 (1936).
(2) Sampson, R. A. *Proc. Roy. Soc. Edinb.* **57**, pt 1 (1936–7).
(3) Shortt, W. H. *Observatory*, **51**, No. 646 (Mar. 1928).
(4) Robertson, David. *Horolog. J.* (Dec. 1928, Jan. and Feb. 1929).
(5) Atkinson, E. C. *J. Sci. Instrum.* **2**, No. 9 (June 1925).
(6) Keelhoff, Fr. *J. suisse Horlog.* (Jan. 1906).
(7) Sampson, R. A. *Proc. Roy. Soc. Edinb.* **38**, pt 1, No. 11 (Jan. 1918).
(8) Haag, J. *J. Math. pures et appl.* **14**, pt 2 (1935).
(9) *Mon. Not. R. Astr. Soc.* **93**, No. 4 (Feb. 1933).
(10) Kimball, A. L. and Lovell, D. E. *Trans. A.S.M.E.* (Dec. 1926).

DISCUSSION

For discussion see p. 753.

THE AMPLITUDE DEVIATION OF RATE OF A PENDULUM: A SECOND EXPERIMENT

By E. C. ATKINSON, M.A.

Received 3 *March* 1938. *Read* 24 *June* 1938

ABSTRACT. In a previous experiment the amplitude deviation was almost equal to the circular deviation. The present experiment was made on a lighter pendulum with a long suspension spring, moving in different surroundings. The amplitudes ranged from 108′ to 224′ as compared with the previous range of 30′ to 70′. The deviation is about 15 per cent larger than the circular deviation and is well represented by the latter plus a linear term. Two other experiments with Graham's escapement are referred to, in which the driving weights are varied. One of these, described by Sir Henry Cunynghame, seems to be hypothetical, for it yields an amplitude giving a minimum rate instead of a maximum one. Guillaume overlooked the large temperature effect produced by an invar suspension spring, which the author found by experience and calculated. Prof. R. A. Sampson sought to find the deviation by observations on a Shortt clock without allowing for impulse deviation. It is pointed out that the deviation for the master pendulum when it is impulsed is less than the deviation for the pendulum when it is free. In addition to the vibration used for time-keeping, a spring-suspended pendulum has a parasitic mode of vibration which the concentrated Shortt impulse is well adapted to set up. Prof. Sampson has analysed the author's previous experiment by the method of least squares and concludes that the solution given is but one of a number of possible solutions. Neither of Sampson's alternatives is a least-squares solution and both involve impossible values of the decrement. The corrected normal equations confirm the original solution.

§ 1. NEED FOR A SECOND EXPERIMENT

Two years ago I described experiments(9) with a spring-suspended pendulum vibrating in air, which showed amplitude deviation agreeing closely with the circular deviation calculated for motion about a centre in vacuo. The result for this pendulum, E_{11}, does not necessarily hold good for other pendulums. For this reason, I tested a grandfather clock by changing the driving weight from time to time during ten weeks in the winter 1936–7.

Until fifteen years ago, this clock was just a good household clock made almost 140 years ago. Then I provided it with a new pendulum which was bracketed to the wall through the back of the clock case. This change converted it into a first-class time-keeper, but not into a precision one. Minor changes followed, and in 1936 I made a new pair of Graham pallets, taking care to make the front faces truly dead, so that the impulse deviation could be correctly calculated.

This seconds pendulum, G, is contrasted with E_{11} of the previous experiment, in table 1. G has a light bob and a very long suspension spring. The long, narrow

Table 1. Two experiments compared

The pendulums

	Bobs			Rods		Case	Air pressure	Suspension spring				
	Height (cm.)	Diameter (cm.)	Weight (g.)	Diameter (cm.)	Weight (g.)	(cm.)	(mm.)	Length l	Width w	Thickness c	Young's modulus e	λ
E_{11} (1934)	16·0	7·4	5740	0·8	440	cylinder diam. = 20	540	1·08	1·27	0·014	$1{\cdot}7\times10^6$	3·96
G (1936–7)	9·6 1·6	4·1 2·4	1430 60	0·32	70	46 × 10 (at bob 7·5)	750	2·54	0·66	0·021	$1{\cdot}5\times10^6$	3·63

G has an auxiliary bob for regulating and a plate opposite to the bob to prevent air reaction between the driving weight and the bob. $\lambda=l\sqrt{(12Mg/ec^3w)}$. *M* is the total mass of the pendulum.

Range of observations

	Amplitude	Rate (sec./day)
E_{11}	30′ to 70′	0·4 to 2·2
G	108′ to 224′	6·2 to 26·2

space in which it moves probably involves more air drag than does the cylindrical case of E_{11}. The space is further reduced opposite to the bob by a shield, which prevents air reaction between the bob and the driving weight.

The range of amplitudes, too, is different in the two experiments. Hence there is a range of rates in the second experiment ten times as large as in the first, which makes up for the larger errors in rate and amplitude which must be expected.

In this paper definitions and explanations given in the previous one will not in general be repeated. Even for the largest amplitude α involved, the circular deviation is represented with sufficient accuracy by $86400\times\alpha^2/16$ sec./day, when α is expressed in radians.

§ 2. RESULTS FOR PENDULUM *G*

The results for pendulum *G* are shown in table 2. The alphabetical sequence is that of amplitude, the numerical sequence, column 2, shows the order of events, large and small amplitudes being taken roughly alternately in order to reduce the

Table 2. Amplitudes and rates [+ means losing rate]

1 Period	2 Order	3 Days	4 Driving weight (kg.)	5 Amplitude (mins.)	6 p.e. angle (mins.)	7 Equiv. p.e. (sec./day)	8 Rate (sec./day)	9 p.e. (sec./day)	10 Impulse deviation	11 Free pendulum	12 Circular deviation
a	2	8	1·10	108·6	0·8	0·08	0·49	0·05	1·61	−1·12	5·39
b	7	10	1·55	124·8	0·7	0·08	2·05	0·07	1·31	+0·74	7·11
c	4	8	2·07	147·0	0·5	0·06	5·28	0·04	1·06	4·22	9·88
d	5	10	2·72	164·8	0·8	0·12	8·03	0·13	0·96	7·07	12·41
e	3	6	3·68	188·6	0·3	0·05	12·58	0·10	0·88	11·70	16·25
f	1	10	4·42	203·7	0·7	0·13	15·19	0·18	0·83	14·36	18·96
g	6	8	5·85	223·8	0·6	0·12	19·68	0·09	0·75	18·93	22·89

effect of a possible drift in rate. With reference to the driving weights, the clock was originally worked by 5·2 kg., but the usual weight now is 1·5, the reduction being partly due to reduced amplitude and largely due to the reduction in loss of energy effected by fixing to the wall. Amplitude is measured on a fixed scale, over which the pointed end of the rod moves. The probable error of amplitude observations is given in decimals of a minute of arc and converted, by the result of the experiment, into seconds per day (col. 6), for comparison with the probable error for rate (col. 9). The two are roughly of the same order, namely 0·1 sec./day.

The rates given in column 8 are the observed rates, reduced to 29·5 in. by applying a barometric correction of 0·4 sec./day per inch. This is the observed variation when $\alpha = 126'$ and includes the remote effect due to the change of amplitude. For the larger angles it is, therefore, likely to be too large. No correction has been applied for temperature (§ 7), and no barometric correction has been applied to amplitudes.

Rates were obtained by daily comparisons with the 10·0-h. Greenwich rhythmic signal, amplitude and barometer being observed about the same time.

Free pendulum rates, column 11, are found by deducting impulse deviation, column 10, from observed rates.

§ 3. FITTING A FORMULA TO THE OBSERVATIONS

Geometrical considerations suggested two solutions which were then computed by the method of least squares. If the free pendulum rates (ordinates) are charted against amplitudes (abscissae), we are at liberty to move the whole group vertically so that the lowest point *a* lies on any curve, for we are concerned only with relative rates, absolute rate being merely a question of regulation; see figure 1.

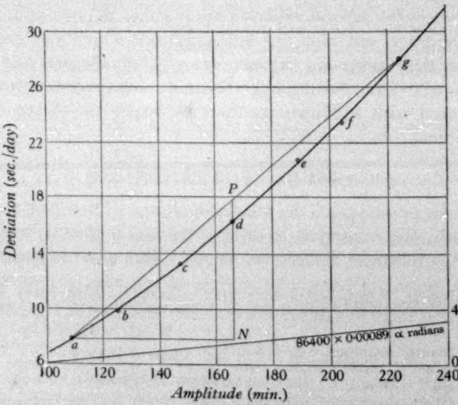

Figure 1. Amplitude deviation. Solution B. Circular deviation +0·0244*m*, where amplitude is in minutes of arc. The curve is a computed one, whilst the points are observed amplitude deviations.

For another point, say g, to be on the curve at the same time, the range for the two points (20·05 sec./day) must be the same as the range for the curve. The corresponding circular deviation range is only 17·50 sec./day, and this must be increased by about 15 per cent to include the two points. The middle point d will lie on a curve containing a and g if the vertical distance Pd of d from ag is equal to the corresponding intercept between the chord and arc of the curve. Now, for the points

$$\begin{aligned} Pd &= PN - dN \\ &= \frac{164{\cdot}8 - 108{\cdot}6}{223{\cdot}8 - 108{\cdot}6} \times 20{\cdot}05 - (7{\cdot}07 + 1{\cdot}12) \\ &= 1{\cdot}59 \text{ sec./day.} \end{aligned}$$

For circular deviation, the corresponding calculation gives 1·51 sec./day. This intercept is 5 per cent less than for the points. There are two simple ways of modifying circular deviation to embrace a and g: (A) We may use a multiple —about 1·15—of it, and (B) we may add a linear term $x\alpha$ to it. (A) will increase the intercept to about 1·73, which is too large for d; (B) will leave it at 1·51, which is too small for d. This suggests a combination of (A) and (B). These considerations concern only three out of seven points and have taken no account of errors due to observation and to erratic behaviour of the clock.

§4. TWO FORMULAE

Solution (A) is expressed by the formula

$$x \times \text{circular deviation} = \text{free pendulum rate} + y,$$

whilst for (B) we have

$$\text{circular deviation} + x \times \text{amplitude} = \text{free pendulum rate} + y.$$

For finding x and y in each case, there are seven equations of condition which have been reduced to the necessary two equations for finding x and y by the method of least squares. I find

$$(A)\ \text{free pendulum rate} + 7{\cdot}23 = 1{\cdot}147 \times \text{circular deviation} \quad \text{......(1)},$$

$$(B)\ \text{free pendulum rate} + 8{\cdot}99 = \text{circular deviation} + 77\alpha \quad \text{......(2)}.$$

Rates are given in table 2, columns 11 and 12. Circular deviation $= 86400 \times \alpha^2/16$, α here and in the linear term of equation (2) being measured in radians. Thus in equation (2) $\alpha^2/16$ becomes $\alpha^2/16 + 0{\cdot}00089\alpha$. When α is expressed as m' (minutes of arc), 77α becomes $0{\cdot}0224m$.

Figure 1 shows solution (B), the sloping straight line showing the linear contribution starting from an arbitrary zero at 100′. Table 3 compares the observed with the computed rates for the two formulae. In (A) the central part of the curve is too low (column 4) whilst the extreme parts are too high: the curvature is too great, which agrees with § 3. In (B) examination of the residuals does not suggest whether the curvature is too large or too small—the erratic variations are too large. The graph gives the impression that no appreciable improvement on solution (B) is

Table 3. Two curves representing rates

A				*B*		
1	2	3	4	5	6	7
Amplitude (mins.)	Free pendulum $+7{\cdot}23$ (sec./day)	$1{\cdot}147\,\dfrac{\alpha^2}{16}$	Observed minus calculated	Free pendulum $+8{\cdot}99$	$\dfrac{\alpha^2}{16}+0{\cdot}00089\alpha$	Observed minus calculated
108·6	6·11	6·18	−0·07	7·87	7·82	+0·05
124·8	7·97	8·15	−0·18	9·73	9·90	−0·17
147·0	11·45	11·35	+0·10	13·21	13·17	+0·04
164·8	14·30	14·24	+0·06	16·06	16·10	−0·04
188·6	18·93	18·64	+0·29	20·69	20·47	+0·22
203·7	21·59	21·74	−0·15	23·35	23·51	−0·16
223·8	26·16	26·25	−0·09	27·92	27·89	+0·03
Root mean square			0·154			0·117

In columns 3 and 6 the formulae have been multiplied by 86,400 to give values in seconds per day.

possible: the main offenders *e* and *f* will be respectively above and below any smooth curve. The root mean squares of the residuals show that (*B*) is a distinctly better solution than (*A*). I offer (*B*) as a suitable formula for pendulum *G*. It can be put in the form free pendulum rate $+9{\cdot}26=86400\,(\alpha+0{\cdot}007)^2/16$, but this does not suggest to me any theoretical meaning for the linear term.

§ 5. THE IMPULSE DEVIATION

If a uniform impulse is delivered to the pendulum commencing when it is $\theta_1{}'$ past the vertical and lasting to $\theta_2{}'$, this will cause the pendulum to lose

$$86400\frac{\delta}{n}\tan\frac{\tau_1+\tau_2}{2}\text{ seconds per day}^{(12)}, \qquad \text{......(3)}$$

where δ is the decrement, $n=2\pi\times$ frequency $=\pi$ for a seconds pendulum, and $\sin\tau_1=\theta_1/\alpha$, $\sin\tau_2=\theta_2/\alpha$. I measured θ_1 and θ_2 by fixing a millimetre scale just above the fork of the lever so that it moved with the pallets. The index consisted of several lines not uniformly spaced. In this way I eliminated, I hope, personal errors in estimating fractions of the millimetre. The beat is adjusted so that θ_2 is the same when escape is from the right pallet as from the left. Then the two θ_1 values are not so nearly equal as I had hoped. For calculating deviation I used the average value. Pivot friction adds largely to the decrement of the pendulum. To secure uniform action it is important for the fork to touch the pendulum on one side only. Hitherto I have secured this by means of a counterpoise, which serves the purpose, but produces a reaction in the bearings and adds to the friction. When amplitude was to be doubled for this experiment, the counterpoise was increased, and with it the decrement. I have now replaced the counterpoise by a light spring at the fork pressing on the other side of the pendulum rod.

Table 2 shows that the change in impulse deviation is less than 5 per cent of the change in rate, so that errors in determining the former do not have an appreciable effect on the result.

§ 6. IMPULSE DEVIATION BALANCING AMPLITUDE DEVIATION

The slowing effect of a dead-beat impulse falls off (see table 2, column 10) with increasing amplitude, whilst the amplitude deviation increases. Equation (3) shows that the deviation, and also its rate of decrease with increase of α, is increased by increasing $\frac{\tau_1+\tau_2}{2}$, i.e. by retarding the impulse and especially by delaying the release of the scape wheel.

Theory indicates that with a much retarded impulse and for amplitudes of, say, 120′, impulse deviation falls more rapidly than amplitude deviation grows, i.e. rate increases with amplitude. Eventually, of course, the latter deviation takes the upper hand, so there is a maximum rate for some angle if the amplitude is changed by increasing the driving weight. Prof. David Robertson has shown me a chart, which Mr A. E. Ball of Messrs Gent sent to him in 1925, relating to a Graham regulator, showing a maximum rate of this kind.

Sir Henry Cunynghame(1) describes the experiment of changing the driving weights with a Graham escapement. He states that a minimum rate will be found and that this is somehow due to friction on the dead faces. I conclude that he had not tried the experiment himself. With reference to this escapement he quotes Airy's formula, but says that the impulse increases the rate.

§ 7. TEMPERATURE ERROR DUE TO SUSPENSION SPRING

When I first installed this pendulum, I was at a loss to explain the very large increase of rate with temperature. As the clock was operating in the open air, the decrease of air-density with rise of temperature would cause an increase in rate which might easily balance, and more than balance, the slowing due to growth of the invar rod and bobs, but this did not suffice to explain why the main bob must be supported a considerable distance above its top. Later the explanation became clear. I had used invar for the spring as well as for the rod and I had omitted to take account of the growth of its elasticity with temperature. I erred in good company, for Dr Guillaume(2), the inventor of invar and of elinvar, deals with the compensation of a pendulum, supplied with an invar spring, in great detail yet omits all reference to the spring except to remark that had it been made of steel allowance would have to be made for the variation in its length.

When λ is as large as with this pendulum (table 1), $\tanh\lambda \doteqdot 1$ and the formula for rate becomes

$$\frac{n^2}{g}=\frac{d+l/\lambda}{d^2+k^2+dl} \qquad \text{......(4)},$$

where d is the distance (cm.) between the bottom of the spring and the centre of mass of the pendulum; hence for a rise of 1° C.

$$\frac{dn}{n}=\frac{l}{4\lambda d}\frac{de}{edT} \qquad \text{......(5)},$$

where T is the temperature (° C.),

$$\frac{de}{edT}=+5{\cdot}0\times10^{-4} \text{ for invar,} \quad -2{\cdot}4\times10^{-4} \text{ for steel,} \quad \pm0{\cdot}5\times10^{-4} \text{ for Elinvar.}$$

Here are figures about the compensation of G, with its main bob of lead 9·6 cm. high and with a brass tube above this screwed to the rod 7·5 cm. up, for a rise of 1° c. The increases are in sec./day.

Expansions, invar and bobs	−0·015	Top half of lead bob	−0·052
Air	+0·037	7·5 cm. of brass tube	−0·054
Spring	+0·075		
	+0·097		−0·106

I do not know any of the coefficients accurately. Since this final compensation in 1928, I do not know whether the pendulum is under-compensated or not. Consequently, in the deviation experiment, I have made no corrections for temperature.

§ 8. DATA FROM A SHORTT PENDULUM

Prof. R. A. Sampson(3) sought to find amplitude deviation from a series of observations of pressure amplitude and rate of SH_4 at Edinburgh in 1930 when the case was leaking. Assuming that the rate could be expressed by the formula

$$x+y\times\text{pressure}+z\times\text{circular deviation},$$

x being a constant, y the increase of rate per inch pressure and z a fraction, sixteen equations of condition were reduced to three by the usual method of least squares. On eliminating x Sampson found that the two equations for y and z were nearly identical and so concluded that the formal solution would have no value. He remarked that from an inspection of the chart he concluded that z was about $\frac{3}{4}$, i.e. that the clock would not show full circular deviation. Since no allowance was made for impulse deviation, the deviation that Sampson refers to is that of the impulsed master pendulum, which is less than that of the same pendulum when free.

As this Shortt master pendulum is often referred to as a "free pendulum", I will discuss the difference.

§ 9. THE SHORTT IMPULSE

Part (*a*) of figure 2 shows the method of applying the impulse, which consists in allowing the jewelled end of a lever to roll down a small wheel attached to the pendulum. The first part of the thrust is very small when the contact is near the top of the wheel, but it increases rapidly with ϕ, and, but for the inertia of the lever, would increase indefinitely until the contact point was in line with the centre of the wheel and the lever axis. In that case, the diagram of the impulse would be the curve T in figure 2, viz. $k\tan\phi$ (ordinate) plotted against $\sin\phi$ (abscissa). The actual diagram is indistinguishable from T in the early stages. I_1 indicates (purely diagrammatically) the later stages of the impulse, which is seen to depart more and more from T as angular acceleration of the lever increases, until a maximum is reached, followed by a rapid fall to zero, before the three points come into line.

With amplitude reduced owing to rising density of air, during Sampson's observations, the accelerations become less for all positions, so that the new diagram I_2 keeps nearer to T, rises to a higher and later peak, and ceases later than before. This change is appreciable only in the later stages of the impulse shown in figure 2 which usually take place after the pendulum is past the vertical. The black part of the diagram indicates the increased impulse, which with normal timing slows the rate of the pendulum and so wipes out part of the free pendulum deviation. Moreover, the phase of all the post-vertical part of the impulse is retarded by reduction of α and this adds further to the slowing of the rate.

If, then, the free pendulum deviation is just equal to the circular deviation, the resultant deviation of the impulsed master pendulum will be a proper fraction of the circular deviation.

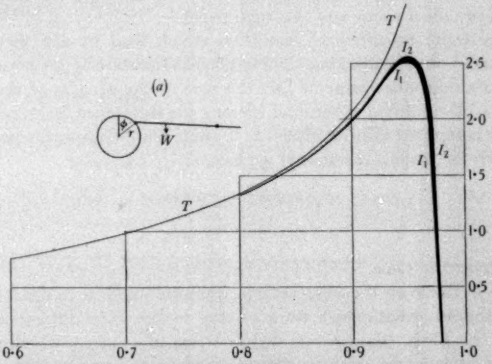

Figure 2. Shortt impulse. Change with amplitude.

The impulse could, of course, be so timed that for one value of the amplitude the change of impulse deviation is zero.

§ 10. THE PARASITIC VIBRATION

A spring-suspended pendulum has two modes of vibration and its motion is generally compounded of these two modes. It can turn about a point, usually a little above the centre of the spring: this mode is used for time-keeping. The other mode which J. Haag(4) calls the "parasitic vibration" is made apparent when the top of the rod of a stationary pendulum receives a blow. In this case the turning point is below the centre of mass of the pendulum. If the impulse could be delivered at this point, it would expend all its energy on the wanted vibration. When the impulse is delivered near the top of the rod, some of the energy takes the form of the parasitic vibration, the more so as the impulse approximates to a blow. The Shortt impulse, with sharp peak, is of a type for producing the second mode, especially as the whole of the energy lost in half a minute is replaced by a single impulse, after the previous parasitic vibration has died out.

I do not think that the presence of the second mode of vibration is harmful for time-keeping, but it adds to the difficulties of computing the effect of the Shortt impulse(13).

§ 11. PROF. SAMPSON'S ANALYSIS OF E_{11} RESULTS

In the same paper, Prof. Sampson analysed the results of my E_{11} experiment(10) by assuming that the observed clock rate

$$a=x+by+cz,$$

where x is a constant, y is the fraction of impulse deviation b which is 'sensible', z is the similar fraction of the circular deviation (see § 13), on the basis of the figures given in tables 1 and 2 of the 1936 paper.

There are eight equations of condition which lead by the method of least squares to three normal equations. These normal equations give values of x, y and z which yield a minimum value of Σv^2, the sum of the squares of the residuals in the equations of condition, a residual v being the difference between an observed value a and a computed value $x+by+cz$. I quote from Sampson's paper: "Eliminating x [from the normal equations] we have

from (1) and (2) $\qquad y-0{\cdot}494z=+0{\cdot}511,$

from (1) and (3) $\qquad y-0{\cdot}508z=+0{\cdot}504$

which are almost the same.

"Treated in this way, the observations are quite unequal to separating the two desiderata. Indeed, what choice we may take makes little difference to the constant arrived at. Thus, take $y=1{\cdot}00$ then $z=1{\cdot}00$, $x=-1{\cdot}10$, which is Atkinson's solution; but if we take $y=0{\cdot}90$ then $z=0{\cdot}80$, $x=-1{\cdot}07$, which is the value indicated on p. 60; but if we take $y=0{\cdot}76$ then $z=0{\cdot}50$, $x=-1{\cdot}06$, which is the value Bloxam reached. I conclude, therefore, that Atkinson's data are insufficient to settle the question but that his agreement is evidence that he has chosen one out of a number of possible solutions."

This would, of course, be true if the equations to which Sampson refers were equations of condition with coefficients affected by experimental error, for small changes in such coefficients make large changes in the values of the unknowns and values of these, which only nearly satisfy the equations, such as those given above, might be regarded as solutions. But the equations are normal equations, derived from equations of condition, for finding values for x, y and z that yield a minimum value of Σv^2. The equations are exact, so that there is, of course, but one solution. If Σv^2 for this solution is not a minimum the equations are wrong. The fact that the two equations for y and z are nearly equal makes solution more laborious, but it introduces no uncertainty as to the result.* The three equations as printed yield a

* Dr R. d'E. Atkinson points out that this fact reduces the weight of the value found for z. In this sense, uncertainly *is* introduced, as is shown by the large value of the probable error.

negative value for z. It appears that 11·51 in equation (2) should be 11·61. With this correction, the two equations for y and z follow approximately correctly and yield $z=0·5$—Bloxam's value. A more exact solution of Sampson's equations is $x=1·039$, $y=0·772$, $z=0·528$. Calculating the residuals and expressing them in msec./day I find $\Sigma v^2=12{,}545$, as compared with 916 for the correct solution and 1232 for $z=1$. The solution, then, is not a least-squares solution and the normal equations are wrong.

I have recomputed these equations and, profiting by Sampson's experience that two significant figures vanish in the last stage of solution, I have sought to secure accuracy in the fourth decimal place in each coefficient by computing each product to five places. It should be remembered that the equations are exact and that a value determined to three places only, such as 19·592, means 19·5920 for the purposes of solution.

§ 12. THE CORRECT NORMAL EQUATIONS

The normal equations are:

$$8x + 19·592y - 8·436z = 2·372 \qquad \text{......(1)},$$

$$19·592x + 59·3568y - 26·2817z = 11·6250 \qquad \text{......(2)},$$

$$8·436x + 26·2817y - 11·7269z = 5·3228 \qquad \text{......(3)},$$

from (1) and (2) $\quad y - 0·494197z = 0·511253,$

from (1) and (3) $\quad y - 0·503599z = 0·501881,$

whence $\quad 0·009402z = 0·009372,$

$$z = 0·997 \pm 0·039,$$

$$y = 1·004 \pm 0·019,$$

$$x = 1·111 \pm 0·007 \text{ sec./day}.$$

With these values the residuals are −2, +20, +4, −17, −13, +6, −1, −1 msec./day, while $\Sigma v^2=916$ as compared with 12,545 for the wrong solution. This result is a neat confirmation of the conclusions arrived at in the 1936 paper, where the solution is $y=z=1$. With regard to the value 0·997 for z, I pointed out that "amplitude deviation appears to grow slightly less rapidly than circular deviation. No importance can, however, be attached to the differences. . . changes in δ of less than 0·5 per cent would wipe out all the differences." I chose a value for x which gave smaller percentage values for the residuals than the least-squares solution.

Where the two penultimate equations are nearly equal the computation of a least-squares solution is unusually arduous. This method is not the only one for reducing the number of equations of condition to the number of equations needed for a unique solution(5, 6, 7, 8). Other methods applied to the present case agree in showing that values of y and of z are in the neighbourhood of unity.

§ 13. THE IMPULSE DEVIATION

In the preceding two sections, I have dealt with an analytical problem without reference to the physical meaning of the quantities concerned.[*] Prof. Sampson's research depended on the possibility of *systematic* error in the determination of impulse deviation amounting to as much as 25 per cent. I referred to two possible sources of error and I did not, perhaps, indicate clearly enough the possible effects. I pointed out that whereas steady amplitudes were ascertained to 0·01′, the angle at which the pendulum picked up the impulse lever was known less accurately. If an error of 0·1′ was committed in finding this, the range of 3·9 sec./day in the deviation would be 0·008 sec./day in error: less than ¼ of one per cent. Then I referred to the determination of decrement as being "the weakest link in the experimental chain". Figure 3, p. 614 shows a series of points, each representing an experimental determination and a line drawn among the points which was used for reading off values of δ/n needed for computing the deviation. There is no systematic error in the points(14); such an error can only come from wrong judgment in drawing the line. A line drawn 1 per cent lower down is clearly wrong (the zero line is not at the bottom of the figure but is near to the bottom line of print of the page), and a line 2 per cent down clears all the points, save two manifestly erratic ones. I think individual values of the deviation may possibly be 1 per cent in error, but a systematic error of this order is highly improbable.

Table 4. Three curves for E_{11}

Losing rates (sec./day)				
Period	Observed rate	Residuals (observed − calculated)		
		$z = 1·0$ $y = 1·0$ $x = 1·102$	0·8 0·905 1·08	0·5 0·761 1·035
a 5	0·723	+3	+27	+73
*b** 1, 6, 7, 8	−0·054	−6	+17	−36
c 2	−0·600	0	−15	−47
d 3	−1·022	−12	−9	−24
e 4	−1·331	−17	+11	+35
Root mean square		0·010†	0·017	0·046
Intercept (§ 3)	0·226	+0·007	−0·034	−0·100
Percentage		3	15	44

* Weighted mean for 4 periods each with $\alpha \fallingdotseq 39·7$.
Prof. Sampson treats these as separate results, but this makes little difference.
† With $x = 1·102$ the residuals have smaller *proportional* values than with $x = 1·095$, for which the root-mean-square value is 0·007.

For small changes of amplitude it is permissible to express amplitude *error* (i.e. rate of change with amplitude of amplitude *deviation*) as $z \times$ circular error:

---

[*] Apart from the method of solution, table 4 shows that 0·8 and 0·5 of the circular deviation (last two columns) give unsatisfactory fits for the observed rates as compared with full circular deviation, the curves being too flat for the points.

z may change with α. To assume for a range of amplitude (from 30′ to 70′) that amplitude deviation $= z \times$ circular deviation is not safe.

The deviation of pendulum G is not satisfactorily expressed in this way. With knife-edge suspension, the law of deviation may be entirely different from this(11).

REFERENCES

(1) Cunynghame, Sir H. H. Roy. Soc. Arts, Cantor Lectures (1908).
(2) Grossmann, J. and H. *Horlogerie Théorique*, **2**, 381.
(3) Sampson, R. A. *Proc. Roy. Soc. Edinb.* **57**, pt 1, No. 4, p. 55 (1936).
(4) Haag, J. *J. Maths. pures et appl.* **14**, pt 2 (1935).
(5) Awbery, J. H. *Proc. Phys. Soc.* **42**, pt 2 (1930).
(6) Campbell, N. R. *Measurement and Calculation*, Chap. 10.
(7) Campbell, N. R. *Phil. Mag.* **39**, 177 (1920).
(8) Denning, W. E. *Proc. Phys. Soc.* **42**, pt 2 (1930).
(9) Atkinson, E. C. *Proc. Phys. Soc.* **48**, 606 (1936).
(10) Atkinson, E. C. *Proc. Phys. Soc.* **48**, 606 (1936), tables 1 and 2.
(11) Atkinson, E. C. *Proc. Phys. Soc.* **48**, 617 (1936).
(12) Atkinson, E. C. *Proc. Phys. Soc.* **42**, pt 2, No. 232, p. 66 (1930).
(13) Atkinson, E. C. *Proc. Phys. Soc.* **42**, pt 2, No. 232, p. 67 (1930).
(14) Atkinson, E. C. *Proc. Phys. Soc.* **50**, pt 5, No. 281, § 3 (1938).

DISCUSSION

Dr A. L. **Rawlings**. There are two or three matters in the paper on dissipation about which I should like to ask Mr Atkinson for more information. In his oral comments this evening he said he had not the means either to attain or to measure very low air pressures in his clock case. From the kinetic theory of gases it is sometimes argued that no substantial reduction of air resistance is to be anticipated unless the pressure is reduced to vanishing point. Some of Mr Atkinson's results—for instance those mentioned after equation (4)—seem contrary to this theory. Does Mr Atkinson think that the elimination of the last $\frac{3}{4}$ in. or so of air pressure would lead to an important diminution of air resistance?

It may be of interest to mention some results obtained with the spinning wheels of gyro compasses as having some bearing on this question. The Sperry compass used in our navy has a steel wheel a foot in diameter and 2 in. thick spun at about 8600 r.p.m. by a built-in electric motor. The wheel is closely surrounded by a casing which is exhausted to about 1 in. of mercury by a very simple hand pump to reduce the power taken by the motor. My own experiments show that when the casing is so exhausted the total power fed into the electrical system is 240 watts. If air at atmospheric pressure is admitted to the casing, the speed of the wheel drops to 6800 and the watts put in rise to 420. Since there is a large fixed loss in the motor, this seems to show that the residuum of windage loss at the lower pressure is very small. Again, if the current is cut off when the wheel is spinning at 9000 r.p.m., its speed falls to half value at the low pressure in 70 minutes, or at atmospheric pressure in 12 minutes.

In considering the impulse-lever loss it has to be remembered that whereas the end of the lever describes an arc of a circle, the pendulum rod which it touches describes some other curve, so that at the point of contact there is rubbing friction which may assume a large value. Every one knows how the absence of a little oil at the crutch of a common clock may make it refuse to go at all. The losses described in § 22 as due to the impulse lever are therefore astonishingly small, and lead one to wonder whether the form of the ground suspension spring has the further advantage of constraining the pendulum to move more nearly in a circular arc.

Dr O. KANTOROWICZ. In recent years the investigation of what is called the damping capacity of engineering materials has become of some importance. As a rule these experiments are made by clamping a rod-shaped test piece into a machine in which it undergoes free torsional oscillations, whose decay is observed and taken as a measure of the damping capacity. In order to avoid additional damping by slip between the rod and the clamps holding it, the clamps are pressed against the rod with great force. It has been considered sufficient to exert on the clamps such a force that the stress per unit of the macrogeometrically described contact area approaches the yield point. Do the author's experiments give any indication whether this assumption is justified?

In order to obtain a uniform bending of suspension springs the author proposes to grind these springs so that they shall be thicker at the suspended end than at the free end. A similar result can of course be obtained by using a spring of uniform thickness and gradually increasing the width of the strip towards the fixed end. I suppose a spring of this form would have smaller internal losses than the spring proposed, on account of the maximum stresses being smaller, since the damping capacity grows with a rather high power of the surface stress.

Mr HOPE JONES. If Mr Atkinson could tell us how much energy was dissipated in the flexure of the suspension spring, and how much was expended in moving the pendulum's apparently rigid support, he would do us good service. I have never experienced difficulty in measuring the total energy dissipated by a pendulum swinging in air or vacuum. One knows the foot-pounds required to maintain it at a certain arc by means of a Synchronome remontoire: remove the maintenance and note the time taken in the fall of the arc, as a check upon the weight of the lever, multiplied by the distance of its fall. That simple procedure was impossible in the bad old days of escapements, when such elemental truths could not be disentangled from the escapement errors which masked them.

May I express the hope that the author will describe his escapement and his method of resetting the gravity lever? Does he use the Synchronome remontoire? On page 739 he describes the well-known modification of the Grimthorpe gravity escapement, in which the pendulum is relieved of the duty of unlocking, but he does not say how the gravity lever is replaced. The pendulum collides with a gravity arm, carries it up to the end of its swing, and returns with it to a lower point, the difference between its lift and fall being the impulse. Variation of arc involves variation in the value of that impulse. The distance which the pendulum has to carry a gravity arm uphill cannot be varied with impunity, particularly since it happens in that part of the path where it should be a point of honour to leave the pendulum alone. Mr Cottingham speaks of it as Gill's, but it was really due to Froment. The names of Liais and Verité in France were associated with it, and later on, Tiede and Knoblich in Germany, whilst LeRoy of Paris calls it Reid-Winnerl, but they are all fundamentally the same. Gill's greatest trouble was contact and his greatest mistake was to provide an impulse every second instead of at long periods. R. J. Rudd made a real free pendulum two years before Gill produced his semidetached escapement based on Froment's. Had they met then, the world would probably not have had to wait another twenty years for a free pendulum.

Mr E. T. COTTINGHAM. With a given suspension it would seem that it needed minute change in form for each particular bob, since the bending point rises with increase in weight of the bob. With thin suspension springs, which some prefer, I feel that critical molecular changes may occasionally occur, from causes little suspected, such as rapid oscillatory changes in their potential caused by a flash of lightning in the vicinity of the clock, or even the slower change in potential due to a passing cloud.

The Foucault effect, due to the earth's rotation, although constant, may be more unfavourable to the clock in certain latitudes. At the poles it exerts a torsional effect on the pendulum; at other places it would act obliquely across the suspension, at the angle of the latitude where the clock is fixed; but at the equator it would act across the bending point of the spring, its most favourable point, and here it may be involved in the true beat of the clock and the zero position of the pendulum. As our present practice makes lighter pendulums possible, I think the knife-edge suspension offers some advantage over the spring. I, too, was concerned in 1912 with probable movement of the support of a pendulum in a heavy iron case resting on three points, until the thought of Newton's rings prompted me to hold two +0·5 D. spectacle lenses in contact with the support by a rod fixed to the wall, with the happy result that the blue ring showed only a slight change in tint with alternate swings of the pendulum, an amount that mirrors or micrometers would not show. I agree with Mr Hope Jones that two other people had used the escapement before the late Sir David Gill, who lent me his drawings, but he was not aware of it, and their illustrations of it were rather crude. Sir David was the first to use it under precision conditions, and that is why I prefer to associate his name with it. Mr Hope Jones's comparison of the Gill clock with the Grimthorpe gravity escapement is not a good one, as the former, like the renowned Shortt, is freed from the frictions of unlocking and has an almost frictionless gravity arm resting on needle points in agate cups, in perfect alignment with the bending point of the spring. The lifting of this by the pendulum, some time before it reaches the end of its swing, disturbs it no more than the rapidly increasing impulse of some escapements.

Dr R. D'E. ATKINSON. The energy-losses due to a clamped suspension spring are similar to those we found when investigating the damping of torsional oscillations in quartz fibres. No form of clamp that we tried was adequate; not even that obtained by fuzing the fibre, after drawing it, into a lump of pyrex. When we drew the fibre from a rod and retained both ends of the rod on the fibre we got decrements about 100 times smaller than had previously been obtained by any means. The resulting shape was of course analogous to that produced in a suspension spring by grinding.

The question what degree of vacuum is adequate to make the damping due to residual gases negligible naturally depends on the magnitude of the other damping agents, but I think the figure of 0·001 mm. given by the author is not too low.

I should like to ask the author if he has looked into the question whether a spring could be so ground that the path of the bob would be cycloidal, so as to eliminate the circular error?

For the AUTHOR'S REPLY see page 856.

AN X-RAY INVESTIGATION OF ATOMIC VIBRATIONS IN MAGNESIUM BETWEEN 86° AND 293° K.

By G. W. BRINDLEY, M.Sc., Ph.D.
Mackinnon Student of the Royal Society

AND

P. RIDLEY, B.Sc., Physics Laboratories, University of Leeds

Received 16 *April* 1938. *Read in title* 10 *June* 1938

ABSTRACT. Measurements are made of the intensities of X-ray reflections from magnesium powder at 86° and 293° K. Absolute values of the ratio I_{86}/I_{293} are obtained by making comparative measurements on a composite specimen of magnesium and aluminium powders. The results are discussed in relation to theoretical work by Zener and others on the effect of lattice vibrations in hexagonal metals on the intensities of X-ray reflections. It is shown that in magnesium the lattice vibrations are almost isotropic but that the mean atomic displacements in the basal plane are about 3 per cent greater than those parallel to the *c* axis. Values are calculated for the mean atomic displacements in these directions at 86° and 293° K., and the results are also expressed in terms of characteristic temperatures Θ_0 (parallel to the *c* axis), equal to 339°, and Θ_{90}, equal to 327°. A consideration of these results, in conjunction with similar results for other hexagonal metals, points to a correlation between the departure of the axial ratio from the ideal value 1·633 and the asymmetry of the lattice vibrations.

§ 1. INTRODUCTION

The results of X-ray investigations of the asymmetry of the lattice vibrations in hexagonal metals carried out during the last few years by one of us^(1, 2) in this laboratory and by Jauncey, Wollan and others^(3, 4, 5, 6) in St Louis, U.S.A., when considered collectively, point to a correlation between the asymmetry of the vibrations and the departure of the axial ratio from the ideal value, 1·633, calculated for a hexagonal close-packed system of spherical atoms having isotropic vibrations. For zinc^(1, 3, 6) and cadmium^(2), which have axial ratios 1·856 and 1·886, the amplitude of the atomic vibrations is markedly greater in the direction of the *c* axis than in the basal plane, whereas for Ag-Cd^(4) and Cu-Zn alloys^(5) in the ε phase, each having an axial ratio of 1·56, the amplitude of vibration is greater in the basal plane than in the direction of the *c* axis. In order to test more thoroughly the idea that the axial ratio gives an indication of the nature of the lattice vibrations, we thought it desirable to examine a metal with an axial ratio approximating to the ideal value, 1·633, and have therefore investigated the case of magnesium, which has an axial ratio of 1·624. The experiments have shown that the lattice vibrations are very nearly isotropic but have a slightly (about 3 per cent) greater amplitude in the basal plane than normal to it, and hence provide additional support for the view that there is a correlation between the departures of the axial ratios from the ideal value, 1·633, and the asymmetry of the lattice vibrations.

§ 2. EXPERIMENTAL

The experimental procedure has been to measure the intensities of X-ray reflections from finely powdered magnesium at room-temperature and at the temperature of liquid air. The change in the magnitude of the atomic vibrations between these temperatures is sufficient to cause a measurable change in the reflected intensities, and from the ratio of the intensities at the two temperatures from different lattice planes the amplitudes of the atomic displacements can be calculated as a function of the temperature and of direction in the crystal lattice.

The method adopted for measuring the intensities resembles that previously described(7) in that the incident radiation is reflected by a flat layer of powder at the centre of a cylindrical camera, and the reflections are recorded on a concentric cylindrical film surrounding the camera. For measurements at liquid-air temperatures we have modified the powder-holder so that it has the form of a shallow cavity 0·5 mm. deep, 2 cm. long and 0·5 cm. wide, in a flat copper sheet at the end of a thin-walled brass tube containing the liquid air; the lower end of this container was of semicylindrical form constructed so that the front surface of the copper sheet was on the axis of the camera, and, since the copper was only 1 mm. thick, the powder was separated from the liquid air by only about 0·5 mm. of metal. To minimize the heat radiation falling on the powder, when the latter has been cooled to liquid-air temperature, from other parts of the camera at room-temperature, the powder-holder was surrounded as completely as possible with copper shields cooled to liquid-air temperature; the X rays pass to and from the powder through a narrow gap in these shields. Throughout these experiments the camera was kept evacuated and became, in effect, a Dewar vessel; this was essential at the lower temperature and was useful also at room-temperature, since it facilitated the maintenance of the temperature at a constant value, namely, 20° C. We have taken the temperature of the powder when it is cooled with liquid air to be 86° K., with an uncertainty of not more than 2°, which is less than 1 per cent of the full temperature range. This value was checked by thermocouple measurements and also by measuring the change in the position of high-order reflections from silver powder when cooled from the temperature of the room to that of liquid air. The entire technique has been checked by measurements on aluminium powder, which showed close agreement with previous measurements by James, Brindley and Wood(8) on single crystals of aluminium cooled from the temperature of the room to that of liquid air, and also with results calculated from the Debye-Waller theory. While this work was in progress a paper by Wollan and Harvey(3) has appeared which describes briefly a camera of somewhat similar construction.

With this type of camera, no difficulties are encountered in measuring the relative intensities of reflections at low temperatures other than those encountered at room-temperature. Absolute values of the reflected intensities were obtained by comparing reflections from magnesium and aluminium powders intimately mixed in a suitable mass-ratio. Wollan and Harvey(3) have recently advocated the use of magnesium oxide as a useful comparison substance since the change of intensity with temperature is very small and can be calculated from the characteristic temperature by means of the Debye-Waller theory. Magnesium oxide is not very suitable as a comparison substance for magnesium, owing to the positions at which the reflections occur; we have preferred aluminium since the reflections are conveniently situated and also because the experiments of James, Brindley and Wood(8) on single crystals of aluminium, and our own (unpublished) measurements on aluminium powder, show that between the temperature of the room and that of liquid air, the intensities of reflection obey closely the Debye-Waller theory.

Measurements were made with copper $\kappa\alpha$ radiation on two separate specimens of magnesium powder prepared by light filing with a Grobet no. 5 file. Previous (unpublished) work by one of us (G. W. B.) on magnesium has shown that it is extremely difficult to prepare specimens of magnesium powder of the flat-layer type which do not show a preferential orientation of the basal plane towards the surface of the layer, and this effect is very marked in the specimens used in the present experiments owing to the strong pressure that must be exerted on the specimens in order to obtain compact powders having good thermal conductivity. We have not, therefore, utilized our intensity-measurements to obtain the scattering factor f for magnesium. Since we are here interested only in the change of the intensities with temperature, preferential orientation of the crystallites is of no importance provided the measurements at both temperatures are made with the powder surface at the same angle to the incident X-ray beam, and special care was taken to satisfy this condition.

§ 3. RESULTS

The experimental results are set out in table 1; part (*a*) of the table gives the intensities of the reflections relative to 100·0 for the $11\bar{2}2$* reflection for the two specimens of powder at the two temperatures, together with the probable percentage errors calculated from the expression

$$\text{probable error} = 0{\cdot}6745\ [(\Sigma\delta^2)/n\,(n-1)]^{\frac{1}{2}},$$

where n is the number of observations and $\Sigma\delta^2$ is the sum of the squares of the residuals. To obtain sufficiently accurate results a large number of films has been measured, and for each film always two and sometimes three independent measurements have been made across different parts of each reflection. In calculating the probable error we have taken for n the number of films measured rather than the total number of measurements; hence the accuracy may be somewhat better than is indicated by the probable percentage errors given in the table.

Part (*b*) of the table summarizes the results for the ratio of the intensities at 86° and 293° relative to unity for the $11\bar{2}2$ reflection; the second and third columns give this ratio for the two specimens separately, and the fourth column gives the mean ratio. In calculating the probable errors, we have taken for the separate ratios the sum of the errors in the quantities involved, and for the mean ratio, which depends on approximately twice as many observations as the separate ratios, we have taken the mean of the errors in the separate ratios divided by $\sqrt{2}$.

---

* The reflecting planes in a hexagonal lattice are usually indexed with respect to four axes. The first three, the a axes, are taken in the basal plane of the structure at intervals of 120°, while the fourth, the c axis, is the hexagonal axis of the lattice and is thus perpendicular to the a axes. It can be shown for any plane that if the indices corresponding to two of the a axes are h, k, then the index corresponding to the third is $\overline{h+k}$. Thus the indices of a plane are expressed in the form $(h, k, \overline{h+k}, l)$.

Table 1. Intensities of X-ray reflections at 86° and 293° K.

(*a*) Relative intensities

Reflections	Specimen I				Specimen II			
	I_{293}	Probable error (per cent)	I_{86}	Probable error (per cent)	I_{293}	Probable error (per cent)	I_{86}	Probable error (per cent)
$11\bar{2}2$	100·0	—	100·0	—	100·0	—	100·0	—
$20\bar{2}1$	63·2	0·7	61·9	0·5	62·8	0·6	62·5	0·6
0004	38·0	0·8	38·6	0·8	36·7	0·8	37·4	0·8
$20\bar{2}2$	24·3	1·1	25·3	1·3	21·6	1·0	23·6	1·1
$10\bar{1}4$	39·4	1·1	42·9	1·3	39·4	1·0	41·6	1·2
$20\bar{2}3$	63·1	0·9	70·5	1·1	60·4	1·0	68·7	0·8
$21\bar{3}1$	84·3	1·2	98·7	1·1	80·2	1·1	96·5	0·8
$11\bar{2}4$	98·0	1·3	115·0	0·9	96·0	1·0	111·6	0·9
$10\bar{1}5$, $21\bar{3}2$	113·3	1·2	136·7	1·1	111·0	0·9	134·8	1·0
$21\bar{3}3$	77·8	1·9	104·8	1·0	74·5	1·3	100·5	1·1

(*b*) Relative and absolute values of I_{86}/I_{293}

Reflections	I_{86}/I_{293}, relative to 1·000 for Mg $11\bar{2}2$						I_{86}/I_{293} absolute
	Specimen I	Probable error (per cent)	Specimen II	Probable error (per cent)	Mean	Probable error (per cent)	
$11\bar{2}2$	1·000	—	1·000	—	1·000	—	$1{\cdot}23_7$
$20\bar{2}1$	$0{\cdot}98_0$	1·2	$0{\cdot}99_5$	1·2	$0{\cdot}98_8$	0·8	$1{\cdot}22_2$
0004	$1{\cdot}01_6$	1·6	$1{\cdot}01_9$	1·6	$1{\cdot}01_8$	1·1	$1{\cdot}26_0$
$20\bar{2}2$	$1{\cdot}04_1$	2·4	$1{\cdot}09_3$	2·1	$1{\cdot}06_7$	1·6	$1{\cdot}32_0$
$10\bar{1}4$	$1{\cdot}08_9$	2·4	$1{\cdot}05_6$	2·2	$1{\cdot}07_2$	$1{\cdot}6_5$	$1{\cdot}32_6$
$20\bar{2}3$	$1{\cdot}11_8$	2·0	$1{\cdot}13_8$	1·8	$1{\cdot}12_8$	1·4	$1{\cdot}39_5$
$21\bar{3}1$	$1{\cdot}17_1$	2·3	$1{\cdot}20_4$	1·9	$1{\cdot}18_8$	1·5	$1{\cdot}47_0$
$11\bar{2}4$	$1{\cdot}17_4$	2·2	$1{\cdot}16_3$	1·9	$1{\cdot}16_8$	1·4	$1{\cdot}44_5$
$10\bar{1}5$, $21\bar{3}2$	$1{\cdot}20_6$	2·3	$1{\cdot}21_5$	1·9	$1{\cdot}21_0$	1·5	$1{\cdot}49_7$
$21\bar{3}3$	$1{\cdot}34_7$	2·9	$1{\cdot}34_9$	2·4	$1{\cdot}34_8$	1·8	$1{\cdot}66_7$

(*c*) Data for standardizing the relative values of I_{86}/I_{293}

Reflections	I_{86}/I_{293}		$\frac{\text{Absolute values}}{\text{relative values}}$
	Relative values, table 1*b*	Absolute values, table 2	
$11\bar{2}2$	1·000	$1{\cdot}25_5$	$1{\cdot}25_5$
$20\bar{2}1$	$0{\cdot}98_8$	$1{\cdot}20_5$	$1{\cdot}22_0$
$20\bar{2}3$	$1{\cdot}12_8$	$1{\cdot}39_4$	$1{\cdot}23_5$
			Mean $1{\cdot}23_7$

From the data given in parts (*a*) and (*b*) of the table it is seen that although the relative intensities of reflection from the two specimens at the two temperatures show differences of the order of several per cent, the ratios of the intensities are in much closer agreement. The differences in the relative intensities may have arisen partly from differences in the degree of orientation of the crystallites, and partly from a small difference in the angular settings of the powders with respect to the incident beam, since the angles were measured only to the nearest 0·5 degree. It is satisfactory to find that the agreement between the ratios of the intensities comes well within the limits of probable error for all the reflections except the $20\bar{2}2$ which was by far the weakest reflection measured. The probable errors in the measured intensities are of the order of 1 per cent, and this is the highest accuracy to be expected from the photographic method of measuring intensities. It is obtainable only by careful measurement of a large number of films, and the labour involved is considerable; altogether in this part of the investigation 46 films have been measured, and two or three independent determinations have been made for each reflection on each film. Comparing the measurements at 86° and 293° we see that the probable errors are slightly less at 86°, and this fact is most marked for the higher order reflections.

Table 2. Comparison of intensities reflected by magnesium and aluminium at 86° and 293° K.

Reflections	Relative intensities		Probable error (per cent)		(I_{86}/I_{293})	
	293° K.	86° K.	293° K.	86° K.	relative	absolute
Al 220	100·0	100·0	—	—	1·000	$1{\cdot}118_6$
Mg $10\bar{1}3$	121·8	129·2	$0{\cdot}5_6$	$0{\cdot}6_1$	$1{\cdot}06_1$	$1{\cdot}18_7$
Mg $11\bar{2}2$	104·9	117·6	$0{\cdot}7_4$	$0{\cdot}5_8$	$1{\cdot}12_1$	$1{\cdot}25_5$
Mg $20\bar{2}1$	66·9	72·0	$1{\cdot}2_1$	$1{\cdot}0_8$	$1{\cdot}07_7$	$1{\cdot}20_5$
Mg $20\bar{2}3$	54·5	67·9	$1{\cdot}3_9$	$1{\cdot}2_3$	$1{\cdot}24_6$	$1{\cdot}39_4$

In order to obtain absolute values of the ratio I_{86}/I_{293}, the intensities of the $10\bar{1}3$, $11\bar{2}2$, $20\bar{2}1$ and $20\bar{2}3$ reflections from magnesium were compared with the 220 reflection from aluminium at the two temperatures; 13 films in all were measured at 293° K. and 15 films at 86° K. The results are set out in table 2, where the columns, in order, give the indices of the reflections, the reflected intensities at 293° and 86° relative to 100·0 for aluminium 220, and the probable percentage errors calculated as before. The sixth column of the table gives the ratio of the intensities at the two temperatures relative to unity for aluminium 220, and the seventh column gives the absolute value of this ratio calculated in the following manner. From their work on single crystals of aluminium, James, Brindley and Wood(8) showed that the exponent M in the equation

$$I_T = Ie^{-2M} \qquad \text{......(1),}$$

which gives the intensity I_T reflected at a temperature T in terms of the intensity I reflected by the atoms at rest, has the form

$$M = (h^2+k^2+l^2)\,\{3{\cdot}87\times 10^{-5}\,T + 0{\cdot}177/T - 277/T^3\} \qquad \text{......(2),}$$

where h, k and l are the indices of the reflections. This expression gives for I_{86}/I_{293} for aluminium 220 the value $1{\cdot}118_6$ and it is in terms of this result that we have standardized our values of the ratio I_{86}/I_{293} for the magnesium reflections. Comparing now the relative values of I_{86}/I_{293} in column 6 of table 1 *b* for the magnesium reflections $11\bar{2}2$, $20\bar{2}1$ and $20\bar{2}3$ with the corresponding absolute values in column 7 of table 2, we see from table 1 (*c*) that the mean conversion factor from relative to absolute values of I_{86}/I_{293} is $1{\cdot}23_7$ and hence we obtain the absolute values of I_{86}/I_{293} given in the final column of table 1 (*b*).

§ 4. DISCUSSION

The main question at issue is to determine whether the lattice vibrations in magnesium between 86° and 293° K. are isotropic, and, if not, to discover the magnitude of the anisotropy. It has been shown⁽⁹⁾ that the exponent M in the equation for the effect of temperature on the reflected intensity, equation (1), is given by

$$M_\psi = 8\pi^2 \overline{u_\psi^2} (\sin\theta/\lambda)^2 \qquad \text{......(3)},$$

where $\overline{u_\psi^2}$ is the mean square displacement in a direction ψ normal to the reflecting planes. In the case of hexagonal crystals, it may easily be shown, as Zener⁽¹⁰⁾ first pointed out, that the mean square displacement in a direction ψ with respect to the c axis can be expressed in terms of the mean square displacements parallel and perpendicular to the c axis, by the equation

$$\overline{u_\psi^2} = \overline{u_0^2} \cos^2\psi + \overline{u_{90}^2} \sin^2\psi \qquad \text{......(4)}.$$

Alternatively, we may write

$$M_\psi = M_0 \cos^2\psi + M_{90} \sin^2\psi \qquad \text{......(5)}.$$

For cubic crystals it has been shown by Debye and Waller that

$$M = \frac{6h^2 T}{mk\Theta^2} [\Phi(x) + x/4] (\sin\theta/\lambda)^2 \qquad \text{......(6)},$$

where Θ is the characteristic temperature which occurs in the Debye theory of specific heat, $x = \Theta/T$, and $\Phi(x)$ is the well-known Debye function. The expression in square brackets, the so-called quantization factor, may conveniently be represented by Q and is of the order of unity provided $T > \Theta$ or $T \sim \Theta$. It follows from the work of Zener, Jauncey and their collaborators⁽¹⁰, ¹¹⁾, that a formula similar to equation (6) may be applied to crystals of lower symmetry provided Θ is regarded as a function of the direction in the crystal and, at high temperatures, also of the temperature. For hexagonal crystals we may write

$$M_\psi = \frac{6h^2 T}{mk} \left(\frac{Q}{\Theta^2}\right)_\psi (\sin\theta/\lambda)^2 \qquad \text{......(7)},$$

or, from equation (5),

$$M_\psi = \frac{6h^2 T}{mk} \left[\left(\frac{Q}{\Theta^2}\right)_0 \cos^2\psi + \left(\frac{Q}{\Theta^2}\right)_{90} \sin^2\psi\right] (\sin\theta/\lambda)^2 \qquad \text{......(8)}.$$

This equation can be compared with the experimental results as follows:

We have $\log_e (I_{86}/I_{293}) = 2(M_{293} - M_{86}) = 2\Delta M,$

whence

$$\frac{\log_e (I_{86}/I_{293})}{(\sin\theta/\lambda)^2} = \frac{12h^2}{mk}\left[\Delta\left(\frac{TQ}{\Theta^2}\right)_0 \cos^2\psi + \Delta\left(\frac{TQ}{\Theta^2}\right)_{90} \sin^2\psi\right]$$

$$= \frac{12h^2}{mk}\left[\left\{\Delta\left(\frac{TQ}{\Theta^2}\right)_0 - \Delta\left(\frac{TQ}{\Theta^2}\right)_{90}\right\} \cos^2\psi + \Delta\left(\frac{TQ}{\Theta^2}\right)_{90}\right] \quad \ldots\ldots(9),$$

where the symbol $\Delta\,(TQ/\Theta^2)$ denotes the change in (TQ/Θ^2) between 86° and 293° K. This last equation indicates that if the atomic vibrations in magnesium are anisotropic, there should be a linear relation between the experimentally determined quantity $\log_e (I_{86}/I_{293}) \,.\, (\sin\theta/\lambda)^{-2}$ and $\cos^2\psi$ from which Θ_0 and Θ_{90} may be calculated. If, however, the vibrations are isotropic, the coefficient of $\cos^2\psi$ in equation (9) will be zero and $\log_e (I_{86}/I_{293}) \,.\, (\sin\theta/\lambda)^{-2}$ will have a constant value from which a mean Θ for the crystal can be obtained.

In table 3 the observed reflections are recorded in order of the angle ψ, which is calculated from the relation

$$\cos\psi = (l/R)\,\{4\,(h^2+kh+k^2)/3 + (l/R)^2\}^{-\frac{1}{2}} \quad \ldots\ldots(10),$$

where h, k and l are the indices of the reflection. The columns of the table, in order, give the indices of the reflections, $(\sin\theta/\lambda)$, ψ and $\cos^2\psi$; the final column gives $\log_e (I_{86}/I_{293}) \,.\, (\sin\theta/\lambda)^{-2}$ together with the probable errors calculated from those in the seventh column of table 1 (*b*). The percentage errors in the quantity

$$\log_e (I_{86}/I_{293}) \,.\, (\sin\theta/\lambda)^{-2}$$

are of the order of 4 per cent for the majority of the reflections, and this is to be compared with corresponding errors of the order of 1·5 per cent in the ratios (I_{86}/I_{293}). This increase in the probable error arises in taking the natural logarithm of the measured ratio.

Table 3. Values of $\log_e (I_{86}/I_{293}) \,.\, (\sin\theta/\lambda)^{-2}$

Reflections	$\left(\frac{\sin\theta}{\lambda}\right)$	ψ	$\cos^2\psi$	$\log_e (I_{86}/I_{293}) \,.\, (\sin\theta/\lambda)^{-2}$
0004	0·384	0°	1·000	1·56 ± 0·08
$10\bar{1}4$	0·425	25·1	0·820	1·57 0·09
$10\bar{1}3$	0·340	32·0	0·719	1·48 0·07
$11\bar{2}4$	0·495	39·1	0·602	1·50 0·06
$10\bar{1}5$	0·513	20·5	0·877 } 0·582	1·53 0·05
$21\bar{3}2$	0·514	68·0	0·140	
$20\bar{2}3$	0·462	51·3	0·391	1·56 0·06
$11\bar{2}2$	0·367	58·4	0·275	1·58 —
$21\bar{3}3$	0·557	58·8	0·268	1·64 0·06
$20\bar{2}2$	0·408	61·9	0·222	1·66 0·10
$20\bar{2}1$	0·373	75·1	0·066	1·44 0·06
$21\bar{3}1$	0·487	78·6	0·039	1·62 0·06

The results show that if there is a variation of $\log_e (I_{86}/I_{293}) \,.\, (\sin\theta/\lambda)^{-2}$ with $\cos^2\psi$ it can only be small; hence any departure from isotropic vibrations must be very small. It is difficult to decide whether there is any real variation in this quantity or whether the departures from a constant value are to be interpreted simply as experimental errors. The arithmetical mean value is 1·56, and most of the values agree with this mean value within the limits of the probable errors. We have, however, examined the results by the method of least squares in order to find the best linear equation to fit them. Writing equation (9) in the form

$$\frac{\log_e (I_{86}/I_{293})}{(\sin \theta/\lambda)^2} = m \cos^2 \psi + c,$$

we find the following values for m and c:

$$\left.\begin{aligned} m &= \frac{12h^2}{mk}\left\{\Delta\left(\frac{TQ}{\Theta^2}\right)_0 - \Delta\left(\frac{TQ}{\Theta^2}\right)_{90}\right\} = -0{\cdot}11_6 \\ c &= \frac{12h^2}{mk}\Delta\left(\frac{TQ}{\Theta^2}\right)_{90} = 1{\cdot}63_2 \end{aligned}\right\}.$$

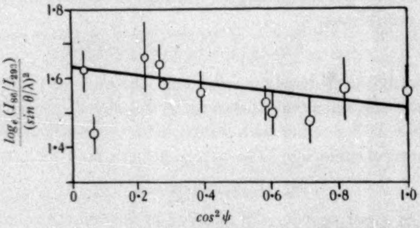

Figure 1. Observed values of $\log_e (I_{86}/I_{293}) \cdot (\sin \theta/\lambda)^{-2}$ plotted against $\cos^2 \psi$. The straight line is calculated by the method of least squares.

The straight line given by these values of m and c is shown in figure 1 together with the experimental values of $\log_e (I_{86}/I_{293}) \cdot (\sin \theta/\lambda)^{-2}$; the vertical line attached to each point indicates the probable error. We see that the straight line passes through the points within the limits of experimental error, with the single exception of the $20\bar{2}1$ which lies so far from the most probable straight line that it was neglected in calculating the best values of m and c. For the two reflections $10\bar{1}5$ and $21\bar{3}2$, which are not resolved, we have calculated a weighted mean value of $\cos^2 \psi$ by weighting the separate values of $\cos^2 \psi$ with the relative intensity of the reflection assuming the scattering factor f for each reflection to be the same; this procedure admittedly gives results which are only approximate, but it serves to show that the measurement in question is not in disagreement with the general run of the others. In view of the uncertainty as to the best way of obtaining a mean $\cos^2 \psi$ for this reflection, we have not included it in the calculation of the constants for the mean line.

With the values given above for m and c, we obtain

$$\Delta\left(\frac{TQ}{\Theta^2}\right)_{90} = 1{\cdot}74_4 \times 10^{-3}$$

and

$$\Delta\left(\frac{TQ}{\Theta^2}\right)_0 = 1{\cdot}62_0 \times 10^{-3},$$

whence, by a graphical solution,* we obtain

$$\left.\begin{aligned}\Theta_0&=339^\circ\\ \Theta_{90}&=327^\circ\end{aligned}\right\}.$$

Assuming that the probable errors in m and c are of the same order as in the quantity $\log_e (I_{86}/I_{293}).(\sin\theta/\lambda)^{-2}$, namely 4 per cent, we find that the corresponding errors in Θ_0 and Θ_{90} are $\pm 7^\circ$. The difference between Θ_0 and Θ_{90} is therefore of the same order as the sum of the probable errors, a result which agrees with the previous statement that the individual values of $\log_e (I_{86}/I_{293}).(\sin\theta/\lambda)^{-2}$ agree with the mean value within the limits of error. We consider, however, that the tendency of the values shown in figure 1 to decrease with increasing $\cos^2\psi$ is a real effect and that, although the measurements cannot be made with sufficient accuracy to give a reliable value of the difference of Θ_0 and Θ_{90}, they are sufficiently accurate to establish the result that Θ_0/Θ_{90} is slightly greater than unity and hence, as we shall proceed to show, that the mean atomic displacement in the direction $\psi=0$, the c axis, is slightly less than the mean displacement in the direction $\psi=90^\circ$, the basal plane, approximately in the ratio 327/339. Combining equations (3) and (7), we have

$$\overline{u_0^2}=\frac{3h^2T}{4\pi^2mk}\left(\frac{Q}{\Theta_0^2}\right),$$

$$\overline{u_{90}^2}=\frac{3h^2T}{4\pi^2mk}\left(\frac{Q}{\Theta_{90}^2}\right).$$

Taking for Θ_0 and Θ_{90} the values 339° and 327°, we obtain the following:

at $T=293^\circ$ K., $(\overline{u_0^2})^{\frac{1}{2}}=0\cdot125$ A. and $(\overline{u_{90}^2})^{\frac{1}{2}}=0\cdot130$ A.,

at $T=86^\circ$ K., $(\overline{u_0^2})^{\frac{1}{2}}=0\cdot078$ A. and $(\overline{u_{90}^2})^{\frac{1}{2}}=0\cdot080$ A.

Also $\Theta_{90}/\Theta_0=0\cdot96_5$

$$(\overline{u_0^2})^{\frac{1}{2}}/(\overline{u_{90}^2})^{\frac{1}{2}}=0\cdot96_5 \quad \text{at} \quad 293^\circ\ \text{K. and} \quad 0\cdot97_1 \quad \text{at} \quad 86^\circ\ \text{K.}$$

An average value of $\overline{u^2}$ for all directions has been calculated from the relation

$$\overline{u_{\mathrm{av}}^2}=\frac{\overline{u_0^2}+2\overline{u_{90}^2}}{3},$$

whence an average characteristic temperature, Θ_{av}, has been derived. We find $(\overline{u_{\mathrm{av}}^2})^{\frac{1}{2}}$ has the values 0·128 A. at 293° K. and 0·080 at 86° K.; the corresponding values of Θ_{av} are 331° at both temperatures. This value of Θ_{av} is of the same order as the value 290° obtained from specific-heat data(13), but the difference is appreciable and may perhaps be explained along the lines suggested in a recent paper by Blackman(12).

§ 5. CONCLUSIONS

The lattice vibrations in magnesium between 86° and 293° are shown to be almost isotropic, the root-mean-square displacements being about 3 per cent greater in the basal plane than parallel to the c axis; this small difference can only be established very approximately, but the measurements are sufficiently accurate to justify the conclusion that there is a small asymmetry in the lattice vibrations, the amplitude being slightly greater in the basal plane, and of the order of magnitude stated. When this result is considered in relation to the results of previous measurements on hexagonal metals, § 1, the total evidence points strongly to the conclusion that there is a correlation between the departures of the axial ratio from the ideal value 1·633 and the asymmetry of the lattice vibrations; metals with c/a greater than 1·633 appear to have mean atomic displacements which are larger parallel to than normal to the c axis, and vice versa. Magnesium, with c/a equal to 1·624, approximates to the ideal but shows a small asymmetry in the lattice vibrations consistent with the axial ratio being slightly less than 1·633.

---

* We have plotted $\Delta\,(TQ/\Theta^2)$ against Θ for a range of values of Θ, from $\Theta=300^\circ$ to $\Theta=380^\circ$; over this range the relation is almost linear.

§ 6. ACKNOWLEDGEMENTS

We wish to thank Prof. Whiddington for his continued interest in the programme of research of which the present work forms a part, and the Department of Scientific and Industrial Research for a maintenance grant to one of us (P. R.).

REFERENCES

(1) Brindley, G. W. *Phil. Mag.* **21**, 790 (1936). (Lattice vibrations in Zn.)
(2) Brindley, G. W. *Proc. Leeds Phil. Soc.* **3**, 200 (1936). (Lattice vibrations in Cd.)
(3) Wollan, E. O. and Harvey, G. G. *Phys. Rev.* **51**, 1054 (1937). (Lattice vibrations in Zn between 85° and 295°.)
(4) Wollan, E. O. *Phys. Rev.* **53**, 203 (1938). (On Ag-Cd alloy; abstract only.)
(5) Howard, R. A. *Phys. Rev.* **53**, 324 (1938). (On Zn-Cu alloy; abstract only.)
(6) Jauncey, G. E. M. and others. *Phys. Rev.* **50**, 408, 413 and 417 (1936); *Phys. Rev.* **51**, 1062, 1065 and 1067 (1937); **53**, 203 (1938). (A group of papers on Zn, mainly diffuse scattering experiments.)
(7) Brindley, G. W. and Spiers, F. W. *Proc. Phys. Soc.* **46**, 841 (1934); **50**, 17 (1938).
(8) James, R. W., Brindley, G. W. and Wood, R. G. *Proc. Roy. Soc.* A, **125**, 401 (1929).
(9) Waller, I. and James, R. W. *Proc. Roy. Soc.* A, **117**, 214 (1927).
(10) Zener, C. *Phys. Rev.* **49**, 122 (1936).
(11) Zener, C. and Bilinsky, S. *Phys. Rev.* **50**, 101 (1936).
Jauncey, G. E. M. and Bruce, W. A. *Phys. Rev.* **51**, 1067 (1937).
(12) Blackman, M. *Proc. Camb. Phil. Soc.* **33**, 380 (1937).
(13) Landolt-Bornstein. *Tabellen*, 2B, 1232 (1931).

CRITICAL FREQUENCY MEASUREMENTS OF WIRELESS WAVES REFLECTED OBLIQUELY FROM THE IONOSPHERE

By F. T. FARMER, Ph.D., Cavendish Laboratory, Cambridge,
C. B. CHILDS, Ph.D. and A. COWIE, B.Sc., Edinburgh University

Communicated by J. A. Ratcliffe, M.A., 28 *April* 1938. *Read in title* 24 *June* 1938

ABSTRACT. Experiments are described which compare the *F*-region skip frequency, for transmission between two distant stations, with that calculated from the normal-incidence characteristics on a simple ray theory. The greatest possible accuracy was aimed at so that the results might resolve an uncertainty left in previous measurements, in which the forms of the oblique and normal incidence *P′f* curves were compared. This involved using a pulse-transmitter at each end of the oblique trajectory to correct for horizontal variations of ionization, and developing a special rapid technique. Measurements were confined to days when the ionosphere was in a completely undisturbed state, as shown by the clean splitting of echoes at normal incidence.

The results showed that the theory, which neglects the earth's magnetic field, is very nearly correct for the ordinary wave over a transmission distance of about 500 km. The precise disagreement is determined, and it is believed that if an accurate theory be developed the results will indicate whether or not the Lorentz term should be included in the analysis.

§ 1. INTRODUCTION

Measurements of the ionization-density in the ionosphere are now available in many parts of the globe. Apart from their physical interest these measurements are made with the object of predicting the transmission characteristics for a trajectory joining any two points. Their use in this way, however, depends entirely on a knowledge of the relationship between vertical and oblique propagation conditions for a given ionized region, and little information is as yet available about this relationship. It is with the object of deriving experimental evidence on this point that the present work has been carried out.

A simple theory relating the group times of travel of two waves, incident vertically and at a known angle on the ionosphere, has been given by Martyn⁽¹⁾. This theory neglects the earth's magnetic field and also the possible effect of the Lorentz term⁽²⁾, but it serves as a useful guide as to the behaviour to be expected at oblique incidence. In a previous paper⁽³⁾ it was shown how, from a normal-incidence *P′f* curve, the corresponding curve (relating equivalent path and frequency) for transmission between two distant points could be deduced by means of this theory, and some experimental results were given which showed good qualitative agreement with the theory. The measurements were made, however, with a transmitter at one end only of the oblique trajectory, and it was not known to what extent the departures found from the simple theory were due to variations of ionization along the path of the wave.

The present paper is an account of a series of experiments in which normal-incidence measurements were made at each end of the trajectory, so that the ionization conditions prevailing at the mid point could be found by interpolation. The technique was developed so as to permit the maximum accuracy in the comparison of normal-incidence and oblique-incidence phenomena. The present discussion of the results is limited to a comparison with the simple theory previously given: it is believed that if later a more complete theory taking into account the earth's magnetic field can be developed, the results will also provide evidence as to whether or not the Lorentz polarization term should be included in the theory.

§2. SPECIAL CONSIDERATIONS

Accurate experiments of the type proposed can only be carried out when the ionosphere is in an entirely undisturbed state. The previous experiments had shown that region E was generally far too irregularly stratified for useful measurements to be made, and it was decided therefore to confine attention to region F. This region also is often in an unsuitable state, the disturbance having the effect of broadening the echoes just before their penetration, and measurements were therefore made only on those occasions when the echoes at normal incidence showed clean splitting even when retarded up to an equivalent height of 800 km. In these cases it was found that the results showed good consistency among themselves.

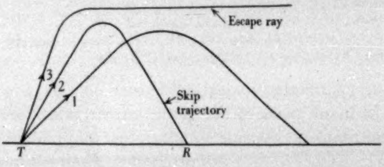

Figure 1

The previous work had shown that the form of the {equivalent-height, frequency} curve for the distant transmission agreed well with that derived by use of the simple theory. In the present work, therefore, most of the experiments consisted in measuring accurately, and as nearly simultaneously as possible, the final skip frequency in the oblique transmission, and the normal incidence $P'f$ curve, so that the exact relationship between them could be found. It is to be noted that the limiting frequency for oblique transmission is fundamentally different from that of penetration at normal incidence: it represents a trajectory which does not reach to the height of maximum density in the layer but is formed by the convergence of the two trajectories present before the skip is reached; see figure 1. It therefore does not involve an increase of absorption as the limiting frequency is approached. On the contrary, the signal strength tends to increase with frequency owing to the focusing effect of the layer on this limiting wave, and the result is, in practice, to make the final frequency extremely well defined. The final frequency is therefore particularly suitable as a quantity for accurate measurement in experiments of this type.

The method of calculation used previously is tedious when a large number of curves are to be handled, and when only the limiting frequency was required it was calculated from the normal-incidence $P'f$ curve by means of a more rapid graphical method due to Smith⁽⁴⁾. This depends on the same theory as the previous method. It may be stated briefly as follows.

A wave of frequency f incident at an angle i on the ionosphere has an equivalent path given by Martyn's theorem

$$P'(f, i) = \sec i \,.\, P'(f \cos i, 0),$$

where $P'(f \cos i, 0)$ is the equivalent path at normal incidence and frequency $f \cos i$.

Breit and Tuve⁽⁵⁾ have shown that, if d is the distance of transmission, then

$$P'(f, i) = d \operatorname{cosec} i.$$

Hence, on elimination of $P'(f, i)$,

$$P'(f \cos i, 0) = d \cot i.$$

Curves are plotted for the fixed distance d and for selected values of f (the oblique-incidence frequency) relating P' to the normal incidence frequency $f \cos i$. The angle of incidence is a variable parameter along any one of these curves. Any curve then shows the equivalent height that must exist at normal incidence and frequency $f \cos i$ if the higher frequency f is to be propagated at an angle i to the distant receiver. The curves are placed over the experimental $P'f$ curve for normal incidence, and it is evident that the highest frequency which can be reflected to the distant receiver is given by the particular curve which is tangential to the observed $P'f$ relationship; see figure 2. The family of curves derived by the above method depends only on the ground distance between the transmitter and receiver, and once plotted it can therefore be applied to all the experimental results. The calculation by this method also shows, by the point of tangency, the equivalent height on the normal-incidence $P'f$ curve which corresponds to the top of the oblique-incidence trajectory. This is of interest in showing what part of the ionosphere is ultimately responsible in reflecting waves to a given distance.

The distance of transmission used in the experiments was 464 km. For this condition the curvature of the earth is just appreciable, and its effect has been allowed for to a first approximation by adding to the equivalent heights measured at the end stations a distance which represents the departure of the earth's surface at the mid point from the chord joining the transmitter and receiver (figure 3). This distance is 4·5 km. in the present instance.

The two magneto-ionic components are propagated independently at oblique incidence, as at normal incidence, and it was shown in the previous work that the {equivalent-path, frequency} curves for each were of the form that would be expected from the normal-incidence curves. Most of the present measurements were made on the ordinary wave alone, since this was likely to be the less affected by the field, and also because the measurements on it were more reliable since the extraordinary wave was always present after the penetration, showing that the signal had not been lost through any other cause. Since at normal incidence the ordinary wave is reflected from a height independent of the field, it is probable that the effect of the field on this wave at oblique incidence will be small, in which case we may expect the calculation based on Martyn's theorem to agree closely with experiment.

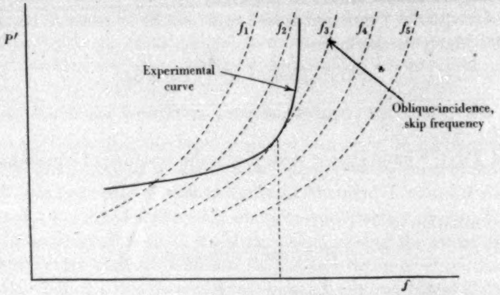

Figure 2

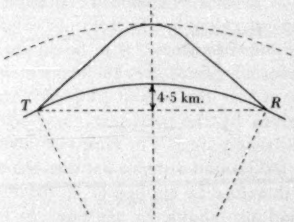

Figure 3

§ 3. EXPERIMENTAL ARRANGEMENTS

The experiments were carried out between Cambridge and Edinburgh, distant 464 km. from one another and situated on a line running approximately north and south magnetically. Pulse transmitters of conventional type were installed at the two stations, that at Cambridge being controlled by a land line from the receiving hut about 1 km. away, while that at Edinburgh was in the same room as the receiver and controlled by hand. Visual observation on a cathode-ray tube was used throughout. For normal incidence a time base synchronized to the local electric mains was employed at each end, and for oblique-incidence measurements a self-synchronizing time base(6) of a type previously described was used.*

* The electric supply mains at the two places were never found to be synchronized.

The experiments were divided into two groups. The first were made before the transmitter at Edinburgh was in use, and consisted of schedules of gradually ascending frequencies transmitted from Cambridge, with 2 min. pause on each frequency, so that measurements of the echo spacing could be made at Edinburgh. Each schedule was followed by a determination of the normal-incidence $P'f$ curve at Cambridge, and the measurements were used to compare the form of the observed $P'f$ curve at oblique incidence with that calculated from the normal-incidence observations.

It was realized from these experiments that the accuracy of comparison of oblique-incidence and normal-incidence curves was impaired not only by the lack of information concerning the latitude variation of ionization, but also by the time delay between the two sets of observations: a complete experiment of this type required 30 min., during which time the region-F ionization might change quite appreciably.

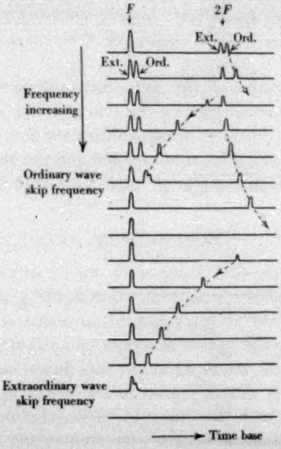
F
2F
Ext.
Ord.
Ext.
Ord.
Frequency increasing
Ordinary wave skip frequency
Extraordinary wave skip frequency
Time base

Figure 4. Echo patterns obtained at oblique incidence on a series of ascending frequencies. The time base was synchronized to the first pulse, no ground wave being received.

The subsequent experiments, in which both transmitters were used, were therefore made by a more rapid technique. The echo spacings in the oblique transmissions were not measured, but attention was confined to determining the exact frequency at which the ordinary wave disappeared. Each experiment lasted only 15 min.: during the first seven a determination was made at Cambridge of the normal-incidence $P'f$ curve, and at Edinburgh of the final penetration frequency of this curve; and during the remaining 8 min. signals having closely spaced frequencies, covering the skip frequency of the ordinary wave and each lasting

30 sec., were transmitted from Edinburgh. These were followed on the receiver at Cambridge, and the echo pattern was sketched so that the point of disappearance was accurately recorded. The type of observations obtained was as shown in figure 4.* Frequency steps of about 0·08 Mc./sec. were used, so that the critical frequency could be estimated with considerable accuracy.

By comparing the penetration frequencies for normal incidence at Cambridge and Edinburgh the variation with latitude was found. It was assumed that the form of the $P'f$ curve was the same at the mid point as at Cambridge, so that from the latitude variation the appropriate curve for the mid point could be determined. An interpolation in time (between successive runs) was also applied to eliminate as far as possible the natural variations in the ionization density. The results obtained in this way showed good agreement, and we consider that the process of interpolation is an essential part of the technique if accurate determinations are to be made.

Since the whole precision of the experiments depended on having a reliable cross calibration of frequency between the two stations, at the end of each period of experiment a test was made in which calibration frequencies, spaced by about 0·5 Mc./sec., were transmitted from one station and the receiver-dial readings were noted at the other. The dial readings were used throughout for recording frequencies.

§4. EXPERIMENTAL RESULTS

The experiments of the first group gave results similar to those shown in the previous paper. A typical case is reproduced in figure 5, in which the upper curves depict the penetration of the ordinary and extraordinary waves at normal incidence, and the lower the corresponding curves at oblique incidence. From the observations on the ordinary wave in the upper figure the theoretical curve for oblique incidence has been calculated; it is shown dotted in the lower figure. It is seen to agree reasonably well in form with the observed curve, and in this particular case also there is quantitative agreement between the frequencies observed and calculated. This is significant in showing that the discrepancy noted in the previous paper (of about 0·25 Mc./sec.) must be at least partly attributable to latitude variations of ionization, and could not have been relied on as the basis of any theoretical computations. These results, therefore, serve merely to confirm the previous work, and their further value depends on eliminating the uncertainty in the absolute relationship between the curves.

Of the experiments in the second group, designed solely for the comparison of critical frequencies, twenty-one gave accurate measurements of the three quantities involved, viz. the normal-incidence $P'f$ curve at Cambridge, the final penetration frequency at Edinburgh, and the skip frequency at oblique incidence. Table 1 shows the results of one of the schedules made during the night 28/29 August 1937, and the interpolation mentioned above. The region-F penetration frequencies at Cambridge and Edinburgh are given in columns 3 and 4, and the latitude variation

---

* This figure also illustrates the behaviour of the extraordinary wave.

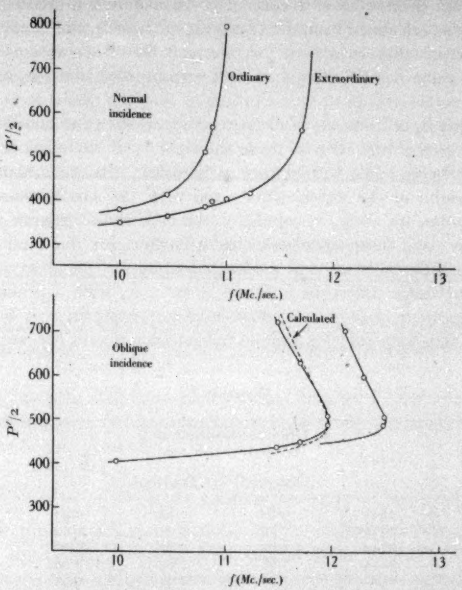

Figure 5. Normal and oblique incidence $P'f$ curves. The absolute values of P' in the oblique curves are estimated from the spacing between first and second reflections, together with the normal-incidence equivalent heights. No ground wave was received.

Table 1

Number of experiment	G.m.t.	F penetration (Mc./sec.)		½ latitude-difference (Mc./sec.)	Calculated skip frequency from Cambridge $P'f$ curve (Mc./sec.)			Observed skip frequency (Mc./sec.)
		Cambridge	Edinburgh		Uncorrected	Corrected for time	Corrected for latitude	
1	2235 2242	6·65	6·45	−0·10	7·01	6·97	6·87	6·88
2	2250 2255	6·57	6·27	−0·15	6·92	6·81	6·66	6·63
3	2305 2310	6·29	6·24	−0·03	6·61	6·56	6·53	6·47
4	2320 2326	6·15	6·13	−0·01	6·47	6·44	6·43	6·30
5	2335 2341	6·10	6·03	−0·03	6·31	6·28	6·25	6·23
6	2350 2357	6·00	5·92	−0·04	6·20	6·20	6·16	6·16

determined from them is given in column 5. In column 6 is given the theoretical skip frequency as calculated from the Cambridge *P′f* curve, and in columns 7 and 8 the same quantity after correction for time and latitude variations respectively. The resulting value is to be compared with the observed skip frequency given in the last column.

Table 2 represents the results of all the experiments after they have been subjected to calculation in this way. Ten of those shown were of the quick-schedule type, the remainder being made with a 30-min. schedule. In order to examine how closely the results of the experiments agree with the simple theory based on Martyn's theorem, we show, in column 5, the differences between the observed skip frequencies and those calculated after correction for time and latitude. In column 6 these differences are expressed as percentages of the observed frequency. The mean percentage difference is found to be 0·47, with a probable error of ±0·13. The mean frequency for normal-incidence penetration is 6·86 Mc./sec., and the mean skip frequency for oblique transmission is 7·17 Mc./sec.

Table 2

Date, 1937	G.m.t.	Oblique-incidence skip frequency (Mc./sec.)		$f_{\text{cal.}} - f_{\text{obs.}}$ (Mc./sec.)	$\frac{f_{\text{cal.}} - f_{\text{obs.}}}{f_{\text{obs.}}}$ %
		Observed	Calculated		
19 May	2245	7·82	7·81	−0·01	−0·13
,,	2315	7·70	7·71	0·01	0·13
,,	2344	7·63	7·65	0·02	0·26
20 May	0014	7·68	7·62	−0·06	−0·78
,,	0112	7·43	7·44	0·01	0·13
27 May	0940	8·73	8·85	0·12	1·40
28 May	1351	7·93	7·97	0·04	0·50
,,	1420	7·70	7·64	−0·06	−0·78
3 June	1425	7·55	7·42	−0·13	−1·72
10 June	2345	7·58	7·62	0·04	0·53
11 June	0055	7·30	7·43	0·13	1·78
28 Aug.	2242	6·88	6·87	−0·01	−0·14
,,	2253	6·63	6·66	0·03	0·45
,,	2310	6·47	6·53	0·06	0·93
,,	2326	6·30	6·43	0·13	2·07
,,	2341	6·23	6·25	0·02	0·32
,,	2357	6·16	6·16	0·00	0·00
29 Aug.	2227	6·90	6·99	0·09	1·30
,,	2242	6·73	6·81	0·08	1·20
,,	2257	6·58	6·68	0·10	1·52
,,	2312	6·51	6·57	0·06	0·92

We conclude from these results that there is very close agreement between the observed skip frequencies and those calculated by means of the theory for the ordinary wave, and we may express the precise relationship by stating that for a wave-frequency of about 7 Mc./sec. the oblique limiting frequency falls short of that calculated from the normal-incidence *P′f* curve by 0·47 ± 0·13 per cent. This value applies, of course, only to the particular ground distance and direction relative to the magnetic field of the experiments.

The extraordinary wave has not been studied so carefully. On twenty-two occasions, however, the frequency-difference between the skips of the ordinary and extraordinary waves at oblique incidence has been measured, and the average value obtained was 0·62 ± 0·013 Mc./sec. for a wave-frequency of about 7 Mc./sec. This value is very nearly the same as that observed at vertical incidence.

It will be noted that in figure 5 the separation between the ordinary and extraordinary curves at oblique incidence is less than this amount, whereas in the normal-incidence curves it is greater. This must be attributed to the slow technique used in those measurements.

§5. ACKNOWLEDGEMENTS

We are deeply indebted to Mr Ratcliffe for his help throughout the course of this work.

We wish also to thank the Royal Society for the loan of a pulse transmitter, and Professors Barkla and Crew for providing generous accommodation in Edinburgh University.

The work has been made possible by grants from the Department of Scientific and Industrial Research, and from the Moray Fund in the University of Edinburgh, for which we are very grateful.

Note added in proof

Since this paper was communicated, Millington has published an extension of Martyn's equivalence theorem to the case of a curved earth. The correction for curvature we have applied above is easily seen to be in agreement with his analysis for the short distance of transmission used in these experiments.

REFERENCES

(1) Martyn. *Proc. Phys. Soc.* **47**, 332 (1935).
(2) Lorentz. *Theory of Electrons*, p. 137.
(3) Farmer and Ratcliffe. *Proc. Phys. Soc.* **48**, 839 (1936).
(4) Smith. *Bur. Stand. J. Res.* **19**, 1013 (1937).
(5) Breit and Tuve. *Phys. Rev.* **28**, 554 (1926).
(6) Falloon and Farmer. *Proc. Phys. Soc.* **48**, 865 (1936).

ELECTRON-DIFFRACTION BY THE SPLIT-SHUTTER METHOD AND A NEW (BACK-REFLECTION) METHOD

By R. JACKSON and A. G. QUARRELL
Department of Applied Science, University of Sheffield

Received 29 *March* 1938. *Read in title* 24 *June* 1938

ABSTRACT. The necessity for using the grazing-incidence method when electron-diffraction is applied to the study of surface structure is emphasized, and precautions to be taken in order to obtain the maximum information from the patterns are discussed. A satisfactory method for obtaining comparison reflection patterns by the split-shutter method is described, and details of a light-tight split-shutter plate-holder are given.

In view of the limitations of the grazing-incidence method the possibility of the back-reflection of electrons is considered, and experiments are described in which high-speed electrons diffracted through angles approaching 180° are recorded photographically, the incident beam being normal to the surface of the specimen. The results obtained do not enable definite conclusions to be drawn concerning the two-dimensional or three-dimensional nature of the mechanism of diffraction involved, but development of the technique should result in a useful method applicable to those specimens which cannot at present be directly examined by electron-diffraction.

§ 1. INTRODUCTION

In the application of electron-diffraction to the study of surface structure, the reflection or grazing-incidence method must be used, because in most cases the removal of the surface layers as a thin film suitable for use as a transmission specimen cannot be justified in view of the possibility that structural changes may be brought about during the stripping process. Thus, the stripping agent may affect the film chemically, or the breaking of the bonds between the surface layers and the matrix may cause atomic rearrangement to take place. In general it will not be possible to determine whether such change has occurred or not.

Unfortunately the reflection method is subject to certain limitations. With polycrystalline reflection specimens, a characteristic pattern will result only if there are, projecting above the general surface, crystallites sufficiently thin to transmit electrons. This condition is usually fulfilled by surfaces which have undergone mild chemical action, but severe treatment may cause the surface to become too rough to be examined at grazing incidence.

In transmission the distance from the diffracting crystal to the photographic plate is the same for all crystals, but in the grazing-incidence method there may be a variation in this length equal to the diameter of the specimen. Thus, for a given diffraction, the radius R is given by

$$R=\lambda L/d,$$

Figure 2. Fe_3O_4.

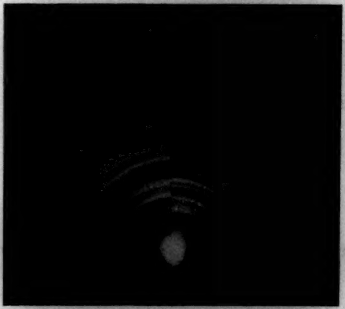

Figure 4. Split-shutter reflection pattern: PbS and $\alpha-Fe_2O_3$.

Figure 6. Back-reflection pattern from quartz single crystal.

where d is the lattice spacing, λ the electronic wave-length and L the distance from crystal to plate. Whilst d and λ are constants, L varies over a range, with a resultant line-broadening which under certain conditions may be considerable. With a camera length of 50 cm. and specimen-diameter of 3 cm. the ring-broadening due to this effect is 0·075 cm. on a ring of normal radius 1·25 cm., whilst if the specimen-size is reduced to 1 cm. the broadening is only 0·025 cm. It is for this reason that the diffractions obtained by reflection are always broader than those obtained by transmission from a comparable specimen. The narrower the rings the more accurately can their radii be determined, and therefore it is advisable to employ small specimens and as long a camera as may be convenient.

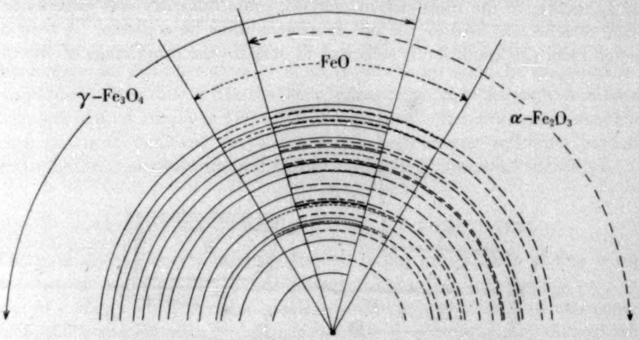

Figure 1. The relative radii of iron-oxide diffractions.

Owing to the short electronic wave-lengths employed, a large number of diffractions are recorded upon a comparatively small photographic plate, and this results in a tendency for the outermost rings to merge together. For a given structure the separation of adjacent rings is greatest for small angles of diffraction, owing to the larger differences in the corresponding lattice spacings; hence these inner rings are the most useful in deciding the structure of the specimen. This may be illustrated by reference to the oxides of iron, figure 1. In the case of Fe_3O_4 and $\alpha-Fe_2O_3$ the diffractions almost coincide, with the exception of the first two or three rings, and unless a satisfactory technique is adopted these inner rings may be cut off by the shadow-edge, or masked by the incoherent scattering around the central spot. Thus, in obtaining the pattern, figure 2, due to Fe_3O_4, the well defined-monochromatic incident beam made possible by focusing was employed. By maintaining a high vacuum in the diffraction chamber, the background, and particularly that in the immediate neighbourhood of the central spot, was almost eliminated, whilst ring-broadening was reduced to a minimum by the combination of small specimen-size with large camera-length. These conditions, combined with low angle of incidence, enable the innermost rings to be clearly seen.

§2. THE SPLIT-SHUTTER METHOD

It has frequently been observed that determinations of lattice spacings made by electron-diffraction are subject to an error of the order of two per cent owing to the difficulty of determining high potentials with accuracy. Further, the important inner rings are liable to a maximum error in measurement because of the smallness of their radii, and for these reasons we have applied the split-shutter method(1) to reflection specimens. This method consists essentially of a comparison of two patterns, obtained under identical conditions, and afforded by the specimen and a standard reference material respectively. Whilst the split-shutter technique was easily applicable to the transmission method, some difficulty was experienced in the case of reflection because the two specimens must be coplanar. A very slight deviation from this condition is sufficient to obscure the inner rings of one of the patterns. Furthermore, the construction of earlier split-shutter plate-holders was such that the diffraction camera had to be used in a dark room. In our work on the oxidation of iron we have found it essential to attain the greater accuracy given by the split-shutter method, but it was necessary for the plate-holder to be light-tight. Accordingly, the plate-holder shown in figure 3 was designed. Features of the design are (i) robust construction, (ii) accurate fitting due to the fact that, once assembled, all joints can be reground without dismantling of the shutters, and (iii) evacuation of the plate-chamber, bearings, and all gas-pockets by ample ducts. The half-shutters *A* and *B* are independently operated through plane ground joints, semi-universal joints being incorporated in the head *C* and the bearing *D*. The aluminium shutter *E* was backed by the fluorescent screen and was operated by means of a third head and bevel gears. The main object of this shutter was to ensure the light-tightness of the gap between the two half-shutters *A* and *B*, but the accuracy of fit made possible by the design was such that this third shutter was hardly necessary.

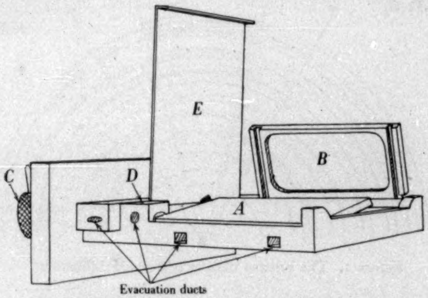

Figure 3. Light-tight split-shutter plate-holder.

§ 3. THE REFERENCE MATERIAL

In split-shutter work the main requirements of the standard reference material are that it shall (i) have a simple, known structure, (ii) be easily and quickly prepared, and (iii) give a reproducible pattern of continuous sharp rings, i.e. consist of a random distribution of fairly large crystals. In addition, for reflection work it is desirable that there shall be a number of rings of small radius to give maximum accuracy for the important diffractions, and furthermore that the reference specimen shall be easily made coplanar with the specimen under examination.

The substance which we have found to fulfil these conditions is lead sulphide, freshly precipitated from lead-nitrate solution, thoroughly washed and made up into a paste with water. The paste is applied, in the form of a thin film, to one-half of the reflection specimen by means of a camel-hair brush. By rotation of the specimen about an axis normal to its plane, either the surface to be examined or the lead sulphide can be brought into the beam without change in the angle of incidence. By this method an accuracy of one-tenth of 1 per cent in the determination of lattice spacings has been achieved. A characteristic split-shutter reflection pattern is shown in figure 4, in which rhombohedral $\alpha-Fe_2O_3$ is compared with PbS.

§ 4. THE BACK-REFLECTION OF ELECTRONS

The grazing-incidence method is limited to the examination of fine wires or surfaces which are virtually plane. This precludes the investigation of a large number of surfaces which occur in practice, since violent chemical attack frequently results in the formation of irregular surfaces made up of large crystals through which the electron beam cannot penetrate. Further, just as X rays cannot be used for the determination of true surface structure because the diffractions caused by the surface layers will be swamped by those due to the underlying material, so the grazing-incidence method of electron-diffraction cannot be used for the examination of isolated areas on the specimen, as for example, corrosion spots, because the electron beam traverses a strip of the specimen and all crystals within this strip contribute to the diffraction pattern. The most obvious way of overcoming these limitations is to use normal instead of grazing incidence of the electron beam.

It is now well known that electron-diffraction from polycrystalline specimens, giving rise to well-defined rings comparatively free from background, is two-dimensional in nature. In effect the Laue condition for diffraction by the line grating parallel to the beam is almost completely relaxed, and the Laue conditions corresponding to two line gratings normal to the beam determine the diffractions which occur. A single line grating normal to the beam gives rise to cones of diffracted rays about the line grating as axis. If we consider two such line gratings defining a two-dimensional lattice, then diffractions due to the two gratings occur in the directions of intersection of the cones. Normally we record those diffractions which occur in the forward direction, yet it is clear that any two such intersecting cones will in general intersect along two directions making angles of ϕ and $(180^\circ-\phi)$

with the incident beam. Furthermore, the indices defining the diffraction occurring at (180° – ϕ) will be the same as those defining the diffraction at ϕ. Provided the intensity of this back-reflection is sufficiently great and is not masked by any other effect, it should be possible to record by means of it patterns having essentially the same characteristics as those obtained by transmission in the forward direction.

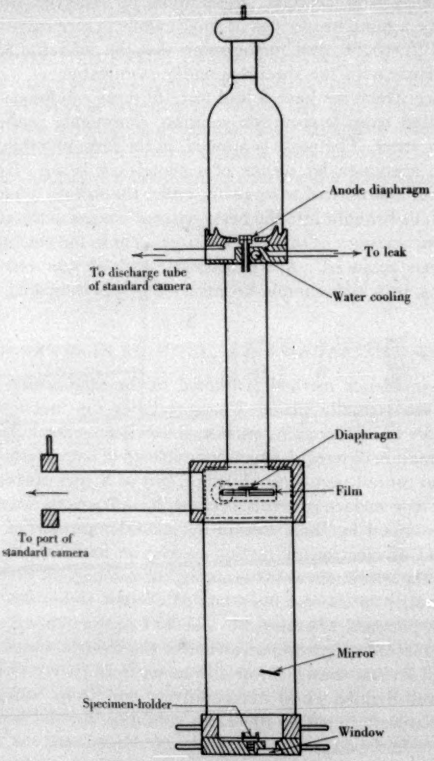
Anode diaphragm
To leak
To discharge tube of standard camera
Water cooling
Diaphragm
Film
To port of standard camera
Mirror
Specimen-holder
Window

Figure 5. Back-reflection camera.

With a view to investigating the back-reflection of electrons we have constructed the simple camera shown in figure 5. The essential difference between this and the standard camera is that the relative positions of the specimen and plate-holder are reversed, and therefore provision must be made for the electrons to pass through a hole punched in the photographic film. Owing to the complications which would be introduced by the diffracted electrons returning within the influence of the magnetic field, focusing was not employed, but the incident beam was limited by two small diaphragms 25 cm. apart. The alignment of discharge tube, diaphragms and specimen was carried out by replacing the specimen by a small fluorescent screen which could be viewed by means of a periscope. Because of the considerable distance of separation of the two diaphragms, maximum intensity of the beam could only be achieved by placing a small bar magnet just below anode-block level to deflect the beam through the lower diaphragm. This served the additional purpose of ensuring that the beam should be appreciably monochromatic.

With exposures of $\frac{1}{2}$ hr. to 1 hr. at 50 to 60 kv. and a camera-length of 30 cm., specimens of (i) a fairly thick layer of polished Aquadag colloidal graphite, (ii) gold foil, and (iii) Armco iron rubbed on no. 00 emery paper, all failed to yield a diffraction pattern, although blackening of the photographic film was observed. Experiments in which one-half of the film was covered with thin black paper proved conclusively that this blackening was not due to X rays. Moreover, when the film was reversed, the celluloid base acted as a shield, completely preventing blackening of the emulsion, which could not, therefore, be attributed to light emitted by the specimen under the action of electrons. It having thus been shown that electrons scattered through angles approaching 180° could be detected photographically, further specimens were examined. On the two-dimensional theory all the specimens so far discussed should have yielded ring patterns, and it is possible that the spreading of the diffracted electrons over such a comparatively large area would result in the intensity being too small for detection in view of the relatively intense background.

An Armco iron specimen, so deeply etched that it would not give a diffraction pattern by the grazing-incidence method, afforded an irregular pattern of from 20 to 30 spots of weak intensity. Further, with the electron beam at normal incidence on a natural (112) face of a rather imperfect quartz crystal, the spot pattern shown in figure 6 was obtained, the exposure being 1 hr. at 45 kv.

These spot patterns cannot be satisfactorily analysed because of the uncertainty which exists as to the exact centre of the pattern, falling as it does somewhere within the hole punched in the film, and therefore it would be imprudent to advance any definite theory as to the mechanism of diffraction involved. The fact that patterns are not always obtained would suggest that the diffraction is three-dimensional, but it would in that case be difficult to explain why five well-defined spots were given by a quartz single crystal with a monochromatic electron beam. Further, as has been mentioned above, the failure to obtain ring patterns from specimens known to consist of random distributions of crystals may well be due to the reduction in intensity caused by the spreading of the diffracted electrons over a relatively large area, and this view is supported by the fact that, whilst the five spots from a quartz single crystal were fairly intense, the more numerous spots yielded by a microcrystalline Armco specimen were very much weaker. It is possible that the Laue condition for the row of atoms parallel to the incident beam is neither completely relaxed nor fully operative, in which case the patterns would have some of the characteristics of both two-dimensional and three-dimensional diffraction.

Whatever the true explanation of these patterns may be, we feel that development of the technique will result in a useful method of investigation, applicable to those specimens which cannot at present be directly examined by electron-diffraction.

REFERENCE

(1) Finch and Quarrell. *Proc. Phys. Soc.* **46**, 148 (1934).

AN INVESTIGATION OF COSMIC-RAY SHOWERS PRODUCED UNDER THIRTY METRES OF CLAY

By J. D. CRAWSHAW, M.Sc.

Communicated by Prof. P. M. S. Blackett, 6 May 1938. Read in title 24 June 1938

ABSTRACT. The vertical intensity of the cosmic radiation and of the cosmic-ray shower-intensity have been measured at ground level and at a station 30 m. below the surface, and the ratio of these two quantities has been shown to be nearly the same at the two levels. A transition curve in lead has been obtained at the Underground station and its shape differs widely from the typical curve obtained at sea level. After a sharp initial rise, the shower-rate remains stationary for thickness of lead up to 8·8 cm., in contrast to the rapid decrease which occurs after the maximum at sea level. The curves obtained underground are shown to be very similar to those obtained by Drigo at sea level under about 2 m. of masonry.

§ 1. INTRODUCTION

THE work described by Follett and Crawshaw⁽¹⁾ on the comparison of both the vertical intensity and the shower intensity of cosmic radiation at ground level and under 30 m. of clay has been continued. The experiments were carried out in the Underground station at Holborn.

In the earlier work, the ratio of the vertical intensity to the maximum shower-rate was shown to be approximately equal at the two levels. The object of the present experiment was to confirm this interesting and rather unexpected result and to obtain a reliable transition curve for showers from lead at the lower level.

§ 2. EXPERIMENTAL ARRANGEMENT

The vertical intensity and the shower-rates were observed by means of the coincident discharges of five Geiger-Müller counters. With five counters the casual-coincidence rate is so small that a correction for it may be omitted.

The counters were 30 cm. long and 1·6 cm. in internal diameter, and were filled at a pressure of 20 cm. of mercury with a mixture of three parts of argon to one part of air. The anode of each counter was a tungsten wire, and the cathode consisted of a cylinder of oxidized copper foil, the whole being sealed into a glass container. The potential applied to each counter was 50 v. above its starting potential. The recording apparatus used is shown in figure 1 and is similar in design to that described by Barasch⁽²⁾.

For successful quintuple recording, the smallest output pulse resulting from discharges in all five counters must be greater than the largest pulse resulting from discharges in all but one of the counters. A quintuple coincidence was recorded when a 6-v. impulse was applied simultaneously to each of the five grids. No false quintuple was observed when a 120-v. impulse was applied simultaneously to any four of the five grids; from this result, it was assumed that a movement of the telephone counter corresponded to a coincident discharge of the five counters. The leads from the anodes of the counters to the grids of the valves were made as short as possible and were screened so as to prevent any mutual-induction effects. Each pentode was enclosed in a screening box.

The apparatus was set up in a laboratory with a thin roof at ground level, five counters being used one above another, and measurements were made of the vertical intensity of the cosmic rays. The axes of these counters were horizontal and the plane containing the axes was vertical.

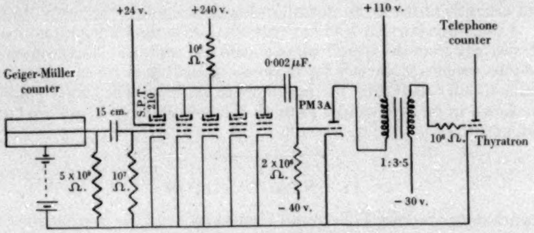

Figure 1. Coincidence recording circuit.

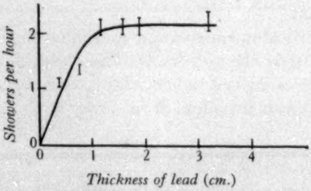

Figure 2. Transition curve for sheet *A*. I, probable error of the determination.

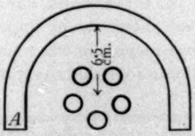

Figure 2A. Arrangement of counters.

For the shower-rate determination, the counters were arranged as shown in figure 2A; their axes were horizontal and formed the apices of a regular pentagon. Such an arrangement requires at least three ionizing particles to discharge it, and thus the showers observed consist of at least three such rays. Observations were made with and without lead over the counters. The lead sheets shown in figure 2A were bent into a nearly semicircular shape and had a thickness of 1·6 cm., since this value gives the maximum shower-rate at ground level.

The apparatus was then taken down to a disused platform in Holborn tube station and was housed in a galvanized iron shed. The platform is about 30 m. below ground level, and above it are strata of different kinds of clay whose mean specific gravity is about 2, giving a total thickness of absorber equivalent to about 60 m. of water. Measurements of the vertical intensity and the transition curves for lead were obtained. As a check on the apparatus, a redetermination of the vertical intensity at ground level agreed with the former value.

§ 3. EXPERIMENTAL RESULTS

Table 1. Vertical intensity

	Total count	Time	Rate per hour
Ground level	1189	4 h. 30 m.	264 ± 5·2
Underground level	454	32 h. 55 m.	13·8 ± 0·45
Ratio of intensities 19·1 ± 0·7			

Table 2. Shower-rates with a hemicylinder of lead, 1·6 cm. thick above the counters. Figure 2

	Total count	Time	Rate per hour
Ground level	331	7 h. 40 m.	43·2 ± 1·6
Underground level	107	49 h. 40 m.	2·15 ± 0·14
Ratio of shower-rates 20·0 ± 1·5			

For the measurement of vertical intensity the counters were equally spaced, the axes of the two outer counters being 12·5 cm. apart. In the pentagonal formation the axes of the counters were 2·7 cm. apart. The shower-rate for the thickness of lead here used decreases with increasing depth below the surface at about the same rate as the primary radiation, in agreement with the former results of Follett and Crawshaw (1).

With the arrangement shown in figure 2A the transition curve up to 3 cm. of lead was measured underground, figure 2. The shape differs markedly from that of the usual air-lead curve at sea level; see, for instance, curve *A* of figure 4, which shows some results obtained by Drigo (4). The shower-rate underground rises with increasing thicknesses of lead up to 1·2 cm. and then remains stationary, while at sea level there is a marked maximum at about 1·6 cm.

To extend the transition curve to greater thicknesses of lead a special frame was constructed to carry the lead sheets, which were bent into circular arcs subtending an angle of 108° at the axis of the bottom counter; this second disposition of lead is represented by *B* in figure 3A. A transition curve, figure 3, was then obtained for thicknesses of lead up to 8·8 cm. The shower-rate is less than with the semicircular sheets, but the commencement of the stationary value occurs at about the same thickness of lead. There is no rapid decrease of shower-rate with increasing thickness of lead up to 8·8 cm.

It is seen that the reduction of the area of lead sheet leads to about a proportional reduction of the shower-intensity. For the case of the hemicylindrical lead sheets, the maximum rate is about 2·15 per hour, whereas in the case of the sheets subtending an angle of 108° with the axis of the bottom counter the maximum rate is about 1·40 per hour. The zenith-angle distribution of the cosmic-ray intensity has already been determined by Follett and Crawshaw⁽¹⁾ at this depth below ground level, and the intensity at angles from the zenith greater than 54° is much too small to explain the observed decrease of intensity unless the harder horizontal rays are more active in producing showers than the softer vertical radiation. The probable explanation is that the showers are so diffuse and contain so many scattered particles that the chance that one will be recorded is almost independent of whether the lead absorber, in which it is produced, is at the side or over the top of the counters. In addition, the average size of a shower probably increases with the area of the lead absorber. This must happen if, as is probable, many of the incident rays coming from the roof of the tunnel are already associated in showers.

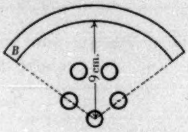

Fig. 3A. Arrangement of counters

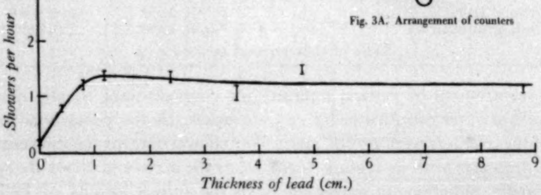

Figure 3. Transition curve for sheet *B*. I, probable error of the determination.

Experiments have been made with lead sheets placed under the counters, but within the limits of experimental error the effect of such sheets is negligible; this shows that no appreciable number of shower particles are projected upwards.

Auger and Rosenberg⁽³⁾ have obtained similar transition curves at depths of 30 and 75 m. water equivalent, but they found that the stationary value of the shower-rate was reached with a considerably smaller thickness of lead than in our experiments in the Underground station. Moreover, they noticed that this thickness decreased with increasing depths below the surface. Perhaps the difference may be due to the difference in the arrangement of counters.

§ 4. DISCUSSION OF RESULTS

Drigo⁽⁴⁾ has obtained transition curves at ground level with increasing thicknesses of light-absorbing material above the lead and counters, figure 4. The remarkable features of his results are that the greater the thickness of absorbing material, the less pronounced is the maximum of the curve, and that the curve *C* obtained with a thickness of light-absorbing material equivalent to 2·7 m. of water is similar to that found at the Underground station, where there is a thickness of 30 m. of clay above the apparatus.

This type of curve thus appears to be characteristic of a transition to lead from a compact mass of material composed of elements of low atomic number. Its shape seems independent of the thickness of material above the lead and counters, provided that this thickness is greater than that equivalent to about 2 m. of water.

On account of the difference between the curves of the transition from air to lead and from masonry to lead, care has to be exercised in comparing the ratio of the shower rates at ground level and at a position 30 m. below this level. In the above experiments, the ratio of the shower-rate to the vertical intensity has been shown to be the same at the two levels, but from a consideration of the curves in figure 4 the shower-rate at sea level, for a thickness of 1·6 cm. of lead, is several times greater for an air-lead transition than for a masonry-lead transition. Thus the ratio of shower-rate to vertical intensity must be actually greater underground than under a few metres of masonry at sea level. This is a rather surprising result, and suggests that either the size or the number of showers produced by the penetrating component must increase as the radiation becomes more penetrating, and so probably more energetic, as a result of filtration.

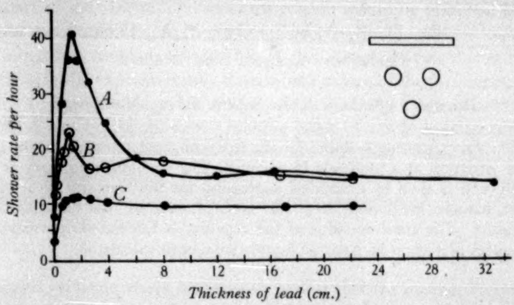

Figure 4. Curves plotted from results of A. Drigo (1935). *A*, filtered by 20 g./cm.^{2} of light material; *B*, filtered by 20 g./cm.^{2} of light material and 88 g./cm.^{2} of lead; *C*, filtered by 270 g./cm.^{2} of light material.

§ 5. ACKNOWLEDGEMENT

The author wishes to thank Prof. Blackett for suggesting this experiment and for his guidance and assistance during its progress. He wishes also to thank Dr H. J. J. Braddick and Dr S. W. Watson for their suggestions and assistance; the London Passenger Transport Board for permission to use the Holborn tube station; and lastly the staff at the station for assistance in many ways.

REFERENCES

(1) Follett and Crawshaw. *Proc. Roy. Soc.* A, **155**, 546 (1936).
(2) Barasch. *Proc. Phys. Soc.* A, **47**, 824 (1935).
(3) Auger and Rosenberg. *C.R. Acad. Sci., Paris*, **202**, 1923 (1936).
Auger and Meyer. *C.R. Acad. Sci., Paris*, **204**, 572 (1937).
(4) Drigo. *Ric. Sci.* **1**, 529 (1935).

THE FREQUENCY OF VIBRATION OF MOLECULES IN LIQUIDS AND ITS RELATION TO VISCOSITY

By D. B. MACLEOD, M.A., D.Sc.
Canterbury College, New Zealand

Received 12 *January* 1938. *Read in title* 25 *March* 1938

ABSTRACT. An expression is found for the variation, with temperature, of the average frequency of vibration of a molecule in a liquid. The absolute frequency is calculated approximately and is used in Andrade's expression for the viscosity of a liquid at the melting point, namely, $\eta = \frac{4}{3} . \nu m/\sigma$, to obtain an expression for the variation of viscosity with temperature. The absolute value of the viscosity is calculated approximately. The internal pressures of several monatomic liquids have been calculated.

---

§1. INTRODUCTION

ANDRADE(1) has developed an expression for the viscosity of a liquid at the melting point, namely

$$\eta = \frac{4}{3} \frac{\nu m}{\sigma} \qquad \text{......(1).}$$

In this expression *m* is the molecular weight of the substance, σ the mean distance between the centres of the molecules and ν the average frequency of vibration of the molecules. The value of the frequency calculated in this way has been shown, for monatomic substances, to be practically identical with that calculated from Lindemann's well-known expression

$$\nu = 2{\cdot}8 \times 10^{12} \sqrt{\frac{T_s}{MV^{\frac{2}{3}}}} \qquad \text{......(2).}$$

Andrade has applied the expression in the above form to the melting point only. In order to account for the variation of viscosity with temperature he assumes that, for the transference of momentum, the molecules must possess a certain mutual potential energy. The number of molecules possessing this energy will be governed by the Boltzmann distribution formula. From this he arrives at the expression

$$\eta v^{\frac{1}{3}} = A e^{c/Tv} \qquad \text{......(3)}$$

for the variation of viscosity with temperature. In arriving at the latter expression he assumes that the average frequency of vibration is independent of temperature. This assumption was made partly because of the difficulty of finding a satisfactory expression for the change of frequency with temperature, and partly because the assumption of a constant frequency gave a more exact representation of the observed values.

Lindemann's expression for the frequency of vibration of an atom at the melting point is based on the assumption that at the melting point the amplitude of vibration of the atoms is approximately equal to their mean distance apart. There is no necessary justification for assuming that the amplitude is actually equal to the distance apart of the atoms. The same expression would be obtained by assuming it to bear a constant ratio, for various substances, to the atomic diameter. The arbitrary numerical constant would thereby be altered, but as this is obtained by comparison with the experimentally determined values of the frequency the general applicability of the formula would not be affected. It is obvious that if the expression is applied to a liquid above the melting point, it would indicate an increase of frequency with rise of temperature, because $\sqrt{T}$ increases much more rapidly than $V^{\frac{1}{3}}$. Such an increase would, of course, preclude the application of equation (1) to liquids above the melting point without further assumptions.

§2. THE CHANGE OF FREQUENCY WITH TEMPERATURE

On general grounds, there is reason to expect that the average frequency of the atoms of a liquid would decrease with rise of temperature. In a solid the frequency is of the order of 10^{12} per sec., whereas in a gas under ordinary conditions the collision frequency is of the order of 10^{9} per sec. Regarding a liquid as an intermediate state between a solid and a gas, we should expect a gradual lowering of the average frequency with rise of temperature.

It is proposed to assume that the movement of a liquid molecule is essentially that of a small sphere vibrating in an envelope slightly larger than itself. Taking the simplest possible analogy of a piston moving in a cylinder, in which the radius of the piston is r, the unoccupied length of the cylinder h and the velocity of the piston c, the frequency for a complete oscillation is given by

$$\nu = \frac{\pi r^2 c}{2\pi r^2 h} \text{ or } \frac{c}{2h} \qquad \text{......(4).}$$

In like manner, the time for a complete oscillation of a liquid molecule can be considered to be the time required by the molecule to sweep out a volume equal to twice the unoccupied volume of its envelope. If V_0 is the specific volume of a liquid at a low temperature, we can consider that the area of a molecule is proportional to $(MV_0/N)^{\frac{2}{3}}$, where M is the molecular weight, N is Avogadro's number, and V_0 is considered to be constant. If at some higher temperature the specific volume is v, then we can consider that the unoccupied portion will be $(v - V_0)$, or the ratio of the unoccupied portion to the occupied portion will be $(v - V_0)/V_0$. The volume of a single molecule can be taken as proportional to MV_0/N, so that the unoccupied volume associated with a single molecule will be

$$\frac{MV_0}{N} \times \frac{v - V_0}{V_0}.$$

Let c be the average velocity of a molecule at the temperature considered. On the above analogy we can expect the frequency to be some simple function of

$$\frac{(MV_0/N)^{\frac{2}{3}}\,c}{2\,(MV_0/N)\,(v-V_0)/V_0},$$

or we can write

$$\nu=\frac{Kc}{2\,(MV_0/N)^{\frac{1}{3}}\,(v-V_0)/V_0} \qquad \text{......(5)}.$$

K should be a small numerical quantity differing from unity because the assumptions are only approximate. V_0 will be considered to be the specific volume at the lowest temperature in the range of temperature over which the measurements are applicable.

The velocity c of a molecule is proportional to $\sqrt{T/M}$, where T is the absolute temperature and M is the molecular weight. We can write, therefore,

$$\nu=\frac{K'}{2\,(MV_0/N)^{\frac{1}{3}}\,(v-V_0)/V_0}\sqrt{\frac{T}{M}} \qquad \text{......(6)}.$$

If now we consider a liquid at its melting point and assume that at the melting point the free space bears a constant ratio to the volume of the molecule for various substances, which is a more generalized form of Lindemann's assumption, the above expression gives for the frequency at the melting point

$$\nu_s \propto \sqrt{\frac{T_s}{M}}\cdot\frac{1}{(MV_0/N)^{\frac{1}{3}}} \qquad \text{......(7)},$$

which is identical with Lindemann's expression. At higher temperatures the frequency will decrease so that at a temperature t the frequency is given by

$$\nu_t=\nu_s\,\frac{v_s-V_0}{v_t-V_0}\sqrt{\frac{T}{T_s}}. \qquad \text{......(8)}$$

v_t-V_0 increases more rapidly than $\sqrt{T}$.

§3. THE VISCOSITY OF A LIQUID

If now we insert the above expression for the frequency into Andrade's expression, equation (1), for the viscosity of liquid at the melting point, we obtain

$$\eta=\frac{4}{3}\,\frac{K'}{(MV_0/N)^{\frac{1}{3}}\,(v-V_0)/V_0}\sqrt{\frac{T}{M}}\cdot\frac{M}{\sigma} \qquad \text{......(9)}.$$

Regarding V_0 as a constant and writing σ as proportional to $v^{\frac{1}{3}}$, we could derive the expression for the variation of viscosity of a liquid with temperature, in which M is constant, as

$$\frac{\eta v^{\frac{1}{3}}}{\sqrt{T}}=\frac{B}{v-V_0}, \text{ where } B \text{ is a constant} \qquad \text{......(10)}.$$

The calculation of the free space from this equation should enable us to obtain approximately the absolute value of the frequency and the absolute value of the viscosity.

In the following tables, the equation

$$\frac{\eta v^{\frac{1}{3}}}{\sqrt{T}}=\frac{B}{v-V_0} \qquad \text{......(11)},$$

which involves two unknowns, B and V_0, is applied to monatomic substances. A comparison is shown of the differences between the calculated and observed values obtained by its use and those from the use of Andrade's expression, equation (3).

Unfortunately the range of experimental data in this class of substance is still very meagre, and the technical difficulties in connexion with the measurement of the viscosity at the relevant temperatures makes it almost impossible to reach the accuracy obtainable with organic substances at ordinary temperatures.

Table 1. Gallium. Spells(2)

Temp. °K.	$\eta_{\text{obs.}}$	Volume cm³	$\frac{\eta v^{\frac{1}{3}}}{\sqrt{T}}$	$\frac{B}{v-V_0}$ (cal.)	Difference between calculated and observed values (per cent)	
					Equation (11)	Equation (3)
303	0·02027	0·9917	$0{\cdot}0_21167$	$0{\cdot}0_31242$	+7·0	—
325·9	0·01894	0·9944	$0{\cdot}0_21042$	$0{\cdot}0_31063$	+2·1	+3·9
373·0	0·01609	1·0000	$0{\cdot}0_38331$	$0{\cdot}0_3833$	0·0	+0·6
422·0	0·01406	1·0060	$0{\cdot}0_36864$	$0{\cdot}0_3673$	−2·0	−1·7
473·0	0·01258	1·0120	$0{\cdot}0_35808$	$0{\cdot}0_3563$	−3·0	−3·4
574·0	0·01029	1·0230	$0{\cdot}0_34333$	$0{\cdot}0_3435$	+0·5	−2·2
675·0	0·00882	1·0345	$0{\cdot}0_33433$	$0{\cdot}0_3351$	+2·3	−0·1
773·0	0·008127	1·0453	$0{\cdot}0_32967$	$0{\cdot}0_3297$	+0·1	−1·6
873·0	0·007637	1·0560	$0{\cdot}0_32632$	$0{\cdot}0_3258$	−2·0	−3·0
1079·0	0·006524	1·0778	$0{\cdot}0_32035$	$0{\cdot}0_32035$	0·0	+1·3
1283·0	0·005915	1·0998	$0{\cdot}0_31705$	$0{\cdot}0_31675$	−1·9	+3·3
1373·0	0·00578	1·1097	$0{\cdot}0_31615$	$0{\cdot}0_31553$	−3·2	+2·7

$(v-V_0)$ at 373° K. is 0·02515.

The differences with gallium over a range of temperature of 1000° are of the same order with the two expressions but are, if anything, more at random with equation (11).

$(v-V_0)$ at 303° K. calculated from first two readings is 0·0229.

Table 2. Potassium. Chiong(3)

Temp. °K.	$\eta_{\text{obs.}}$	Volume cm³	$\frac{\eta v^{\frac{1}{3}}}{\sqrt{T}}$	$\frac{B}{v-V_0}$ (cal.)	Difference between calculated and observed values (per cent)	
					Equation (11)	Equation (3)
337·2	0·005535	0·9894	$0{\cdot}0_32996$	$0{\cdot}0_32897$	−3·3	—
340·0	0·005256	0·9903	$0{\cdot}0_32842$	$0{\cdot}0_32841$	0·0	+0·3
340·9	0·005230	0·9906	$0{\cdot}0_32825$	$0{\cdot}0_32823$	0·0	+0·3
352·4	0·004930	0·9940	$0{\cdot}0_32630$	$0{\cdot}0_32631$	0·0	−0·3
372·5	0·004540	1·0000	$0{\cdot}0_32353$	$0{\cdot}0_32353$	0·0	0·0
392·6	0·004188	1·0060	$0{\cdot}0_32118$	$0{\cdot}0_32127$	+0·4	−0·4
428·5	0·003707	1·0167	$0{\cdot}0_31807$	$0{\cdot}0_31813$	+0·3	−0·6
448·5	0·003530	1·0227	$0{\cdot}0_31680$	$0{\cdot}0_31678$	−0·1	+0·4
480·7	0·003249	1·0323	$0{\cdot}0_31497$	$0{\cdot}0_31497$	0·0	+0·6
555·5	0·002750	1·0546	$0{\cdot}0_31196$	$0{\cdot}0_31196$	0·0	−0·2
625·5	0·002457	1·0756	$0{\cdot}0_31007$	$0{\cdot}0_31007$	0·0	0·0

The volume has been calculated from the expression given in the Landolt-Börnstein tables as follows:

$$V_t = V_{372\cdot 5}\ 1 + 0{\cdot}0_3 299\ (t - 372{\cdot}5). \quad v - V_0 \text{ at } 372{\cdot}5^\circ \text{ K. is } 0{\cdot}0565.$$

The agreement with the author's expression is strikingly good in the case of this substance.

$v - V_0$ at 337·2° K. calculated from values at 337·2° K. and 352·4° K. is 0·0330.

Table 3. Sodium. Chiong[(3)]

Temp. ° K.	$\eta_{\text{obs.}}$	Volume cm.³	$\dfrac{\eta v^{\frac{1}{3}}}{\sqrt{T}}$	$\dfrac{B}{v - V_0}$ (cal.)	Difference between calculated and observed values (per cent)	
					Equation (11)	Equation (3)
371·0	0·007264	0·9988	$0{\cdot}0_3 3772$	$0{\cdot}0_3 3697$	−2·1	—
372·6	0·007142	0·9994	$0{\cdot}0_3 3697$	$0{\cdot}0_3 3637$	−1·7	—
375·4	0·006856	1·0000	$0{\cdot}0_3 3539$	$0{\cdot}0_3 3580$	+1·1	—
393·4	0·006170	1·0051	$0{\cdot}0_3 3116$	$0{\cdot}0_3 3153$	+1·2	+0·3
428·4	0·005322	1·0146	$0{\cdot}0_3 2585$	$0{\cdot}0_3 2581$	−0·2	−0·3
432·1	0·005225	1·0158	$0{\cdot}0_3 2526$	$0{\cdot}0_3 2523$	−0·1	−0·1
446·7	0·004942	1·0198	$0{\cdot}0_3 2354$	$0{\cdot}0_3 2347$	−0·3	−0·2
456·4	0·004760	1·0225	$0{\cdot}0_3 2244$	$0{\cdot}0_3 2242$	−0·1	−0·2
479·7	0·004431	1·0290	$0{\cdot}0_3 2043$	$0{\cdot}0_3 2024$	−1·0	−0·7
491·0	0·004239	1·0321	$0{\cdot}0_3 1933$	$0{\cdot}0_3 1933$	0·0	0·0
562·0	0·003506	1·0519	$0{\cdot}0_3 1504$	$0{\cdot}0_3 1506$	+0·1	−0·3
628·0	0·003015	1·0703	$0{\cdot}0_3 1231$	$0{\cdot}0_3 1249$	+1·4	+0·7

$(v - V_0)$ at 375·4° K. is 0·0377.

The volume has been calculated from the expression given in the Landolt-Börnstein tables, namely

$$V_t = V_{375\cdot 4}\,[1 + 0{\cdot}0_3 278\ (t - 375{\cdot}4)].$$

$(v - V_0)$ at 371° K. calculated from values at 371·0° K. and 393·4° K. is 0·0290.

Table 4. Tin. Stott[(4)]

Temp. ° K.	$\eta_{\text{obs.}}$	Volume cm.³	$\dfrac{\eta v^{\frac{1}{3}}}{\sqrt{T}}$	$\dfrac{B}{v - V_0}$ (cal.)	Difference per cent
513	0·0191	1·0000	$0{\cdot}0_3 843$	$0{\cdot}0_3 843$	0·0
573	0·0167	1·0054	$0{\cdot}0_3 697$	$0{\cdot}0_3 690$	−1·0
673	0·0138	1·0144	$0{\cdot}0_3 535$	$0{\cdot}0_3 529$	−1·2
773	0·0118	1·0235	$0{\cdot}0_3 428$	$0{\cdot}0_3 428$	0·0
873	0·0105	1·0326	$0{\cdot}0_3 359$	$0{\cdot}0_3 359$	0·0
973	0·00945	1·0416	$0{\cdot}0_3 307$	$0{\cdot}0_3 310$	+1·0
1073	0·0087	1·0507	$0{\cdot}0_3 270$	$0{\cdot}0_3 272$	+0·8

The volume has been calculated from the expression

$$V_t = V_{513}\,[1 + 0{\cdot}0_4 905\ (t - 513)],$$

based on the results of Lewis[(5)].

$v - V_0$ at 513° K. is 0·0242.

Table 5. Bromine. Thorpe and Rodger[(6)]

Temp. ° K.	$\eta_{\text{obs.}}$	Volume cm³	$\dfrac{\eta v^{\frac{1}{3}}}{\sqrt{T}}$	$\dfrac{B}{v-V_0}$ (cal.)	Difference per cent
273	0·012575	1·0000	$0{\cdot}0_{3}7610$	$0{\cdot}0_{3}7590$	−0·3
283	0·01109	1·0108	$0{\cdot}0_{3}6613$	$0{\cdot}0_{3}6613$	0·0
293	0·009935	1·0219	$0{\cdot}0_{3}5845$	$0{\cdot}0_{3}5843$	−0·1
303	0·008985	1·0335	$0{\cdot}0_{3}5218$	$0{\cdot}0_{3}5207$	−0·2
313	0·00817	1·0454	$0{\cdot}0_{3}4685$	$0{\cdot}0_{3}4685$	0·0
323	0·00747	1·0576	$0{\cdot}0_{3}4235$	$0{\cdot}0_{3}4250$	+0·3

$(v-V_0)$ at 273° K. is 0·0733.

Table 6. Mercury

Temp. ° K.	$\eta_{\text{obs.}}$	Volume cm³	$\dfrac{\eta v^{\frac{1}{3}}}{\sqrt{T}}$	$\dfrac{B}{v-V_0}$ (cal.)	Difference per cent
253	0·0186	0·9963	$0{\cdot}0_{2}1171$	$0{\cdot}0_{3}1169$	−0·2
273	0·0170	1·0000	$0{\cdot}0_{2}1029$	$0{\cdot}0_{3}1029$	0·0
293	0·0157	1·0037	$0{\cdot}0_{3}919$	$0{\cdot}0_{3}919$	0·0
323	0·0141	1·0091	$0{\cdot}0_{3}787$	$0{\cdot}0_{3}795$	+1·0
373	0·0122	1·0183	$0{\cdot}0_{3}636$	$0{\cdot}0_{3}646$	+1·6
473	0·0102	1·0368	$0{\cdot}0_{3}475$	$0{\cdot}0_{3}470$	−1·0

$(v-V_0)$ at 273° K. is 0·0309.

These tables show that equation (11) follows the experimental values with an error not much greater than the probable experimental uncertainty.

§4. THE FREE SPACE AT THE MELTING POINT

On the basis of Lindemann's assumption, the free space at the melting point should bear, approximately, a constant ratio to the total volume for various substances. Of the substances given above, bromine will be shown to fit in more satisfactorily with the organic substances and will be discussed with them.

Table 7 tabulates the values of the free space calculated for the remaining elements and gives the values computed for the melting points.

Table 7

	Temp. ° C.	$v-V_0$	Melting point ° C.	(i) $v-V_0$ at melting point	(ii) $v-V_0$ at melting point
Mercury	0	0·0309	−39	0·0237	0·0237
Tin	240	0·0242	232	0·0232	0·0232
Gallium	100	0·0252	30	0·0170	0·0224
Sodium	103	0·0384	97	0·0366	0·0291
Potassium	100	0·0565	62	0·0446	0·0320

In the neighbourhood of the melting point, the viscosities of gallium, sodium and potassium show definite anomalies whether calculated by Andrade's equation (3) or by equation (11). The last column gives the free space for these substances calculated from the experimental values immediately above the melting point. While the values in column (i) can hardly be called approximately constant, those in column (ii) are much more so. The very high compressibilities of sodium and potassium in the solid form would suggest that in these elements the atoms themselves are compressible. If that is the case, some portion of their very large coefficients of expansion may be due to an actual increase in the volume of the atom as the substance expands. The expansion of the free space would, therefore, be less than that calculated from the ordinary coefficient of expansion. Such an anomaly would account for the higher value for these substances. In the method of approach of Lindemann and Andrade this difficulty would not appear. A more extended range of data is necessary to establish the constancy or otherwise of the free space at the melting point, calculated in this way. In the meantime the values can be said to be of the same order and, in the case of mercury, tin and gallium, approximately constant.

§5. CALCULATION OF THE ABSOLUTE FREQUENCY

It is now possible to attempt the calculation of the absolute frequency from equation (5).

The values for sodium at 103° C., which is not far from the melting point, are $(v-V_0)/V_0=0{\cdot}0384$, $M=23$, $N=6{\cdot}06\times 10^{23}$ and $\rho=0{\cdot}93$; $V_0=1/\rho$; c is obtained from the known kinetic energy of a molecule at 0° C., namely $5{\cdot}62\times 10^{-14}$ ergs, and the mass of the sodium atom, namely $23\times 1{\cdot}64\times 10^{-24}$ gram, by the formula

$$c=\sqrt{\frac{2\times 5{\cdot}62\times 10^{-14}\times 376}{23\times 1{\cdot}64\times 10^{-24}\times 273}}\ \text{cm./sec.}$$

Taking K as unity, this gives the absolute frequency of the sodium atom as $2{\cdot}42\times 10^{13}$. Andrade's value for sodium is $4{\cdot}6\times 10^{12}$. The value is, therefore, five times too great. This might be considered too great a numerical factor, even after allowance for the approximate nature of the initial assumptions. It will be shown that for the organic substances the numerical factor is much lower and that its large value in the case of the elementary substances is probably connected with their very small molecular volume.

§6. ORGANIC SUBSTANCES

There is little doubt that organic substances, with falling temperature, tend to undergo some sort of loose association of the molecules, varying according to the nature of the substance. Such an association would involve an alteration in the effective molecular weight. It might be expected, therefore, that the simple expression (11) would apply less satisfactorily to organic substances over any extended range of temperatures. It still remains, however, approximately true for those liquids which are ordinarily considered to be unassociated. A more exact agreement can, of course, be obtained by introducing an arbitrary coefficient and writing

$$\frac{\eta v^{\frac{1}{3}}}{\sqrt{T}}=\frac{B}{(v-V_0)^n} \qquad \text{......(12).}$$

The value of n for unassociated substances is very close to unity. This type of expression has been discussed by the author in earlier papers(7, 8, 9). The value of the free space, calculated over a small range of temperature from equation (11), is not very different from that obtained from the expression

$$\eta = \frac{B}{v - V_0} \qquad \text{......(13).}$$

It was shown by the author(9) that the specific volume of a liquid can be accurately represented by the expression

$$\pi_0 e^{c''/Tv} = \frac{RT}{v - V_0},$$

where $\pi_0 e^{c''/Tv}$ is considered to be the internal pressure of the liquid. It was also shown that if the molecular weight changed owing to any loose association of molecules, it would be expected to change so that

$$M = M_0 e^{c'/Tv}.$$

Substituting for $1/(v - V_0)$ the quantity $\pi_0 e^{c''/Tv}/RT$, and representing any change in the molecular weight as covered by the expression $M = M_0 e^{c'/Tv}$, we obtain the following possible expressions for the viscosity of a liquid, in which the molecular weight is not necessarily constant.

$$\frac{\eta v^{\frac{1}{3}}}{\sqrt{T}} = \frac{K_0 e^{c'/Tv}}{v - V_0} \qquad \text{......(14)}$$

$$= \frac{K_0 e^{c'/Tv}\, \pi_0 e^{c''/Tv}}{RT}$$

$$= \frac{K e^{c/Tv}}{T}$$

or

$$\eta v^{\frac{1}{3}} \sqrt{T} = K e^{c/Tv} \qquad \text{......(15),}$$

this latter equation involving only two unknowns. The use of these expressions will be shown as applied to diethyl ketone for which Thorpe and Rodger(6) give the expression for the relation between temperature and volume as

$$V_t = V_0\,[1 + 0{\cdot}0_2 11534t + 0{\cdot}0_5 1884t^2 + 0{\cdot}0_8 3202t^3] \qquad \text{......(16),}$$

an expression involving four unknowns.

The equation

$$\pi_0 e^{c''/Tv} = \frac{T}{v - V_0} \qquad \text{......(17)}$$

is applied to the volumes calculated from the equation (16). Equation (17) involves only three unknowns. The calculated values are obtained from the values of the constants, which unfortunately have to be obtained by the method of trial and error, thus: $V_0 = 0{\cdot}9000$, $c'' = 418{\cdot}1$, $\pi_0 = 587{\cdot}4$.

It is obvious that an expression of this type represents the specific volume of a liquid with considerable accuracy.

Table 8. Diethyl ketone

Temp. ° C.	Volume cm³	$v-V_0$	$\dfrac{T}{v-V_0}$	$\pi_0 e^{c''/Tv}$	Difference per cent
0	1·0000	0·1000	2730	2717	−0·5
10	1·0117	0·1117	2535	2531	−0·2
20	1·0238	0·1238	2367	2367	0·0
30	1·0363	0·1363	2223	2225	+0·1
40	1·0493	0·1493	2096	2098	+0·1
50	1·0627	0·1627	1985	1986	0·0
60	1·0766	0·1766	1885	1885	0·0
70	1·0909	0·1909	1795	1796	0·0
80	1·1059	0·2059	1714	1714	0·0
90	1·1213	0·2213	1640	1641	0·0
100	1·1373	0·2373	1572	1574	+0·1

If now we take the value of V_0 as 0·9000, which has been determined independently of viscosity data, and insert it in equation (14), we have an equation which involves only two unknowns, namely K_0 and c'. This expression gives a very accurate representation of the experimental values. The values of the constants are: $c' = 160{\cdot}0$, $K_0 = 0{\cdot}0_3 1995$, $V_0 = 0{\cdot}9000$.

Table 9. Diethyl ketone

Temp. ° C.	$\eta_{\text{obs.}}$	$\eta_{\text{calc.}}$
0	0·00595	0·00593
10	0·00525	0·00524
20	0·00466	0·00467
30	0·004195	0·004194
40	0·003795	0·003792
50	0·003445	0·003445
60	0·00315	0·00315
70	0·00289	0·00289
80	0·002655	0·002654
90	0·00245	0·00245
100	0·00226	0·00227

It will be seen that the experimental values are almost exactly reproduced.

By eliminating $(v-V_0)$ we obtain the equation

$$\eta v^{\frac{1}{3}} \sqrt{T} = K e^{c/Tv},$$

where $c = c' + c'' = 578{\cdot}1$ and $K = K_0 \times \pi_0 = 0{\cdot}1172$. In the following tables this equation is applied to several liquids, and a comparison is made of the differences between the observed and calculated values obtained by its use with those by the use of Andrade's expression, equation (3). The values of $(v-V_0)$, calculated from the approximate equation

$$\frac{\eta v^{\frac{1}{3}}}{\sqrt{T}} = \frac{B}{v-V_0} \qquad \text{......(18)},$$

along with the divergences from the observed values, are also given. From the approximate value of $(v-V_0)$ thus obtained the absolute frequency has been calculated in the manner illustrated for sodium. The absolute viscosity is then obtained from equation (1). The observed value is shown in brackets.

Table 10. Diethyl ketone

Temp. ° C.	$\eta_{\text{obs.}}$	$\eta v^{\frac{1}{3}}\sqrt{T}$	$Ke^{c/Tv}$	Difference per cent	From Andrade's formula	$\frac{B}{v-V_0}$
0	0·00595	0·0983	0·0974	−0·9	−0·4	+1·6
10	0·00525	0·0886	0·0883	−0·3	−0·2	+0·3
20	0·00466	0·0805	0·0805	0·0	−0·1	0·0
30	0·004195	0·0739	0·0739	0·0	0·0	−0·8
40	0·003795	0·0682	0·0682	0·0	−0·2	−1·0
50	0·003445	0·0632	0·0632	0·0	−0·3	−1·1
60	0·00315	0·0589	0·0588	−0·2	−0·4	−1·1
70	0·00289	0·0551	0·0550	0·2	−0·3	−0·7
80	0·002655	0·0516	0·0516	0·0	0·0	0·0
90	0·00245	0·0485	0·0485	0·0	+0·4	+0·5
100	0·00226	0·0456	0·0458	+0·4	+0·8	+1·5

$c=578{\cdot}1$; $K=0{\cdot}1172$; $(v-V_0)$ at 0° C. $=0{\cdot}0701$; $\nu_0=3{\cdot}36\times10^{12}$; $\eta_0=0{\cdot}01056$ (0·00595).

Table 11. Octane

Temp. ° C.	$\eta_{\text{obs.}}$	Volume cm^3	$\eta v^{\frac{1}{3}}\sqrt{T}$	$Ke^{c/Tv}$	Difference per cent	From Andrade's formula	$\frac{B}{v-V_0}$
0	0·00703	1·0000	0·1161	0·1152	−0·8	−0·4	7·0
10	0·006125	1·0119	0·1035	0·1030	−0·5	−0·3	2·0
20	0·00538	1·0238	0·09282	0·09282	0·0	0·0	0·0
30	0·004785	1·0360	0·08427	0·08428	0·0	−0·2	−1·5
40	0·00428	1·0485	0·07690	0·07697	+0·1	−0·2	−2·0
50	0·003855	1·0612	0·07068	0·07070	0·0	−0·2	−2·1
60	0·003495	1·0745	0·06531	0·06518	−0·2	−0·6	−2·1
70	0·00318	1·0882	0·06058	0·06042	−0·3	−0·6	−1·7
80	0·002905	1·1025	0·05638	0·05625	−0·2	−0·5	−1·3
90	0·00266	1·1174	0·05257	0·05257	0·0	−0·3	−0·6
100	0·002445	1·1331	0·04922	0·04922	0·0	0·0	0·0
110	0·002255	1·1496	0·04624	0·04626	0·0	0·0	+0·4
120	0·002075	1·1670	0·04332	0·04358	+0·6	+0·7	+1·4

$c=655{\cdot}6$; $K=0{\cdot}1044$; $(v-V_0)$ at 0° C. $=0{\cdot}0543$; $\nu_0=3{\cdot}52\times10^{12}$; $\eta_0=0{\cdot}0137$ (0·00703).

Table 12. Carbon tetrachloride

Temp. ° C	$\eta_{\text{obs.}}$	Volume cm^3	$\eta v^{\frac{1}{3}}\sqrt{T}$	$Ke^{c/Tv}$	Difference per cent	From Andrade's formula	$\frac{B}{v-V_0}$
0	0·01346	1·0000	0·2223	0·2192	−1·4	−1·4	+3·5
10	0·01133	1·0122	0·1914	0·1914	0·0	0·0	0·0
20	0·00969	1·0245	0·1672	0·1681	+0·5	+0·6	−1·1
30	0·00842	1·0371	0·1484	0·1494	+0·7	+0·7	−1·2
40	0·00738	1·0502	0·1328	0·1337	+0·7	+0·7	−1·4
50	0·00654	1·0636	0·1200	0·1205	+0·4	+0·5	−0·6
60	0·005835	1·0776	0·1092	0·1092	0·0	0·0	0·0
70	0·00524	1·0932	0·1000	0·0995	−0·5	−0·8	+0·1

$c=793{\cdot}1$; $K=0{\cdot}1199$; $(v-V_0)$ at 0° C. $=0{\cdot}0494$; $\nu_0=3{\cdot}75\times10^{12}$; $\eta_0=0{\cdot}0217$ (0·0135).

Table 13 gives the absolute frequency and the absolute viscosity calculated for a large number of liquids at temperatures approximately 20° below their boiling points. The free space was obtained by means of equation (18) from observed values at two temperatures 20° and 10° below the boiling point. In calculating the absolute value, K was taken as unity. The last column gives the numerical ratio of the calculated value to the observed value. It is practically constant for this class of substances, which includes bromine and nitrogen peroxide, and is much smaller than the ratio for the metals. The organic substances are distinguished from the metals by their much larger atomic volumes as well as for their greater free space. It might be expected that the error due to the approximations made would become greater as the scale is reduced; in the gaseous state the time between collisions is long compared to the time of the actual collision, whereas in a liquid a molecule is practically in a state of continual collision; the actual nature of the collision, which is relatively unimportant in a gas, becomes one of the determining factors in a liquid. A considerable numerical correction is therefore to be expected. In the case of the organic substances the value actually required is certainly not unreasonable.

Table 13

Substance	Temp. ° C.	$\nu \times 10^{-12}$	$\eta_{\text{calc.}}$	$\eta_{\text{obs.}}$	Ratio
Pentane	10	2·00	0·00550	0·00256	2·15
Heptane	70	1·50	0·00516	0·00253	2·04
Octane	100	1·22	0·00456	0·00244	1·87
Propyl chloride	20	2·17	0·00691	0·00352	1·97
Propyl bromide	50	1·55	0·00773	0·00388	2·00
Propyl iodide	80	1·24	0·00830	0·00420	1·99
Carbon tetrachloride	50	1·99	0·01230	0·00654	1·88
Chloroform	40	1·83	0·00910	0·00465	1·96
Propylene bromide	120	1·56	0·01194	0·00535	2·23
Benzene	60	2·63	0·00836	0·00391	2·14
Ethyl benzene	110	1·53	0·00586	0·00282	2·08
Ethyl sulphide	70	1·60	0·00543	0·00279	1·95
Carbon bisulphide	20	2·36	0·00847	0·00367	2·30
Methyl propyl ether	10	2·13	0·00624	0·00277	2·25
Dipropyl ether	60	1·64	0·00589	0·00277	2·13
Diethyl ether	10	2·02	0·00592	0·00259	2·28
Propyl acetate	80	1·78	0·00673	0·00304	2·21
Methyl formate	10	2·65	0·00745	0·00384	1·94
Nitrogen peroxide	0	2·66	0·01140	0·00528	2·16
Bromine	0	5·75	0·02910	0·0126	2·30
Potassium	62	16·9	0·0336	0·0056	6·00
Sodium	97	31·9	0·0466	0·0075	6·20
Mercury	0	10·9	0·1557	0·0170	9·00
Gallium	30	28·5	0·1697	0·0204	8·32
Tin	240	22·2	0·1900	0·0191	10·0

§7. THE INTERNAL PRESSURE OF THE LIQUIDS

It is of interest to calculate the internal pressures Π of the elements on the assumption that they are given approximately by the expression

$$\Pi = \frac{RT}{(v - V_0)\, M/\rho}.$$

Table 13 sets out the values obtained in atmospheres. The approximate value of their coefficients of cubical expansion are also given.

Table 14

Substance	Temp. ° C.	Π	α
Tin	240	104,600	$0{\cdot}0_3 10$
Gallium	100	108,000	$0{\cdot}0_3 11$
Mercury	0	50,500	$0{\cdot}0_3 18$
Sodium	100	43,000	$0{\cdot}0_3 28$
Potassium	64	18,600	$0{\cdot}0_3 30$
Bromine	0	12,200	$0{\cdot}0_2 10$

Except in the case of potassium, the coefficients of expansion are approximately inversely proportional to the internal pressures. There is an obvious relation between the internal pressure of a liquid and its viscosity, as both are largely governed by the free space.

§8. ACKNOWLEDGEMENTS

In conclusion, I wish to express my thanks to Dr F. W. G. White, Professor of Physics at Canterbury College, and to Mr C. J. Banwell, M.Sc., for helpful criticism and encouragement.

Note added in proof

My attention has been drawn to the recent papers by Eyring in the *Journal of Chemical Physics* on the physical properties of liquids, to which no reference is made in this paper. Unfortunately the journal is not available in Christchurch and I was unaware of the contents of Eyring's papers when I was preparing mine. Any conclusions, therefore, arrived at in this paper are independent of those arrived at by Eyring.

I have now obtained copies of Eyring's papers but I find that his method of approach is different from mine, though he makes use of the terms "free volume" and "internal pressure" in his discussion. The expression "free space or volume" as understood in the present paper has been defined both in it and my earlier papers (7, 8, 9) and evidence has been brought forward to show that it corresponds to the free-volume term in Van der Waals's equation. In calculating the internal pressure of a liquid Van der Waals has been followed in that only attractive static forces have been considered. It is of interest, however, to note that the values of the intrinsic cohesive pressures for potassium, sodium and mercury, given above, are of the same order and bear a similar relationship to one another as do those given by Richards for the same substances in a paper published in the discussion by the Faraday Society on Cohesion and Related Problems, November 1927. The following table sets out the values obtained by the author and by Richards:

Substance	Richards	Author
Potassium	15,300	18,600
Sodium	33,000	43,000
Mercury	41,300	50,500

REFERENCES

(1) Andrade. *Phil. Mag.* **17**, 497 and 698 (1934).
(2) Spells. *Proc. Phys. Soc.* **48**, 299 (1936).
(3) Chiong. *Proc. Roy. Soc.* A, **157**, 264 (1936).
(4) Stott. *Proc. Phys. Soc.* **45**, 530 (1933).
(5) Lewis. *Proc. Phys. Soc.* **48**, 102 (1936).
(6) Thorpe and Rodger. *Philos. Trans.* A, **185**, 397 (1894); **189**, 71 (1897).
(7) Macleod. *Trans. Faraday Soc.* **19**, 6 (1923).
(8) Macleod. *Trans. Faraday Soc.* **21**, 151 (1925).
(9) Macleod. *Trans. Faraday Soc.* **32**, 872 (1936).

THE RELATION BETWEEN IONOSPHERIC TRANSMISSION PHENOMENA AT OBLIQUE INCIDENCE AND THOSE AT VERTICAL INCIDENCE

By G. MILLINGTON, Marconi's Wireless Telegraph Co. Ltd.,
Research and Development Department

Received 25 January 1938. Read in title 10 June 1938

ABSTRACT. This paper gives a modification for a curved earth of Martyn's theorems, relating oblique-incidence ionospheric phenomena with observed conditions at vertical incidence. The theorems in their modified form are shown to hold, as regards both equivalent frequency and absorption, for a relatively thin layer above the earth's surface. It is assumed that the ionic density has the same vertical gradient everywhere between the transmitter and receiver, and that the effect of the earth's magnetic field can be neglected. Methods of allowing approximately for these two factors are discussed. A set of transmission curves is derived, with which the skip frequency at any given distance from the transmitter can be obtained graphically from an observed *P'f* curve at vertical incidence. Similar curves are given for deducing equivalent heights and angles of elevation at oblique incidence, together with graphs of the maximum receivable frequency at extreme distances and the maximum distance of single-hop transmission, as functions of the height of the layer. The application of the theorem is thus reduced, for the benefit of engineers, to a simple technique of using a number of standard curves in conjunction with a given *P'f* curve.

§ 1. INTRODUCTION

THE problem of determining the characteristics of long-distance transmission through the ionosphere, as regards the maximum usable frequency and the absorption en route, is a very important one from the point of view of the engineer who has to allocate wave-lengths for any projected service. It would be a difficult and tedious business to make ionospheric measurements for a comprehensive set of conditions at oblique incidence, and it would be very useful if the required data could be deduced from observations made at vertical incidence by the standard *P'f* technique.

Martyn⁽¹⁾ has shown that a simple relation does actually exist between results taken at vertical incidence and those which would be obtained at oblique incidence, provided that three assumptions are made: (1) that the gradient of electronic density is everywhere vertical and similar along the oblique path, (2) that the earth's magnetic field is negligible, and (3) that the earth is flat. The first assumption is roughly satisfied if, for instance, the whole of the transmission path lies in a region of bright daylight, or if the transmission, regarded as a single hop, is referred to the ionospheric conditions at the mid point of the path where the reflection takes place. The second assumption is approximately justified at short distances, but at longer distances it leads to values of maximum usable frequency for the extraordinary ray which are too big. The third assumption also leads to values which are considerably too big for long distances.

It is difficult to assess the error due to the neglect of the earth's magnetic field, owing to the complexity of the analysis involved in the magneto-ionic theory. It is, however, possible to examine the effect of the earth's curvature in some detail and to express the result as a modification of Martyn's theorem. In this paper the general ray theory of a curved earth and ionosphere is developed in a form suitable for the discussion of transmission at very oblique incidence, in which the ray may leave the earth almost tangentially. The results obtained are presented in a set of curves for use in practical cases, and some discussion is given of their application to long-distance transmission problems.

§ 2. GENERAL RAY THEORY FOR A CURVED EARTH

Figure 1 represents a ray leaving a transmitter T at an angle of elevation α, and arriving at a receiver R at a distance y along the surface of the earth. If ϕ is the angular distance, and r_0 is the radius of the earth, $y = r_0 \phi$. PQ is an element ds of the ray path, corresponding to a height h above the surface of the earth and to an angular distance $d\phi$. In the figure, SQ represents dh and $PS = (r_0 + h)\, d\phi$, while the angle of elevation QPS at P is θ. We therefore have

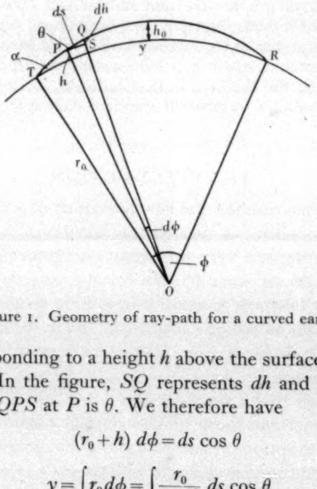

Figure 1. Geometry of ray-path for a curved earth.

$$(r_0 + h)\, d\phi = ds \cos\theta$$

and

$$y = \int r_0 d\phi = \int \frac{r_0}{r_0 + h}\, ds \cos\theta \qquad \text{......(2·1).}$$

But if the refractive index of the ionosphere at P is μ, and is taken as unity on the earth at T, the fundamental ray equation for the curved earth is

$$\mu\,(r_0 + h) \cos\theta = r_0 \cos\alpha \qquad \text{......(2·2),}$$

so that equation (2·1) may be written

$$y=\int\left(\frac{r_0}{r_0+h}\right)^2\cos\alpha\,\frac{ds}{\mu}.$$

Now if h_0 is the height to which the ray penetrates at its apex, it follows that y lies between the values

$$\cos\alpha\int\frac{ds}{\mu}\quad\text{and}\quad\left(\frac{r_0}{r_0+h_0}\right)^2\cos\alpha\int\frac{ds}{\mu}.$$

But $\int\frac{ds}{\mu}$ is the equivalent path P'_{ob} given by ct, where t is the time taken for the ray to pass from T to R, and c is the velocity of the ray in free space. We may therefore write

$$y=\left(1-\gamma\frac{h_0}{r_0}\right)P'_{\text{ob}}\cos\alpha \qquad \text{......(2·3)},$$

where γ is of the order of unity.

This relation shows that whatever the law of the gradient in the ionosphere and however long the ray path may be, the flat-earth relation $y=P'_{\text{ob}}\cos\alpha$ is only slightly modified, provided that h_0/r_0 is very small compared with unity. Strictly speaking γ can only be determined if we know the relation between the electronic density N and the height h. To study further the form of P'_{ob}, we must make use of the well-known relation

$$1-\mu^2=\frac{Ne^2}{\pi mf^2} \qquad \text{......(2·4)},$$

where e and m are the electronic charge and mass, and f is the frequency of the wave. N is a function of the height h, so that it is convenient to write equation (2·4) as

$$1-\mu^2=\frac{g(h)}{f^2} \qquad \text{......(2·5)},$$

where

$$g(h)=\frac{Ne^2}{\pi m} \qquad \text{......(2·6)}.$$

Now from figure 1, $ds=dh/\sin\theta$, so that

$$P'_{\text{ob}}=\int\frac{ds}{\mu}=2\int_0^{h_0}\frac{dh}{\mu\sin\theta} \qquad \text{......(2·7)}.$$

But if $h/r_0\ll 1$, we have from equation (2·2)

$$\sin^2\theta\doteqdot 1-\left(1-\frac{2h}{r_0}\right)\frac{\cos^2\alpha}{\mu^2},$$

i.e.

$$\mu^2\sin^2\theta\doteqdot\sin^2\alpha+\frac{2h}{r_0}\cos^2\alpha-(1-\mu^2).$$

Using equation (2·5) and writing f_{ob} for the frequency used at oblique incidence, we have

$$\mu^2\sin^2\theta=\sin^2\alpha+\frac{2h}{r_0}\cos^2\alpha-\frac{g(h)}{f^2_{\text{ob}}} \qquad \text{......(2·8)}.$$

At the apex of the path where $h=h_0$ and $\theta=0$, and μ from equation (2·2) is given by $r_0 \cos\alpha/(r_0+h_0)$, we have from equation (2·8)

$$\frac{g\,(h_0)}{f^2{}_{\mathrm{ob}}}=\sin^2\alpha+\frac{2h_0}{r_0}\cos^2\alpha \qquad \text{......(2·9)}.$$

Now if a frequency f at vertical incidence reaches a height h_0 where $\mu=0$, we have

$$g\,(h_0)=f^2 \qquad \text{......(2·10)}.$$

Corresponding to a frequency f at vertical incidence we may therefore define an equivalent frequency f_{ob} at oblique incidence, such that at the apex of its path it reaches the same height h_0, and from equations (2·9) and (2·10) we see that f_{ob} and f are connected by the relation

$$f^2{}_{\mathrm{ob}}=\frac{f^2}{\sin^2\alpha+\dfrac{2h_0}{r_0}\cos^2\alpha},$$

i.e.

$$f_{\mathrm{ob}}=\frac{f\,\mathrm{cosec}\,\alpha}{\sqrt{(1+2h_0r_0^{-1}\cot^2\alpha)}} \qquad \text{......(2·11)}.$$

Equation (2·8) may now be written

$$\mu\sin\theta=\frac{\sqrt{(1+2h_0r_0^{-1}\cot^2\alpha)}}{f\,\mathrm{cosec}\,\alpha}\sqrt{\left\{\frac{f^2\,(1+2hr_0^{-1}\cot^2\alpha)}{(1+2h_0r_0^{-1}\cot^2\alpha)}-g\,(h)\right\}}.$$

Putting this value into equation (2·7), we get

$$P'_{\mathrm{ob}}=\frac{2f\,\mathrm{cosec}\,\alpha}{\sqrt{(1+2h_0r_0^{-1}\cot^2\alpha)}}\int_0^{h_0}\frac{dh}{\sqrt{\left\{\dfrac{f^2(1+2hr_0^{-1}\cot^2\alpha)}{(1+2h_0r_0^{-1}\cot^2\alpha)}-g\,(h)\right\}}} \qquad \text{...(2·12)}.$$

If P' is the equivalent path at vertical incidence for the frequency f, we have, by putting $\alpha=90^\circ$ in equation (2·12),

$$P'=2f\int_0^{h_0}\frac{dh}{\sqrt{\{f^2-g\,(h)\}}} \qquad \text{......(2·13)},$$

and for a flat earth at oblique incidence we have, by putting $r_0=\infty$ in equation (2·12),

$$P'_{\mathrm{ob}}=2f\,\mathrm{cosec}\,\alpha\int_0^{h_0}\frac{dh}{\sqrt{\{f^2-g\,(h)\}}},$$

i.e., from equation (2·13),

$$P'_{\mathrm{ob}}=P'\,\mathrm{cosec}\,\alpha.$$

This is Martyn's theorem relating the equivalent path P'_{ob} for oblique incidence with initial angle of elevation α for a frequency f_{ob}, given from equation (2·11) by $f\,\mathrm{cosec}\,\alpha$, with the equivalent path P' at vertical incidence for a frequency f.

We cannot accurately interpret the general expression for the curved earth given in equation (2·12) unless we know the form of $g\,(h)$ as a function of h, i.e. unless we know the nature of the gradient of electronic density, whereas for the flat-earth case the theorem holds independently of any assumed form of the gradient. But from the form of the integrand in equation (2·12) we can see that the integral in the expression for P'_{ob} is greater than the corresponding integral in the expression for P' in equation (2·13), so that we know that

$$P'_{\text{ob}} > P' \operatorname{cosec} \alpha / \sqrt{(1 + 2h_0 r_0^{-1} \cot^2 \alpha)}.$$

Now if we exclude very small values of α and only consider values for which $h_0 r_0^{-1} \cot^2 \alpha \ll 1$, i.e. for which $\tan \alpha \gg \sqrt{(h_0/r_0)}$, it can be seen that in general the integral in equation (2·12) is only slightly greater than the corresponding integral in equation (2·13). Near the apex of the ray, where the denominator in the integral approaches zero, we also approach the condition where h becomes h_0, and the denominator approaches $\sqrt{\{f^2 - g(h)\}}$ as in the integral in equation (2·13). By assuming a layer of the form $g(h) = ah - bh^2$ having a maximum density at a height $a^2/2b$, and by choosing a and b so that $g(h_0)$ is equal to f and $a^2/2b$ is only slightly greater than h_0, we can show that in a typical case in which the ray is near to the escape condition, P'_{ob} is only slightly greater than $P' \operatorname{cosec} \alpha$. Thus in general it appears that when $h_0 r_0^{-1} \cot^2 \alpha \ll 1$, the relation $P'_{\text{ob}} = P' \operatorname{cosec} \alpha$ is still very nearly true, while equations (2·3) and (2·11) give approximately $y = P'_{\text{ob}} \cos \alpha$ and $f_{\text{ob}} = f \operatorname{cosec} \alpha$ respectively, so that $\tan \alpha = P'/y$.

These relations are formally the same as for a flat earth, but it must be remembered that they have been shown to hold even when the ray travels to a long distance, so that y is measured round the surface of the earth, and the angle α, considered as the initial angle of elevation on the curved earth, may be markedly different from the corresponding angle in the flat earth case.

Martyn has also given an analogous theorem relating the absorption at oblique incidence for the frequency f_{ob} with that at vertical incidence for the frequency f. If the absorption occurring over the length ds of the path is represented by the factor $\exp[-\kappa\, ds]$, the absorption coefficient is given by

$$\kappa = \frac{\nu}{2c\mu} \frac{g(h)}{f^2_{\text{ob}}} \qquad \text{......(2·14)},$$

where $g(h)$ is given by equation (2·6) as before, and ν is the collisional frequency of the electrons and is a function of h.

We have
$$\kappa\, ds = \frac{\nu}{2c\mu} \frac{g(h)}{f^2_{\text{ob}}} \frac{dh}{\sin\theta},$$

so that
$$\int_{\text{oblique}} \kappa\, ds = 2 \int_0^{h_0} \frac{\nu}{2c\mu} \frac{g(h)}{f^2_{\text{ob}}} \frac{dh}{\sin\theta}.$$

Again substituting from equation (2·8) for $\mu \sin\theta$, and from equation (2·11) for f_{ob}, we get

$$\int_{\text{oblique}} \kappa\, ds = \frac{\sin\alpha \sqrt{(1 + 2h_0 r_0^{-1} \cot^2 \alpha)}}{cf} \int_0^{h_0} \frac{\nu g(h)\, dh}{\sqrt{\left\{\frac{f^2 (1 + 2hr_0^{-1} \cot^2 \alpha)}{(1 + 2h_0 r_0^{-1} \cot^2 \alpha)} - g(h)\right\}}}.$$

It is obvious that with the same limitations the absorption theorem still holds, namely

$$\int_{\text{oblique for } f_{\text{ob}}} \kappa\, ds = \sin\alpha \int_{\text{vertical for } f} \kappa\, ds.$$

If we write $\exp[\int -\kappa\, ds]$ as a reflection coefficient ρ, then

$$\frac{[\log \rho]_{\text{oblique for } f_{\text{ob}}}}{[\log \rho]_{\text{vertical for } f}} = \sin \alpha \qquad \text{......(2·15).}$$

The condition $\tan \alpha \gg \sqrt{(h_0/r_0)}$ which we have assumed implies a serious limitation to the application of the theorem to long-distance transmission at very oblique incidence. This limitation has arisen because we have considered the ionosphere to extend down to the surface of the earth, whereas actually we know that it exists as well-defined layers of thickness small compared with their height above the ground. Suppose, therefore, that we consider a layer whose lower edge is at a height H above the ground, and in which the maximum density occurs at a height h_0 above this edge, then a ray leaving the earth tangentially will enter the layer with an angle of elevation α for which $\tan \alpha = \sqrt{(2H/r_0)}$. As this is large in comparison with $\sqrt{(h_0/r_0)}$, our condition is always satisfied for such a layer.

§ 3. ANALYSIS FOR A THIN LAYER ABOVE THE EARTH'S SURFACE

In figure 2 the ray enters the layer at T' and leaves it again at R', and the straight-line portions TT' and RR' of the path between the earth and the layer can be determined in terms of the height of the layer and the angle of elevation α at which the ray enters the layer. Corresponding to the arc $T'R'$ of the circle of radius $r_0 + H$, which we will call y_2', is an arc $T''R''$ on the surface of the earth. Calling this arc y_2, and each of the arcs TT'' and $R''R$, y_1, we have

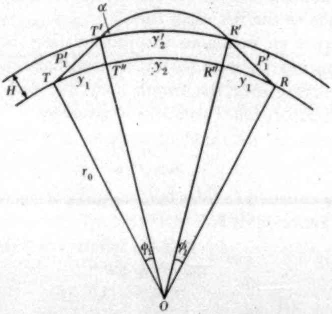

Figure 2. Geometry of ray-path for a curved earth when the lower edge of the ionosphere is at a height H.

$$y = 2y_1 + y_2 \qquad \text{......(3·1).}$$

If we call each of the paths TT' and $R'R$, P_1', and the equivalent path in the layer P_2', then the total equivalent path P'_{ob} is now given by

$$P'_{\text{ob}} = 2P_1' + P_2' \qquad \text{......(3·2).}$$

If ϕ_1 is the angle subtended at the centre of the earth, O, by y_1, then from $\triangle TOT'$

$$\frac{r_0+H}{r_0}=\frac{\cos(\alpha-\phi_1)}{\cos\alpha}.$$

Therefore
$$1+\frac{H}{r_0}=\cos\phi_1\,[1+\tan\alpha\tan\phi_1]$$
$$\doteqdot\left(1-\frac{\phi_1^2}{2}\right)(1+\phi_1\tan\alpha),$$

whence
$$\phi_1^2-2\tan\alpha\,.\,\phi_1+\frac{2H}{r_0}=0$$

and
$$y_1=r_0\phi_1=r_0\tan\alpha-r_0\sqrt{(\tan^2\alpha-2H/r_0)} \qquad \ldots\ldots(3\cdot3).$$

This approximation is close enough, and gives the limits $\tan\alpha=\sqrt{(2H/r_0)}$ and $y_1=\sqrt{(2r_0H)}$ when $\phi_1=\alpha$, and the ray leaves the earth tangentially. Also for large values of $\tan\alpha$, y_1 approximates to $H/\tan\alpha$, as it should.

Inspection now shows that the analysis simplifies considerably, if we assume that on entering the layer the ray suffers a slight diminution of angle given by changing α to α', where

$$\tan\alpha'=\tan\alpha/(1+H/r_0) \qquad \ldots\ldots(3\cdot4).$$

In justification of this procedure, we notice that the change produced in α is only of the order of error involved in determining y_1 as above, and that the ratio of α/α', which has a maximum value of $(1+H/r_0)$ when α is small, decreases to unity as α approaches 90° at vertical incidence. Applying the curved-earth theory as developed in the previous section, we now have

$$P_2'=y_2'\sec\alpha'=(P'-2H)\operatorname{cosec}\alpha' \qquad \ldots\ldots(3\cdot5),$$

where P', referring to the frequency f at vertical incidence, is still measured from the earth's surface. The frequency f_{ob} can still be written, to the accuracy to which we are justified in working, as

$$f_{\text{ob}}=f\operatorname{cosec}\alpha \qquad \ldots\ldots(3\cdot6).$$

Now
$$y_2=\frac{y_2'}{1+H/r_0}=\frac{P'-2H}{(1+H/r_0)\tan\alpha'}, \quad \text{from equation } (3\cdot5),$$

i.e. from equation (3·4)
$$y_2=(P'-2H)\cot\alpha \qquad \ldots\ldots(3\cdot7).$$

The assumption in equation (3·4) was designed to remove the $1+H/r_0$ term from y_2, and to give it in the form in equation (3·7). Now from equations (3·1) and (3·3)

$$y-y_2=2r_0\tan\alpha-2r_0\sqrt{(\tan^2\alpha-2H/r_0)},$$

i.e.
$$(y-y_2)^2-4(y-y_2)\,r_0\tan\alpha=-8r_0H \qquad \ldots\ldots(3\cdot8).$$

By analogy with the flat-earth case it is convenient to write

$$\tan\alpha=\frac{kP'}{y} \qquad \ldots\ldots(3\cdot9),$$

where k is a modification factor to be determined. If further we write

$$P' = 2mH \qquad \text{......(3·10)},$$

i.e.

$$m = \frac{h'}{H},$$

where h' is the equivalent height for the frequency f at vertical incidence, so that m is a parameter expressing the penetration of the ray into the layer, then equation (3·7) may be written

$$y_2 = \frac{m-1}{km} y \qquad \text{......(3·11)},$$

and

$$y - y_2 = 2y_1 = \left(\frac{km - m + 1}{km}\right) y \qquad \text{......(3·12)}.$$

With this substitution equation (3·8) reduces down to

$$y = \left[\frac{km}{km - m + 1}\right] \sqrt{\{8r_0 Hm (k-1)\}} \qquad \text{......(3·13)},$$

$\sqrt{(8r_0 H)}$ represents the distance to which a ray leaving the earth tangentially would go if it were reflected as from a mirror at a height H above the earth, i.e. as from the layer without any penetration, for which $m = 1$. This suggests that we should write

$$l = \frac{y}{\sqrt{(8r_0 H)}} \qquad \text{......(3·14)},$$

so that equation (3·13) becomes

$$l = \left(\frac{km}{km - m + 1}\right) \sqrt{\{m(k-1)\}} \qquad \text{......(3·15)}.$$

Values of l greater than unity imply that there must be some penetration into the layer if the ray is to travel to the assumed distance y, and for a given value of l which is greater than unity, there exists a minimum possible value of m which corresponds to the ray that leaves the earth tangentially. Corresponding to this value of m there will be a maximum possible value of k. From equations (3·9) and (3·10) we have

$$\tan\alpha = \frac{2kmH}{y} = \frac{km}{l} \sqrt{\frac{H}{2r_0}}$$

by substitution from equation (3·14).

By writing $k_{\max}$ and $m_{\min}$ for the tangential ray, we get

$$\tan\alpha = \sqrt{\frac{2H}{r_0}} = \frac{k_{\max} m_{\min}}{l} \sqrt{\frac{H}{2r_0}}$$

and

$$k_{\max} m_{\min} = 2l.$$

Combining this with equation (3·15) we get

$$m_{\min} = 2l - 1, \quad \text{where } l > 1$$

and

$$k_{\max} = \frac{2l}{2l-1}, \quad \text{where } l > 1.$$

When $l<1$ the maximum value of k occurs when $m=1$ and $k=1+l^2$. The maximum possible value of k is thus 2 when $l=1$ and $m=1$, it being remembered that by definition m cannot be less than unity.

Strictly speaking equation (3·15) has to be solved for k for assumed values of l and m, but in practice l is calculated for assumed values of k and m, and then k is plotted as a function of l for a series of values of m, as shown in figure 3. Since equation (3·15) only contains k, l, and m, one set of curves suffices to represent all combinations of P', H and y. The curves are drawn to represent the limiting conditions that $m>1$, and that when $l>1$, $m>2l-1$, and they are arbitrarily cut off at $m=3$, as the parts retained cover most practical conditions.

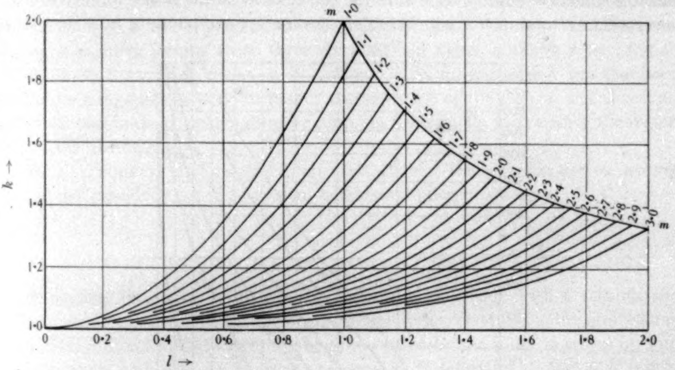

Figure 3. Curves showing k as a function of l for various values of m.

From the general shape of the curves we can see at a glance when the factor k exceeds any arbitrary value chosen as the point at which Martyn's theorem needs modification. For assumed values of H and y, l is determined from equation (3·14), and from a given value of P' on the $P'f$ curve at vertical incidence, m is given by equation (3·10). For the values of l and m so obtained, k is read off the curves, and $\tan\alpha$ is then derived from equation (3·9). The equivalent frequency f_{ob} is then obtained from equation (3·6). In this way the value of f_{ob} for each point on the $P'f$ curve can be obtained, but as it is a somewhat lengthy process we seek a simple graphical method for converting the values of f into the required values of f_{ob}.

§4. CONSTRUCTION OF TRANSMISSION CURVES

It is convenient to adopt the technique suggested by Smith(2) in a recent research paper published by the National Bureau of Standards. We notice that equation (3·6) expresses f_{ob} by its equivalent vertical-incidence value multiplied by cosec α, so that it should be possible by the use of a logarithmic scale to devise a sliding process, as with a slide rule, to convert the vertical-incidence values to the required oblique incidence values. Suppose that we have an experimental $P'f$ curve, and that we assume that it corresponds to a layer whose lower edge is at a height H above the surface of the earth. (Since $P' = 2h'$, whereas in practice h' is plotted against f, it will be better from now on to refer to $h'f$ curves.) For a given point (h', f) we work out the value of $\tan\alpha$ for a given distance y as above. α does not depend on f but only on h', and so a graph of h' as ordinates and $\sin\alpha$ as abscissae can be constructed. Such a graph with $\sin\alpha$ on a logarithmic scale is called a transmission curve.

If now the $h'f$ curve is plotted with f on a logarithmic scale as abscissa, and the transmission curve is slid over it until the two coincide at the height h', the ordinate corresponding to $\sin\alpha = 1$ will lie on the ordinate corresponding to a frequency $f \operatorname{cosec}\alpha$, which from equation (3·6) is equal to f_{ob}. We can thus read off directly the equivalent frequency f_{ob} corresponding to any point on the $h'f$ curve. As the transmission curve is moved from right to left, it initially touches the $h'f$ curve, and the corresponding value of f_{ob} represents the skip frequency. For values of f_{ob} between the skip frequency and the critical frequency at vertical incidence, the transmission curve will cut the $h'f$ curve in two places corresponding to the low-angle and high-angle pair of rays which, as is well known, are obtained at oblique incidence under these conditions. From the abscissa scale of $\sin\alpha$ on the transmission curves the value of $\sin\alpha$ can be read off directly, for any point at which the transmission curve cuts the $h'f$ curve, for insertion into equation (2·15) to relate the absorption at oblique incidence with that measured at vertical incidence.

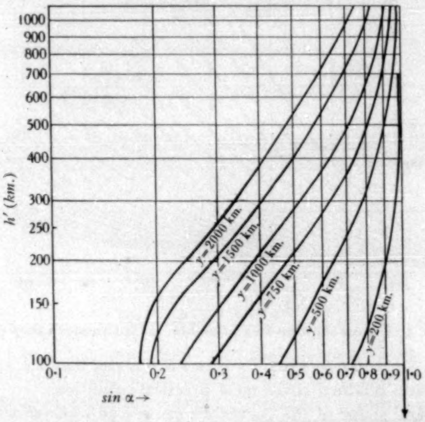

Figure 4. Transmission curves for various distances from the transmitter.

For short distances the transmission curves depend very little on the choice of H within the practical range, because the value of k is always very near to unity. For values of y over 1000 km. the curves differ appreciably for different values of H, but run together for large values of h'. For extreme distances for which $y > \sqrt{(8r_0H)}$, i.e. $l > 1$, we must remember that the transmission curve can only be drawn for values of h' greater than $(2l-1)H$. This may mean under certain conditions that transmission by a single hop to these distances is only possible by the high-angle ray.

In practice it would be inconvenient to have to use a separate transmission curve for each assumed value of H, and a composite curve can be made which will be accurate enough, and within the limits to which we are justified in working. We assume that from $h'=100$ km. to $h'=150$ km. we may take H equal to 100 km., and that from $h'=200$ km. to $h'=250$ km. we may take H equal to 200 km. while for all values of h' above 300 km. we may take H equal to 300 km. We then draw a composite curve joining these three sections, and figure 4 shows a set of such curves drawn for various values of the distance y. In these curves h' has also been plotted on a logarithmic scale to reduce the steepness of the curves, and this is an advantage also in the corresponding $h'f$ curves in reducing the steepness in the region of the critical frequency.

Before discussing the practical application of these transmission curves, we will turn to the consideration of equivalent heights at oblique incidence.

§5. EQUIVALENT HEIGHT ANALYSIS AT OBLIQUE INCIDENCE

At vertical incidence, with the standard pulse technique with a cathode-ray indicator and a linear time base, the displacement of the echo beyond the ground-ray pulse gives a direct measurement of the time t taken by the pulse to travel up into the ionosphere and back, i.e. it gives a measure of P' (equal to ct) and of h' (equal to $P'/2$). But at oblique incidence, if we assume the ground-ray pulse to be still present, the displacement of the echo corresponds to the difference between the equivalent path P'_{ob} and the distance y over the ground. If therefore we define the equivalent height h'_{ob} in terms of the displacement of the echo from the ground ray, we have*

$$h'_{\text{ob}} = \tfrac{1}{2}(P'_{\text{ob}} - y).$$

Even when we are beyond the range of the ground ray it is convenient to keep to this definition rather than to use $h'_{\text{ob}} = \frac{1}{2}P'_{\text{ob}}$, since, although changes of h'_{ob} with P'_{ob} will be the same on either definition for a given value of y, at extreme distances while P'_{ob} gets very large, $(P'_{\text{ob}} - y)$ tends to smaller values. If a transmitter being used for a $P'f$ run at vertical incidence were observed on a receiver at the distance y, the variation in the position of the reflected pulse would give a measure of the variation of h'_{ob} with frequency. Corresponding to the $h'f$ curve obtained at vertical incidence there is an $\{h'_{\text{ob}}, f_{\text{ob}}\}$ curve at oblique incidence, which we refer to the position of the ground ray as datum.

Except at extreme distances, we can obtain a relation between h'_{ob} and h' in a simple way. We consider first the difference between P_1' and y_1 in figure 2. From the triangle TOT'' we have immediately

---

* It is important to notice that equivalent height as here defined is different from the height of the equivalent triangular path in the flat-earth case. It is the equivalent height to which the echo displacement at oblique incidence would correspond if it were obtained at vertical incidence.

$$P_1' = r_0 \sec\alpha \sin\phi_1 = y_1 \sec\alpha \frac{\sin\phi_1}{\phi_1} \qquad \ldots\ldots(5\cdot1),$$

so that when ϕ_1 is small

$$P_1' - y_1 \doteqdot y_1(\sec\alpha - 1) \qquad \ldots\ldots(5\cdot2).$$

Also assuming that the ratio of P_2' in the layer to y_2' is large compared with the ration of y_2' to y_2, i.e. neglecting a factor $(1+H/r_0)$, we have

$$P_2' \doteqdot y_2 \sec\alpha$$

and

$$P_2' - y_2 = y_2(\sec\alpha - 1) \qquad \ldots\ldots(5\cdot3).$$

Combining equations (5·2) and (5·3), and allowing for the two P_1' portions in the path P'_{ob}, we get

$$P'_{\mathrm{ob}} - y = y(\sec\alpha - 1) \qquad \ldots\ldots(5\cdot4).$$

With the formula for $\tan\alpha$ in equation (3·9), and the relation $P' = 2h'$, equation (5·4) leads to

$$h'_{\mathrm{ob}} = h' k \tan\frac{\alpha}{2} \qquad \ldots\ldots(5\cdot5).$$

This is the flat-earth case modified by the factor k. At the extreme distances, where the angles of elevation concerned may be small, we can no longer ignore the terms of the order of H/r_0 omitted above. Returning to equation (5·1), we write

$$\begin{aligned} 2P_1' &= 2y_1 \sec\alpha\,(1 - \phi_1^2/6) \\ &= 2y_1 \sec\alpha - \tfrac{1}{3}(y_1^3/r_0^2)\sec\alpha \qquad \ldots\ldots(5\cdot6). \end{aligned}$$

Substituting for y from equation (3·12), we have

$$\frac{1}{3}\frac{y_1^3}{r_0^2}\sec\alpha = \frac{\sec\alpha}{3r_0^2}\,\frac{1}{8}\left(\frac{km-m+1}{km}\right)^3 y^3.$$

We now substitute for y^2 from equation (3·13), and for y from equation (3·9), and find that

$$\frac{1}{3}\frac{y_1^3}{r_0^2}\sec\alpha = \frac{1}{3}P'\frac{H}{r_0}(k-1)(km-m+1)\operatorname{cosec}\alpha \qquad \ldots\ldots(5\cdot7).$$

For P_2' we must now use the form in equation (3·5), i.e.

$$P_2' = (P' - 2H)\operatorname{cosec}\alpha',$$

and from equation (3·4)

$$\operatorname{cosec}\alpha' \doteqdot \operatorname{cosec}\alpha\left[1 + \frac{H}{r_0}\cos^2\alpha\right].$$

Thus

$$P_2' = (P' - 2H)\operatorname{cosec}\alpha + (P' - 2H)\frac{H}{r_0}\cos^2\alpha\,.\operatorname{cosec}\alpha,$$

and using equations (3·7) and (3·10) this becomes

$$P_2' = y_2 \sec\alpha + P'\left(1 - \frac{1}{m}\right)\frac{H}{r_0}\cos^2\alpha\operatorname{cosec}\alpha \qquad \ldots\ldots(5\cdot8).$$

Combining equations (5·6), (5·7) and (5·8), we have

$$h'_{\text{ob}} = h'\left(k\tan\frac{\alpha}{2} + A\frac{H}{r_0}\operatorname{cosec}\alpha\right) \qquad \ldots\ldots(5\cdot9),$$

where

$$A = \left(1-\frac{1}{m}\right)\cos^2\alpha - \tfrac{1}{3}(k-1)(km-m+1) \qquad \ldots\ldots(5\cdot10).$$

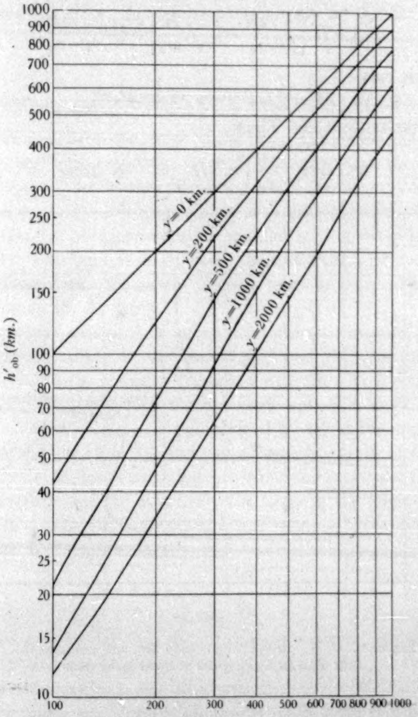

Figure 5. The equivalent height h'_{ob} as a function of h' for various distances from the transmitter.

We notice that although cosec $\alpha = 1$ at vertical incidence when $\alpha = 90°$, A is zero since $k = 1$ and $\cos\alpha = 0$, whatever the depth of penetration into the layer determined by m. The value of h'_{ob} therefore reduces to h' as it should. For small angles of elevation at extreme distances the correction term becomes comparable with the term $k\tan\frac{\alpha}{2}$. As a check if we consider the ray leaving the earth tangentially and with mirror reflection, for which $k=2$, $m=1$, $\alpha=\sqrt{(2H/r_0)}$, so that $A=-\frac{2}{3}$ and $h'=H$. Then

$$k\tan\frac{\alpha}{2}=\sqrt{\frac{2H}{r_0}}$$

and

$$\frac{H}{r_0}\operatorname{cosec}\alpha=\sqrt{\frac{H}{2r_0}},$$

$$h'_{\text{ob}}=H\left[\sqrt{\frac{2H}{r_0}}-\frac{2}{3}\sqrt{\frac{H}{2r_0}}\right]=\frac{2}{3}H\sqrt{\frac{2H}{r_0}}.$$

But in this simple case

$$h'_{\text{ob}}=r_0\,[\tan\phi_1-\phi_1]=\tfrac{1}{3}r_0\alpha^3,$$

since $\phi_1=\alpha$ for the tangent ray. Thus

$$h'_{\text{ob}}=\tfrac{1}{3}r_0\left(\frac{2H}{r_0}\right)^{\frac{3}{2}}=\tfrac{2}{3}H\sqrt{\frac{2H}{r_0}}\quad\text{as above.}$$

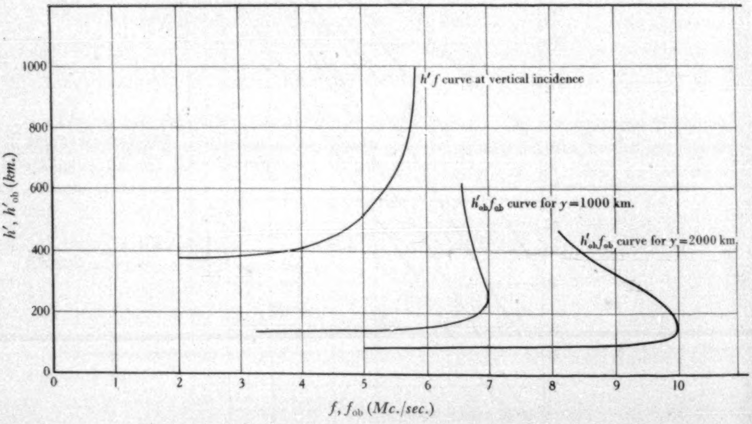

Figure 6. $h'_{\text{ob}}f_{\text{ob}}$ curves for $y=1000$ km. and $y=2000$ km., for a given $h'f$ curve at vertical incidence.

We have seen that for a given H and y the angle α is a function of h' only, so that it follows from equation (5·9) that h'_{ob} is a function of h' only. We can, therefore, draw a curve of h'_{ob} against h' for a set of values of H and y. Figure 5 shows such a set for various values of y, where the curves are again made composite to compromise for the variation with H. These curves have also been drawn on logarithmic scales. By using these curves in conjunction with the transmission curves in figure 4, the $h'_{\text{ob}}f_{\text{ob}}$ curve for any distance y corresponding to a given $h'f$ curve at vertical incidence can be quickly drawn out. Figure 6 shows a typical $h'f$ curve drawn on an ordinary linear scale. This is redrawn with h' and f on logarithmic scales, and for any point $h'f$ the value of f_{ob} for the chosen distance y is obtained by using the appropriate transmission curve. The value of h' is then used to find h'_{ob} from the appropriate curve in figure 5. It is quite a quick process to tabulate h'_{ob}, f_{ob} for a series of points on the $h'f$ curve, and the result of so doing for $y = 1000$ km. and 2000 km. is shown in figure 6. We can see from this figure the advantage of defining h'_{ob} as $\frac{1}{2}(P'_{ob} - y)$ rather than as $\frac{1}{2}P'_{ob}$, since it allows us to draw the $\{h'_{ob}, f_{ob}\}$ curves conveniently on the same axes as the $h'f$ curve.

§6. THE CONSTRUCTION OF {RANGE, ANGLE-OF-ELEVATION} CURVES

We can see at once from the shape of the $\{h'_{ob}, f_{ob}\}$ curves the relative positions of the low-angle and high-angle rays on any frequency above the critical frequency at vertical incidence, up to the skip frequency where the two rays coalesce. It would be useful, however, to be able to predict the results which would be obtained at any given frequency at oblique incidence, without having to work out the whole of the $h'_{ob}f_{ob}$ curve. This we can do by using the transmission curves, in conjunction with the vertical-incidence $h'f$ curve, to work from the assumed value of f_{ob} to the equivalent points on the $h'f$ curve.

The ordinate corresponding to $\sin\alpha = 1$ on the transmission curves is set over the ordinate corresponding to the chosen f_{ob}, and then the intersection of the transmission curve for the assumed distance y with the $h'f$ curve gives the values of h' (in the general case when both the low-angle and high-angle rays are present), from which the values of h'_{ob} can be obtained by using the appropriate curve in figure 5. From the values of f_{ob} and the equivalent values of f we can calculate $\sin\alpha$, and obtain the angles of elevation α at which the rays enter the layer. At short distances the angle α will be effectively the same as the angle of elevation α_0 at the ground, but at extreme distances the true relation between α_0 and α must be used; from equation (2·2) this is

$$\cos\alpha_0 = \left(1 + \frac{H}{r_0}\right)\cos\alpha.$$

But, as we have seen in deriving the transmission curves, the angle α for a given distance y and equivalent height h' is only a function of h', so that it is possible to plot out a series of curves for α_0 against h' analogous to the $\{h', h'_{ob}\}$ curves in figure 5. For the extreme distances the angle of elevation will depend considerably upon the value of H chosen, but up to about $y = 2000$ km. we can draw a single set of curves, as in the case of h'_{ob}, and such a set is given in figure 7.

From these curves it is possible to construct a set of curves showing the distance y to which a ray travels, as a function of the initial angle of elevation α_0 for a series of frequencies, assuming, of course, the form of the $h'f$ curve at vertical incidence. The curves in figure 8 were actually worked out from an assumed sine-squared law of gradient in the layer, in which H is taken as 200 km. and the maximum density occurs 300 km. above the ground. They are taken from a paper by T. L.

Eckersley(3), which should be consulted for details of the method of computation. These curves show in another way that for a given range or distance there are two possible rays for each frequency between the penetration frequency at vertical incidence and the skip frequency corresponding to the nose of the $h'_{ob}f_{ob}$ curve.

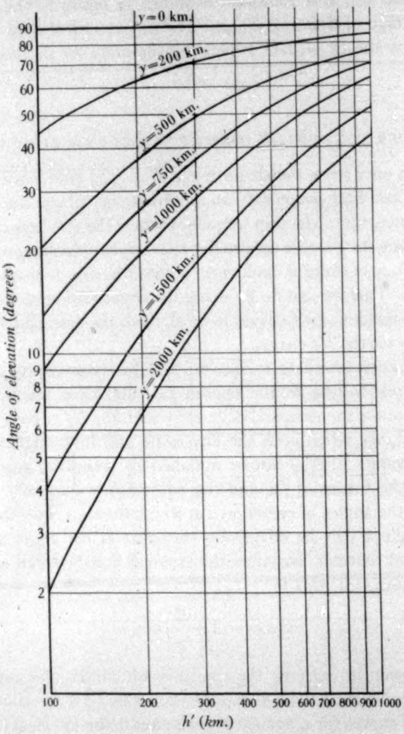

Figure 7. Angle of elevation as a function of h' for various distances from the transmitter.

They also show clearly why the skip frequency appropriate to a given distance is the maximum frequency receivable at that distance, since although the layer can return higher frequencies to the earth, they will for all angles of elevation be transmitted over the point in question, and come to earth again at some point beyond. For each frequency above the penetration frequency at vertical incidence there is a critical angle at which the ray escapes, and this angle is in general only slightly greater than the skip angle corresponding to the minimum range or skip distance.

The energy contained between these two angles at the transmitter is thus spread out on return to the earth from the skip distance to all greater distances; Eckersley's paper(3) may be consulted for a more detailed discussion of this point. This effect, coupled with the high absorption due to long traverse in the denser parts of the layer, explains why in practice the upper limb of the $h'_{ob}f_{ob}$ curve is extremely weak, and why it can only be observed in the region of the skip frequency.

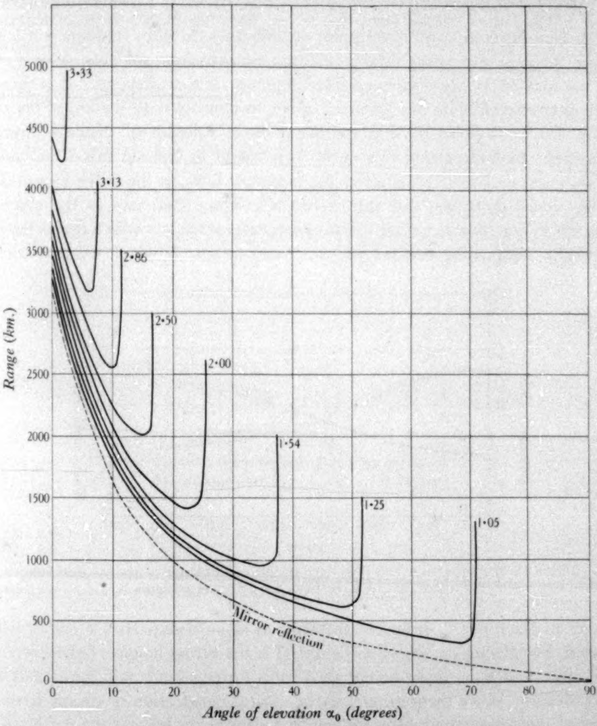

Figure 8. Range curves as a function of the angle of elevation for various values of f_{ob}/f_0.

The $h'_{ob}f_{ob}$ curve at any distance can be associated with the set of curves in figure 8 by considering the section of the curves made by the appropriate abscissa. We can see at once the important point that the nose of the $h'_{ob}f_{ob}$ curve does not correspond to the penetration frequency at vertical incidence, but that as derived from Martyn's theorem it corresponds to a point some way down the $h'f$ curve at vertical incidence. The part of the curve above this point becomes on application of the theorem (i.e. by the use of the transmission-curve technique) the upper or high-angle limb of the $h'_{ob}f_{ob}$ curve.

§7. THE CONSTRUCTION OF {SKIP-FREQUENCY, DISTANCE} CURVES

It is obvious from a practical point of view that the skip frequency at a given distance is a very important factor in oblique transmission problems, since it represents the maximum possible receivable frequency at that distance. It is therefore useful, in connexion with any given $h'f$ curve, to plot out with the aid of the transmission curves a curve of skip frequency as a function of distance from the transmitter. In interpreting this curve it is useful to bear in mind the complementary picture of figure 8, since it shows clearly how, as the range increases, the skip frequency increases, and approaches at extreme distances to the maximum escape frequency corresponding to the penetration of the ray which leaves the earth tangentially. Returning to equations (2·9) and (2·10), in which we may consider the layer to reach to the surface of the earth as far as the analysis is concerned, we replace h_0 by $(H+h_{\max})$, where as before H is the actual height of the lower edge of the layer, and $h_{\max}$ is the height above this lower edge at which the maximum density occurs. If we then write f_0 as the critical penetration or escape frequency at vertical incidence, the escape frequency f_{ob} for a ray leaving the earth with an angle of elevation α_0 is given by

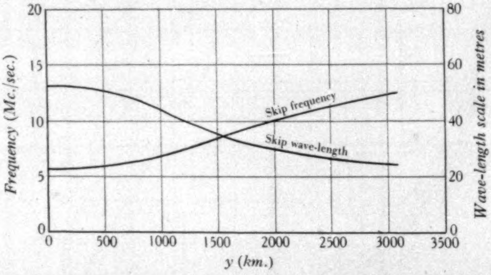

Figure 9. Skip frequency and skip wave-length as a function of the distance from the transmitter, derived from the $h'f$ curve in figure 6.

$$f_{ob}=f_0\Big/\sqrt{\left\{\sin^2\alpha_0+\frac{2\,(H+h_{\max})}{r_0}\cos^2\alpha\right\}}.$$

For large angles of elevation this reduces to the flat-earth case of $f_0/\sin\alpha_0$, but for the tangent ray $\alpha_0=0$, and the maximum escape frequency is $f_0\sqrt{\{r_0/2\,(H+h_{\max})\}}$.

Figure 9 shows a {skip-frequency, distance} curve deduced from the $h'f$ curve given in figure 6; the corresponding {skip-wave-length, distance} curve is also shown, since it is often useful for the engineer to think in terms of wave-length rather than of frequency. It will be seen that as the distance increases, the skip frequency approaches an upper limit, and in identifying it with the maximum escape frequency as above, we have to assign a value to $(H+h_{\max})$, i.e. the actual height above the ground at which the maximum density occurs. If we assume that $h_{\max}$ is small compared with H, we can take as an approximate value the value of h' corresponding to the lower limit of the $h'f$ curve under consideration (in the present case 380 km.). It is therefore useful to have a curve of $\sqrt{(r_0/2H)}$ as a function of H, given in figure 10, as a factor for obtaining the limiting frequency at extreme distances, from the penetration frequency at vertical incidence.

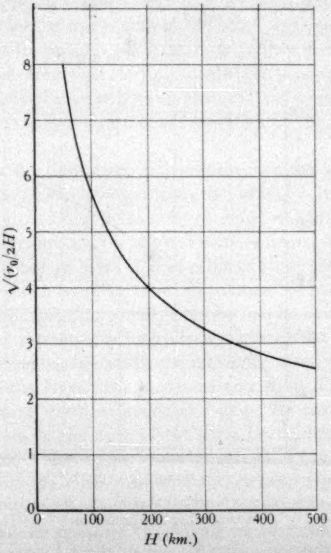

Figure 10. $\sqrt{(r_0/2H)}$ as a function of H, to give the limiting value of f_{ob}/f_0 at extreme distances.

We have to bear in mind here a point which has already been raised—that when the lower edge of the layer is at a height H, rays can only reach distances greater than $\sqrt{(8r_0H)}$ by a single hop when the equivalent frequency at vertical incidence penetrates to an equivalent height of at least $(2l-1)\,H$, l being the parameter given by equation (3·14). At these longer distances, say those greater than 2000 km., the shape of the transmission curves becomes increasingly dependent on the value of H assumed, and as far as the simple geometrical picture of the ray-path is concerned, the detailed analysis given above gives a clearer idea of what is happening than the simplified picture given by Smith; his picture is equivalent to assuming that at oblique incidence there is mirror reflection at a height h', the corresponding equivalent height at vertical incidence.* If we put $m=1$ in equation (3·13) so that

$$k=\frac{y^2}{8r_0H}+1,$$

and if we substitute in equation (3·9), remembering that P' is here $2h'$, and that H is h', we get

$$\tan\alpha=\frac{2h'}{y}+\frac{y}{4r_0}.$$

Smith uses $\cot\phi_0$ instead of our $\tan\alpha$, and gives

$$\cot\phi_0=\frac{h'+r_0(1-\cos\theta)}{r_0\sin\theta},\quad \text{where } \theta\doteq y/2r_0,$$

which gives $$\frac{2h'}{y}+\frac{y}{4r_0}\quad \text{when } \theta \text{ is small.}$$

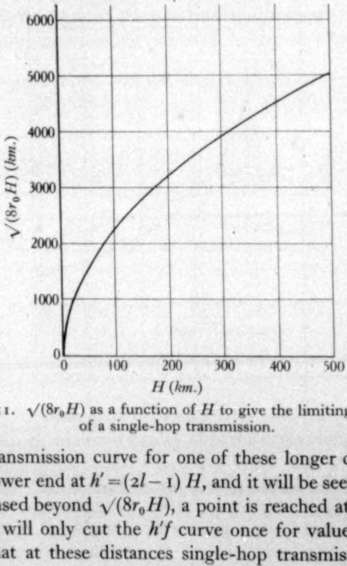

Figure 11. $\surd(8r_0H)$ as a function of H to give the limiting distance of a single-hop transmission.

If we draw a transmission curve for one of these longer distances, we have to terminate it at its lower end at $h'=(2l-1)H$, and it will be seen that as the distance considered is increased beyond $\surd(8r_0H)$, a point is reached at which the truncated transmission curve will only cut the $h'f$ curve once for values of f_{ob} greater than f_0. This implies that at these distances single-hop transmission is only possible with a high-angle ray. In practice, therefore, we should not expect to get a workable signal by a single hop much beyond the distance $\surd(8r_0H)$. It is therefore useful to have a curve of $\surd(8r_0H)$ as a function of H, and this is given in figure 11.

The analysis can be applied to the case of multiple hops by considering, in the case of n hops, the distance y/n for the determination of f_{ob}. The equivalent h'_{ob}

* While this paper has been in the press, N. Smith(4) has published another paper in which he gives a further correction for the curvature of the earth.

will be n times the value of h'_{ob} so obtained. In this way we can study the formation of multiple-echo patterns, and see how at long distances the first echo received may correspond to $n=3$, 4 or even more, where smaller values of n only are possible for the heavily attenuated high-angle ray. In this connexion it is again interesting to refer to the discussion on multiple echoes given on pp. 410 to 412 of Eckersley's paper(3).

§8. THE EFFECT OF A HORIZONTAL GRADIENT OF ELECTRONIC DENSITY AND OF THE EARTH'S MAGNETIC FIELD

As was pointed out in the introduction, the above analysis has been worked out on the assumption that there is no horizontal gradient of electronic density and no magnetic field. We have seen that starting from these premises the analysis can be developed to take account of the earth's curvature even at long distances, but we must now consider to what extent our results are modified by the inclusion of these two factors.

The presence of a horizontal density-gradient will in general cause a ray to emerge at a different angle of elevation from that at which it entered the layer, and unless the transmission is along a contour of equal maximum electronic density or at right-angles to the contours, the ray will suffer a lateral deviation. By assuming some law for the horizontal gradient it is possible to study these effects analytically, but it is clear that they both modify the simple picture we have analysed. The error will be greatest for a transmission at very oblique incidence across the density contours, in which the ray remains for long distances in the layer.

If we consider a single hop in which the incidence is not too oblique, so that the ray is actually only in the layer for a comparatively short distance, we can assume that there is no horizontal gradient over this region. We can then refer the process to the density conditions at the apex of the path, i.e. mid-way between the transmitter and the receiver. This implies that the vertical $h'f$ measurements should be made at this mid point. In testing out the theory over a given distance it is not necessarily feasible to make vertical-incidence measurements at the mid point, but as a compromise it may be possible, by making measurements at both ends of the path and averaging them, to get an idea of the characteristics at the mid point.

The effect due to the earth's magnetic field is very difficult to assess owing to the complexity of the magneto-ionic theory. In this theory the magnetic field enters through the term τ, which is the ratio of the gyromagnetic frequency f_H to the transmitted frequency. As is well known, at vertical incidence the extraordinary escape frequency exceeds the ordinary escape frequency by $f_H/2$ when τ is small. Now if we assume that at vertical incidence the $h'f$ curve for the extraordinary ray when plotted logarithmically is of the same shape as the curve for the ordinary ray, but shifted to the right, as in figure 12, so that the extraordinary escape frequency is greater by $f_H/2$ than the ordinary escape frequency, and if we then apply the transmission-curve technique to each, the $h'_{ob}f_{ob}$ curves obtained will be similar in shape and have the same shift, owing to the use of a logarithmic scale. The noses P and Q of the curves will correspond to two similar points O and E on the $h'f$ curves, and their actual separation in frequency will be $\frac{1}{2}f_H$ cosec α, where α is the angle of elevation appropriate to the equivalent height h' for the particular distance we are considering. (We are assuming that the frequencies at O and E are sufficiently near to their respective escape frequencies for their difference to be considered as $\frac{1}{2}f_H$.) The appropriate value of cosec α is simply given by the ratio of f_{ob}/f, the frequencies at P and O.

Referring again to the curves in figure 8, we see that the skip frequency for a given distance escapes through the layer for an angle which is only slightly greater than the skip angle, so that we may for the purposes of the present argument identify approximately the skip frequency with the frequency of the ray which just escapes when transmitted at the skip angle. Now by assuming an oblique transmission with a vertical magnetic field, it can be seen that if we consider the value of the difference of the escape frequencies ($f_{\text{ext}} - f_{\text{ord}}$) as a function of the angle of elevation α, then, provided τ is less than about 0·7, the value decreases below the value at vertical incidence as α decreases from 90°, and reaches a flat minimum before increasing up to infinity as α approaches zero. Moreover, this minimum occurs when $\alpha \doteqdot 36^\circ$ independently of the actual value of τ, and*

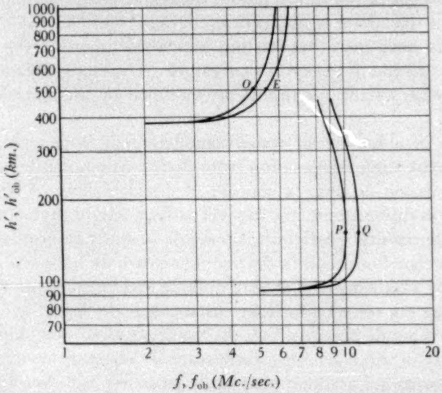

Figure 12. $h'_{\text{ob}}f_{\text{ob}}$ curves for ordinary and extraordinary rays derived from the equivalent $h'f$ curves, assuming that the equivalence theorem can be applied.

$$(f_{\text{ext}} - f_{\text{ord}})_{\text{oblique}} \doteqdot \frac{2\cdot 6\tau}{1+\tau}(f_{\text{ext}} - f_{\text{ord}})_{\text{vertical}}.$$

Thus instead of a factor of cosec α (which $= 1\cdot 7$ when $\alpha = 36^\circ$), we have a factor which is less than unity.

---

* I am indebted to Mr T. L. Eckersley for some analysis from which these results have been deduced.

From these results it seems safe to deduce that for most practical cases the value of $(f_{\mathrm{ext}} - f_{\mathrm{ord}})$ at the noses of the $h'_{\mathrm{ob}}f_{\mathrm{ob}}$ curves decreases as the distance from the transmitter increases, instead of increasing as the simple application of the theorem would suggest. Actually the shape of the $h'_{\mathrm{ob}}f_{\mathrm{ob}}$ curve cannot strictly be obtained from the vertical-incidence $h'f$ curve by means of the transmission curves, but it is reasonable to suppose that the process will be nearly true for the ordinary ray. If then for the vertical-incidence $h'f$ curve for the ordinary ray we construct the {skip-frequency, distance} curve as for figure 9, and take this to be correct for the ordinary ray, we know that the corresponding extraordinary curve will start with a separation of $\frac{1}{2}f_H$, and will then gradually close in towards the ordinary curve as the distance is increased.

Some idea of the way in which the two curves will converge can be obtained from the relation in terms of τ given above. This would seem to be a better way of allowing for the effect of the magnetic field than, say, applying the transmission curve technique to a curve sketched in between the vertical incidence $h'f$ curves for the ordinary and extraordinary rays.

§9. PRACTICAL APPLICATION OF THE ANALYSIS

The analysis we have been considering has its most practical application in the prediction of the behaviour of short waves over long distances, for determining the choice of frequencies to be used over any given route. Such routes can be divided into two classes according as they are of medium distance, where single-hop transmission is possible, or of extreme distance where the transmission is only possible by multiple hops. The latter case may be taken first, and as regards the optimum frequency to be used, we can restrict ourselves to the consideration of the case where the individual hops themselves represent long distances and low angles of elevation, since steeper angles imply lower usable frequencies and more overall attenuation.

In an idealized case the problem may be treated as a succession of similar hops, each one of which can be treated as for a single-hop transmission. In practice, however, owing to the changing density conditions en route, the path of any given order of echo will consist of a series of unequal hops, and the angle at which the ray enters and leaves the layer may change along the route. Moreover the signal which is received at an extreme distance will in general be the resultant of several low-angle rays, and the assessment of the total absorption under these conditions will be a complex problem. Actually the overall absorption is found to be equivalent to a transmission through a succession of grades of ionic density, so that the attenuation can be represented by $e^{\Sigma(-k_1 d_1)}$. Theoretically the coefficients k should be deducible by applying the absorption theorem to vertical-incidence measurements for a set of low-angle rays. In practice, however, they are obtained by analysing a large mass of practical long-distance transmission data. In determining the practicability of a given route, we have to consider the two major factors of electron limitation and absorption, and to remember that to some extent they represent opposing conditions.

We cannot go further here into this aspect of the problem, but it is obvious that in analysing any given route it would be most useful to know the density-distribution at every point along the route, so that it might be possible to deduce the absorption and the limiting frequency for low-angle rays for the different parts of the route. This serves to emphasize the need for regular vertical-incidence measurements at a large number of places in different parts of the world, so that the probable density-distributions at any place at any time and season may be predicted.

Coming now to the consideration of single-hop transmissions, and applying the transmission-curve technique, we have in practice to take account of the fact that the $h'f$ curve is not usually a curve of the simple type given, for instance, in figure 6, but results from the combined effects of the E and F layers. It is easily seen that a lower layer, for which the vertical-incidence escape frequency is less than that for a higher layer, may nevertheless control the skip frequency when both layers are present together. Thus in summer when the F_1 layer is well defined, it may control the skip frequency beyond a certain distance from the transmitter, and at still greater distances the E layer may take charge, although the vertical escape frequency may be considerably less than for the F_2 layer. This latter effect is especially likely in summer, because the E maximum density is then greater than in winter, while the F_2 density is considerably less and the layer-height markedly greater than in winter, and it accounts for the fact that distant stations working on, say, 15 m. are sometimes out of the skip, when a casual measurement of the F_2 escape frequency would suggest that the limiting wave-length should be much longer.

In deducing, therefore, from the vertical $h'f$ curve the {skip-frequency, distance} curve of the type shown in figure 9, this possible shielding of the F layer by the E layer has to be taken into account, but provided that the set of transmission curves is applied to the complete $h'f$ curve, this is allowed for in the graphical process, which shows immediately the distance at which the lower layer takes charge.

For an assumed value of H we have seen that we should not expect to get a workable signal much beyond a distance $\sqrt{(8r_0H)}$ given in figure 11, and that at this distance the maximum transmissible frequency is approaching the maximum escape frequency $f_0\sqrt{(r_0/2H)}$, where f_0 is the vertical escape frequency. In practice these theoretical limits must be somewhat reduced. It is necessary to allow a small margin of safety in order not to work too near to the edge represented by the skip frequency. Further, the factor should be reduced to allow for the actual depth of penetration into the layer; and since a ray leaving the transmitter tangentially would be heavily absorbed by the ground before getting clear, it is usual to assume that the initial angle of elevation should be somewhat greater than zero, say about 5°, and the polar diagram of the aerial is usually adjusted accordingly. These considerations lead to the choice of an optimum frequency which is less than the skip frequency, and some corresponding arbitrary factor could be incorporated as a reduction factor in the curves of figures 10 and 11. But it is felt that it is better to give the ideal curves, and to indicate in general terms, as above, the necessary modifications. The method of allowing for the effect of the earth's magnetic field has been given above to take account of the fact that the extraordinary ray, rather than the ordinary ray, determines the maximum usable frequency, whereas the vertical-incidence $h'f$ curve for the ordinary ray is used for deducing the oblique-incidence curve.

Mention has already been made of the importance in accurate work of knowing the density-distribution at the mid point of the path rather than at either end, especially for experiments designed to test out the fundamental soundness of the analysis. When a pulse transmission is received at a medium distance from the transmitter, the echo pattern obtained can be very complex as a result of possible multiple hops, low-angle and high-angle pairs, ordinary and extraordinary pairs due to magneto-ionic splitting, and simultaneous reflections from different layers. From a knowledge of the vertical-incidence $h'f$ curve, the positions of the various possible echoes for the given distance and frequency can be predicted, and this provides a check on the theory, and conversely aids in the interpretation of the complex echo pattern actually obtained.

By keeping a watch on the vertical-incidence conditions, the course of a $P't$ run on a fixed frequency at a given distance can be deduced. For instance, if a run is taken during the evening, when the general level of electronic density is falling, the appearance of the high-angle ray and its movement in towards the corresponding low-angle ray, with eventual coalescence as the signal goes into the skip, can be interpreted in a simple graphical way, by considering the gradual shift to the left of the $h'_{\mathrm{ob}}f_{\mathrm{ob}}$ curve, as the $h'f$ curve moves to the left with decreasing density.

§ 10. CONCLUSION

Although the analysis given in this paper admittedly refers to an ideal case, and the necessary modifications (in particular that due to the earth's magnetic field) can only be expressed in a rather qualitative way, it is found in practice to be very useful in the explanation of oblique-incidence transmission phenomena. Graphs such as figures 3, 4, 5, 7, 10 and 11, which can be applied to any given $h'f$ curve to give curves of the type shown in figures 6, 8 and 9, will, it is hoped, form a helpful tool in the hands of those who are engaged on oblique-incidence and long-distance transmission problems.

REFERENCES

(1) Martyn, D. F. *Proc. Phys. Soc.* **47**, 332 (1935).
(2) Smith, N. *Bur. Stand. J. Res.* **19** (July 1937).
(3) Eckersley, T. L. *J. Instn Elect. Engrs*, **71**, 423, 424 (1932).
(4) Smith, N. *Bur. Stand. J. Res.* **20** (May 1938).

THE NUCLEAR MAGNETIC MOMENT OF COPPER

By S. TOLANSKY, Ph.D. and G. O. FORESTER, B.Sc.
Manchester University

Communicated by Prof. P. M. S. Blackett, F.R.S., 30 *April* 1938.
Read in title 24 *June* 1938

ABSTRACT. The doublet hyperfine structures of the resonance lines of the copper arc spectrum, λ3247 and λ3274, have been measured with a quartz Lummer plate. The lines are produced free from reversal effects, the doublet separations being respectively 379 and 405×10^{-3} cm^{-1}. The following hyperfine structure interval factors are calculated: $3d^{10}4s\,^2S_{\frac{1}{2}} = 197{\cdot}5$, $3d^{10}4p\,^2P_{\frac{1}{2}} = 14$ and $3d^{10}4p\,^2P_{1\frac{1}{2}} = 4{\cdot}8$ (all in cm$^{-1} \times 10^{-3}$). The mean nuclear magnetic moment for the two copper isotopes, 63 and 65, is derived from the ground state, $3d^{10}4s\,^2S_{\frac{1}{2}}$. The value found is $\mu = 2{\cdot}47$ nuclear magnetons, this being probably a better estimate than that given by other terms, since the ground state is spherically symmetrical and thus not affected by quadrupole moment of the nucleus. By adopting Schüler and Schmidt's value for the ratio of the magnetic moments of the two isotopes, it is found that $\mu\,(^{63}\text{Cu}) = 2{\cdot}43$ and $\mu\,(^{65}\text{Cu}) = 2{\cdot}54$ nuclear magnetons.

§ 1. INTRODUCTION

The nuclear spins of the two copper isotopes, 63 and 65, have been determined by Ritschl(1), who measured hyperfine structures in a number of the lines of the CuI spectrum. The spins of both the isotopes are the same, namely $\frac{3}{2}$. The spectrum was excited in a liquid-air-cooled hollow cathode, and amongst the lines measured were the two very intense resonance lines,

$$\lambda 3247\ (3d^{10}4s\,^2S_{\frac{1}{2}} - 3d^{10}4p\,^2P_{1\frac{1}{2}})$$

and

$$\lambda 3274\ (3d^{10}4s\,^2S_{\frac{1}{2}} - 3d^{10}4p\,^2P_{\frac{1}{2}}).$$

From these the hyperfine structure splitting in the ground term $3d^{10}4s\,^2S_{\frac{1}{2}}$ can be derived, and as this in effect arises from a single *s* electron it is a term very well suited for the calculation of the nuclear magnetic moment. Fermi and Segré(2), using Ritschl's data for this term, have evaluated a mean magnetic moment, assuming that the moments are nearly the same for both isotopes. They give $\mu = 2{\cdot}42$ nuclear magnetons. Schüler(3) has recalculated this from the same data, and after stating that Fermi and Segré have made a small numerical error, gives $\mu = 2{\cdot}74$. This is no doubt a misprint, since in a later paper Schüler and Schmidt(4) quote $\mu = 2{\cdot}44$ as the value given by Ritschl's measurements upon the ground term.

Schüler and Schmidt(4) have repeated Ritschl's observations upon two lines, λ5700 ($3d^9 4s^2\,^2D_{1\frac{1}{2}} - 3d^{10}4p\,^2P_{1\frac{1}{2}}$) and λ5782 ($3d^9 4s^2\,^2D_{1\frac{1}{2}} - 3d^{10}4p\,^2P_{\frac{1}{2}}$), which, it will be noted, include as upper terms the upper levels of the two resonance lines. These investigators showed that the interval rule is not obeyed in the $3d^9 4s^2\,^2D_{1\frac{1}{2}}$ term, and from it they derived both nuclear quadrupole moments and nuclear magnetic moments. The latter were found to be different for the two isotopes, the calculated values being μ (^{63}Cu) = 2·52 and μ (^{65}Cu) = 2·64, and the weighted mean μ for both isotopes = 2·56. The value given for the quadrupole moment q is

$$-0{\cdot}1 \pm 0{\cdot}1 \times 10^{-24}\ \text{cm}^2.$$

The calculation of these quantities presupposes that the observed irregularities in the intervals are entirely to be attributed to a nuclear deviation from spherical symmetry, and it is clear from the high probable error given for q that uncertainties due to incomplete resolution will introduce small errors into the calculation of μ.

If there is a real quadrupole moment, the value of μ derived from the ground term is to be preferred since, being an S term, it is spherically symmetrical and therefore unaffected by any nuclear deviations from symmetry. It is thus clear that accurate measurements of hyperfine structure for the ground term are desirable. However, a difficulty exists here because the resonance lines are extremely sensitive to self-reversal. Early measurements by Back(5) were vitiated by the existence of complete self-reversal. Frisch(6) and Green and Wulff(7) examined these lines with concave gratings but, consequently, the order of accuracy was not high. Sibaiya(8) has attempted to measure the separations of the components by allowing complete self-reversal to take place, measuring to the centre of the reversal. The separation he reports for one line is in close agreement with that given here, but in the other line there is a deviation by 4 per cent.

Ritschl(1), who, owing to the use of a superior source, has no doubt succeeded in measuring these lines more accurately than the other observers quoted, discusses the question of self-reversal. The hollow cathode employed by him had an 8-mm. bore and was 10 cm. long. The result was that even with currents of only 50 ma. the resonance lines were completely reversed. He was obliged to use a current of 30 ma., with consequent long exposure, before he could eliminate reversal. He points out that, in spite of this, the lines were broadened, and he considers that his accuracy of measurement was not very high. That there still existed a certain amount of reversal is shown by the fact that the intensity ratio of the doublets seen by him was 2 : 1 instead of the theoretical ratio 5 : 3. The instruments used by Ritschl for measuring the structures were a reflection echelon and a Fabry-Perot interferometer coated with Hochheim alloy.

In the present paper are given details of measurements made upon the copper resonance lines, which have been obtained entirely free from reversal effects.

§ 2. EXPERIMENTAL DETAILS

The copper resonance lines λ3247 and λ3274 were obtained by accident in a water-cooled hollow-cathode tube which was being used to examine hyperfine structures in the spectra of iodine. The tube was a modified Schüler tube, the upper part of the cathode being a brass tube about 8 cm. in diameter and 18 cm. long, the lower hollow cathode portion having a bore of 1 cm. and a length of 15 cm. The lower portion was made of oxidized iron and was lined with platinum. Helium containing iodine vapour was continuously circulated through the tube at a pressure of 2 mm. Under these conditions the narrow hollow cathode was filled with light and a rich iodine spectrum was emitted. When the helium pressure was reduced, a sudden change in the nature of the discharge took place at a critical pressure. The discharge left the narrow hollow cathode and filled the wide upper portion of the cathode cylinder. A peculiar change in the iodine emission spectrum was noticed. This will be discussed elsewhere. At the same time the copper resonance lines appeared in the discharge, and it is clear that they originated in the copper in the brass tube constituting the upper, and normally unused, portion of the discharge tube.

Even with currents reaching up to 500 ma., no trace of any other copper lines could be found, from which it is clear that the concentration of copper in the discharge must have been exceedingly minute. It is possible that the iodine attacked the brass wall and formed copper iodide, which would break up under bombardment and thus liberate free copper atoms into the discharge. Under all conditions of excitation, and even with currents up to 400 ma., the lines remained exceedingly sharp, the hyperfine-structure components showing no trace of reversal and exhibiting intensity-ratios of approximately the theoretical values. This is remarkable when it is remembered that currents of 30 ma. produced a certain amount of reversal in Ritschl's experiments. It is not quite clear whether the discharge in the brass tube is a hollow-cathode discharge, but if it is, then the current-density must be very low. Ritschl's current-density was about 60 ma./cm^2, whereas when we used 150 ma., our current density was 3 ma./cm^2, if the whole tube was acting as a hollow cathode. This may explain why the lines are so sharp. On the other hand, the excitation mechanism is probably quite different from that which obtains in the normal hollow cathode, since we obtain good exposures, through the interferometer, in fifteen minutes, whereas Ritschl pointed out that with his current-densities long exposures were required. Whether the iodine or the tube diameter is the cause, the fact remains that the individual hyperfine-structure components were very sharp and yet the lines were strong. The separations could be measured with an accuracy of the order of 0·25 per cent.

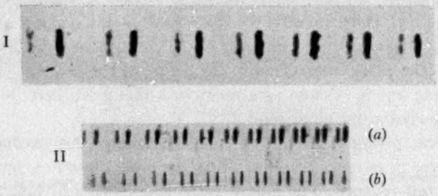

Figure 1. I, structure in λ 3247 (× 10); II (*a*), structure in λ 3247 (× 4); II (*b*), structure in λ 3274 (× 4).

The structures in the lines were measured with a quartz Lummer plate and checked with the aid of a variable-gap quartz Fabry-Perot interferometer coated with aluminium. The Lummer plate, recently acquired from Adam Hilger Ltd., is a particularly fine one and is free from ghosts. When extreme overexposure is used, single lines show a shading off to one side, but under normal working conditions the instrument is entirely ghost-free. It is made of crystalline quartz, the length being 20 cm. and the thickness 0·342 cm. The resolving-power is high when the extraordinary ray is used, particularly when the emergence angle is near grazing. It may be pointed out that even in the visible region, where high reflecting coefficients are available, the Lummer plate is superior to the Fabry-Perot interferometer when the structures are so large that only a small-gap Fabry-Perot interferometer can be used.

The Lummer plate was set up before the slit of a quartz spectrograph. The latter was made in the laboratory and has a collimator focal length of 30 cm. and a camera focal length of 100 cm. The interferometer fringes were projected with a quartz fluorite achromat of focal length 21 cm., so that the effective focal length used for photographing the fringes was 70 cm. Since the Lummer plate is thin, the dispersion is large. In spite of the magnification, the individual components were very sharp, figure 2.

Since we are able to measure separations to 1 part in 1000 with this Lummer plate, Dr Simeon, of Messrs Adam Hilger Ltd., has kindly recalculated the dispersions for us. He has given us dispersions to four figures over the range 6500 to 2000 A.

§ 3. OBSERVATIONS AND ANALYSIS

Both the lines λ3247 and λ3274 were found to be simple doublets each consisting of two components with intensity-ratio visually estimated as 1·5 : 1. (The theoretical ratio is 1·66 : 1, which is some 10 per cent greater. Such a difference can hardly be distinguished visually and we may safely assume that the theoretical intensities are those which actually occur.) In both lines the weaker component is towards the violet. The separation in λ3247 is 379×10^{-3} cm.$^{-1}$, and in λ3274 it is 405×10^{-3} cm.$^{-1}$, the error in each case not being much greater than 1×10^{-3} cm.$^{-1}$

Although Ritschl's lines were broadened, the separations he reports are very close to those given here. In table 1 are the separations according to Sibaiya, Ritschl and the authors.

Table 1

Wave-length	Separation (cm. × 10^{-3})		
	Sibaiya	Ritschl	Authors
3247	366	371	379
3274	406	405	405

Attention may be drawn to the fact that Sibaiya's lines were completely reversed and Ritschl's lines somewhat broadened, while our lines were quite sharp. Only λ3247 seems to be affected by the reversal, the separation of the components diminishing with increasing amount of reversal.

In Ritschl's measurements the uncertainty due to the widths of the lines was such that he predicted a separation of 394×10^{-3} cm.$^{-1}$ for λ3247. This value he accepted for the purpose of analysis and he was unable to show that it is actually incorrect. This has led him to assign an incorrect value to the structure of the $3d^{10}4p\ ^2P_{1\frac{1}{2}}$ term. Schüler and Schmidt also prove that this term is wrongly analysed, from a consideration of the structures in λ5700 and λ5782. Ritschl's measurements lead to a structure of 390×10^{-3} cm.$^{-1}$ for the ground term.

In figure 2 are drawn the lines reported here and those studied by Schüler and Schmidt, the latter being dotted. The broken line λ5105 is one of those measured by Ritschl and utilized by Schüler and Schmidt in deriving a value for the nuclear magnetic moment. The dotted lines exhibit isotope displacement, and from their structures Schüler and Schmidt conclude that the hyperfine-structure separations in the $3d^{10}4p\ ^2P_{\frac{1}{2}}$ level are respectively 28×10^{-3} cm.$^{-1}$ for the more abundant isotope (63) and 29×10^{-3} cm.$^{-1}$ for the less abundant isotope (65). The isotope abundance ratio is about 2·1 : 1. The mean interval factor of this term for the two isotopes, given independently by Ritschl, is 28×10^{-3} cm.$^{-1}$ The lines involved are in both cases highly complex and incompletely resolved. A careful examination of the structure diagram given by Schüler and Schmidt for λ5782, which is more completely resolved than λ5700, shows that while the value 28×10^{-3} cm.$^{-1}$ is certainly correct for the lighter isotope, some uncertainty exists as to whether the separation for the heavier isotope actually differs by the very small amount suggested; if the nuclear magnetic moments are different, the small variation will be expected. We shall assume here that the structure in the $3d^{10}4p\ ^2P_{\frac{1}{2}}$ term is 28×10^{-3} cm.$^{-1}$ for both the isotopes, and it is quite certain that no appreciable error is introduced into our analysis of the structure of the ground term, since this does not exhibit a measurable isotope displacement, owing no doubt to the fact that the *d* electron shell is here complete.

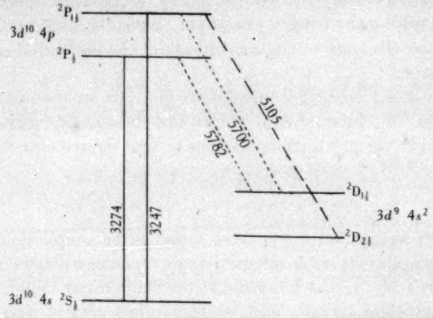

Figure 2

The analysis of the structure of λ3274 is shown in figure 3. The arrow heads, drawn at the centres of gravity of each close unresolved pair of components, represent the positions of the observed lines. On the basis of this analysis the separation in the $3d^{10}4s\ ^2S_{\frac{1}{2}}$ ground term is 395×10^{-3} cm.$^{-1}$

Figure 4 shows the analysis for the line λ3247. In this case the lower term is made to have the separation 395×10^{-3} cm.$^{-1}$ already derived, and a value adopted for the interval factor in the upper term which will make the centre of gravity of the two components 379×10^{-3} cm.$^{-1}$ apart. It can be justifiably assumed that the interval rule holds in the upper term, since deviations will only introduce a second order effect. The interval factor calculated by this method for the upper term, $3d^{10}4p\ ^2P_{1\frac{1}{2}}$ is $4{\cdot}8 \times 10^{-3}$ cm.$^{-1}$ This is in remarkably exact agreement with that found by Schüler and Schmidt for the same term by means of the line λ5700. These authors give the separation as $4{\cdot}8 \times 10^{-3}$ cm.$^{-1}$ for the more abundant isotope and estimate $5{\cdot}0 \times 10^{-3}$ cm.$^{-1}$ as the separation for the less abundant isotope. The difference between these can be neglected. The close agreement for the structure derived from quite independent lines confirms the analysis made by Schüler and Schmidt and by us, and in particular it shows that the value 395×10^{-3} cm.$^{-1}$ for the ground term is very accurate.

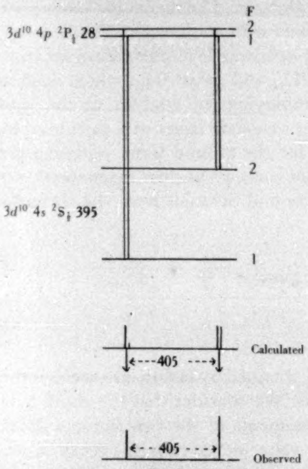

$3d^{10}\ 4p\ ^2P_{\frac{1}{2}}$ 28
F
2
1
2
$3d^{10}\ 4s\ ^2S_{\frac{1}{2}}$ 395
1
405
Calculated
405
Observed

λ3274

Figure 3

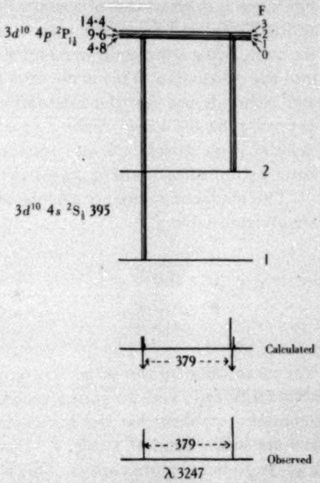

14·4
$3d^{10}\ 4p\ ^2P_{1\frac{1}{2}}$
9·6
4·8
F
3
2
1
0
2
$3d^{10}\ 4s\ ^2S_{\frac{1}{2}}$ 395
1
379
Calculated
379
Observed

λ 3247

Figure 4

The interval factors for the terms we have observed are shown in table 2.

Table 2

Term	Interval factor (cm.$^{-1} \times 10^{-3}$)
$3d^{10}4s\ ^2S_{\frac{1}{2}}$	197·5
$3d^{10}4p\ ^2P_{\frac{1}{2}}$	14·0
$3d^{10}4p\ ^2P_{1\frac{1}{2}}$	4·8

The differences in $\lambda 3247$ in table 1 can be accounted for, if it is assumed that there is preferential absorption of the component $\Delta F = 2 \rightarrow 1$. Thus it is the line coming from the higher F level of the term with higher J that is more absorbed.

§ 4. THE NUCLEAR MAGNETIC MOMENT

As has previously been pointed out, the ground state $3d^{10}4s\ {}^2S_{\frac{1}{2}}$ is well suited for the calculation of the nuclear magnetic moment of copper, since the term configuration is in effect that of a single penetrating electron. The theory of Goudsmit⁽⁹⁾ and of Fermi and Segré⁽²⁾ can therefore be applied with confidence. Furthermore, the state, being spherically symmetrical, nuclear quadrupole moment does not enter into the calculation. This is not true for $3d^9 4s^2\ {}^2D_{1\frac{1}{2}}$ and $3d^9 4s^2\ {}^2D_{2\frac{1}{2}}$, which Schüler and Schmidt use for the calculation of μ, employing the analysis of the lines $\lambda\lambda 5700$, 5782 and 5105. Since 2·44 is the nuclear magnetic moment μ calculated by Schüler from Ritschl's value, 390×10^{-3} cm.⁻¹, for the ground term, replacing the latter by our measurement, 395×10^{-3} cm.⁻¹ gives $\mu = 2{\cdot}47$ nuclear magnetons.

The magnetic moments calculated by Schüler and Schmidt from the ${}^2D$ terms are given in table 3.

Table 3

Term	Mean μ	μ (^{63}Cu)	μ (^{65}Cu)
$3d^9 4s^2\ {}^2D_{1\frac{1}{2}}$	2·56	2·52	2·64
$3d^9 4s^2\ {}^2D_{2\frac{1}{2}}$	2·5		

The mean value for the $3d^9 4s^2\ {}^2D_{\frac{1}{2}}$ term has been obtained by taking into account the abundance ratio and weighting according to this. We consider that the above data definitely establish that the nuclear magnetic moments of the two isotopes differ and are in the ratio of 1·048 : 1. However, the value we give for the mean μ, i.e. 2·47, is probably more correct. This is due partly to the absence of perturbation and partly to the fact that a penetrating s electron is involved. This latter point is important, since the formula for the magnetic moment is likely to be more correct here. If we adopt the ratio 1·048 : 1 for the two isotopes, we can derive magnetic moments for them. Thus we have finally the values shown in table 4.

Table 4

Term	Mean μ observed	μ (^{63}Cu) calculated	μ (^{65}Cu) calculated
$3d^{10}4s\ {}^2S_{\frac{1}{2}}$	2·47	2·43	2·54

§ 5. ACKNOWLEDGEMENT

The Lummer plate and the optical parts of the spectrograph were purchased with the aid of a grant made to one of us (S. T.) by the Government Grants Committee of the Royal Society.

We wish to thank Dr Simeon for recalculating the dispersions of the Lummer plate.

REFERENCES

(1) Ritschl, R. *Z. Phys.* **79**, 1 (1932).
(2) Fermi, E. and Segrè, E. *Z. Phys.* **82**, 729 (1933).
(3) Schüler, H. *Z. Phys.* **88**, 323 (1934).
(4) Schüler, H. and Schmidt, Th. *Z. Phys.* **100**, 113 (1936).
(5) Back, E. *Ann. Phys., Lpz.*, **70**, 368 (1936).
(6) Frisch, S. *Z. Phys.* **71**, 89 (1931).
(7) Green, J. B. and Wulff, J. *Nature, Lond.*, p. 409 (1931).
(8) Sibaiya, L. *Proc. Ind. Acad. Sci.* **1**, 321 (1934).
(9) Goudsmit, S. *Phys. Rev.* **43**, 636 (1933).

THE SPECIFIC HEAT OF NICKEL FROM 100° C. TO 600° C.

By C. SYKES, D.Sc. and H. WILKINSON, Ph.D.

Communicated by Prof. N. F. Mott, F.R.S., 22 March 1938. *Read in title* 10 *June* 1938

ABSTRACT. The {specific-heat, temperature} curves for four different types of nickel have been determined, and the effects of method of manufacture, heat treatment, and chemical composition have been ascertained. The results, together with those obtained by previous investigators, are reviewed, and an attempt made to evaluate the most probable $\{C_p, T\}$ curve for nickel for the temperature range 100° c. to 600° c.

---

§ 1. INTRODUCTION

STONER⁽¹⁾ has made an analysis of certain experimental values for the specific heat of nickel with a view to obtaining some indication of the dependence of electronic energy on temperature and magnetization for a ferromagnetic material. The treatment followed by him is, briefly, as follows. After subtraction of a calculated dilatation correction $(C_p - C_v)$ from the measured specific heat C_p to obtain C_v, C_v is considered as the sum of three terms, so that $C_v = C_Q + C_E + C_M$. C_Q is the main contribution to the specific heat, connected with lattice energy, represented by a Debye expression and calculated when a reasonable estimate of the characteristic Debye temperature Θ_D has been made. C_E and C_M together comprise an electronic specific heat, C_M being the part of it associated with the spin orientation of the electrons and hence with the magnetization, while C_E is associated with changes in translational state.

Theoretical estimates of C_E are made, and from low-temperature measurements of specific heat $(C_Q + C_M)$ is found by difference, as $(C_v - C_E)$; the Debye temperature Θ_D governing the values of C_Q can be most accurately deduced from specific heats at low temperatures, where C_M is small, by comparison, and an approximate estimate of its value is sufficient. The value of Θ_D then gives values of C_Q for all temperatures and so leads to values for C_M. From C_M estimates of the molecular field coefficient are made for comparison with those found by other methods.

The object of the present paper is to present the results of new precise determinations of the specific heat of nickel which, while in general confirming the values previously adopted, serve as additional criteria for the choice of values of the specific heat in cases in which previous results are not in sufficiently good agreement to enable reliable theoretical deductions to be made.

Although almost all previous investigators claim an accuracy of at least 2 per cent in the measurement of specific heat, comparison of their results shows discrepancies in excess of that amount. The lack of agreement has been ascribed to differences in the degree of purity, method of manufacture, metallographic structure and heat treatment of the specimens. On the other hand, no investigator has studied the effect of impurities using identical apparatus and technique. Consequently, it appeared probable that some part of the discrepancies were, in fact, experimental error.

Above the Curie point the C_M term vanishes and the specific heat C_v is made up of two terms C_Q and C_E. As the lattice energy contribution C_Q is of the order of 80 per cent of the measured value C_p, relatively small errors in C_p give rise to large percentage errors in the value of C_E obtained by difference. The effect of impurities on C_p should be relatively small, yet some of the greatest discrepancies between the results of previous workers occur in the region above the Curie point. Using four different types of nickel prepared in a variety of ways, we have investigated this part of the {specific-heat, temperature} curve very carefully and find that any differences which can be ascribed to the presence of impurities or insufficient annealing are of the order of our experimental error, namely 2 per cent.

Impurities undoubtedly affect the Curie temperature, for instance 1 per cent of cobalt raises it by about 12° C. whereas the addition of 1 per cent of silicon lowers it by 70° C. It has been suggested that the shape of the {specific-heat, temperature} curve in the neighbourhood of the Curie point is very sensitive to the presence of impurities, and that for perfectly pure nickel, free from strain, the curve should drop very steeply to a minimum just above the Curie point, indicating that the co-ordination of electron spin even for small groups of atoms vanishes completely at the Curie point. On the other hand, by analogy with superlattice formation, local co-ordination above the Curie point would be expected, and this would give rise to a tail on the {specific-heat, temperature} curve. Our experimental technique is better adapted to the investigation of the rapid variation of C_p in the Curie-point region than any previously used, as it permits continuous measurements of instantaneous specific heat to be made as the temperature of the specimen is varied. All the specimens examined, irrespective of their heat treatment, gave {specific-heat, temperature} curves in which no sharp minimum occurred just above the Curie point and it is concluded that this feature of the curve is not particularly sensitive to traces of impurity or variations in heat treatment.

§ 2. EXPERIMENTAL ARRANGEMENTS

Method. The apparatus and technique employed were identical with those used in investigations on superlattice transformations in the alloys Cu_3Au (3) and CuZn (4), and has been fully described elsewhere (5). The principle is as follows. The specimen is heated electrically *in vacuo* at about 1·5° C. per minute inside a copper enclosure which is heated independently at the same rate. The temperature-difference between specimen and enclosure is kept small, namely ±0·5° C. A small differential heating or cooling-rate of the specimen relative to the enclosure is measured by observing the deflection of a sensitive galvanometer which is energized by a differential thermocouple. Rapid changes in specific heat appear as changes in the differential heating-rate, and by taking readings of the galvanometer at half-minute intervals data are obtained from which the instantaneous specific heat may be calculated at temperature-intervals of 1° C. if desired.

In the temperature-range from 400° C. to 600° C. the specific-heat measurements have been supplemented by experimental measurements of the differences of total energy content. A copper voltameter is used to integrate the current which is supplied to raise the temperature of the specimen from 400° C. to 600° C. The current is passed intermittently so that the temperatures of specimen and enclosure never vary by more than ±0·3° C. These measurements serve as a reliable check on the direct measurements of the {specific-heat, temperature} curve and will be discussed in § 3.

Material. Four types of nickel designated I, II, III and IV have been examined. The chemical analysis is given in table 1. Samples II and III are very pure. I has a low Curie point, and IV a high Curie point. The selection is thus reasonably representative.

Table 1

Material	Impurities (per cent)							
	Iron	Cobalt	Carbon	Copper	Manganese	Silicon	Sulphur	Oxygen
I Commercial	0·15	0·45	—	—	0·03	0·19	—	—
II Mond pellets	0·031	Nil	0·025	0·007	—	—	0·004	—
III Powder	0·04	Nil	trace	—	—	—	—	trace
IV Cathode	0·01	0·41	—	0·04	—	—	—	—

The specific-heat specimens were prepared in the form of closed hollow cylinders 1 in. in diameter and 1¼ in. long, and weighed approximately 100 g. Sample I was machined from a forged bar 1⅛ in. in diameter and is typical of material classed as commercially pure nickel. Samples II, III and IV were prepared from raw material very kindly provided by the Mond Nickel Company through the agency of Mr W. T. Griffiths and Dr L. B. Pfeil. The analyses given for these materials refer to the raw material before melting or sintering and were supplied by the Mond Nickel Laboratories. Samples II and IV were melted in a high-frequency furnace in high vacuum, the pressure being less than 10^{-3} mm. of mercury, and then hammered to a suitable shape before being machined. Sample III was prepared by sintering a block of pressed powder *in vacuo* at 900° C., that is to say, the material was not melted. The sintered block was slightly porous, having an apparent density 85 per cent that of melted nickel. It machined quite satisfactorily. Except where the contrary is stated the specific-heat specimens after being machined were heated *in vacuo* to 900° C. and cooled at 1° C. per minute to room-temperature before measurements were made.

Accuracy. In a previous paper(5) the errors likely to arise in specific-heat measurements made by the method used in this investigation have been discussed at length for the temperature range 100° C. to 400° C. Absolute errors arise in the determination of power input of ±0·2 per cent, of heating rate ±0·4 per cent and from faulty experimental conditions due to uncertainties regarding the e.m.f. of the differential thermocouple ±0·2 per cent. Observational errors are found to be within the limits of ±0·75 per cent, but these can substantially be eliminated by taking a large number of experimental points. Consequently it is reasonable to conclude that the maximum absolute error will not exceed ±1 per cent, with a probable error of ±0·5 per cent. This claim is made for results recorded in this paper for the region 100° C. to 400° C. with the exception of a 10° C. interval immediately above the Curie point. In this region the specific heat falls very rapidly, and errors in determining the differential heating rate (which can be neglected in general) become appreciable, with a consequent increase in the observational error to about twice the normal value, viz.: ±1·5 per cent. Again these errors have been minimized graphically from a large number of experimental points, and we estimate the absolute error in this region to be within ±1·5 per cent.

In the region from 400° C. to 600° C. the accuracy falls off rapidly, primarily owing to uncertainty regarding the e.m.f. of the differential thermocouple. The experimental method involves the assumption that the e.m.f. of the differential thermocouple is known when specimen and enclosure are at the same temperature. Experience indicates that, even after special precautions have been taken in the preparation of the thermocouples, no two thermocouples give exactly the same e.m.f. at the same temperature, nor is the e.m.f. exactly reproducible. For a true difference in temperature of 1° C. between specimen and enclosure the corresponding radiation correction amounts to 1·6 per cent of the specific heat at 400° C. and 5 per cent at 600° C. Consequently, the e.m.f. for zero temperature-difference must be known and reproducible to an amount corresponding to 0·2° C. at 600° C., i.e. 1 part in 3000, in order that errors in specific heat due to this cause alone shall not exceed ±1 per cent. Our experience is that the limit of accuracy of the differential thermocouple is of this order at 600° C. Observational errors also increase in consequence of experimental difficulties encountered in heating the copper enclosure at a steady rate at high temperatures.

In order to minimize errors due to these difficulties as far as possible, we have supplemented specific-heat measurements by measurements of differences of energy-content from 400° C. to 600° C. Duplicate measurements have been made with the differential thermocouple reversed and with different thermocouples. In this way errors due to choice of an incorrect e.m.f. for zero temperature-difference between specimen and enclosure are eliminated, and only errors due to lack of reproducibility remain. The measurements are independent of any precise determination of the heating rate, and agree for a definite arrangement of the differential thermocouple to within ±0·4 per cent. The absolute accuracy of the mean values of the energy-content difference is estimated to be within ±1 per cent. As a check the change in energy-content of copper from 400° C. to 600° C. has been determined. The result, 20·79 cal./g., agrees with that found by Jaeger by the calorimeter method, 20·60 cal./g. to within 1 per cent.

The experimentally determined values of specific heat have been used to give the shape of the {specific-heat, temperature} curve, and the actual curves have been

Table 2

Specific heat of nickel (cal./g. per ° c.) × 10^4

Temperature (° c.)		0	10	20	30	40	50	60	70	80	90	100
	I	Commercially pure nickel						1060	1077	1095	1111	
	II	Vacuum melted pure Mond						1055	1079	1096	1111	
0	III	Pressed powder							1066	1088	1106	
	IV	Cathode nickel						1060	1080	1096	1112	
	Mean of II and III								1072	1092	1108	
	I	1128	1143	1156	1169	1181	1191	1202	1210	1220	1230	
	II	1125	1138	1149	1160	1170	1180	1188	1197	1205	1214	
100	III	1121	1136	1146	1158	1170	1181	1191	1199	1207	1215	
	IV	1128	1140	1154	1165	1177	1187	1196	1204	1213	1222	
	Mean of II and III	1123	1137	1147	1159	1170	1180	1190	1198	1206	1214	
	I	1240	1251	1262	1275	1287	1300	1315	1330	1349	1368	
	II	1225	1236	1249	1262	1279	1294	1310	1324	1340	1355	
200	III	1225	1236	1248	1260	1275	1289	1303	1318	1334	1348	
	IV	1231	1243	1256	1269	1283	1296	1310	1325	1340	1354	
	Mean of II and III	1225	1236	1248	1261	1277	1292	1307	1321	1337	1352	
	I	1386	1404	1424	1452	1460	1322	1292	1279	1270	1266	
	II	1371	1388	1407	1428	1454	1492	1420	1322	1302	1282	
300	III	1363	1379	1405	1426	1454	1495	1373	1308	1280	1271	
	IV	1369	1385	1400	1419	1441	1470	1534	1335	1294	1275	
	Mean of II and III	1367	1384	1406	1427	1454	1493	1396	1315	1291	1276	
	I	1263	1260	1258	1256	1256	1256	1257	1258	1259	1261	
	II	1269	1261	1256	1252	1251	1251	1253	1257	1260	1265	
400	III	1264	1260	1257	1255	1253	1252	1252	1252	1254	1256	
	IV	1265	1260									
	Mean of II and III	1267	1261	1256	1254	1252	1251	1252	1254	1257	1260	
	I	1263	1265	1270	1274	1279	1283	1287	1292	1297	1302	1306
	II	1270	1276	1281	1287	1293	1299	1305	1311	1317	1322	1328
500	III	1259	1264	1269	1275	1281	1286	1293	1301	1307	1315	1324
	IV											
	Mean of II and III	1265	1270	1275	1281	1287	1292	1299	1306	1312	1318	1326

drawn to give the correct energy-contents, see table 2. We estimate that the maximum absolute error in specific heat increases from ± 1 per cent at 400° c. to ± 2 per cent at 600° c.

The temperature measurements were made with a thermocouple which was regularly checked against a platinum-platinum-rhodium thermocouple. This standard couple was calibrated very carefully (5). The temperature scale is considered accurate to ± 1·5° c.

The effect of eddy currents in the nickel specimen produced by the alternating current used to heat the copper enclosure has been examined. The specific-heat curve of a sample of soft iron was measured first under a.-c. heating and secondly under d.-c. heating. No difference could be detected. It is concluded that the various copper screens incorporated in the apparatus effectively shield the specimen.

§ 3. EXPERIMENTAL RESULTS

Annealed material. Four experiments were carried out on each type of nickel, and the specific heat was calculated at about 25 different temperatures for each experiment. These 100 or so points were plotted and the best curve was drawn through them; the majority of the points lay within 0·5 per cent of this mean curve in the region 100° c. to 400° c. The values of specific heat given in tables 2 and 3 from 100° c. to 400° c. were read off from these mean curves.

Table 3. Curie-point region

Specific heat (cal./g. per ° c.) × 10^4

Temperature (° c.)	I	II	III	IV	Mean of II and III
325	1437	—	—	—	—
330	1452	1428	1426	1419	1427
335	1474	—	—	—	—
339·5	**1510**	—	—	—	—
340	1460	1454	1454	1441	1454
342	1400	—	—	—	—
345	1358	1470	1471	1454	1470
350	1322	1492	1495	1470	1493
352	—	1504	1508	—	1506
354	—	1520	1524	1487	1522
356	—	1543	1547	1498	1545
357	—	1562	1563	—	1562
357·5	—	—	**1576**	—	—
358	—	**1586**	1470	1511	**1580**
359	—	1460	1395	—	—
360	1292	1420	1373	1534	1396
361	—	—	—	1550	—
362	—	1384	1352	1578	1368
363	—	—	—	**1600**	—
364	—	1364	1338	1420	1351
365	—	—	—	1390	—
370	1279	1330	1308	1335	1319
375	—	1312	1290	1310	1301

Four determinations of differences in the energy-content were made on each material for the temperature range 400° c. to 600° c. The mean results obtained are given in table 4 together with the mean deviations.

Table 4

Sample	Difference of energy-content from 400° c. to 600° c. (cal./g.)	Deviation
I	25·45	0·05
II	25·58	0·14
III	25·42	0·19
IV	25·64	0·02
Mean	25·52	

These data and direct specific-heat measurements were combined to give the values of specific heat recorded in table 3 for the range 400° c. to 600° c., but measurements of specific heat were not made for specimen IV in this range.

The mean results for each type of nickel in the neighbourhood of the Curie-point (330 to 380° c.) are plotted in figure 1.

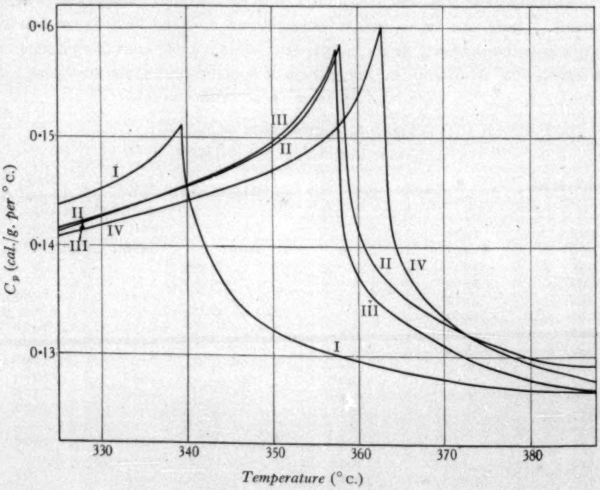

Figure 1.

§ 4. DISCUSSION OF EXPERIMENTAL RESULTS

Samples II and III are both of high purity, i.e. 99·9 per cent nickel, and their {specific-heat, temperature} curves are identical within the limits of experimental error over the greater part of the temperature range; see table 2.

Allowing for the slight difference of about 1° c. between the Curie points of samples II and III, see figure 1, there is a difference decreasing from 2 per cent to 1 per cent in the range 360° C. to 390° C.; as this is of the same order as the experimental error expected in the Curie-point region, it is concluded that the difference in behaviour between the two materials even in this region is quite small.

Sample IV gives similar results to samples II and III from 400° C. to 600° C., table 4; from 100° C. to 320° C. the values of C_p are about 0·5 per cent higher. The Curie point is much higher, namely 363° C., owing to the presence of cobalt. Allowing for this difference in Curie point it will be found that curve IV can be superposed almost exactly on curve III in the Curie-point region, figure 1. Consequently the addition of 0·4 per cent of cobalt has not materially modified the shape of the tail of {specific-heat, temperature} curve.

Sample I, containing appreciable quantities of impurities, in particular silicon, has a low Curie temperature, namely 340° C., and a low maximum specific heat, namely 0·152 cal./g. per ° C. If this curve is transposed 18° C., the difference in Curie temperature between samples I and III, it will be found to lie between curves II and III, so that apart from the decreased maximum specific heat the behaviour in the Curie-point region is not markedly different from that of samples II, III and IV. In the region below the Curie point the values of C_p lie consistently higher than for the other samples; see table 2. This is to be expected since the contribution to C_p by the magnetic transformation is restricted to lower temperatures. A comparison of the total difference of energy-content for the temperature range of 200° C. below the Curie point has been made for samples I and II. The results are 26·05 cal./g. for I and 26·43 cal./g. for II; so that the total change is not great.

From 400° C. to 550° C. the values of C_p for sample I are in satisfactory agreement with those for the other samples. Above 550° C. the results are lower by about 1·5 per cent, suggesting that the rate of rise of C_p in this region is somewhat slower than for the pure materials.

From this survey of the experimental results on annealed material we conclude that over the range of compositions tested the presence of impurities does not materially affect either the shape of the tail of the {specific-heat, temperature} curve in the neighbourhood of the Curie point or the values of the specific heat above the Curie point. On the other hand, both the Curie point and the maximum specific heat are sensitive to the presence of impurities.

§ 5. INFLUENCE OF METHOD OF PREPARATION OF SPECIMEN

Melting procedure. Samples I, II and III were produced in three distinct ways. The commercially pure nickel I would be melted in air, cast into an ingot of cross section about 4 in. square, forged, and then rolled to a diameter of 1⅛ in. The Mond nickel II was melted *in vacuo* and the reduction in diameter by forging was in this case only about 10 per cent. Sample III was prepared from powder of particle-size approximately 10^{-2} mm. and was sintered at 900° C., a temperature well below the melting point of nickel (1450° C.) so that very little grain growth could take place. In view of the experimental results obtained, it is clear that neither the tail on the {specific-heat, temperature} curve nor the values of C_p above the Curie point are markedly sensitive to the mode of manufacture, crystal-size or the like.

Effect of heat treatment. The results listed in table 3 were obtained on the different samples heat-treated in an identical manner. We have carried out a number of experiments on samples III and IV to determine whether variation in heat treatment produced any changes in the C_p curve.

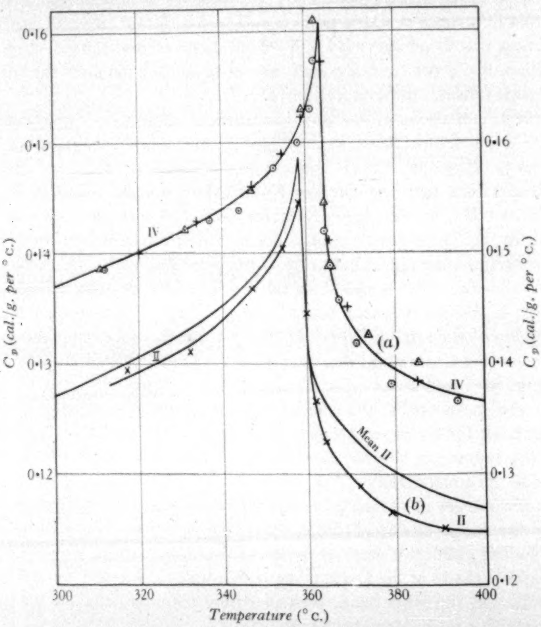

Figure 2. ⊙, IV quenched 700° c.; +, IV cooled from 600° c. at 1° c./min.; △, IV cooled 1° c./min., from 900° c.; ×, II annealed 300 h. at 350° c.

Two specimens of cathode nickel, sample IV, were prepared. One was cooled from 900° c. at 1° c. per minute, and the other was quenched from 700° c. in water. The {specific-heat, temperature} curves were taken, and an additional curve was taken on the quenched sample after it had been cooled at 1° c. per minute from 600° c. The experimental points obtained are shown in figure 2 (*a*) for the Curie-point region. Within the limits of error they all fall on the mean curve. A specimen of vacuum-melted Mond nickel, sample II, was annealed at 350° c. for 300 hours *in vacuo*. The {specific-heat, temperature} curve obtained is shown in figure 2 (*b*) together with the mean curve for sample II. The change, if any, produced by this annealing treatment is very small. We conclude from the above experiments that the {specific-heat, temperature} curves of pure nickel are not particularly sensitive to heat treatment.

It is conceivable that our experimental method might smooth out any minimum on the {specific-heat, temperature} curve. This point has been checked experimentally in connexion with another investigation. A specimen of iron was fitted with an insert of zinc weighing about 1 g., which was 1 per cent of the total weight of the specimen. The {specific-heat, temperature} curve was determined and at the melting point of zinc a sharp maximum was observed. The anomaly in the {specific-heat, temperature} curve was restricted to a temperature-interval of about 4° C. The tail on the specific heat curves, figure 1, which stretches over some 30° C., is thus a genuine property of the samples under investigation.

§ 6. COMPARISON OF EXPERIMENTAL RESULTS WITH PREVIOUS RESULTS

General. Table 5 gives the values of C_p (specific heat per gram-atom) found by various investigators for the temperatures given in degrees absolute in column 1. The estimated accuracy given by each investigator is also tabulated.

Table 5

Atomic heat C_p (cal./gram-atom per ° C.)

Temperature (° K.)	Lapp	Grew	Ahrens	Moser	Klink-hardt	Sykes and Wilkinson	Transposed Sykes and Wilkinson	Most probable values
350	6·51	6·60	6·52	6·46	—	—	—	6·51
400	6·75	6·86	6·84	6·69	—	6·78	—	6·76
450	7·05	7·14	7·14	7·04	—	7·07	—	7·07
500	7·42	7·49	7·52	7·48	—	7·48	—	7·47
550	7·88	7·90	8·01	7·78	—	7·82	—	7·83
600	8·45	8·55	8·72	8·28	—	8·34	8·36	8·37
610	8·67	8·79	8·95	8·43	—	8·49	8·55	8·49 (8·57)
620	8·95	9·05	9·18	8·62	—	8·69	8·78	8·69 (8·80)
622	9·04	9·12	9·22	8·66	—	8·74	8·89	8·74 (8·88)
624	9·13	9·18	9·28	8·80	—	8·80	9·02	8·80 (8·99)
626	9·23	9·25	9·36	8·87	—	8·89	9·28	8·89 (9·13)
628	—	Interpolated		—	—	—	—	9·02 (8·61)
630	7·80	8·70	8·25	8·22	—	9·28	8·12	9·28 (8·20)
635	7·42	8·25	8·18	7·93	—	8·04	7·87	8·04 (7·88)
640	7·43	7·98	8·06	7·72	—	7·87	7·74	7·87 (7·72)
650	7·44	7·70	8·00	7·48	7·31	7·62	—	7·50
700	—	—	—	7·32	7·35	7·37	—	7·35
750	—	—	—	7·31	7·42	7·37	—	7·37
800	—	—	—	7·33	7·51	7·48	—	7·44
850	—	—	—	7·36	7·68	7·66	—	7·50 (7·57)
Estimated error (per cent)	±2	±2	±2	±0·5	±3	±1 to ±2		

The purity of the samples used was as shown in table 6. We shall compare the results obtained on these materials with the mean result for samples II and III. All investigators used an aneroid method; the energy necessary to raise the specimen over a small temperature interval of about 2° C. was determined. The mean specific heat over the temperature-interval was assumed equal to the instantaneous specific heat at the mean temperature. Lapp, Grew and Ahrens used wires which were heated electrically by the passage of current. Klinkhardt heated a massive specimen by means of electron bombardment. In both these methods the temperature of the enclosure surrounding the specimen was held constant throughout the course of the experiment, and a radiation correction had to be made for loss of heat by the specimen. Moser heated his specimen electrically in a tightly fitting silver calorimeter, and arranged that the temperature of the surroundings should increase at substantially the same speed as the specimen. In this way he reduced the radiation correction. Grew, Ahrens and Klinkhardt carried out their experiments *in vacuo* to reduce heat losses, Moser used a reduced pressure of argon, and Lapp appears to have worked with air at atmospheric pressure.

Table 6

Investigator	Material	Impurities (per cent)						
		Iron	Copper	Carbon	Silicon	Magnesium	Manganese	Sulphur
Lapp	Nickel wire	0·19	0·06	0·04	0·02	0·18	—	—
Grew	Nickel wire (Hilger)	Impurity 0·03 per cent						
Ahrens	Wire, carbonyl nickel	Stated to be of high purity						
Ahrens	Wire, Rein nickel	0·2	0·07	—	0·04	—	0·18	—
Moser	Mond nickel	0·1	—	—	0·003	0·07	—	0·003
Klinkhardt	Vacuum melted nickel	—	—	—	—	—	0·5	—

The temperature range, 350° K. *to* 610° K. Ahrens's results, given in table 5, refer to his carbonyl nickel. Klinkhardt's results at low temperatures are not included as his material had a very low Curie point owing to the presence of manganese. The agreement from 350° K. to 610° K. is satisfactory; it is ± 1·5 per cent, which is within the range of estimated errors provided the results of Ahrens are not considered. For reasons which will be given later in connexion with the range 650° K. to 850° K., it is highly probable that his results are high throughout the major portion of the temperature range 350° K. to 650° K. by an amount greater than 2 per cent.

In the ninth column of table 5 we list probable values which are obtained by giving each experimental method an equal weight independent of the number of the determinations made by that method; thus we give Lapp and Grew a weight of 1, Moser and our own results, column 7, a weight of 2. Ahrens's results are neglected.

The Curie-point region, 610° C. *to* 650° K. The results obtained are shown graphically in figure 3. Apart from the one result obtained by Lapp, all the curves agree in showing a well-defined tail. The sharp minimum found by Lapp cannot be attributed to high purity (in view of the analyses), or to an especially prolonged heat treatment, since none is specified. It is conceivable that the wire sample had a pronouncedly fibrous structure which differentiated it from material used by other investigators, yet Grew and Ahrens, who also used wire, did not confirm Lapp's result.

In our opinion the wire method is not particularly suitable for high-temperature measurements of specific heat in view of the relatively high surface-to-mass ratio, which necessitates large radiation corrections. In Lapp's measurements at the Curie point this correction amounted to 18 per cent though in our experiments it seldom exceeded 0·5 per cent. The correction is sensitive to variation in emissivity and gas pressure; neither Grew, Lapp nor Ahrens give any precise details regarding the methods adopted to keep the gas pressure constant. With wires fluctuations in gas pressure above 5×10^{-3} mm. of mercury will affect the radiation correction to an appreciable extent. Additional difficulties arise from the necessity for controlling the temperature of the surroundings carefully, a change of 0·005° C. per minute being important. These considerations throw doubt on Lapp's result and on the results obtained by the wire method in general. It is significant that in the range from 400° C. to 500° C., figure 4, the deviations in the results obtained by the three different methods used by Klinkhardt, Moser, and Sykes and Wilkinson are much smaller than the deviations in the results obtained by different investigators using the wire method.

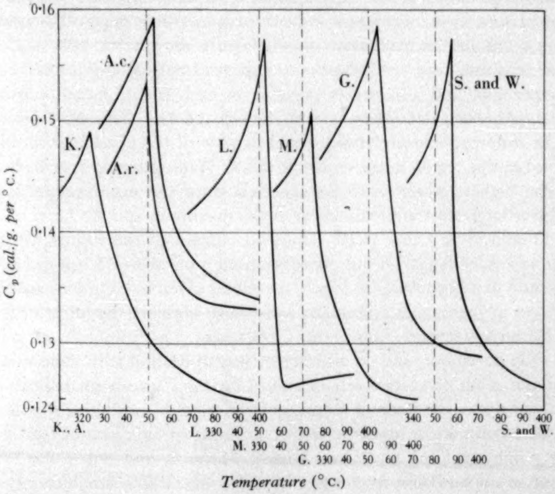

Figure 3.

As we have previously pointed out, our results in figure 1 indicate that the tail on the {specific-heat, temperature} curve is not sensitive to the presence of impurity or normal variations in heat treatment. Ahrens's results on carbonyl nickel (A.c.), figure 3, and Rein nickel (A.r.) of widely differing composition, confirm this conclusion.

The variation in Curie point found by different observers is much greater than the probable experimental errors and is no doubt caused by the presence of impurities. Whilst Lapp's impure nickel and Ahrens's Rein nickel give relatively high Curie points, indicating that some of the impurities must be self-compensating, their effect on the magnetic properties is not certain and the results obtained with these materials together with those obtained with Klinkhardt's are considered to be unreliable. The samples which are known to be reasonably pure, namely carbonyl iron (Ahrens), Mond nickel (Moser), Hilger nickel (Grew), and our samples II and III, have Curie points at 353° c., 354° c., 358° c. and 357·5° c. respectively. The variation is outside the limits of our experimental error and it appears that the residual impurities present in the samples still exert an appreciable effect. For comparison purposes the ratio of the maximum specific heat to the specific heat at 400° c. is a reasonable criterion, since it eliminates to a great extent variations due to differing Curie temperature and also errors peculiar to each set of measurements. This ratio is 1·19 (Ahrens), 1·20 (Moser), 1·23 (Grew) and 1·25 from our own measurements. The differences are relatively small in view of the experimental difficulties encountered in this region in consequence of the rapid change in specific heat. Our value is the highest which is to be expected since the experimental method is likely to give the nearest approximation to the maximum specific heat.

The differences in Curie point render discussion of the results in the range 610° K. to 640° K. difficult. If our curve, column 7 of table 5, Curie point 630° K., is transposed* to a position 4° K. lower, the values given in column 8 are obtained, and these are in reasonable agreement with those obtained by other investigators (Ahrens being neglected). Above the Curie point, i.e. from 626° K. to 640° K., there are wide deviations, and no satisfactory way of dealing with them is apparent.

In column 9 are given two sets of values for the Curie-point region; the first comprises our own experimental values, column 7, with maximum specific heat at 630° K.: the second set in brackets, with maximum specific heat at 626° K., is obtained by weighting Lapp and Grew 1 each, Moser 2, and Sykes and Wilkinson (table 5, column 8) 2. Both sets of figures give the same difference in energy-content from 610° K. to 640° K. to within ± 0·1 per cent.

The range from 400° c. *to* 600° c. (650° K. *to* 850° K). The experimental results available are plotted in figure 4. Although our measurements indicate that impurities have a very small effect on the {specific-heat, temperature} curve in this region, the deviations are very high, amounting to 7 per cent from 400° c. to 450° c. Recently, in an investigation of the {specific-heat, temperature} curve of β brass from 240° c. to 500° c., Moser's results and our own were in satisfactory agreement, and an independent check was available from a direct energy-content measurement made by Ruer and Kremers: all three experimental methods gave the same result to within ± 0·5 per cent. An error of 7 per cent in either Moser's result or our own at 400° c. to 450° c. is therefore extremely unlikely, and for this reason we have neglected Ahrens's results throughout, as they appear to be consistently high. The remaining results differ within the reasonable limits of 5 per cent over the region 400° C. to 600° C.

---

* This transposition does not modify appreciably the values of C_p below 610° K. or above 640° K.

The value of C_p given in column 9 of table 5 at 650° K. is obtained by weighting Lapp and Grew 1 each, Klinkhardt 2, Moser 2, and Sykes and Wilkinson 2. From 700° K. to 800° K. Klinkhardt, Moser, and Sykes and Wilkinson are weighted equally; i.e. each experimental method is considered to be as accurate as any other, in agreement with the arrangement adopted for the most probable {specific-heat, temperature} curve below the Curie point. The value of C_p at 850° K. with this method of weighting is 7·57 cal./gram-atom, which would indicate that Moser's result is in error by 3 per cent.

In the preceding paragraphs we have endeavoured to evaluate the most probable {specific-heat, temperature} curve for nickel on the basis of the existing experimental data. In selecting the data we have been guided by the experimental results given in §§ 4 and 5, which deal with the effects of impurity and the method of preparation of the samples. In weighting the data, each experimental method has been given equal weight because it appeared highly probable that the differences between results obtained by different methods were much more likely to be associated with inherent difficulties in the individual technique employed than with errors in measurement. The values recorded in column 9 should be correct within 0·5 per cent up to the Curie point and 1 per cent above it.

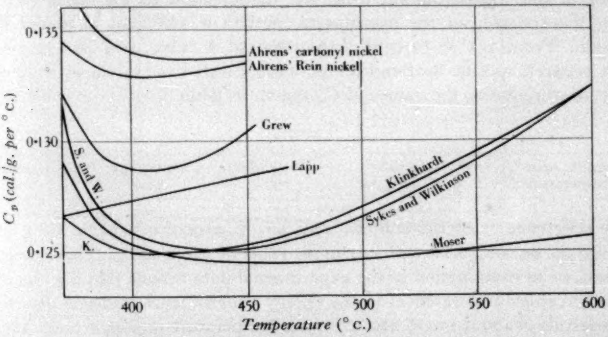

Figure 4. Specific heat from 400° C. to 600° C.

The agreement between our results, column 7, and the most probable values given in column 9 is very satisfactory over the range of temperature 350° K. to 600° K. and 650° K. to 850° K., where direct comparison can be made. In the Curie-point region, 610° K. to 640° K., some uncertainty exists as to the precise form of the {specific-heat, temperature} curve depending on the value chosen for the Curie temperature. The two sets of values given in column 9 are equally satisfactory.

Energy-content measurements. In the region above the Curie point, where the specific heat changes slowly with temperature, measurements by the calorimeter method should afford a check on those made by the various aneroid methods under discussion. Wust[12] gives the difference in energy-content of nickel between 400° C. and 600° C. as 25·89 cal./g., the actual value observed by him being 25·56 cal./g. Our value for samples II and III is 25·50 cal./g.

Bronsen[13], using the calorimeter method and very pure nickel (99·98 per cent), has determined C_p up to 500° C. and finds values of 7·43 cal./gram-atom at 670° K., 7·40 at 720° K. and 7·38 at 770° K., which are in good agreement with those given in columns 7 and 9 of table 5. His value for the Curie point was 358° C. ± 2° C.

Ewart[14] has recently published measurements which purport to show that a hexagonal modification of nickel exists between 345° C. and 351° C., forming very slowly from the cubic modification on either side. Whilst this work forms the main evidence from specific-heat data for such a modification, it is conceivable that other investigators, including ourselves, did not observe the effect owing to the sluggish character of the transformation from one modification to the other. We doubt whether the accuracy of the calorimeter method is sufficient to justify Ewart's conclusion. From 351° C. to 950° C. the material is cubic, and assuming a linear relation between specific heat and temperature Ewart has evaluated, from energy-content measurements, the values of C_p shown in table 7.

Table 7

Specific heat C_p	0·1267	0·1281	0·1295	0·1310
Temperature (° C.)	400	500	600	700

The difference in energy-content from 400° C. to 600° C. is 25·62 cal./g., a value which should be compared with our mean value of 25·52 cal./g. This agreement is fortuitous, as an examination of the experimental data reveals that the true specific heats, deduced from differences in the energy-content measurements over temperature-intervals of about 100 to 200° C. in this temperature region, actually vary by as much as 10 per cent from those recorded in table 7, whilst the energy-content measurements are liable to an error of ±4 per cent.

The evidence from calorimetric data, whilst in good agreement with the results in column 9, table 5, is not sufficiently extensive or precise to give a really satisfactory check.

§ 7. DISCUSSION OF RESULTS

In his theoretical treatment Stoner[1] used the results due to Lapp and Grew over the temperature range 100° K. to 750° K. and Klinkhardt's results from 650° K. upwards. He derives two curves for the variation of C_E, the electronic specific heat, with temperature. One, figure 5 (*a*), is based on the assumption that the electron spins are parallel, and the other, figure 5 (*b*), is the corresponding curve for equal numbers of oppositely directed spins. If the assumption that the observed electronic specific heat at low temperatures, represented by the initial part of figure 5 (*a*), is entirely due to change in the translational state of the electrons is correct, then we should expect that above the Curie point, where there are equal numbers of oppositely directed spins, the electronic specific heat would be represented by the upper part of figure 5(*b*). Using Stoner's values for C_Q and $(C_p - C_v)$, we find the values shown in table 8 for C_E above the Curie point:

Table 8

Temperature (° K.)	650	700	750	800	850
Electronic specific heat C_E	1·30	1·11	1·09	1·13	1·22

These fall on the curve for parallel spins, and an error of 3 per cent in C_p would be necessary to lift them on to the other curve. As an error of this magnitude is unlikely, the relation, figure 5(*a*), between C_E and temperature for parallel spins seems the more probable. The electronic specific heat above the Curie point cannot correspond to parallel spins, and the fact that the observed points fall closely on figure 5(*a*) in this region appears to indicate either that there was an over-simplification in the assumptions underlying the derivation of the curves or that there are other additional factors which have to be taken into account. Whatever the explanation for this anomaly, it seems appropriate to use figure 5(*a*) for extrapolation to temperatures below the Curie point since it gives the best fit above this point.

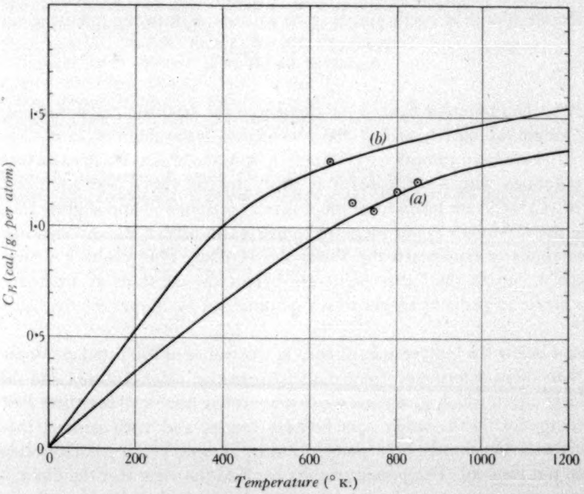

Figure 5

The values of C_M are determined by subtracting from C_p the dilatation term $(C_p - C_v)$, the lattice-vibration term C_Q, and the electronic-specific-heat term C_E. As Stoner overestimated C_E his resulting values for C_M are too small. We have redetermined C_M for the temperature interval 450° K. to 630° K., using the data given by Stoner for C_Q and $(C_p - C_v)$, while the values of C_E were read off from the curve figure 5(*a*). The resulting values of C_M are as shown in table 9.

Table 9

Temperature (° K.)	450	500	550	600	610	620	622	624	626	628	630
C_p	7·07	7·47	7·83	8·37	8·49	8·69	8·74	8·80	8·89	9·02	9·28
C_Q	5·72	5·77	5·80	5·83	5·83	5·84	5·84	5·84	5·84	5·84	5·84
$C_p - C_V$	0·22	0·26	0·30	0·36	0·37	0·38	0·38	0·39	0·39	0·40	0·40
C_E	0·74	0·81	0·88	0·94	0·95	0·96	0·96	0·97	0·97	0·97	0·97
C_M	0·39	0·63	0·85	1·24	1·34	1·51	1·56	1·60	1·69	1·81	2·07
$\frac{1}{2}(\partial\sigma_0^2/\partial T)$	3·3	4·2	5·8	8·7	9·5	10·4	10·7	11·1	11·8	12·6	13·3
$N\rho$ (c.g.s.u. $\times 10^5$)	0·84	1·07	1·05	1·00	1·00	1·03	1·04	1·03	1·02	1·02	1·11

The molecular field coefficient may be calculated from the following equation:

$$N\rho = C_M . J \Big/ \frac{1}{2}\frac{\partial\sigma_0^2}{\partial T} . A,$$

where N is the molecular field, ρ the density, σ the intrinsic magnetization, A the atomic weight of nickel, and J the mechanical equivalent of heat. Values of $\frac{1}{2}(\partial\sigma_0^2/\partial T)$ have been compiled by Stoner⁽¹⁵⁾ from the Weiss-Forrer data for a small nickel specimen with a Curie point at 352°. In the above derivation of C_M the values of $(C_p - C_v)$ are taken from those given by Stoner⁽¹⁾ and slightly transposed to bring the maximum to our measured Curie point of 630° K., and to arrive at $N\rho$ we have similarly transposed the Weiss-Forrer data. The resulting values of $N\rho$ from 500° K. up to the Curie point are practically constant at $1·04 \times 10^5$. This value is about 10 per cent higher than that obtained by Stoner for the Curie-point region.*

At and below the temperature of 600° K. the values of $N\rho$ listed above are much larger than those determined from measurements on magnetization and the magnetocaloric effect, which give $N\rho = 5·5$ to $5·0 \times 10^4$ at 600° K. That these low values are incompatible with earlier specific-heat results and with general theoretical considerations has already been pointed out by Stoner, and a possible explanation has been put forward. The present results confirm the view that the discrepancy is not due to errors in specific-heat measurements. Assuming that the value of C_p at 600° K. is in error by 1 per cent, i.e. that the true value is 8·29 cal./g., we find that $C_Q + (C_p - C_v)$ is 6·19 cal./g., leaving 2·10 cal./g. for $C_E + C_M$. If C_M is 0·62 cal./g., the value necessary to make $N\rho$ equal to 5×10^4, then $C_E = 1·48$ cal./g., which is 0·38 cal./g. higher than the value of C_E at 700° K. and corresponds to an error of 4 per cent in the measured value of C_p at this temperature.

---

* Dr Stoner has informed us "that further consideration of the problem has shown that the character of the variation of C_E below the Curie point is much more complex than was previously supposed. Detailed calculations are not completed, but the indications are that the values of $N\rho$ calculated by the present method can be regarded only as lower limits to the molecular field coefficient."

§ 8. ACKNOWLEDGEMENTS

The authors are indebted to the Department of Scientific and Industrial Research for the grant made to one of them (H. W.); to the Metropolitan-Vickers Electrical Co. Ltd. for kindly providing the necessary facilities, and to Dr A. P. M. Fleming, C.B.E., Director and Manager of Research and Education Departments, for his personal interest in the investigation. The authors thank Professor W. L. Bragg, F.R.S., and Dr E. C. Stoner, F.R.S., for their kindness in discussing the subject-matter of the paper from time to time.

REFERENCES

(1) Stoner. *Phil. Mag.* **22**, 81 (1936).
(2) Hansen. *Der Aufbau der Zweistoff-Legierungen* (Berlin, 1936).
(3) Sykes and Jones. *Proc. Roy. Soc.* A, **157**, 213 (1936).
(4) Sykes and Wilkinson. *J. Inst. Met.* **61**, 223 (1937).
(5) Sykes and Jones. *J. Inst. Met.* **59**, 257 (1936).
(6) Lapp. *Ann. Phys., Lpz.*, **12**, 442 (1929).
(7) Grew. *Proc. Roy. Soc.* A, **145**, 509 (1934).
(8) Ahrens. *Ann. Phys., Lpz.*, **21**, 169 (1934).
(9) Moser. *Phys. Z.* **37**, 737 (1936).
(10) Klinkhardt. *Ann. Phys., Lpz.*, **84**, 67 (1927).
(11) Ruer and Kremers. *Z. anorg. Chem.* **184**, 208 (1929).
(12) Wust. *Die Temperatur Wärmeinhaltskurven der Technisch-Wichtigen Metalle* (Berlin, 1918).
(13) Bronsen. *Canad. J. Res.* **14**, 194 (1936).
(14) Ewart. *Proc. Akad. Wet. Amst.* **39** (1936).
(15) Stoner. *Philos. Trans.* **235**, 165 (1936).

THE CONSTRUCTION OF MOLECULAR MODELS OF DIELECTRICS

Demonstration given on 8 *April* 1938

BY L. HARTSHORN, D.SC.

In an investigation of the dielectric properties of some synthetic resins the need was felt for models which would give a general idea of the molecular structure of materials of this type; that is to say, of organic compounds with large molecules, which are formed by the linking together of simple molecules by polymerization or condensation. A typical example is the phenol-formaldehyde resin familiar to most physicists as Bakelite. This is commonly used in two forms, one which is fusible and readily soluble in such common solvents as acetone and alcohol and is used for making varnishes, and another which is insoluble and almost vitreous in character and is used in the form of insulating sheets, rods, tubes and mouldings.

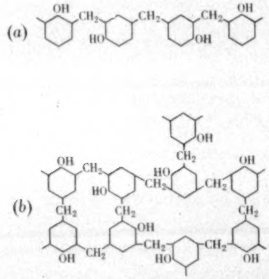

Figure 1. Structure of phenol-formaldehyde resins (*a*) fusible; (*b*) heat-hardened.

It is believed from chemical evidence that the structure is more or less such as may be represented by the formulae shown in figure 1. In each case we have benzene rings with hydroxyl groups attached, arising from the phenol molecules, linked together by methylene groups, —CH_2— from the formaldehyde molecules. The structure of the fusible resin is fairly easily visualized: it is that of a simple chain. The structure of the hardened resin is, however, difficult to visualize. It may be regarded as a kind of irregular lattice-structure obtained by cross-linking a number of neighbouring chains. The structure lacks the regularity of a crystal, and it is evident that the ordinary graphical formula can give very little idea of the spatial relations between its constituent atoms and groups. I have found a model constructed with wooden balls to represent the various atoms very informative in this respect.

When the need for these models first arose, I naturally turned to the well-known work of Sir William Bragg and the workers at the Royal Institution, and also the models of proteins recently shown to the Physical Society by Dr Winch. I soon found that the construction of models may absorb a good deal of time and money, and having now arrived at a relatively cheap and simple method of construction, I propose to describe it in the hope that it may be useful to those who have similar problems. It will be found that with a stock of a few kinds of wooden balls of the type to be described, a model of the molecule of almost any organic material may be constructed in a few minutes, and although it will have no pretensions to accuracy of dimensions, it will bring out features of the structure which are not easily grasped without the use of models.

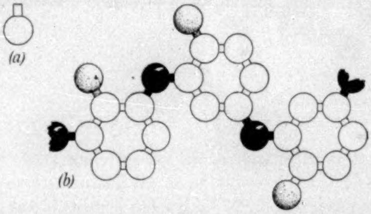

Figure 2. (*a*) Ball foot as purchased; (*b*) Model for fusible phenol-formaldehyde resin (Novolak).

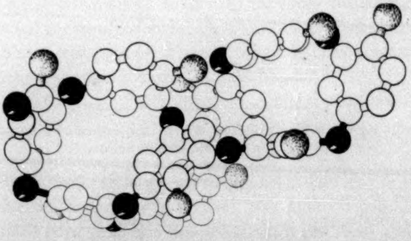

Figure 3. Model for hardened phenol-formaldehyde resin (Bakelite). (Heat-hardened Bakelite.)

The method of construction will be understood by reference to the models for the two phenol-formaldehyde resins already mentioned. That for the fusible resin is shown in figure 2, and that for the hardened resin in figure 3. Both models are built of units of three kinds only, white balls in hexagon formation representing aromatic carbon atoms assembled into benzene rings, black balls linking together the hexagons and representing —CH_2— groups, and spotted balls representing OH groups. The hydrogen atoms must be regarded as buried within the carbon and oxygen atoms to which they are attached, since X-ray analysis fails to detect the H atoms as separate units in such compounds as have been analysed. Thus three types of ball are required to represent (1) aromatic carbon atoms for building benzene hexagons, (2) aliphatic carbon atoms each with four bonds symmetrically arranged so as to occupy the four corners of an imaginary tetrahedrom whose centre coincides with that of the ball, and (3) oxygen atoms with two bonds or points of attachment.

These atomic units are all made from "ball feet",* which consist of wooden balls attached to short cylindrical stems, figure 2 (*a*). They are obtainable very cheaply in three sizes, of diameters ½, ¾ and 1¼ in. In order to make the hexagons, the balls are placed in a simple jig, figure 4, which consists merely of a board drilled with holes into which the pegs of the ball feet will fit, and mounted at an angle of 60° to the horizontal. The ball is drilled centrally with a vertical drill of the same diameter as the peg of the ball foot. It is then rotated about its peg through 180° and again drilled. Six balls, drilled in this way and arranged so that the stem of one fits into a hole in the next, form a benzene molecule, the hydrogen atoms being represented by the holes which are left empty. The aliphatic carbon atoms are made in the same way, but in this case the angle of the jig is 71° instead of 60°, and the ball is rotated about its peg through 120° instead of 180° after each drilling operation, so that each of these balls has three holes and one peg, with their axes inclined to one another at the tetrahedral angle of 109° and therefore representing the four bonds. Additional pegs to fit the holes are cut from dowel rods when required. The balls are very easily coloured by dipping them into black, red, green or yellow ink. The ¾-in. ball is the most convenient one for most purposes. It serves for both carbon and oxygen atoms since X-ray data obtained for organic compounds show that these atoms are of about the same size. The chlorine atom is considerably bigger, and may be represented by the 1¼-in. ball. A slightly smaller size would be more nearly to scale, but no other sizes appear to be produced so cheaply.

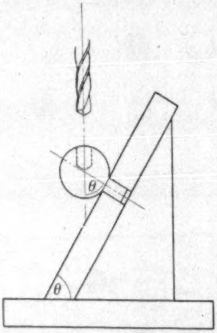

Figure 4. Jig for drilling ball-feet. $\theta=60^\circ$ for aromatic carbon atoms. $\theta=71^\circ$ for aliphatic carbon atoms.

It is a simple matter to prepare a stock of a few dozen balls of each of these kinds, and with them molecular models of the kind shown are very quickly assembled. The models shown represent (1) fusible phenol-formaldehyde resin (Novolak).

---

* Supplied by Messrs Hobbies, Ltd., 16, New Oxford St., London, W.C. 1.

This is a chain structure, assembled as shown in figure 2; (2) hardened phenol-formaldehyde resin (Bakelite), figure 3, a structure of an irregular lattice type. It cannot be claimed that this model represents in detail the actual structure of any one molecule, but it is reasonable to suppose that the benzene rings preserve their usual configuration, and that the possible positions and orientations of the links of the structure are fixed by the geometry of these hexagons and the tetrahedral carbon atoms. Obviously many cross-linked structures differing in their details could be assembled from the same numbers of atoms of the various kinds, and there is at present no means of discriminating between the various possibilities. The model does, however, give some idea of the general features of the structure, such as its rigidity, the open spaces, and the distribution of the OH groups, which, being polar, greatly affect the dielectric properties; (3) polystyrene, figure 5. This may be regarded as an aliphatic hydrocarbon chain with benzene rings attached to it. The material is a clear transparent resin with excellent insulating properties. On the scale of the model a complete molecule would be represented by a chain some 30 m. long; (4) chlorinated rubber, figure 6, another chain compound. The large chlorine atoms are easily distinguished.

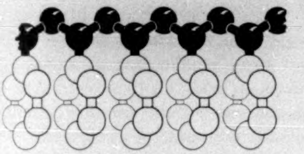

Figure 5. Model for polystyrene.

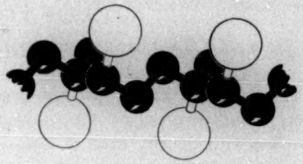

Figure 6. Model for chlorinated rubber.

Models of methyl methacrylate, cellulose acetate, and chlorinated diphenyl also were shown.

I am much indebted to Mr E. J. Pratt for preparing the illustrations. For the sake of clearness a portion of the peg of each ball is shown; in practice the peg is not usually visible after it has been inserted into the appropriate socket in order to link together two balls. The problem of giving an impression of the models by means of photographs or diagrams is one of considerable difficulty, a fact which serves to emphasize the usefulness of the model.

THE DISSIPATION OF ENERGY BY A PENDULUM SWINGING IN AIR

THE AMPLITUDE DEVIATION OF RATE OF A PENDULUM: A SECOND EXPERIMENT

By E. C. ATKINSON, M.A.

See page 756 *of this volume*

AUTHOR'S REPLY TO DISCUSSION

Do not Dr Rawlings's observations with the gyro wheel show that the viscosity of air increases with the density? I am not sure that the changes in pendulum resistance prove this to be the case, because, in addition to skin-friction loss, energy is dissipated by the movement of the air. Would not this component increase with density even if viscosity remained constant? I cannot answer the question about low pressure loss from my own experience, but I refer Dr Rawlings to Loomis's observations (§ 13) and to Dr R. d'E. Atkinson's remark in this discussion.

My observations show that the loss of energy due to the rubbing friction of the impulse lever on the pendulum rod may be very small. For small amplitudes the relative motion is of the second order only, if a point on the rod does not describe a circle or if the axis of the lever is too high or too low, and in such cases the losses are probably negligible. On the other hand, when the lever axis is in the wrong vertical plane, either displaced to one side of the right one or inclined to it, slip is of the first order and energy loss may be serious.

I cannot answer Dr Kantorowicz's question about yield point. I used brass chaps and I doubt whether the rivets clamped the faces tight enough together to reach the yield point even of the brass. When a spring is made non-uniform by varying the width instead of the thickness the internal loss will be far less, as Dr Kantorowicz suggests. This form has the disadvantage for pendulum suspension of making a less compact spring.

Mr Hope Jones makes the calculation of input of energy appear simpler than it really is, for part of the energy released by the fall of the lever remains with it as kinetic energy. Using data about the Synchronome lever which Mr Hope Jones gave me 10 years ago, I conclude that of 94 ergs released about 71 are transferred to the pendulum when the amplitude is 50′ and 68 when it is 60′.

I do not use the Synchronome remontoire, but I replace the gravity lever with an electromagnet just as Mr Cottingham did, except that I use a thermionic valve in such a way that contact between pendulum and impulse lever lowers the grid voltage and so cuts off the anode current which energizes the electromagnet. With suitable screens attached to pendulum and armature lever this voltage change can be made by means of a photoelectric cell but I doubt whether this method is as reliable as the simpler one.

As variation of the arc of the impulse, to which Mr Hope Jones refers, is the worst fault of the gravity impulse, it is important to guard against it. When the armature lever comes fully into contact with the clean ends of the stop screws the arc is very nearly constant. In order to test whether all is well, I switch on a telephone circuit which is completed by contact between lever and screw. The sound at make shows whether the contact is clean and whether there is recoil.

The Foucault effect produces twist in the suspension spring and so affects its rigidity for the normal motion. Has Mr Cottingham managed to calculate the moment necessary to counter the effect? Lack of symmetry in the pendulum produces an alternating twist in the spring and I suspect that this is likely to be more harmful than the Foucault effect.

It is interesting that Mr Cottingham used Newton's rings so long ago to observe the motion of a pendulum support. If one could measure the motion in this way and also measure the loss of energy due to motion through a cycle of known amplitude, it would be possible to separate the spring loss from the bracketing loss, as Mr Hope Jones desires.

Dr Atkinson's observations on decrement with clamped and with all-one-piece quartz fibres are very interesting. I do not know whether a spring can be ground so as to secure cycloidal motion of the bob, for I have not dealt with the second-approximation terms of the equations of motion. I think Haag alone has attempted to obtain these terms. If Dr Atkinson will read Haag's paper, he will perhaps be able to clear up some of my difficulties and doubts.

REVIEWS OF BOOKS

Isaac Newton 1642–1727, by J. W. N. SULLIVAN, with a memoir of the author by CHARLES SINGER. Pp. xx+275. (Macmillan & Co., Ltd.) 8*s*. 6*d*. nett.

This book, over which Sullivan spent considerable time during his last ten years, presents a very interesting but unusual account of Newton's life and work. Most readers of Newton's biography will have noticed how in several respects his behaviour differed very much from what one would normally expect of a discoverer. Thus he put on one side his work on gravitation, when it had reached a most interesting stage in 1666, although he then "minded mathematics and philosophy more than at any time since". A portion of his book on optics published in 1704 was "written at the desire of some Gentlemen of the Royal Society, in the Year 1675...and the rest was added about twelve Years after to complete the Theory." He goes on to say "to avoid being engaged in Disputes about these Matters, I have hitherto delayed the printing, and should still have delayed it, had not the importunity of Friends prevailed upon me." Most of his scientific work was accomplished by the time he was forty-five, when, in one tremendous effort lasting eighteen months, he composed the *Principia*; but it might never have been written had it not been for an almost accidental discussion with Halley and "the importunity of friends". He was apparently indifferent to the claims of others, such as Hooke, and in connexion with Leibnitz his case was at first argued by his friends.

Sullivan aims at explaining these unusual characteristics and suggests as the solution of the problem that Newton was not interested in philosophy and did not regard even his greatest discoveries as being of importance. It is surprising to find it suggested that our greatest mathematical physicist was not really interested in science and that he only worked when, for accidental reasons, the spirit moved him. Nevertheless the explanation seems to fit the facts in many instances.

Thus when he "compared the force required to keep the moon in her orb with the force of gravity at the surface of the earth and found them answer pretty well", that ended the matter. Various hypotheses have been advanced to explain this. Pemberton suggested that he used an incorrect value for the length of a degree of latitude, but it is known that he had access to a reasonably correct one. Adams and Glaisher suggested that it was not until 1685, when Newton proved that a sphere attracted as if its mass were concentrated at its centre, that he felt that the law of gravitation was established. This proof made exact what he formerly regarded as approximate, much to his own surprise. Be that as it may, Newton in 1666 was personally satisfied "pretty well".

To Sullivan this dropping of the subject indicates his lack of interest. He was more interested in alchemy and in religion, and apparently regarded it as more important "to justify the ways of God to man" than to explain the motions of the heavens.

Similarly in connexion with the claims of Hooke and of Leibnitz, he ignores them until they seem to affect his personal honour. He is then aroused and writes severely to Hooke and superintends the preparation of the second edition of the *Commercium Epistolicum*. He is aroused from his duties at the Mint and his religious studies by the problems of Bernoulli, which he solves in a night, since he feels they are a challenge and attack on his method of fluxions. He is aroused for a moment only.

Thus we have a picture of Newton indifferent to science and perhaps, like Pascal, half ashamed of spending his time in mathematics, and like Cavendish not interested in publication of his work. Sullivan presents his arguments most convincingly and they are supported by lengthy and pertinent extracts from Newton's letters and those of his contemporaries. These apart from Sullivan's thesis are interesting side-lights on a very interesting period of English science. It is, of course, impossible to say whether Sullivan's explanation is correct. It seems to explain much, but it does not explain Newton's most regular attendances at the meetings of the Royal Society over which he presided from 1703 until 1727, when, though in a poor state of health, he presided for the last time three weeks before his death.

H. B.

Probleme der Technischen Magnetisierungskurve. Herausgegeben von R. Becker, Göttingen. Pp. v + 172, with 102 illustrations. (Berlin. Springer, 1938.) RM: 16.50.

The contents of this book consist of the contributions made at a colloquium held in Göttingen in October 1937, to discuss ferromagnetic problems of technical importance, and they are of interest to all who are concerned with such problems. It may be said at the outset that many of the speakers appeared to attach great significance to the properties of boundaries between magnetic domains. Thus, the first contribution by K. J. Sixtus on the researches carried out on the propagation of large Barkhausen discontinuities and their theoretical interpretation is followed by another in which W. Döring examines the energy relations in the transition region of separation between two oppositely magnetized portions of a wire which represents a discontinuity spreading along the latter. On account of its technical interest, coercivity loomed large in the discussions. M. Kersten in his contribution reviews the modern conceptions of coercive force, and he also placed emphasis on the information which the investigation of large Barkhausen discontinuities has provided and upon the conception of a wall or transition region between adjacent domains magnetized anti-parallel to one another.

The reviewer found the sections on magnetic viscosity to be the most interesting. This subject has been more or less completely ignored in modern works, mainly because the observed effects are generally quite small. G. Richter, however, gives an abreviated account of his magnetometer and ballistic studies of the pronounced effects exhibited by carbonyl iron, which shows marked induction changes up to 100 seconds after the magnetizing field has become steady. Richter shows that magnetic viscosity and ordinary hysteresis effects are not intimately related. His main results are confirmed by H. Schulze, who gives a summary of the results of an alternating-current study of the phenomena which was recently published by the Siemens-Werken. He measures the power losses in a carbonyl iron core by means of a Maxwell inductance-capacity bridge and separates them into magnetic viscosity, hysteresis and eddy-current losses. He shows that the viscosity losses can be divided into two parts, one independent of and the other dependent upon the frequency of the alternating field. The latter part provides a kind of resonance curve when plotted as a function of the temperature of the specimen for a constant frequency f, the relation between f and the absolute temperature T_r at which the viscosity is a maximum being given by

$$\log 2\pi f=\theta\left(\frac{1}{T_0}-\frac{1}{T_r}\right)=34{\cdot}7-\frac{10{,}600}{T_r}$$

for the material in the virgin state. Schulze explains his results on the assumption that a pure and recrystallized specimen of carbonyl iron in the virgin state consists of parallel, threadlike domains magnetized in parallel and antiparallel directions.

The final contributions describe new ways and apparatus for applying magnetic analysis to problems of metallic structure. Here the reviewer is not happy about some of the basic assumptions and interpretations. In particular, he deprecates the use of the term "spezifische technische Sättigung $I_{\infty,T}$" to denote what he would himself describe as the "spontaneous magnetization in zero applied field $I_{0,T}$" at a temperature T. However, the book is full of interest and is to be heartily commended.

L. F. B.

Negative Ions, by H. S. W. Massey. Cambridge Physical Tracts. Pp. xiv + 105. (Cambridge University Press.) 6*s*. net.

This work is the first of a series of Cambridge Physical Tracts issued under the joint editorship of Professor Oliphant and Mr Ratcliffe. It is the aim of the editors that these tracts may present such surveys of subjects as the authors might give in a short course of specialized lectures. They are therefore intended not to be exhaustive but to deal more particularly with work on which the authors can speak with direct experience gained through their own investigations. Such a tract avoids one objection to a full monograph, complete with all references to published papers and to allied subjects which, in a rapidly advancing subject, becomes so soon out of date. In these tracts, bound in a stiff paper cover and issued at a moderate price, revision or additions in subsequent years will be much more practicable, and it is to be hoped that other authors will come forward to supply a real need in the busy life of the average physicist.

The material collected by Dr Massey in a hundred pages is full of interest and is well selected. The first two chapters summarize the experimental evidence for the existence of certain atomic and molecular negative ions in gases, and discuss from the wave-mechanical standpoint why one would expect stable ions in certain cases and not in others. The third chapter, on modes of formation, is of particular interest and deals with the processes of electron-capture and the experiments of Tate and Lozier, Bailey, and Bradbury. In the last chapter, on negative ions in glow discharges and the upper atmosphere, the author draws attention to a number of problems which still await solution, and makes tentative suggestions as to the role played by negative ions in the conducting layers of the ionosphere.

The tract may be confidently recommended as a critical and original treatment of a subject which has not previously been adequately summarized. A. M. T.

Direct and Alternating Current Potentiometer Measurements, by D. C. Gall, F.Inst.P. Pp. xiv + 231. (Chapman & Hall.) 15*s*.

This book constitutes volume IV of the series of *Monographs on Electrical Engineering* edited by Mr H. P. Young. The author is well known as a designer of electrical instruments, and has himself originated instruments of the classes which form the subject of the volume.

The direct-current potentiometer has long been a familiar instrument both to physicist and engineer. Its accuracy and the multiplicity of its uses, direct and indirect, are well recognized. The alternating-current potentiometer is its younger brother, a decidedly subtler and more complicated personality. In 1897 Clark Fisher produced his book on *The Potentiometer and its Adjuncts*; in this the alternating-current instrument is not even mentioned, although the idea of it had already begun to take practical form. The first complete alternating-current potentiometer, that of Drysdale, appeared in 1908. Its reception was not at first general, and even as late as 1922, in the *Dictionary of Applied Physics*, we find the alternating-current potentiometer disposed of in three quarters of a page, whilst the direct-current instrument claims fourteen pages.

The book before us is, we believe, the first since Fisher's to be devoted entirely to the subject of potentiometers; about one quarter of it (five chapters) is allotted to the direct-current class, and three quarters (eight chapters) to the alternating-current class of instrument. Doubtless this proportion is not intended to indicate the relative order of importance, but rather to implement the view that the time is ripe for a full-dress introduction of the manifold applications and merits of the new-comer. We feel sure the book will be sincerely welcomed by the physicist as well as the engineer. The description of the various forms of instruments of the direct-current and alternating-current types is given with the wealth of practical detail and suggestion that would be expected from the author, and the notes and bibliography appended to most of the chapters facilitate access to the whole field of potentiometer measurements.

Of the chapters on the direct-current instruments no more need be said than that fresh material will be found even for the expert. The reader's attention is however directed mainly to the alternating-current types of potentiometers. Two chapters are devoted to descriptions of the instruments, and four chapters to their applications, which range from the calibration of ammeters, voltmeters and watt-meters to measurements of impedance of all kinds, the determination of iron losses, the testing of current and potential transformers, and the measurement of magnetic fields. The author has developed the rectangular-coordinate type of alternating-current potentiometer, and the interest of the reader will naturally turn to his account of his own instrument. It will be found that the balance is held fairly between the polar and the coordinate types, applications to which one or the other type is peculiarly adapted being pointed out. One valuable chapter is devoted to the precautions to be attended to when the most precise measurements are required. In a penultimate chapter the representation of alternating-currents or voltages by complex quantities is explained in its application to the calculation of results from measurements made with the coordinate type and with the polar type of potentiometer respectively. A brief historical chapter brings the book to its close.

If a criticism may be made it is that more care might occasionally have been allowed in the exposition of theory and the unambiguous choice of symbols. The manipulation of alternating-current quantities undoubtedly presents difficulties to the learner, and in view of the necessity of distinguishing clearly between instantaneous value, amplitude, effective value, and vector value, special regard to a systematic notation and nomenclature is demanded. This impression should not impede for a moment the recourse of any reader interested in electrical measurements to the benefits to be derived from this valuable and timely book.

D. O.

Elementary Practical Physics, by N. H. Black and H. N. Davis. Pp. viii + 710. (New York: The Macmillan Co., 1938.) 8*s*. 6*d*. net.

This is not, as many English readers might expect it to be, an elementary laboratory manual. It is mainly devoted to what we might call, for want of a better brief title, "Everyday Physics", or since the cyclotron, which gets over two pages of description, is not yet an everyday object even of the laboratory, perhaps "Elementary Applied Physics" would be a less misleading title.

The book does deal very largely with the physics of everyday life—the motor-car provides the first object-lesson—and the authors (a Harvard physicist and a former Harvard engineer) form an obviously suitable team for the writing of such a treatise. One of their avowed aims is the teaching of physics "in the light of its social and industrial uses", and this aim is followed throughout the book. Considerable space is, however, given to quite recent developments, of which the "practical" applications lie largely in the future.

The text is brightly written, and is supplemented by a large number of diagrams and an excellent selection of most searching questions, so worded as to catch the attention and linger in the memory—e.g., "Does the cardboard jacket on a dry cell serve any useful purpose except advertising?" The questions range far outside the subject-matter of the text, and the reader is enjoined to consult reference books in attempting to answer them, "to keep his eyes open outside the classroom and to ask questions of artisans and business-men". This seems on the face of it excellent advice, and it is difficult to believe that it can be the same authors who on another page (299) advocate the starting of a first-class squabble thus: "Will potatoes cook faster if more gas is turned on to make the water boil faster? *Discuss it with your mother*." The authors again show, we feel, less than their usual acumen when they encourage the young reader to float silver coins on mercury—the success of this experiment may very well be accepted as an act of faith.

The book is further embellished by portraits of outstanding physicists, intelligently arranged. Thus, Joule is paired with Kelvin on one page, and Henry with Faraday on another. The authors have succeeded in securing a rather rare photograph of Moseley, which they have fittingly placed with Rutherford's, and Marconi's portrait is associated with that of Hertz—we may hope that a place will be found for Maxwell in the next edition. The portraits—of which there are many others—add considerably to the interest of the book.

Any intelligent youngster could learn a good deal of interesting physics from this volume, and a senior who had studied it carefully might be less apt to leap like a startled faun at the well-known gambit: "Look here, you're a physicist, you can tell me why...."

The book is an experiment, interesting and on the whole very successful. In view of its size and the lavish way in which it is illustrated, the price is remarkably low. H. R. R.

On Understanding Physics, by W. H. WATSON, M.A., Ph.D., F.R.S.C. Pp. xii + 146. (Cambridge University Press.) 7*s.* 6*d.*

Prof. Watson, who is Assistant Professor of Physics in McGill University, has evidently been troubled, like many other experimental physicists, by the repercussions of so-called modern physics on philosophy. He is particularly concerned with the philosophers' writings around the discoveries made by experiment. This book contains his reflections, which are based largely on the views of Dr Ludwig Wittgenstein. The problems are treated from the standpoint of the logician rather than from that of the mathematical physicist, though "language is, of course, a more complicated symbolism than mathematics". The chapter on "Methods of Representation" is particularly good and should be read with equal interest by both experimental and theoretical physicists. On the controversial question of determinism the author says "...the new theories of physics will not do for us what not a few men have wanted them to do, namely, to get rid of determinism" (p. 80). And on discontinuity he says "if it happens that discontinuity is accepted, and with it limits on the precision with which an electromagnetic field can be specified, perhaps we shall be fortunate enough to avoid the mistake of attempting to use the new physical theory as a peg on which to hang 'philosophy'" (p. 141).

Although the book makes difficult reading, which is inherent in its nature, it is one of those which serves to give scientists in general and physicists in particular a view of the recent outstanding advances in physics, in relation to the background of philosophical thought; it also serves to restrain the making of broad generalizations from theories propounded for the purpose of linking together, in logical order, discoveries made by experimentalists.

H. R. L.

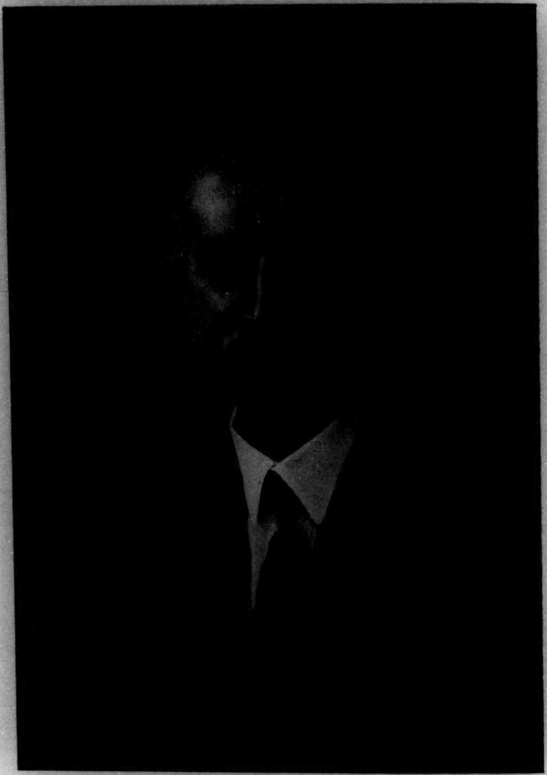

THOMAS SMITH, M.A., F.INST.P., F.R.S.

President of the Physical Society, 1936 *to* 1938

Frontispiece